Utilizing ultra-performance chromatography high-resolution mass spectrometry to investigate fatty acid mediated antibiotic tolerance

A Dissertation Presented for the
Doctor of Philosophy
Degree
The University of Tennessee, Knoxville

Brittni M. Woodall
May 2023

DEDICATION

To my precious grandfather Pop- I wish you were here to see me accomplish this milestone. I know how proud you would be. I miss you dearly. Go Vols.

ACKNOWLEDGEMENTS

There are so many people to thank for supporting me on this journey and I hope each person listed below understands the profound impact they have made on my life either personally and/or professionally. I would first like to thank my advisors Dr. Shawn R. Campagna and Dr. Elizabeth M. Fozo for convincing me to invest time in science and fostering my creativity over the last 6 years. Without them, I would have never stumbled into this field and found my passion for exploration. Additionally, I would like to thank Dr. Michael Best, Dr. Thanh Do and Dr. Colleen Crouch for providing valuable feedback regarding scientific ideas and challenging me to grow into the scientist I am today.

Of course, I must thank my lab family. Dr. Abigail Farmer, Dr. Eric Tague, Dr. Josh Powers, Dr. Caleb Gibson, Dr. Stephen Dearth, Dr. Allen Bourden, Dr. Brandon Kennedy, and Dr. Alexander Fisch were all fantastic mentors in my early training and made long days enjoyable. I owe a huge thank you to each of these individuals for their mentorship and for being fantastic role models. A special thank you to Dr. Hector Castro for telling me when I was being too difficult and providing honest advice when I needed it. I would also like to thank Dr. Katarina Jones and Dr. Courtney Christopher for helping push me to the finish line. You both have offered advice, encouragement, and friendship when I needed it most. To my other lab members, thank you for providing wholesome conversation, listening to presentations, and providing feedback on documents. To my best friend Lindsay Brown, I owe so much to you. There is no doubt I would have quit two years ago if it weren't for you. Thank you for everything: coffee dates, chipotle, making me love tofu, helping me with broken instruments, the list goes on and on… but most importantly, thank you for not letting me quit. There is no other name I would rather be swapped with mine for the last 4 years.

Last and certainly not least, thank you to my family and friends. My parents Donita and Gary Woodall have always supported my wildest dreams and are the reason why I am here today. To my brother Peyton, although you are a handful, I hope to have set an example for you: do what makes you happy, even if no one understands. To my grandparents, thank you for your support and words of wisdom. Thank you to my aunts, uncles, and cousins for always picking up the phone when I needed to talk and for reminding me that even during hard times to smile. Kayla and Adam, Erica and Z, Jacob, John, Marissa, Tess and Jordan, Abigail and Erika, thank you all for everything. You all have supported me, given me space to have fun and enjoy my time off, and provided the best company. I am forever thankful for each of you.

ABSTRACT

The lipid membrane is the first component necessary to sustain life. To maintain homeostasis, segregate cellular machinery, provide protection from the environment, and reproduce, an organism must establish a boundary in which the processes can occur. Throughout the last two decades, research has propelled our knowledge of lipid membranes much beyond original hypotheses. Once thought of to be static and uniform, the understanding of the lipid membrane has evolved to encompass a structure that is responsive, unique, and intricately constructed by the organism itself. By chance or by choice, organisms adapt the lipid membrane according to the environment for which they are in. Many of these adaptations or alterations of the lipid membrane have been implicated to play a large role in human health and disease pathology; one example includes the ability of bacteria to circumvent antimicrobial drugs by altering cellular membrane components. In the chapters following, the unique link between fatty acid supplementation and antimicrobial drug tolerance will be investigated utilizing a variety of techniques including ultra-performance liquid chromatography high resolution mass spectrometry, genetic mutagenesis, and stable isotope tracing.

Daptomycin is a lipopeptide designed to target Gram-positive bacteria, yet since the discovery of daptomycin the 1980's, instances of resistance or tolerance to the drug have been reported in several strains of Enterococci. Despite the efforts of many researchers, the mechanism by which resistance or tolerance occurs in Enterococcal strains is not yet understood although significant links to lipid membrane alterations have been reported. Chapter 1 demonstrates how daptomycin impacts the membrane of both susceptible populations and fatty acid protected populations. Susceptible and protected bacterial populations responded to daptomycin by altering percent of total lipid species present; therefore, a genetic approach was utilized to investigate the role of individual lipid species in Chapter 2. Mutagenesis studies carried out in Chapter 2 demonstrated the ability of *E. faecalis* to respond to genetic and environmental perturbation. Additionally, specific strains generated in this chapter had altered survival in the presence of membrane damaging agents. Chapter 3 focused on the design of an analytical technique capable of tracing basal and environmental nutrient fluxes using stable isotopes. Results from this study concluded *E. faecalis* is capable of altering its membrane in the presence of oleic acid by placing oleic acid onto acyl tails of lipids species as well as direct incorporation into the membrane as free fat.

Together, this body of work highlights the importance of cross discipline collaboration in efforts to improve the quality and longevity of human life. Yet at a fundamental level, this work reminds us to always consider parts of science others may rule out as lackluster.

PREFACE

The contents of this document submitted for the degree of Doctor of Philosophy at the University of Tennessee, Department of Chemistry have been directed by Dr. Shawn R. Campagna and Elizabeth M. Fozo. As part of collaborative efforts, both advisors have provided conceptualization of ideas for the research reported herein. This work is original, with the exceptions of reported publications included as Chapters 2:

Woodall, B. M., et al. (2021). "Enterococcus faecalis Readily Adapts Membrane Phospholipid Composition to Environmental and Genetic Perturbation." *Frontiers in Microbiology* **12**.

TABLE OF CONTENTS

LIST OF TABLES

LIST OF FIGURES

INTRODUCTION

Lipid membrane

Persistence. A word to some that signifies tenacity, determination, or perseverance, however, to others the definition might be much simpler. Response to change is a conserved behavior across species. All organisms respond to external stimuli received from their environment and alter their behaviors accordingly. These behaviors can be simple, such as our pet's response to command "sit", or complex, such as microbial intelligence altering its metabolism in response to available nutrients in the environment. While one behavior results in a tasty treat, the other results in the ability to survive. In order to survive, one must first create a boundary by which it can separate itself from the environment; this boundary is defined as the lipid membrane.[1] The lipid membrane serves many vital roles for the cell including signaling, aiding in protein function, and energy production/storage.[2-4] Organisms craft intricate designs of molecules contributing to the overall structure and function of the lipid membrane.

Generalized definitions of lipids include any organic molecule that is not soluble in water, of which include sterols, sphingolipids, terpenes, fatty acids, and phospholipids.[5] While each organism contains unique ratios and modifications of the abovementioned lipid classes, phospholipids remain the most abundant.[6] Phospholipids have a conserved structure composed of non-polar regions containing acyl groups referred to as "acyl tails" which can vary in number of carbons and degrees of unsaturation contributing to the physical properties of the lipid membrane.[2] Decreasing the saturation of the membrane (or increasing unsaturation) alters the rigidity of the membrane, concomitantly altering the function of membrane associated processes such as protein or ion channel function. Cell toxicity has been observed under conditions which cause the membrane to be too fluid, thus membrane fluidity or rigidity is an important factor to consider as it is vital ratio to maintain for cell survival.[7] In addition to the acyl tails, phospholipids also contain a glycerol backbone that can be linked to various polar molecules through phosphate linkages. These polar regions of the lipid are termed "head groups" and can consist of additional glycerol molecules, ethanolamine, choline, serine, inositol, or glucose.[2] These headgroups are not conserved across species, and while present in some, not all headgroup classes are produced or observed in a specific organism.

Bacteria have demonstrated significant ability to alter the lipid membrane in response to environmental and genetic cues. These single celled microorganisms are often thought to be simpler in terms of complexity given they do not contain cellular organelles such as mitochondria or endoplasmic reticulum nor do they perform DNA replication within the site of a nucleus however; while these processes might appear to make the organism less complex, cellular structures such as the cell wall and lipid membrane are of utmost importance to aid in performing critical functions.[8] Species including *Escherichia coli*, *Bacillus*

subtills, and *Streptococcus pneumoniae* have demonstrated capabilities to control spatial growth, cellular division, and morphology through the use of cell wall and cell membrane components.[9, 10] Formation of membrane domains and segregation of protein machinery in or at the membrane occurs to aid supporting structural components, performing essential metabolic reactions, and assembling signaling complexes.[2] Given the cellular membrane plays a key role in cell viability and survival, understanding how bacteria adapt or alter this structure is essential for understanding the overall function of the cell. As complex and adaptable as they seem, lipid membranes continue to prove their relevance as the years progress.

Metabolomics and Lipidomics

Although comprised of many parts, nature conserves a method to the madness as interruption or dysfunction of this integral structural component has been implicated to play a role in a myriad of diseases including cardiac and neurodegenerative disease, many cancers, and even antibiotic resistant infections.[11-13] While studying the structure and function of the lipid membrane contributes to the global understanding of cellular biology, links to health and human disease are yet another reason additional research is needed to understand these dynamic structures. The field of “omics” was developed to fully characterize any and all biological molecules within the living cell, with hopes of gaining a deeper understanding of how cells function and communicate.[14] All cells contain genetic material (genomics) which can be transcribed to messenger information (transcriptomics) for further translation into proteins (proteomics).[15] Proteins then act within a cell to break and build bonds, keeping the cell alive. Studying metabolic processes consists of characterizing both the polar (metabolomics) and non-polar (lipidomics) molecules responsible for maintaining the cells living state.[16]

The field of mass spectrometry has contributed greatly to the ability to perform routine, high- throughput analysis of these molecules providing reproducible, precise quantitative and qualitative data.[17] Most mass spectrometry workflows include the use of a separation technique prior to the arrival of molecules to the instrument. Techniques such as liquid chromatography separate molecules of similar structural and/or physical properties in order to maximize instrumental response and provide quantitative data.[17, 18] For both metabolome and lipidome analysis, two types of chromatography are routinely utilized: normal phase and reverse phase chromatography. While both types of chromatography are useful, each type has unique pros and cons to consider when selecting a liquid chromatography mass spectrometry analysis platform including the analyte type and polarity of the molecules of interest. Hydrophilic interaction liquid chromatography (HILIC) is an attractive technique for separation of small, polar compounds as there are copious types of stationary phases commercially available which can be utilized to selectively separate or target functional groups on polar molecules.[19] Metabolomics workflows often utilize HILIC

chromatography, as separation of polar molecules is easily accomplished via polar stationary phase selection; however, lipidomics workflows can also utilize HILIC chromatography by targeting the headgroup or other functionalized regions on the molecule.[20, 21] While HILIC chromatography for lipidome analysis can save on analysis time and cost, it can be difficult to discern structural information such as acyl tail carbon number or unsaturation with traditional HILIC separations as the technique segregates lipids according to their head group composition. Given these limitations, reverse phase is an attractive platform for lipidomics analysis due to its ability to distinguish lipids based on their hydrophobic properties which include acyl tail length and conformation.

While the structural heterogeneity among metabolic molecules is high, mass spectrometers can also aid in providing structural information through the use of fragmentation.[22] Various types of fragmentation are routinely used throughout metabolomics and lipidomics workflows and are chosen primarily based on the instrument platform utilized as each mass spectrometer contains unique fragmentation abilities. Orbitrap mass spectrometers are attractive platforms to utilize for routine ‘omics analyses due to the ability to have both high resolution and mass accuracy for full scan and fragmentation scan data.[23] Within these instruments, ions of interest can be analyzed within the orbitrap, moved to a selective fragmentation cell where collisional energy is utilized to break chemical bonds, producing fragments which can then be reanalyzed by the orbitrap again. The data generated from these experiments can aid in producing information regarding the structural conformation of the molecule as ion fragments have a unique mass to charge ratio. Over the last decade, several data analysis tools have been developed to aid in processing datasets in which fragmentation techniques are utilized, however; interpretation and spectra matching remain laborious and time consuming.[24, 25]

When considering the advantages of mass spectrometry analysis for biological small molecule characterization including high reproducibility and sensitivity and quick measurement time, the ability to trace metabolite generation or modification should also be included. Biological systems adapt external and internal pathways to modify or utilize molecules for metabolic processes. Beyond studying these molecules directly, isotope tracing techniques can be utilized to trace the flow of nutrients through a pathway or system, providing insight into the state of the system beyond quantitative or qualitative values.[26] Stable isotope probes including ^{15}N, ^{13}C, and ^{2}H have been employed monitor nutrient cycling and metabolic flux through a variety of systems.[27] As isotope probes are introduced into the system, metabolites and lipids are modified via the mass of the incorporated probe. The differences in masses between metabolites utilizing the labeled nutrient can be monitored via mass spectrometry as labeled metabolites are produced with unique mass to charge ratios. Isotope tracing techniques can be utilized to probe biological systems gaining a deeper understanding of how metabolic processes influence nutrient cycling and distribution.

Outline of Dissertation

As some forms of antimicrobial resistance or tolerance have been linked to bacterial lipid membrane alterations, the studies provided within this dissertation utilize lipidomics and metabolomics workflows to probe bacterial behaviors in response to antimicrobial drugs, host derived nutrient sources, and genetic perturbations. The first study investigates daptomycin mediated membrane alterations in the presence and absence of host derived fatty acids due to their hypothesized role in providing drug tolerance. A dual omics approach was used to characterize the metabolome and lipidome under several conditions. The second study investigates membrane alterations from a genetic perspective. Mutant strains were generated lacking specific phospholipid classes. Lipidomics and membrane challenge assays investigated the bacterial response to these alterations in the presence of host derived fatty acids. The last study focuses on the development of a novel analytical technique capable of tracing *de-novo* lipid biosynthesis as well as exogenous nutrient fluxes to gain a better understanding of how host fatty acids alter the lipid membrane of the bacteria.

REFERENCES

1. van Meer, G.; Voelker, D. R.; Feigenson, G. W., Membrane lipids: where they are and how they behave. *Nat Rev Mol Cell Biol* **2008,** *9* (2), 112-24.
2. Harayama, T.; Riezman, H., Understanding the diversity of membrane lipid composition. *Nature Reviews Molecular Cell Biology* **2018,** *19* (5), 281-296.
3. Nakamura, M. T.; Yudell, B. E.; Loor, J. J., Regulation of energy metabolism by long-chain fatty acids. *Progress in lipid research* **2014,** *53*, 124-144.
4. Shimizu, T., Lipid mediators in health and disease: enzymes and receptors as therapeutic targets for the regulation of immunity and inflammation. *Annual review of pharmacology and toxicology* **2009,** *49*, 123-150.
5. Fahy, E.; Cotter, D.; Sud, M.; Subramaniam, S., Lipid classification, structures and tools. *Biochim Biophys Acta* **2011,** *1811* (11), 637-47.
6. Alberts, B. J., A Lewis J, et al., *The Lipid Bilayer*. 4th edition ed.; Garland Science: Molecular Biology of the Cell, 2002.
7. Maxfield, F. R.; Tabas, I., Role of cholesterol and lipid organization in disease. *Nature* **2005,** *438* (7068), 612-621.
8. Schroeder, F., Fluorescence probes in metastatic B16 melanoma membranes. *Biochimica et Biophysica Acta (BBA)-Biomembranes* **1984,** *776* (2), 299-312.
9. MacDermott-Opeskin, H. I.; Gupta, V.; O'Mara, M. L., Lipid-mediated antimicrobial resistance: a phantom menace or a new hope? *Biophys Rev* **2022,** *14* (1), 145-162.
10. Vailati-Riboni, M.; Palombo, V.; Loor, J. J., What Are Omics Sciences? In *Periparturient Diseases of Dairy Cows: A Systems Biology Approach*, Ametaj, B. N., Ed. Springer International Publishing: Cham, 2017; pp 1-7.
11. Bell, M.; Blais, J. M., "-Omics" workflow for paleolimnological and geological archives: A review. *Science of The Total Environment* **2019,** *672*, 438-455.
12. Clish, C. B., Metabolomics: an emerging but powerful tool for precision medicine. *Cold Spring Harb Mol Case Stud* **2015,** *1* (1), a000588.
13. Gowda, G. A.; Djukovic, D., Overview of mass spectrometry-based metabolomics: opportunities and challenges. *Methods Mol Biol* **2014,** *1198*, 3-12.
14. Guillarme, D.; Ruta, J.; Rudaz, S.; Veuthey, J.-L., New trends in fast and high-resolution liquid chromatography: a critical comparison of existing approaches. *Analytical and Bioanalytical Chemistry* **2010,** *397* (3), 1069-1082.
15. Kind, T.; Fiehn, O., Advances in structure elucidation of small molecules using mass spectrometry. *Bioanalytical Reviews* **2010,** *2* (1), 23-60.
16. Aebersold, R.; Burlingame, A. L.; Bradshaw, R. A., Western blots versus selected reaction monitoring assays: time to turn the tables? *Mol Cell Proteomics* **2013,** *12* (9), 2381-2.
17. Young, L. M.; Saunders, J. C.; Mahood, R. A.; Revill, C. H.; Foster, R. J.; Tu, L.-H.; Raleigh, D. P.; Radford, S. E.; Ashcroft, A. E., Screening and

classifying small-molecule inhibitors of amyloid formation using ion mobility spectrometry–mass spectrometry. *Nature Chemistry* **2015,** *7* (1), 73-81.
18. Chen, G.; Pramanik, B. N.; Liu, Y.-H.; Mirza, U. A., Applications of LC/MS in structure identifications of small molecules and proteins in drug discovery. *Journal of Mass Spectrometry* **2007,** *42* (3), 279-287.
19. Banerjee, S., Empowering Clinical Diagnostics with Mass Spectrometry. *ACS Omega* **2020,** *5* (5), 2041-2048.

CHAPTER I
A bifurcated omics approach for the investigation of fatty acid mediated antibiotic protection in *Enterococcus faecalis*

A version of this chapter is expected to be included in future publication. Proposed Authors: Brittni M. Woodall, Elizabeth M. Fozo, Shawn R. Campagna

EMF, BMW, and SRC contributed to study design. BMW and EMF prepared cell cultures. BMW performed lipidomics extraction, mass spectral analysis, data processing and interpretation, and prepared manuscript. SRC and EMF provided funding for the project.

1.1 Abstract

Daptomycin was reported to alter the lipid membrane of *Enterococcus faecalis (E. faecalis)* by significantly decreasing percent of total phosphatidylglycerol (PG) species while increasing the percent of total free fatty acid (FFA) species, phosphatidic acid (PA), and cardiolipin (CL) detected. Metabolome analysis of bacterial cultures treated with daptomycin detected 6 significantly altered metabolites, however, partial least squares discriminatory analysis (PLS-DA) and principle component analysis (PCA) did not validate these findings. Oleic acid supplementation did not inhibit daptomycin from altering the lipidome of *E. faecalis* as percent of total ion species for PG species decreased, while FFA, PA, and CL species increased when comparing oleic acid supplemented and daptomycin treated cultures to the oleic acid supplemented cultures. Additionally, supplementation with oleic acid alone was not reported to significantly alter the metabolome (compared to vehicle control). Comparing bacterial cultures supplemented with oleic acid and treated with daptomycin to those treated with daptomycin resulted in similar percent of ion totals, however; heatmap analysis reported significant alterations in acyl tail composition between the two groups. The metabolome of bacterial populations supplemented with oleic acid and treated with daptomycin was also reported to contain 22 significant metabolite features compared to populations only treated with daptomycin. These metabolic pathways included amino acid biosynthesis, nucleotide metabolism, vitamin/cofactor metabolism, 2-oxocarboxylic acid metabolism, ABC transporters, and central carbon/fatty acid metabolism.

1.2 Introduction

With the global rise in antibiotic tolerance and resistance accompanies a need for further exploration into bacterial metabolism to aid in understanding mechanisms by which these behaviors occur. Enterococci compose a group of Gram-positive bacteria identified by the Centers for Disease Control and Prevention and World Health Organization to pose high threat levels due to their resistance to several antibiotic classes.[1, 2] One specific species of Enterococci, *Enterococcus faecalis*, is known to cause infections in the human host when exposed to environments outside of the gastrointestinal tract such as the urinary tract, cardiac, and lymphatic systems.[3-5] Daptomycin is a lipopeptide developed to combat resistant enterococcal species such as vancomycin resistant enterococcus (VRE), however recent studies have reported an emergence of

tolerance or resistance to this drug as well.[6-9] Although tolerance and resistance to daptomycin is well characterized within the literature among clinical isolates and case studies, the mechanism by which these processes occur is still widely debated.[8, 10-12] Ongoing research remains multifaceted in types of approaches used to generate hypotheses related to daptomycin tolerance. Genetic, biochemical, and analytical techniques have been employed to aid in the advancement of knowledge to combat this growing threat.[6, 13-16]

In pathogenic environments, *E. faecalis* is exposed to different nutrient sources, such as fatty acids, compared to their commensal state. Host fluids such as bile and serum are reported to be contain higher amounts of fatty acids C16:0, C18:1, and C18:2 while the gut microbiome is composed mainly of short chain fatty acids.[17-19] Independent exposure to oleic and linoleic acids (C18:1 and C18:2) have been implicated to induce daptomycin tolerance under laboratory conditions.[20-22] In addition to inducing tolerance, oleic and linoleic acids also alter the lipid membrane by shifting percent of total lipid species as well as altering acyl tail composition.[21] Although cellular membrane alterations have been consistently implicated to play a role in daptomycin tolerance, a precise mechanism of tolerance has not been validated.[6, 15, 16, 20-23] Daptomycin resistant strains were reported to contain lower abundances of PG, L-PG, and CL compared to a susceptible control however, genetic mutagenesis studies suggested L-PG and CL species are not solely responsible for tolerance.[15, 21] While the body of literature surrounding daptomycin tolerance is large, characterization of the lipidome in the presence of the drug has not yet been published.

The lipidome of *E. faecalis* has been well characterized, however, current literature has overlooked the contribution of polar metabolites in lipid biosynthesis. Amino acid metabolism, DNA replication and repair, and primary carbon metabolism are all capable of directly influencing the structure of the lipid membrane.[24-26] Previous studies of Gram-positive organisms including *Staphylococcus aureus* and *Streptococcus mitis oralis* have suggested alterations in the metabolome comparing susceptible versus non-susceptible strains via nuclear magnetic resonance metabolomics techniques; however, these studies do not report findings of metabolome alterations in the presence of the drug itself.[27, 28] To address these concerns, we designed a bifurcated experiment capable of monitoring both the polar metabolome and the lipidome in the presence of daptomycin with the addition of oleic acid in attempt to elucidate the relationship between fatty acid supplementation and daptomycin tolerance.

1.3 Materials and Methods

1.3.1 Bacterial growth conditions

Bacterial strains, Enterococcus faecalis (OG1RF), were grown statically in brain heart infusion medium (BHI; BD Difico) at 37°C. Overnight cultures were inoculated into fresh BHI medium to an optical density at 600 nm (OD600) of 0.01 to begin growth. At an OD600 of 0.3 cell cultures were exposed to oleic acid

(20ug/mL) or vehicle control (ethanol equal volume) for 30 minutes. After 30 minutes of supplementation, bacterial cultures were split and treated with daptomycin and calcium chloride (15 ug/mL and 1.5 mM respectively) or vehicle control (ethanol equal volume). Cell cultures were incubated for an additional 30 minutes and harvested for metabolomic and lipidomic analysis. All chemicals were purchased from Millipore Sigma.

1.3.2 Cell harvest and extraction

Bacterial cultures were harvested for metabolomic and lipidomic analysis independently. Cell pellets were generated for lipid analysis via centrifugation (2729xg for 10 minutes). Supernatant was removed and cells were washed with 1X phosphate buffered saline 3 times. After washing was completed cell pellets were flash frozen and stored at -80°C until extraction. Lipid extraction was performed as previously described. In brief, cell pellets were resuspended in extraction solvent (95% ethanol, water, diethyl ether, pyridine, 4.2 N ammonium hydroxide; 15:15:5:1:0.18) and glass beads were added. After vortexing, cells were placed in 60°C water bath for 1 hour. After incubation, cells were centrifuged and supernatant was removed and dried under N2. An additional 5mL of extraction solvent was added, pellets were vortexed, and incubated at 60°C for an additional hour. Once incubation was complete, centrifugation was performed and organic supernatant was combined and dried under N2. Resulting solids were resuspended in 9:1 methanol: chloroform and stored at 4°C prior to UHPLC-HRMS analysis.

Cell culture was harvested for metabolomic analysis via filtration. Polycarbonate filters (0.4 microns; Fisher 09-300-71) were placed on a vacuum filtration apparatus and 1 mL of cell culture was harvested. After harvest, cell filters were placed in prechilled (4°C) extraction solvent (1.3mL; 40:40:20 methanol: acetonitrile: water with 0.1% formic acid) and incubated for 20 mins at -20°C. Following incubation, extraction solvent was removed and transferred to an Eppendorf tube for drying. The filter was then washed with 400uL of extraction solvent and incubated for an additional 20 mins at -20°C. Once incubation was complete, filters were washed with an additional 300uL of extraction solvent, extraction solvent was combined and dried under N2. Resulting solids were resuspended in 300uL of water and stored at 4°C prior to analysis.

1.3.3 Ultra- high performance liquid chromatography high-resolution mass spectrometry analysis

Bacterial lipid profiling was performed as previously described with minor adaptation. A Vanquish ultra-high performance liquid chromatography system coupled to an Exploris 120 (Thermo Scientific) mass spectrometer operated in positive and negative mode. A Thermo C30 column 2.1x150 mm (2.6 pore size) was utilized to separated 2 uL of sample. Full chromatographic parameters can be found in the supporting information. Eluent was introduced to the mass spectrometer utilizing heated electrospray ionization. Full mass spectrometry

parameters can be found in supporting information. Lipid classes free fatty acid (FFA), cardiolipin (CL), lysyl- phosphatidyl glycerol (L-PG), PG (phosphatidylglycerol), and phosphatidic acid) PA were detected in negative mode while monoglucosyl-diacylglycerol (MGDG) and diglucosyl-diacylglycerol (DGDG) species were detected in positive mode as ammonium adducts. The mass spectrometer was operated in DDA mode with full scan spectra acquired from 100-2,000 m/z at 120,000 resolution. MS2 scans were produced via stepped collisional energy 25, 50, and 75 eV from a scan range of 100-2000 *m/z* and a resolution of 30,000. The mass spectrometer was calibrated in both modes prior to analysis.

Metabolic profiling was also adapted from previous publication. A Vanquish ultra-high performance liquid chromatography system coupled to an Exploris 120 (Thermo Scientific) mass spectrometer operated in positive mode. A Xbridge BEH amide column, 150x2mm (2.5 pore size; Waters) was utilized to separate 2 uL of sample. Full chromatographic parameters can be found in supporting information. Eluent was introduced into the mass spectrometer utlizing heated electrospray ionization. Full mass spectrometry parameters can be found in supporting information. Metabolites were detected as [M+H] species unless otherwise noted. The mass spectrometer was operated in DDA mode with full scan spectra acquired from 70-1000 *m/z* at 120,000 resolution. MS2 scans were acquired utilizing stepped collisional energy at 25, 50, and 75 eV from a scan range of 70-1000 *m/z* and a resolution of 30,000. The mass spectrometer was calibrated prior to analysis.

1.3.4 Data analysis

MSConvert (ProteoWizard) was utilized to convert .raw files (Thermo Scientific) acquired by the mass spectrometer to .Mzml. ElMAVEN (Elucidata, open-source software), was utilized to integrate peak areas (less than 10ppm error) and verify retention times. Both metabolomics and lipidomics data were matched to curated libraries verified in-house to contain accurate retention time and *m/z* for identified compounds. All data were normalized to OD_{600} at the time of cell harvest in order to account for any growth effects antibiotics or other treatments could have on the bacterial populations. Metabolomics data were also scaled utilizing Pareto Scaling. Metaboanalyst was utilized to perform partial least squares discriminatory analysis (PLS-DA), principle component analysis (PCA), and volcano plot analysis. Percent of ion totals for lipid species were created by summing averaged ion abundances for each lipid class. Heatmaps were generated in R studio as the ratio of averaged species. P- values for heatmaps are depicted as ***<0.01, **=0.01-0.05, *=0.05-0.1.

1.4 Results

1.4.1 Daptomycin significantly impacts the lipidome of Enterococcus faecalis both in the absence and presence of oleic acid

Bacterial populations exposed to daptomycin for 30 minutes demonstrated significant lipidome alterations compared to vehicle control. Overall, daptomycin is reported to alter the abundance of lipid classes including FFA, CL, DGDG, MGDG, PA, and PG. Percent of ion totals for FFA increased 5% to 11% (p-value 0.05), CL totals increased 9% to 21% (p-value 0.0009), PA totals increased 1% to 5% (p-value 0.09), and for PG totals decreased 79% to 63% (p-value 0.005) upon exposure to daptomycin (Figure 1.1A); Further analysis of lipid classes determined 35 individual lipid species contained significant fold changes (Figure 1.1B). An additional descriptive modeling technique, PLS-DA, was employed to validate differences between the two groups (daptomycin treated versus vehicle control). PLS-DA reports two distinct groups, non-overlapping with 95% confidence confirming statistical differences between bacterial cultures treated with daptomycin versus those exposed to the vehicle control (Figure 1.1C). Supplementing bacterial cultures with oleic acid prior to daptomycin exposure also led to alterations in total abundance of lipid classes compared to oleic acid supplementation alone. In the presence of oleic acid, exposure to daptomycin significantly altered the percentage of CL, PA, and PG species detected in the lipidome. CL totals increased 12% to 18% (p-value 0.01), PA totals increased 1% to 4% (p-value 0.01) and PG totals decreased 71% to 63% (p-value 0.01) when exposed to daptomycin in the presence of oleic acid (Figure 1.2A). Furthermore, 43 individual lipid species were reported to contain significant fold changes (Figure 1.2B). PLS-DA reports two distinct groups (oleic acid+ daptomycin versus oleic acid only) with 95% confidence (Figure 1.2C).

1.4.2 Treatment with daptomycin results in similar percent of lipid species totals regardless of oleic acid supplementation, yet acyl tail composition is significantly altered

Bacterial cultures supplemented with oleic acid prior to treatment with daptomycin contained similar percent of ion totals for all lipid classes including FFA, CL, PA, PG, L-PG, DGDG, and MGDG compared to cultures only treated with daptomycin. Statistical analysis did not report p-values less than 0.05 when comparing percent of ion totals for bacterial cultures supplemented with oleic acid and treated with daptomycin to those only treated with daptomycin (Figure 1.1A and 1.2A). While percent of total ion profiles for both cultures are indistinguishable, the acyl tail composition of individual lipid species detected in bacterial cultures supplemented with oleic acid and treated with daptomycin versus those treated with daptomycin only contain significant differences. 45 lipid species contained significant fold changes when comparing bacterial cultures supplemented with oleic acid and exposed to daptomycin to bacterial cultures only exposed to daptomycin. Of these 45 lipids, 14 lipids were higher in

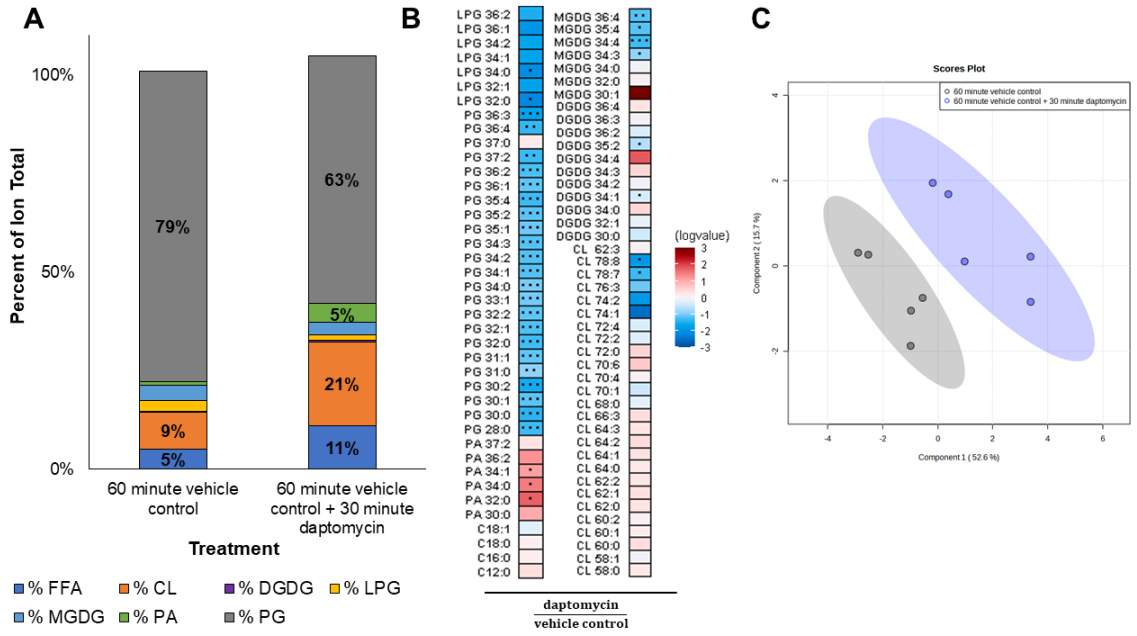

Figure 1.2 Daptomycin alters lipid profile of *E. faecalis*. A) Percent of ion totals detected in bacterial cultures treated with vehicle control or daptomycin. Vehicle control: 5% FFA, 9% CL, 0% DGDG, 3% L-PG, 4% MGDG, 1% PA, and 79% PG. Daptomycin treatment: 11% FFA*, 21% CL*, 0% DGDG, 1% L-PG, 3% MGDG, 5% PA*, and 63% PG*. *P= 0.05 B) Heatmap of lipid features detected in bacterial cultures (daptomycin treatment/ vehicle control). ***P=<0.01, **P= 0.01-0.05, *P=0.1-0.05. C) PLS-DA 2D plot of lipid features detected in vehicle control (grey) versus daptomycin treated (blue). n=5 unless stated otherwise in the text.

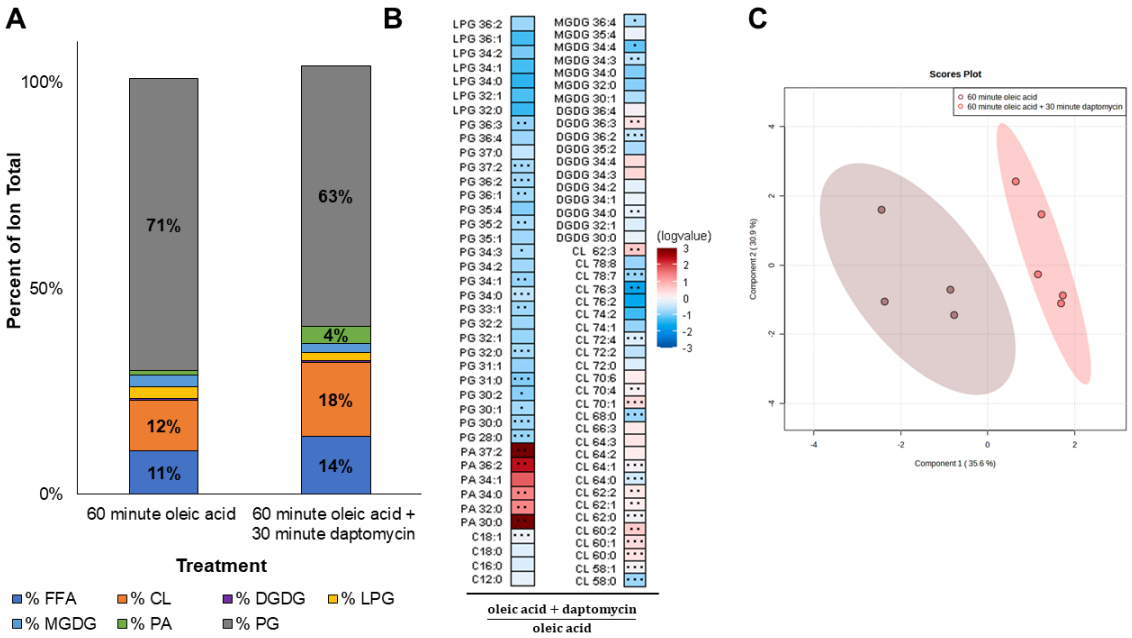

Figure 1.1 Daptomycin alters lipid profile of *E. faecalis* in the presence of oleic acid. A) Percent of ion totals detected in bacterial cultures treated with oleic acid or oleic acid and daptomycin. Oleic acid: 11% FFA, 12% CL, 0% DGDG, 3% L-PG, 3% MGDG, 1% PA, and 71% PG. Oleic acid and daptomycin treatment: 14% FFA*, 18% CL*, 0% DGDG, 2% L-PG, 2% MGDG, 4% PA*, and 63% PG*. *P= 0.05 B) Heatmap of lipid features detected in bacterial cultures (oleic acid and daptomycin treatment/ oleic acid only). ***P=<0.01, **P= 0.01-0.05, *P=0.1-0.05. C) PLS-DA 2D plot of lipid features detected in oleic acid supplemented (maroon) versus oleic acid and daptomycin treated (red). n=5 unless stated otherwise in the text.

abundance in cultures supplemented with oleic acid and treated with daptomycin while 31 lipids were lower in abundance in cultures supplemented with oleic acid and treated with daptomycin (compared to cultures only treated with daptomycin). All 14 lipids which were detected in higher abundance contained at least one unsaturated acyl tail (Figure 1.3).

1.4.3 Oleic acid supplementation and daptomycin treatment are both required to significantly alter metabolism of E. faecalis

Exposing bacterial populations to daptomycin for 30 minutes was reported to cause few significant metabolome alterations. Metabolomic studies detected 68 metabolites in the two treatment groups (vehicle control and daptomycin treated for 30 minutes) of which 6 were reported to be significantly altered when comparing the daptomycin treated cultures to the vehicle control. The following metabolites were detected containing fold changes greater than 2 and a p-value of less than 0.1: Adenosine diphosphate (ADP), hydroxyindoleacetate, adenosine monophosphate (AMP), trehalose 6-phosphate, serine and ornithinine (Figure 4A). PLD-SA was utilized to validate these results, however, did not provide any separation between the two groups when analyzing cross-validated components (Figure 4B). An additional unsupervised scoring method, PCA, was also employed to predict group separation; both groups were plotted overlapping with 95% confidence (Appendix).

Oleic acid supplementation prior to daptomycin exposure led to alterations in the metabolome compared to cultures exposed to daptomycin only. Metabolic analysis detected the presence of 68 metabolites of which 22 metabolites contained a significant fold change and p-value (Figure 1.5, Table 1). PLS-DA confirmed group separation with minor overlap in 95% confidence ranges (Figure 1.5). Pathway analysis of the 22 metabolites reported to be significant identified 12 metabolites involved in amino acid metabolism, 6 metabolites involved in nucleotide metabolism, 2 metabolites involved in butonate metabolism, 1 metabolite involved in ABC transporter metabolism, and 1 metabolite involved in central carbon/ fatty acid metabolism (Table 1).

Supplementation with oleic acid for 60 minutes did not significantly alter metabolism of *E. faecalis*. Metabolomic analysis detected the presence of 68 metabolites in bacterial cultures. Comparing bacterial populations supplemented with oleic acid to those supplemented with vehicle control two significantly decreased metabolites: hydroxyindoleacetate and AMP. Cross validation for PLS-DA failed for all four components and PCA plotted the two groups overlapping with 95% confidence (Appendix).

1.5 Discussion

A bifurcated omics approach was employed in order to monitor both the polar and non-polar metabolites impacted by the presence of either fatty acid or daptomycin as well as both treatments combined. Considering high resolution lipidomic analyses of *E. faecalis* OG1RF treated with daptomycin are not widely

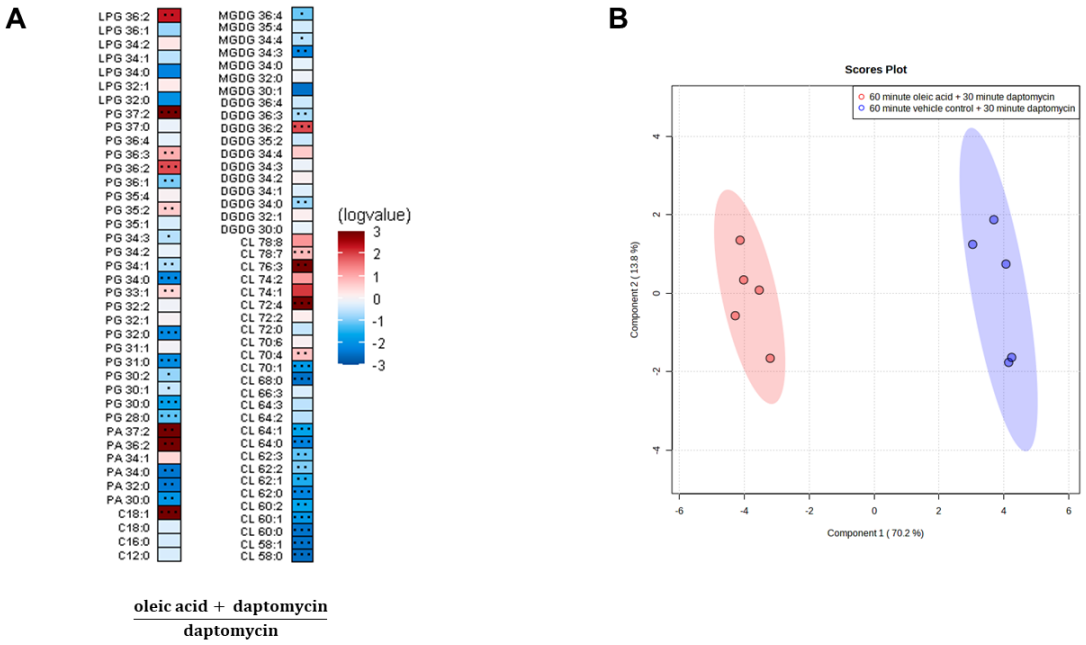

Figure 1.2 Oleic acid supplementation alters lipidome of *E. faecalis* in the presence of daptomycin. A) Heatmap of lipid features detected in bacterial cultures (oleic acid and daptomycin treatment/ daptomycin). ***P=<0.01, **P= 0.01-0.05, *P=0.1-0.05. C) PLS-DA 2D plot of lipid features detected in oleic acid supplemented and daptomycin treated (red) versus daptomycin treated (blue). n=5 unless stated otherwise in the text.

A

B

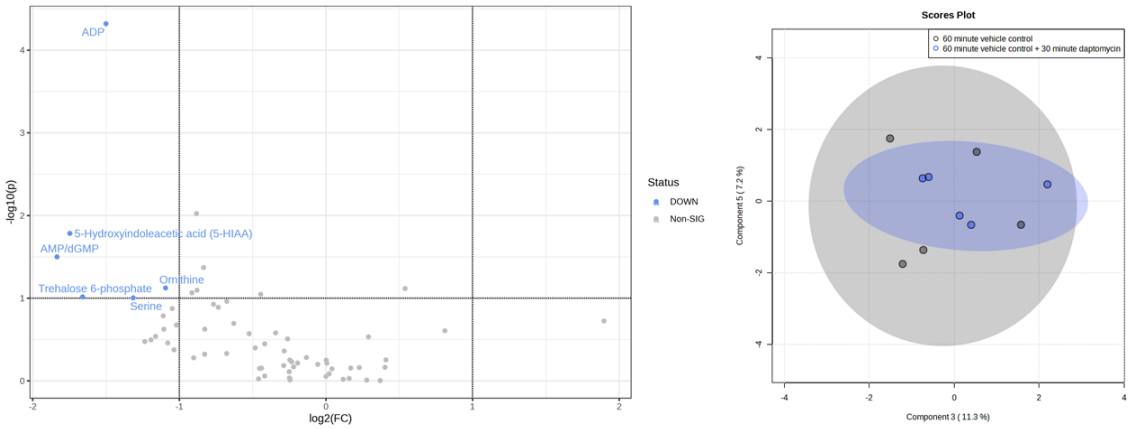

Figure 1.3 Treatment with daptomycin does not cause significant metabolome alterations. A) Volcano plot analysis predicting significant metabolites features. Fold change >2 and p-value<0.05 threshold values were used. C) PLS-DA 2D plot of metabolome features detected in vehicle control versus daptomycin treated bacterial cultures. n=5 unless stated otherwise in the text.

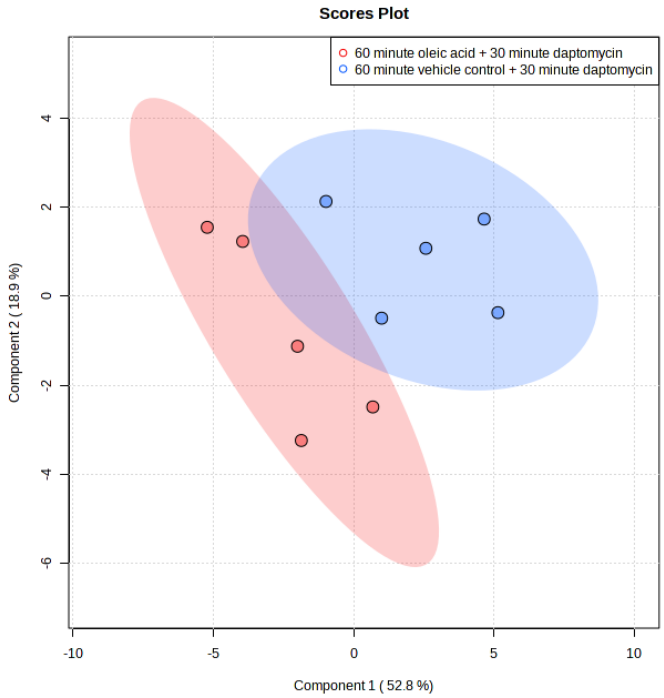

Figure 1.4 Oleic acid supplementation alters metabolome in the presence of daptomycin. PLS-DA 2D plot of metabolome features detected in oleic acid supplemented and daptomycin treated versus daptomycin treated bacterial cultures. n=5 unless stated otherwise in the text.

Table 1.1 Metabolites reported to be significantly altered in bacterial cultures supplemented with oleic acid and treated with daptomycin compared to daptomycin treatment only.

Metabolite	oleic acid+daptomycin/ daptomycin	P-value	Pathway
N-Acetyl-beta-alanine	0.2396	0.0024	**Amino acid metabolism**
Guanidoacetic acid	0.2739	0.0015	**Amino acid metabolism**
Hydroxyindoleacetate	0.2972	0.0592	**Amino acid metabolism**
Deoxyinosine	0.3059	0.0434	**Nucleotide metabolism**
Adenine	0.3557	0.0137	**Nucleotide metabolism**
Dimethylglycine	0.3893	0.0189	**Amino acid metabolism**
Uridine	0.4139	0.0487	**Nucleotide metabolism**
Adenosine	0.4178	0.0773	**Nucleotide metabolism**
Alanine/Sarcosine	0.4264	0.0169	**Amino acid metabolism**
Inosine	0.4388	0.0666	**Nucleotide metabolism**
Phenylalanine	0.4389	0.0789	**Amino acid metabolism**
Methionine	0.4423	0.0759	**Amino acid metabolism**
Arginine	0.4462	0.0766	**Amino acid metabolism**
Leucine/Isoleucine	0.4483	0.064	**Amino acid metabolism**
Homoserine/Threonine	0.4702	0.0292	**Amino acid metabolism**
Guanine	0.4796	0.0829	**Nucleotide metabolism**
Biotin	0.4818	0.0401	**Cofactor/ vitamin metabolism**
Nicotinamide	0.4908	0.0173	**Cofactor/ vitamin metabolism**
2-Oxobutanoate	2.6103	0.0229	**2- Oxocarboxylic acid metabolism**
Acetoacetate	2.6103	0.0229	**Amino acid/ butonate metabolism**
Carnitine	2.8145	0.0163	**ABC transporters**
Acetyl-CoA	4.241	0.0672	**Central carbon/ fatty acid metabolism**

reported in the literature, this study was designed to further probe fatty acid mediated protection from daptomycin. Recent studies have investigated lipidome differences in strains susceptible to daptomycin versus resistant. Hines et al suggested resistant *E. faecalis* strain R712 contained decreased PG species compared a non-resistant strain S613. In this study, treating bacterial populations with daptomycin for 30 minutes decreased the total abundance of PG detected in the membrane compared to the vehicle control. Additionally, PA species, CL species, and FFA's were significantly increased upon exposure to daptomycin. While decreases in PG species were previously reported to be associated with resistance to the antimicrobial drug daptomycin, these results suggest regardless of susceptibility, daptomycin alters the membrane.[6, 15, 29] Furthermore, there are additional lipid classes that are altered in response to treatment with the drug including increases in PA, CL, and FFA's. Heatmap analysis identified several PA species significantly increased in the daptomycin treated culture. As PA species are a precursor to PG, L-PG, and CL biosynthesis, this could signify lipid synthesis is occurring in attempt to rescue cell death caused by daptomycin. It is also possible that *E. faecalis* is synthesizing other anionic lipid species in the form of CL and PA in attempt to maintain homeostasis due to the decreased production of PG.

While significant lipidome alterations are reported upon treatment with daptomycin, alterations in the metabolome are reported to contain fewer significant species. Of the 68 metabolites detected, only 6 were reported to contain both significant fold changes and p-values. All 6 metabolites were lower in abundance in bacterial cultures treated with daptomycin compared to those treated with vehicle control. Metabolites involving carbon or sugar metabolism (trehalose 6-phosphate and (ornthinine), energy storage (AMP/ ADP) as well as amino acid metabolism (indoleacetate and serine) are decreased in cultures treated with daptomycin. These metabolites alterations could suggest decreased cell survival; however, cross validation analyses did not corroborate these results. PLS-DA and PCA did not report significant differences in metabolites detected in cultures treated with daptomycin versus those exposed to the vehicle control. It should be discussed this study considered the effects of daptomycin after 30 minutes of exposure as reported tolerance was observed during that time frame; however, it is possible that daptomycin further alters the metabolome with longer exposure times to the drug.[20]

Supplementation with oleic acid has been widely reported to alter the membrane of E. faecalis under many conditions (genetic and environmental) including both percentage of lipid classes and acyl tail components.[20-22, 30, 31] While supplementation with oleic acid provides protection from the antimicrobial drug daptomycin, it is not understood if oleic acid can inhibit daptomycin from altering the membrane. These results suggest, exposing bacterial cultures to oleic acid for 30 minutes prior to treatment with daptomycin does not inhibit daptomycin mediated membrane alterations from occurring as significant alterations between daptomycin treated (oleic acid + daptomycin) and fatty acid

control (oleic acid only) were detected (Figure 1.2A). As discussed above, exposure to daptomycin decreases the percent of PG detected in the membrane as well as increases PA, CL, and FFA species. Bacterial cultures supplemented with oleic acid prior to daptomycin exposure exhibit similar response as those bacterial cultures treated with daptomycin only. The heatmap analysis comparing oleic acid supplemented and daptomycin treated cultures to oleic acid supplemented only cultures reports significantly higher abundances of PA species 30:0, 32:0, 34:0, 36:2, and 37:2. Similar trends were reported upon treatment with daptomycin only, however the fold changes reported with oleic acid supplementation are larger and encompass more lipids to contain significance. This finding could suggest 1.) Bacterial populations are actively synthesizing lipids in response to daptomycin exposure and oleic acid aids in providing carbon substrate for acyl tail construction or 2.) daptomycin is interfering in global lipid synthesis such that any lipid species downstream of PA cannot be synthesized. These results support option 1.) as both the percent of ion totals as well as the heatmap suggest active biosynthesis of other lipid species such as CL although the precise origin of the increase in FFA cannot be determined (de-novo versus exogenous supplementation) without the use of other analytical techniques such as isotope tracing.

Although considerable membrane alterations have been reported due to oleic acid supplementation, metabolome analysis performed in this study does not suggest significant metabolic alterations due to supplementation of the fatty acid. As this organism is not capable of undergoing fatty acid oxidation processes, oleic acid cannot be oxidized and utilized in other metabolic processes such as the TCA cycle, glycolysis, or amino acid biosynthesis, yet literature has reported oleic acid to transcriptionally regulate *de-novo* fatty acid biosynthesis via the *fab* operon.[32, 33] Should oleic acid impact fatty acid biosynthesis through regulatory processes, alterations in metabolic pathways contributing to *de-novo* biosynthesis such as pyruvate metabolism and beta alanine metabolism could show significant decreases upon the addition of oleic acid to bacterial culture; however, those pathways are not reported to be significantly altered under the conditions of this study.

As supplementation with oleic acid protects bacterial populations from daptomycin mediated cell death, comparison between protected and non-protection bacterial cultures was necessary to elucidate a possible mechanism of protection.[20-22, 31] Comparing cell cultures supplemented with oleic acid prior to daptomycin treatment versus those treated daptomycin only (no fatty acid) resulted in zero significant differences in ion totals for lipid classes FFA, CL, L-PG, MGDG, DGDG, and PG. (Figure 1.1A Figure 1.2A). Additionally, previous research suggests genetic modification resulting in a loss of function for the production L-PG and CL do not inhibit oleic acid mediated protection.[21] While both cultures supplemented with daptomycin contain similar headgroups totals, PLS-DA suggested significant differences between the two groups. The heatmap reported significant increases in lipids containing a C18:1 acyl tail, which is

characteristic of oleic acid supplementation. These results suggest fatty acid mediated daptomycin tolerance does not arise via alterations in percentage of total lipid classes or one individual lipid class; however, alterations in acyl tail composition could be the driving factor. Molecular dynamics simulations have investigated the role of unsaturated fatty acids within the lipid bilayer reporting branching along the acyl tail increased the relative size of lipids containing branches or methyl additions which concomitantly decreased lipid bilayer thickness suggesting an increase in membrane fluidity.[34] Additionally, studies have linked oleic acid supplementation to increased membrane fluidity in other Gram-positive species via anisotropy techniques.[35] These links to altered membrane fluidity, lipid size, and bilayer thickness with the incorporation of unsaturated fatty acids should not be overlooked and should be further investigated. The results reported in this study suggest strong correlations between increased unsaturated lipid abundance and daptomycin tolerance.

In addition to acyl tail alterations, significant alterations in the metabolome of protected versus non protected bacterial cultured were detected (oleic acid + daptomycin versus daptomycin only). Metabolites involved in 2-oxocarboxylic acid, amino acid/ butonate, ABC transporters and central carbon/fatty acid metabolism were reported be significantly increased in cultures supplemented with oleic acid prior to daptomycin exposure. Alpha keto acids produced from 2-oxocarboxylic acid metabolism are precursors to both acetoacetate and acetyl CoA which are utilized for de-novo fatty acid biosynthesis. These results suggest oleic acid supplementation in the presence of daptomycin could contribute to sustained fatty acid biosynthesis compared to cultures treated with daptomycin only.

1.6 Conclusions

The results reported in this study suggest lipidome alterations occur in the presence of daptomycin regardless of susceptibility or tolerance induced by oleic acid supplementation. Treatment with daptomycin leads to a large decrease in total PG species, although increases in total FFA, PA, and CL are also detected. While supplementation with oleic acid is reported within the literature to provide protection from daptomycin mediated cell death, in the presence of oleic acid daptomycin is still capable of altering the membrane. Additionally, comparing bacterial cultures supplemented with oleic acid and treated with daptomycin to cultures only treated with daptomycin, percent of ion totals are nearly identical. While percent of total species remain consistent, the acyl tail composition of lipids supplemented with oleic acid and treated with daptomycin are significantly altered compared to lipids only treated with daptomycin. Metabolome analysis of these two groups (oleic acid + daptomycin versus daptomycin only) reported the largest number of significant metabolic features detected within the study (22 total) linking several pathways including amino acid biosynthesis, nucleotide metabolism, vitamin/cofactor metabolism, 2-oxocarboxylic acid metabolism, ABC transporters, and central carbon/fatty acid metabolism to sustained fatty acid

biosynthesis in the presence of the drug. While this study did not investigate implications of membrane fluidity in the presence or absence of oleic acid or daptomycin, these results suggest further experimentation is warranted to further investigate these processes.

REFERENCES

1. CDC, A., Antibiotic resistance threats in the United States. *US Department of Health and Human Services: Washington, DC, USA* **2019**.
2. Ayobami, O.; Willrich, N.; Reuss, A.; Eckmanns, T.; Markwart, R., The ongoing challenge of vancomycin-resistant Enterococcus faecium and Enterococcus faecalis in Europe: an epidemiological analysis of bloodstream infections. *Emerging Microbes & Infections* **2020,** *9* (1), 1180-1193.
3. Fiore, E.; Van Tyne, D.; Gilmore, M. S., Pathogenicity of Enterococci. *Microbiol Spectr* **2019,** *7* (4).
4. Cetinkaya, Y.; Falk, P.; Mayhall, C. G., Vancomycin-Resistant Enterococci. *Clinical Microbiology Reviews* **2000,** *13* (4), 686-707.
5. Jett, B. D.; Huycke, M. M.; Gilmore, M. S., Virulence of enterococci. *Clinical Microbiology Reviews* **1994,** *7* (4), 462-478.
6. Mishra, N. N.; Bayer, A. S.; Tran, T. T.; Shamoo, Y.; Mileykovskaya, E.; Dowhan, W.; Guan, Z.; Arias, C. A., Daptomycin Resistance in Enterococci Is Associated with Distinct Alterations of Cell Membrane Phospholipid Content. *PLOS ONE* **2012,** *7* (8), e43958.
7. Davlieva, M.; Zhang, W.; Arias, C. A.; Shamoo, Y., Biochemical Characterization of Cardiolipin Synthase Mutations Associated with Daptomycin Resistance in Enterococci. *Antimicrobial Agents and Chemotherapy* **2013,** *57* (1), 289-296.
8. Tran, T. T.; Munita, J. M.; Arias, C. A., Mechanisms of drug resistance: daptomycin resistance. *Annals of the New York Academy of Sciences* **2015,** *1354* (1), 32-53.
9. Munoz-Price, L. S.; Lolans, K.; Quinn, J. P., Emergence of Resistance to Daptomycin during Treatment of Vancomycin-Resistant Enterococcus faecalis Infection. *Clinical Infectious Diseases* **2005,** *41* (4), 565-566.
10. MacDermott-Opeskin, H. I.; Gupta, V.; O'Mara, M. L., Lipid-mediated antimicrobial resistance: a phantom menace or a new hope? *Biophys Rev* **2022,** *14* (1), 145-162.
11. Jonas, B. M.; Murray, B. E.; Weinstock, G. M., Characterization of emeA, anorA Homolog and Multidrug Resistance Efflux Pump, inEnterococcus faecalis. *Antimicrobial Agents and Chemotherapy* **2001,** *45* (12), 3574-3579.
12. Paulsen, I. T.; Banerjei, L.; Myers, G. S. A.; Nelson, K. E.; Seshadri, R.; Read, T. D.; Fouts, D. E.; Eisen, J. A.; Gill, S. R.; Heidelberg, J. F.; Tettelin, H.; Dodson, R. J.; Umayam, L.; Brinkac, L.; Beanan, M.; Daugherty, S.; DeBoy, R. T.; Durkin, S.; Kolonay, J.; Madupu, R.; Nelson, W.; Vamathevan, J.; Tran, B.; Upton, J.; Hansen, T.; Shetty, J.; Khouri, H.; Utterback, T.; Radune, D.; Ketchum, K. A.; Dougherty, B. A.; Fraser, C. M., Role of Mobile DNA in the Evolution of Vancomycin-Resistant Enterococcus faecalis. *Science* **2003,** *299* (5615), 2071-2074.

13. Nguyen, A. H.; Hood, K. S.; Mileykovskaya, E.; Miller, W. R.; Tran, T. T., Bacterial cell membranes and their role in daptomycin resistance: A review. *Front Mol Biosci* **2022,** *9*, 1035574.
14. Arias, C. A.; Panesso, D.; McGrath, D. M.; Qin, X.; Mojica, M. F.; Miller, C.; Diaz, L.; Tran, T. T.; Rincon, S.; Barbu, E. M.; Reyes, J.; Roh, J. H.; Lobos, E.; Sodergren, E.; Pasqualini, R.; Arap, W.; Quinn, J. P.; Shamoo, Y.; Murray, B. E.; Weinstock, G. M., Genetic basis for in vivo daptomycin resistance in enterococci. *N Engl J Med* **2011,** *365* (10), 892-900.
15. Hines, K. M.; Waalkes, A.; Penewit, K.; Holmes, E. A.; Salipante, S. J.; Werth, B. J.; Xu, L., Characterization of the Mechanisms of Daptomycin Resistance among Gram-Positive Bacterial Pathogens by Multidimensional Lipidomics. *mSphere* **2017,** *2* (6), e00492-17.
16. Kotsogianni, I.; Wood, T. M.; Alexander, F. M.; Cochrane, S. A.; Martin, N. I., Binding Studies Reveal Phospholipid Specificity and Its Role in the Calcium-Dependent Mechanism of Action of Daptomycin. *ACS Infect Dis* **2021,** *7* (9), 2612-2619.
17. Cummings, J. H.; Pomare, E. W.; Branch, W. J.; Naylor, C. P.; Macfarlane, G. T., Short chain fatty acids in human large intestine, portal, hepatic and venous blood. *Gut* **1987,** *28* (10), 1221-7.
18. Akoto, L.; Vreuls, R. J. J.; Irth, H.; Pel, R.; Stellaard, F., Fatty acid profiling of raw human plasma and whole blood using direct thermal desorption combined with gas chromatography–mass spectrometry. *Journal of Chromatography A* **2008,** *1186* (1), 365-371.
19. Begley, M.; Gahan, C. G. M.; Hill, C., The interaction between bacteria and bile. *FEMS Microbiology Reviews* **2005,** *29* (4), 625-651.
20. Saito, H. E.; Harp, J. R.; Fozo, E. M., Incorporation of exogenous fatty acids protects Enterococcus faecalis from membrane-damaging agents. *Appl Environ Microbiol* **2014,** *80* (20), 6527-38.
21. Woodall, B. M.; Harp, J. R.; Brewer, W. T.; Tague, E. D.; Campagna, S. R.; Fozo, E. M., Enterococcus faecalis Readily Adapts Membrane Phospholipid Composition to Environmental and Genetic Perturbation. *Frontiers in Microbiology* **2021,** *12*.
22. Brewer, W.; Harrison, J.; Saito, H. E.; Fozo, E. M., Induction of Daptomycin Tolerance in Enterococcus faecalis by Fatty Acid Combinations. *Applied and Environmental Microbiology* **2020,** *86* (20), e01178-20.
23. Zhang, T.; Muraih, J. K.; Tishbi, N.; Herskowitz, J.; Victor, R. L.; Silverman, J.; Uwumarenogie, S.; Taylor, S. D.; Palmer, M.; Mintzer, E., Cardiolipin prevents membrane translocation and permeabilization by daptomycin. *J Biol Chem* **2014,** *289* (17), 11584-11591.
24. Yang, P. L., Metabolomics and Lipidomics: Yet More Ways Your Health Is Influenced by Fat.
25. Parsons, J. B.; Rock, C. O., Bacterial lipids: metabolism and membrane homeostasis. *Prog Lipid Res* **2013,** *52* (3), 249-76.

26. White, S. W.; Zheng, J.; Zhang, Y.-M.; Rock, C. O., THE STRUCTURAL BIOLOGY OF TYPE II FATTY ACID BIOSYNTHESIS. *Annual Review of Biochemistry* **2005,** *74* (1), 791-831.
27. Parrett, A.; Reed, J. M.; Gardner, S. G.; Mishra, N. N.; Bayer, A. S.; Powers, R.; Somerville, G. A., Metabolic changes associated with adaptive resistance to daptomycin in Streptococcus mitis-oralis. *BMC Microbiology* **2020,** *20* (1), 162.
28. Gaupp, R.; Lei, S.; Reed, J. M.; Peisker, H.; Boyle-Vavra, S.; Bayer, A. S.; Bischoff, M.; Herrmann, M.; Daum, R. S.; Powers, R.; Somerville, G. A., Staphylococcus aureus Metabolic Adaptations during the Transition from a Daptomycin Susceptibility Phenotype to a Daptomycin Nonsusceptibility Phenotype. *Antimicrobial Agents and Chemotherapy* **2015,** *59* (7), 4226-4238.
29. Rashid, R.; Cazenave-Gassiot, A.; Gao, I. H.; Nair, Z. J.; Kumar, J. K.; Gao, L.; Kline, K. A.; Wenk, M. R., Comprehensive analysis of phospholipids and glycolipids in the opportunistic pathogen Enterococcus faecalis. *PLoS One* **2017,** *12* (4), e0175886.
30. Saito, H. E.; Harp, J. R.; Fozo, E. M., Enterococcus faecalis Responds to Individual Exogenous Fatty Acids Independently of Their Degree of Saturation or Chain Length. *Appl Environ Microbiol* **2018,** *84* (1).
31. Harp, J. R.; Saito, H. E.; Bourdon, A. K.; Reyes, J.; Arias, C. A.; Campagna, S. R.; Fozo, E. M., Exogenous Fatty Acids Protect Enterococcus faecalis from Daptomycin-Induced Membrane Stress Independently of the Response Regulator LiaR. *Applied and Environmental Microbiology* **2016,** *82* (14), 4410-4420.
32. Zhu, L.; Zou, Q.; Cao, X.; Cronan, J. E., Enterococcus faecalis Encodes an Atypical Auxiliary Acyl Carrier Protein Required for Efficient Regulation of Fatty Acid Synthesis by Exogenous Fatty Acids. *mBio* **2019,** *10* (3), e00577-19.
33. Chilambi, G. S.; Gao, I. H.; Yoon, B. K.; Park, S.; Kawakami, L. M.; Ravikumar, V.; Chan-Park, M. B.; Cho, N.-J.; Bazan, G. C.; Kline, K. A.; Rice, S. A.; Hinks, J., Membrane adaptation limitations in Enterococcus faecalis underlie sensitivity and the inability to develop significant resistance to conjugated oligoelectrolytes. *RSC Advances* **2018,** *8* (19), 10284-10293.
34. Poger, D.; Caron, B.; Mark, A. E., Effect of Methyl-Branched Fatty Acids on the Structure of Lipid Bilayers. *The Journal of Physical Chemistry B* **2014,** *118* (48), 13838-13848.
35. Flegler, A.; Iswara, J.; Mänz, A. T.; Schocke, F. S.; Faßbender, W. A.; Hölzl, G.; Lipski, A., Exogenous fatty acids affect membrane properties and cold adaptation of Listeria monocytogenes. *Scientific Reports* **2022,** *12* (1), 1499.

APPENDIX

Lipidomics chromatography and mass spectrometry parameters

Chromatography parameters for lipidomic analysis utilized 10mM ammonium formate with 0.1% formic acid 60:40 acetonitrile: water for solvent A. Solvent B consisted of 10mM ammonium formate and 0.1% formic acid 90:10 2-propanol:acetonitrile. The gradient is as follows : 0-2 min 30% B, 3 min 40% B, 7 min 50% B, 8 min 60% B, 10 min 65% B, 12 min 68% B, 13 min 70% B, 16 min 75% B, 20 min 80% B, 23-28 min 98% B, 32 min 100% B, 34 min 90% B, 35-40 min 30% B a flow rate of 0.15 µL/min. Eluent was introduced into the mass spectrometer using a heated- electrospray ionization source with the following parameters: spray voltage (static) 3500 V for positive mode and 2500 V for negative mode, sheath gas 35 (Arb), aux gas 7 (Arb), ion transfer tube 320 °C. Ions of respective diacylglycerol (DAG) and monoglucosyl-diacylglycerol (MGDG) species were detected in positive mode as ammonium adducts while phosphatidylglycerol (PG), lysyl-phosphatidylglycerol (L-PG), cardiolipin (CL), and free fatty acids (FFA) were detected in negative mode. The mass spectrometer was operated in data dependent acquisition (DDA) mode for which the full scan spectra (100-2,000 *m/z*) were collected at 120,000 resolution and the MS^2 spectra were collected at stepped collisional energies of 25, 50, and 75 eV at a resolution of 30,000. The mass spectrometer was calibrated every 24 hours in both modes.

Metabolomics chromatography mass spectrometry parameters

Chromatography parameters for metabolomics analysis utilized 20mM ammonium acetate and 20 mM ammonium hydroxide (pH 9.4) 95:5 acetonitrile: water as solvent A while solvent B consisted of 100% acetonitrile. The gradient is as follows: 0 min, 90% B; 2 min, 90% B; 3 min, 75%; 7 min, 75% B; 8 min, 70%, 9 min, 70% B; 10 min, 50% B; 12 min, 50% B; 13 min, 25% B; 14 min, 25% B; 16 min, 0% B, 20.5 min, 0% B; 21 min, 90% B; 25 min, 90% B. Total running time is 25 min at a flow rate of 150 µl/min. Eluent was introduced into the mass spectrometer via heated electrospray ionization in positive mode under the following parameters: static spray voltage of 3500 V, sheath gas 35 (arb), aux gas 7 (arb), sweep gas 0 (arb), RF lens percentage 65, ion transfer tube temp 320 °C, vaporizer temperature 275 °C.

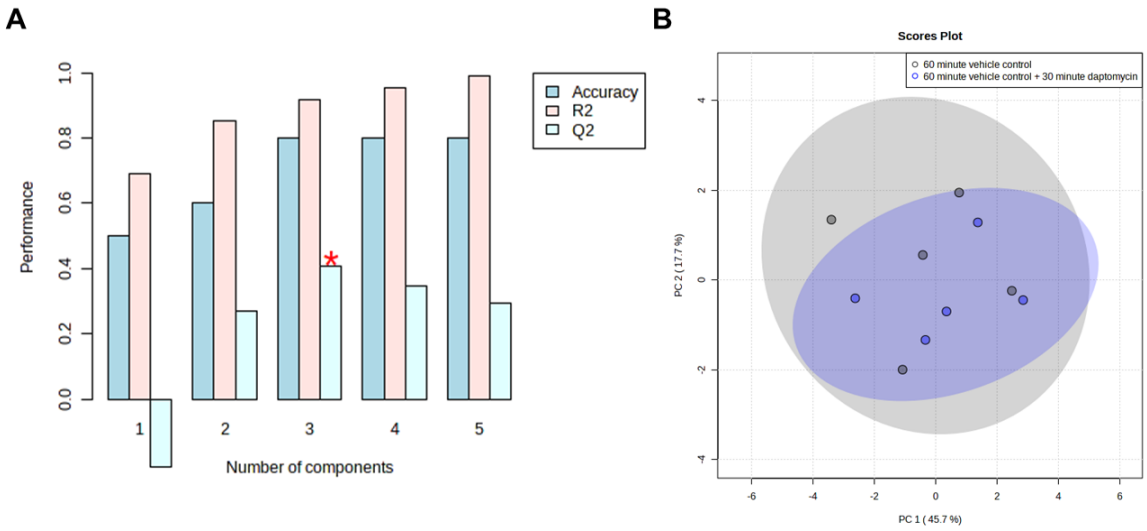

Figure S1.1 A) Cross validation scores for PLS-DA comparing metabolite features for bacterial cultures treated with daptomycin or vehicle control. B) PCA plot for metabolite features detected in bacterial cultures treated with daptomycin (blue) or vehicle control (grey). n=5 unless otherwise stated in the text.

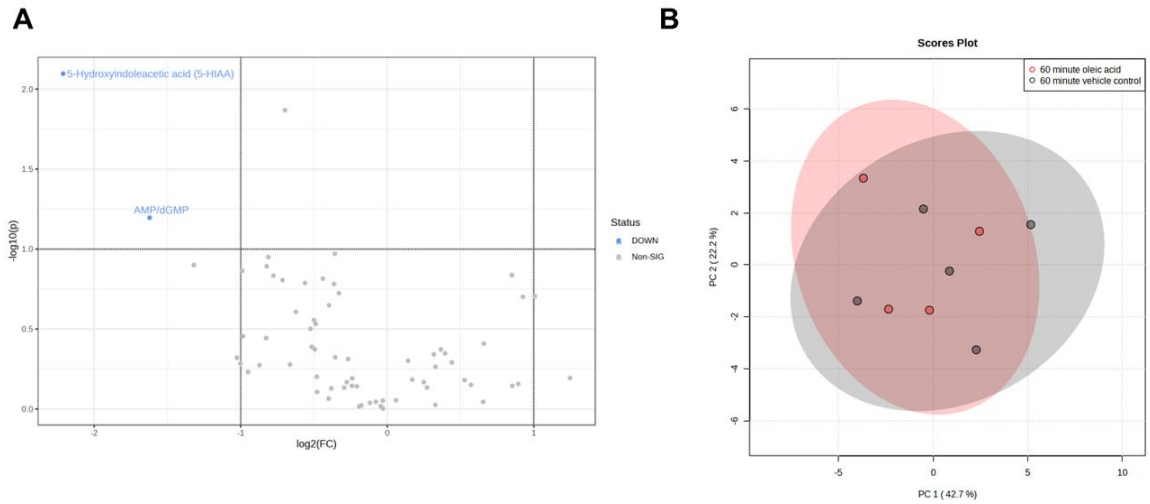

Figure S1.2 A) Volcano plot analysis for metabolite features detected in bacterial cultures supplemented with oleic acid compared to vehicle control. FC>2, P<0.05. B) PCA plot for metabolite features detected in bacterial cultures supplemented with oleic acid (red) and vehicle control (grey). n=5 unless otherwise stated in the text.

CHAPTER II
Enterococcus faecalis readily adapts membrane phospholipid composition to environmental and genetic perturbation

A version of this chapter was originally published by Woodall B. M, et al.:

Brittni M. Woodall, John R. Harp, William T. Brewer, Eric D. Tague. Shawn R. Campagna, Elizabeth M. Fozo. *Enterococcus faecalis* readily adapts membrane phospholipid composition to environmental and genetic perturbation. *Frontiers in Microbiology*. 2021 May 21; 12:616045. doi: 10.3389/fmicb.2021.616045. PMID: 34093456. PMCID: PMC8177052.

BMW performed lipid analyses and subsequent data analyses. JRH generated all strains and constructs, prepared cells for fatty acid analyses performed daptomycin sensitivity assays and growth analyses. BMW, EMF, WTB prepared cells for lipid analyses. EDT performed initial lipid analyses. WTB performed SDS sensitivity analyses and assisted with figure construction. BMW, JRF, EMF, SRC contributed to the writing of the manuscript. EMF and SRC directed the project.

2.1 Abstract

The bacterial lipid membrane, consisting both of fatty acid (acyl) tails and polar head groups, responds to changing conditions through alteration of either the acyl tails and/or head groups. This plasticity is critical for cell survival as it allows maintenance of both the protective nature of the membrane as well as functioning membrane protein complexes. Bacteria that live in fatty-acid rich environments, such as those found in the human host, can exploit host fatty acids to synthesize their own membranes, in turn, altering their physiology. *Enterococcus faecalis* is such an organism: it is a commensal of the mammalian intestine where it is exposed to fatty-acid rich bile, as well as a major cause of hospital infections during which it is exposed to fatty acid containing-serum. Within, we employed an untargeted approach to detect the most common phospholipid species of *E. faecalis* OG1RF via ultra-high performance liquid chromatography high-resolution mass spectrometry (UPLC-HRMS). We examined not only how the composition responds upon exposure to host fatty acids but also how deletion of genes predicted to synthesize major polar head groups impact lipid composition. Regardless of genetic background and differing basal lipid composition, all strains were able to alter their lipid composition upon exposure to individual host fatty acids. Specific gene deletion strains, however, had altered survival to membrane damaging agents. Combined, the enterococcal lipidome is highly resilient in response to both genetic and environmental perturbation, likely contributing to stress survival.

2.2 Introduction

The bacterial cellular envelope, consisting of the cell wall and membrane, is the first line of defense from environmental stresses.[1] In particular, the cellular membrane that is composed primarily of lipids, is critical as it blocks the

accumulation of toxins, senses changing conditions, houses protein signaling systems that are critical for stimulating gene expression changes, and provides a location for the major energetic complexes.[2] The majority of these lipids are phospholipids that consist of a polar head group and fatty acid (acyl) tails; though other lipid species, including sulfolipids and glycerophospholipids, exist and are vital for a variety of processes and functions across many species.[3, 4]
The lipid composition of any species is not static and bacteria will often alter their lipid composition in response to environmental perturbations. These alterations are needed to allow protein complexes to function properly. For example, as temperature decreases, so does molecular movement; bacteria will increase the proportion of monounsaturated fatty acids in their membranes to maintain fluidity under these conditions.[5, 6] In regards to other stressors, a variety of fatty acid tail alterations can occur that are critical for survival.[4] Additional studies have concluded that specific polar head groups are also necessary for stress survival. For example, depletion of cardiolipin in *Escherichia coli* leads to pleiotropic effects on its physiology.[7]

Enterococcus faecalis, a Gram-positive bacterial commensal and pathogenic species, has been shown to alter its membrane fatty acid content in response to laboratory growth conditions.[8-11] Under these conditions, the fatty acid profile contains primarily the saturated fatty acid palmitic acid ($C_{16:0}$) and an unsaturated fatty acid, *cis*-vaccenic acid ($C_{18:1cis11}$). Within the host, *E. faecalis* is surrounded by the fatty acid rich fluids, bile (as an intestinal commensal) and serum (when pathogenic). Previous studies demonstrated that the organism will uptake the fatty acids from these fluids, in particular oleic acid ($C_{18:1cis9}$) and linoleic acid ($C_{18:2\ cis\ 9,12}$), and utilize these species in its membrane.[8, 9] Supplementation with an individual fatty acid will lead to the provided species dominating the fatty acid composition, which can have significant impacts on cellular growth, morphology, and stress responses.[10] This supplementation also leads to a decrease in native enterococcal fatty acids found within the membrane.

The above-mentioned studies have focused primarily on the fatty acid tail alterations that can occur, and fewer studies have focused on understanding the changes in intact lipid species. In *E. faecalis*, several lipid head groups have been confirmed along with the presence of free fatty acids within the membrane: phosphatidylglycerol (PG), lysyl-phosphatidylglycerol (L-PG), cardiolipin (CL), diacylglycerol (DAG), and monoglucosyl-diacylglycerol (MGDG).[12-16] The glycolipids, DAGs, and MGDGs, are important precursors of lipoteichoic acid found in Gram positive bacteria. Of the phospholipid species, phosphatidylglycerol is dominant in the membrane and serves as a precursor for both CL and L-PG. Cardiolipin is typically derived from the addition of two phosphatidylglycerol moieties to a bridging glycerol, leading to a phospholipid that contains four fatty acid tails.[17] L-PG is also derived from PG and is formed from the addition of a lysine to the headgroup.[18] The proportion of these specific lipid classes can change during growth in liquid culture. For example, specific PG

species decreased as the culture entered stationary phase, while L-PG increased.[15] A study by Tague and coworkers also demonstrated that prolonged exposure to oleic or linoleic acid led to changes in the proportion of PG and L-PG species, as well as accumulation of either fatty acid within the membrane of *E. faecalis* OG1RF.[16] Others have shown that an enterococcal strain resistant to the antibiotic daptomycin had reduced levels of PG species compared to its sensitive derivative, suggesting that genetic perturbations will also alter lipid content.[13, 14] Given these findings, the plasticity of the phospholipid composition of *E. faecalis* was examined using untargeted lipidomics to monitor membrane changes in response to environmental and genetic perturbations. An ultra-high performance liquid chromatography high-resolution mass spectrometry (UHPLC-HRMS) approach was used to identify those tail and polar head group combinations most likely to occur within the membrane: this allowed us to detect as many as 63 species (5 free fats, 9 PG's, 4 L-PG's, 11 CL's, 12 DAGs, 16 MGDs). Specifically, the response of the organism to changing environments through short-exposures to host-derived fatty acids was examined and strains deleted for genes in phospholipid biosynthesis were used to better determine how the organism would compensate for the loss of specific lipid synthetic capabilities.

2.3 Materials and Methods

2.3.1 Bacterial growth conditions

E. faecalis strains were grown statically in brain heart infusion medium (BHI; BD Difco) at 37°C. For the determination of generation time (long-term supplementation), overnight cultures were diluted into fresh BHI medium to an optical density at 600 nm (OD_{600}) of 0.01 with either oleic acid ($C_{18:1\ cis\text{-}9}$, 20 µg ml^{-1}), linoleic acid ($C_{18:2\ cis\text{-}9,12}$, 10 g ml^{-1}) or solvent control (equal volume ethanol) and grown until stationary phase.[8] For all other fatty acid exposure experiments, referred to as short-term supplementation and used for lipid compositional analyses, overnight cultures were diluted into fresh BHI medium as described above and grown until an OD_{600} of ~0.25.[10] Fatty acid supplements (20 µg ml^{-1} oleic acid ($C_{18:1\ cis\text{-}9}$) or 10 µg ml^{-1} linoleic acid ($C_{18:2\ cis\text{-}9,\ 12}$)) or an equal volume of ethanol was added and cultures were incubated at 37°C for an additional 30 min to eliminate any possible negative effects on growth.[9] All fatty acids and chemicals were purchased from Millipore-Sigma unless noted otherwise. Counter-selection for *E. faecalis* cultures was performed on MM9YEG agar plates (final concentration: 1X M9 salts, 0.25% yeast extract, 250µg ml^{-1} 5-bromo-4-chloro-3-indolyl-β-D-galactopyranoside (X-gal), and 0.5% glucose) containing 10 mM *p*-Cl-phenylalanine (*p*-Cl-Phe) (Kristich et al., 2007). *Escherichia coli* strains were grown in LB medium at 37°C with shaking. Antibiotics were used at the following concentrations when needed: erythromycin, 10µg ml^{-1} (*E. faecalis*) or 100µg ml^{-1} (*E. coli*); spectinomycin, 1000µg ml^{-1}; fusidic acid, 25 µg ml^{-1}; rifampicin, 250 µg ml^{-1}.

2.3.2 Generation of bacterial deletion strains

The strains and plasmids used in this study and the sequence of all oligonucleotides are provided in the Appendix. Generation of deletion strains of *E. faecalis* OG1RF was through the method of Kristich *et al*.[19] To delete the *mprF2* gene and two predicted cardiolipin synthase genes, ~1000 bp flanking either OG1RF_RS03930 (*mprF2*), OG1RF_RS01975 (*cls1*) or OG1RF_RS06840 (*cls2*) were amplified from *E. faecalis* OG1RF genomic DNA. The two products for each gene region were then spliced together using external primers. Primers containing complementary overlaps with the spliced gene regions were used to amplify pCJK47.[19] The amplified inserts and vectors were assembled using NEB Gibson Assembly Master Mix. The assembled products were transformed into *E. coli* strain EC1000. Once verified, pMprF2 (to generate *ΔmprF2*), pJRH1 (to generate *Δcls1*) and pJRH2 (to generate *Δcls2*) was transformed into an *E. faecalis* conjugative donor strain (CK111/pCF10-101). After clonal selection, conjugative donors containing pMPRF2, pJRH1 or pJRH2 were mixed with an OG1RF recipient at a ratio of 1-part donor to 9 parts recipient. After conjugation, cells were placed on recipient (rifampicin, fusidic acid, erythromycin and X-gal) or donor (spectinomycin and erythromycin) selection media. Blue colonies from the recipient plates were then re-isolated on the same selective media. Isolated colonies were grown to stationary phase in BHI in the absence of selection, diluted, and then isolated on MM9YEG. White colonies were tested for erythromycin sensitivity and sequenced for verification.

2.3.3 GC FAME preparation and analysis

Cells were grown via short term supplementation as outlined in bacterial growth conditions above. 15 ml aliquots of cells were harvested via centrifugation (2739x*g* for 10 min), washed twice with 10 ml of 1X phosphate buffered saline (PBS), pelleted, and stored at -80°C prior to shipment to Microbial ID, Inc. (Newark, DE). Cells were then subjected to saponification with a sodium hydroxide-methanol mixture, a methylation step, and hexane extraction prior to GC-FAME analysis.[20]

2.3.4 Membrane challenge assays

Cells were diluted to an OD_{600} of 0.01 in BHI medium, incubated until exponential phase (OD_{600} of ~ 0.225-0.25), and then supplemented with either solvent control, 20 μg ml^{-1} oleic acid ($C_{18:1\ cis\text{-}9}$) or 10 μg ml^{-1} linoleic acid ($C_{18:2\ cis\text{-}9,\ 12}$) for 30 minutes.[10] 10 ml of cells were harvested and washed twice with 10 ml of 1X PBS and then resuspended in BHI (SDS challenge) or BHI containing 1.5mM $CaCl_2$ (daptomycin challenge) and treated with either a final concentration of 0.05% SDS or 15 μg ml^{-1} of daptomycin, given the inherent sensitivity of the *Δcls1/cls2* strain. Serial dilutions were plated onto BHI agar at the times indicated in the text. The log ratio of survivors over time was calculated for *n*=3 biological replicates and shown are the averages and standard deviations for each experiment

2.3.5 Phospholipid extraction for UHPLC-HRMS

Cells were grown as indicated above and 5 ml were harvested by centrifugation (2739x*g* for 10 min). The supernatants were removed and the remaining pellets were washed with 15 ml of PBS and stored in conical vials at -80°C prior to lipid extraction. Lipids were extracted using a method of Guan and coworkers with modifications.[21] Briefly, pellets were brought to room temperature and resuspended in 5 ml of extraction solvent (95% ethanol, water, diethyl ether, pyridine, 4.2 N ammonium hydroxide; 15:15:5:1:0.18) Glass beads were added and cells were vortexed for 30 s before being heated at 60°C for 1 h. After incubation, the organic solvent was removed via pipetting and placed in a respectively labeled glass dram vial, leaving glass beads behind. An additional 5 ml of extraction buffer was added to the vial, contents were vortexed and incubated for another hour at 60°C. At this time, the organic extracts were combined and dried under a stream N_2. The resulting solids were resuspended in 300 µL of 9:1 methanol:chloroform and stored at -20°C until UHPLC-HRMS analysis.

2.3.6 Ultra-high performance liquid chromatography high resolution mass spectrometry (UHPLC-HRMS)

Lipid profiling was performed in the manner of Bird et al. with modification.[22] Samples were stored at 4°C prior to analysis. An UltiMate 3000 ultra-high performance liquid chromatography system (UHPLC, Dionex, Sunnyvale, CA) was used to inject 10µl of sample onto a CORTECS C18 column (90 Å, 2.7µm, 2.1mm x 150mm; Waters) controlled at 40°C. Mobile phase A was 60:40 acetonitrile/water with 10 mM ammonium formate as a buffer and 0.1% formic acid while mobile phase B consisted of 90:10 2-propanol/acetonitrile with 10 mM ammonium formate as a buffer and 0.1% formic acid. The gradient used follows: *t*=0 min: 32% solvent B flow rate of 0.30 ml/min, t=1.5 min: 32% solvent B flow rate 0.4 ml/min, t=2.5 min: 45% solvent B flow rate 0.4 ml/min, t=5 min: 52% solvent B flow rate 0.3 ml/min, t=8.0 min 58% solvent B flow rate 0.3 ml/min, t=11.0 min 68% solvent B flow rate 0.4 ml/min, t=14.0 min 75% mobile phase B flow rate of 0.4 ml/min, t=18.0 min 80% solvent B flow rate of 0.4 mL/min, t=21 98% solvent B flow rate 0.45 ml/min, t=25.0 min 32% solvent B flow rate 0.3 ml/min until equilibration at 30 mins. Eluent was introduced to the mass spectrometer via an electrospray ionization (ESI) source, with the following parameters: sheath gas 30 (arbitrary units), aux gas 8 (arbitrary units), sweep gas 3 (arbitrary units), spray voltage 3 kV, capillary temperature 300°C. Mass analysis was performed using an Exactive Plus (Thermo Scientific, Waltham, MA) mass spectrometer operated in dual polarity mode. Ions of respective DAG and MGDG species were detected in positive mode while free fat, PG, L-PG, and CL were detected in negative mode. Masses were detected in full scan mode within a scan range of 100-1500 *m/z*, operated at a resolution of 140,000, with an automatic gain control target of (AGC) of $3x10^6$ ions, and a maximum IT time of 100 ms. Full scan data was complemented with all ion fragmentation data at a

resolution of 35,000 utilizing 35 eV collisional energy. The mass spectrometer was calibrated every 24 hours.

2.3.7 Data processing and statistical analysis

A list of potential lipids was created using GC FAME data to determine which fatty acids were expected within the biological samples (Appendix).[8, 10, 12] This list of chemical formulas (Appendix) allowed detection of 6 lipids classes based on calculated mass. External standards were analyzed to verify retention time and charge state. External standards included MGDG (34:1), DAG (36:2), DAG (36:4), PG (36:0), L-PG (36:2), and CL (72:4). All lipid standards were purchased from Avanti Polar Lipids Inc. (Alabaster, AL). Raw data acquired from Xcalibur were converted to mzML format utilizing MS convert from ProteoWizard. El MAVEN was utilized to integrate exact masses of predicted lipid species with an error of less than 5ppm. The integrated intensities were normalized to the optical density (OD_{600} nm) of the culture at the time of extraction. A Grubbs' test was utilized to exclude any outliers within the biological replicates in the data set. An alpha value of 1.67 was chosen for the Grubbs test to represent a confidence interval of 95 percent. After Grubbs analysis, outliers residing outside the 95 percent confidence interval were removed; the average peak area, standard deviation, and coefficient of variation were then calculated. Any remaining data points with a representative coefficient variation greater than 30 percent were removed to aid in confirmation of presented data. Heatmaps were constructed by determining the ratio of normalized, log transformed intensities of experimental values over control values. A paired student's *t*-test was utilized to determine significance. Three dots denote $P < 0.01$; two dots indicate *P* value between 0.01-0.05; one dot, *P* value between 0.05-0.1. Percentage of total graphs were constructed by summing ion totals of all detected lipids into specific lipid categories and presenting respective lipid classes as a percentage of total ions detected.

2.4 Results

2.4.1 Supplementation with host fatty acids increases specific lipid species according to tail group

Previous research utilizing fatty acid methyl ester (FAME) analysis has shown that *E. faecalis* OG1RF can incorporate exogenous fatty acids including oleic acid and linoleic acid from host fluids, altering its membrane fatty acid content and sensitivity to membrane damaging agents.[8-11] However, alterations to intact lipid species consisting of head group and fatty acid tails were not examined. To address this question, we examined lipid species of OG1RF using UHPLC-HRMS (Material and Methods) and GC-FAME analysis (Appendix). Cells were subject to brief exposure to one of three conditions: solvent control (ethanol), oleic acid, or linoleic acid, as these host-derived fatty acids are readily utilized by the organism and trigger stress protection.[10, 11] Short-exposures were

also used as the addition of these fatty acids, particularly to some gene deletion strains, impacted generation time if they were given at the time of dilution (see below). The lipid species detected in this analysis are listed with their chemical formulas and can be found in Appendix. While LC-MS can detect thousands of unique masses, we focused specifically on these species (Appendix) as they represent the most commonly detected tail species and headgroups.[8, 10, 12, 14-16]

Under our control conditions, OG1RF had a lipid profile dominated by PGs (54% of total species), although DAGs (22% of total), MGDAGs (19% of total), free fat (3% of total), L-PGs (1% of total), and CLs (1% of total) were also detected (Figure 2.1A). When examining which individual species were most prevalent, we noted PG 32:0, PG 34:1, PG 34:2 and PG 36:2 were detected at high levels (>10^7): these species corresponded well with the GC-FAME analyses of fatty acid tail profiles with $C_{16:0}$ and $C_{18:1cis11}$ being the dominant tails (Appendix). Similarly, CL 66:1, DAG 34:1, DAG 36:2, MGDG 34:1 were all highly expressed as well.

While PG species are responsible for nearly 54% of the lipids detected in this method for our growth conditions, upon short term supplementation with oleic ($C_{18:1cis9}$) or linoleic ($C_{18:2cis9,12}$) acids, found in host fluids bile and serum, there were major alterations in the contribution of the individual lipid classes compared to the control (Figure 2.1A). Cells pulsed with oleic acid were increased in free fatty acids, CL, and MGDG, with a resulting decrease in PG and DAG species. There was a large increase in the amount of free $C_{18:1}$ detected in the membrane, which correlates with the GC-FAME data where the combined $C_{18:1}$ species (consisting of both native *cis*-vaccenic acid, $C_{18:1cis11}$ and oleic acid, $C_{18:1cis9}$) in oleic acid comprised over 65% of total fatty acids detected after oleic acid supplementation, while they were only 40% in the control cultures (Appendix). Lipid species correlating to one or more $C_{18:1}$ tails were also increased including, PG 36:2, L-PG 36:2, CL 70:4, CL 70:3, and MGDG 36:2. Other species that likely did not possess oleic acid tails, were significantly increased including CL 68:1, CL 68:0, CL 72:6, MGDG 35:1, MGDG 34:2, MGDG 32:1, and MGDG 26:4.

Short term exposure to linoleic acid also resulted in large alterations of the lipid profile from control. This included large increases in the proportion of detected free fatty acids and cardiolipin species; like supplementation with oleic acid, there was an overall decrease in PG species compared to control (Figure 2.1A). The amount of free $C_{18:2}$ within the membrane was a major driver for the detected free fatty acids within the membrane (Figure 2.1B; >10^8), again corresponding to the GC-FAME analysis (Appendix; 24% of total fatty acids detected via this method). While there was an increase in specific cardiolipin species upon linoleic acid supplementation, these species (CL 64:0, CL 64:1, CL 66:0, CL 66:1, CL 68:0, CL 68:1) would not possess a linoleic acid tail; however many were also conserved upon oleic acid supplementation.

Given the increase in cardiolipin species upon supplementation with either oleic or linoleic acid, we hypothesized these changes may be critical for maintaining proper membrane function in these growth environments. [13, 23-26]

Figure 2.5 *Enterococcus faecalis* OG1RF lipid composition is altered upon exposure to host fatty acids. (A) Percent totals of lipid species in solvent control: free fatty acids (2.7%), PG (53.7%), L-PG (1.1%), CL (1.1%), DAG (22.4%), and MGDG (19.0%), oleic acid: free fatty acids (16.8%), PG (46.7%), L-PG (1.5%), CL 3.3%), DAG (6.1%), and MGDG (25.6%), linoleic acid: free fatty acids (39.5%), PG (36.6%), L-PG (2.6%), CL (3.4%), DAG (1.4%), and MGDG (16.6%). Species were normalized to $OD_{600\ nm}$. (B) Heat-map of fold changes upon fatty acid supplementation vs. solvent control; OA, oleic acid supplementation; LA, linoleic acid supplementation. Shown are the average fold changes of those detected lipid species above limit of detection for *n* = 5 samples. **P* = 0.1–0.05; ***P* = 0.05–0.01; ****P* < 0.01

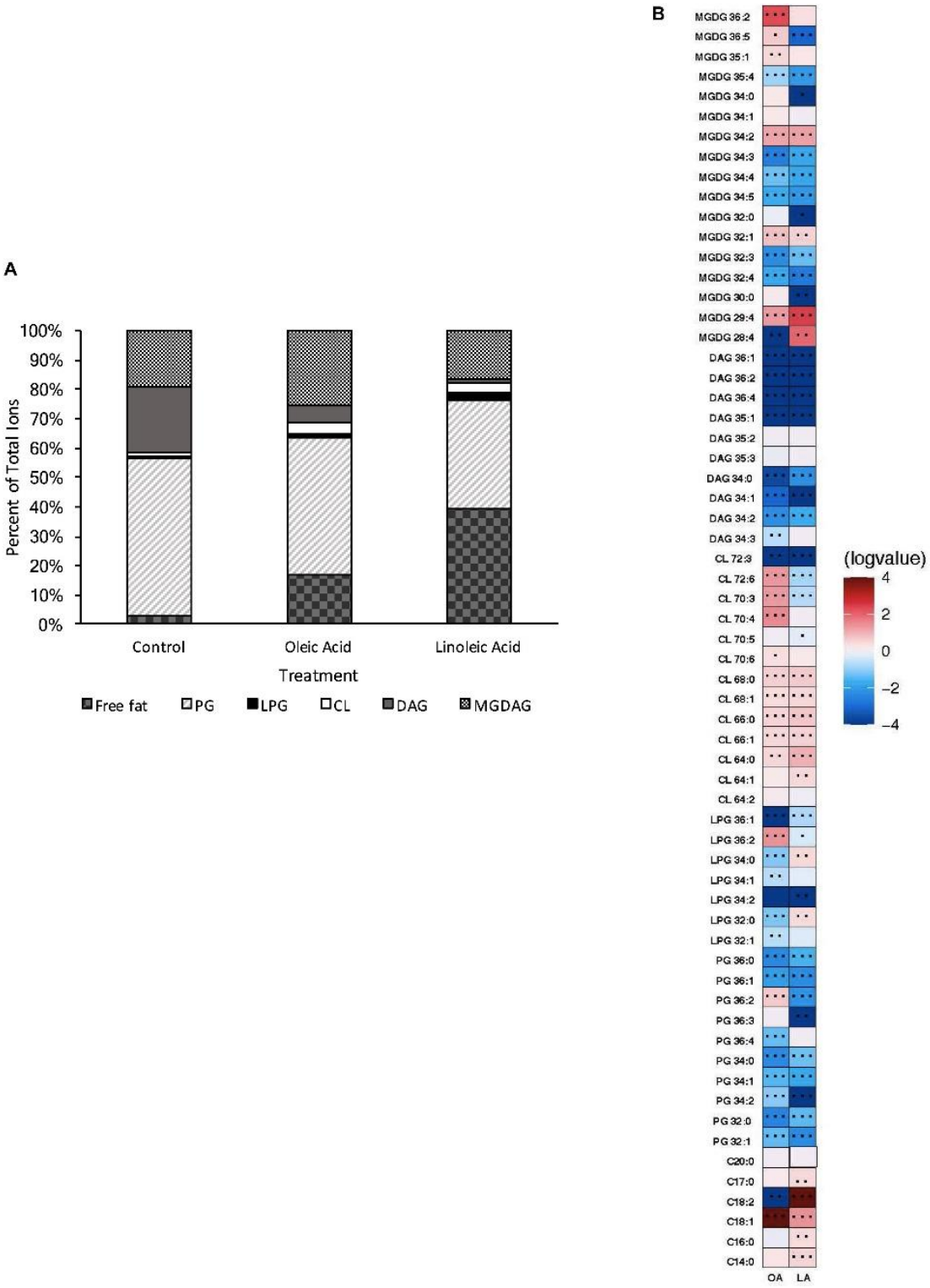
A
100%
90%
80%
70%
60%
50%
40%
30%
20%
10%
0%
Percent of Total Ions
Control
Oleic Acid
Linoleic Acid
Treatment
Free fat
PG
LPG
CL
DAG
MGDAG
B
MGDG 36:2
MGDG 36:5
MGDG 35:1
MGDG 35:4
MGDG 34:0
MGDG 34:1
MGDG 34:2
MGDG 34:3
MGDG 34:4
MGDG 34:5
MGDG 32:0
MGDG 32:1
MGDG 32:3
MGDG 32:4
MGDG 30:0
MGDG 29:4
MGDG 28:4
DAG 36:1
DAG 36:2
DAG 36:4
DAG 35:1
DAG 35:2
DAG 35:3
DAG 34:0
DAG 34:1
DAG 34:2
DAG 34:3
CL 72:3
CL 72:6
CL 70:3
CL 70:4
CL 70:5
CL 70:6
CL 68:0
CL 68:1
CL 66:0
CL 66:1
CL 64:0
CL 64:1
CL 64:2
LPG 36:1
LPG 36:2
LPG 34:0
LPG 34:1
LPG 34:2
LPG 32:0
LPG 32:1
PG 36:0
PG 36:1
PG 36:2
PG 36:3
PG 36:4
PG 34:0
PG 34:1
PG 34:2
PG 32:0
PG 32:1
C20:0
C17:0
C18:2
C18:1
C16:0
C14:0
OA
LA
(logvalue)
4
2
0
−2
−4

Therefore, we generated a strain deleted for the two genes predicted to be responsible for cardiolipin synthesis: cardiolipin synthase 1 (ΔOG1RF_RS01975- *Δcls1*) and cardiolipin synthase 2 (ΔOG1RF_RS06840- *Δcls2*)

2.4.2 Deletion of both cardiolipin synthase genes is required for full depletion of cardiolipin synthase

Both single gene deletion strains, *Δcls1* (cardiolipin synthase 1; OG1RF_RS01975) and *Δcls2* (ΔOG1RF_RS06840- *Δcls2*) were analyzed via UHPLC-HRMS. Each strain was able to produce detectable levels of cardiolipin (Appendix). However, the deletion strains did not necessarily have other changes in common (Figures 2.2A, 2.3A). For *Δcls1* we noted significantly higher levels of $C_{18:1}$ while *Δcls2* had increased PG 32:0, PG 36:3, and several MGDG species (Figure 2.2B, 2.3B).

Supplementation with either oleic or linoleic acid led to an accumulation of many CL species in both single gene deletion strains. Similarly, the deletion strains, like the parental strain, had elevated levels of PG 36:2 and L-PG 36:2, as well as free $C_{18:1}$ within their membranes when provided oleic acid (Figure 1.1B, 2.2B, 2.3B), which corresponded with the increase in total $C_{18:1}$ measured via GC-FAME (Appendix). Linoleic acid, however, resulted in the accumulation of specific species, dependent upon the genetic background of the strain. While both *Δcls1* and *Δcls2* accumulated PG 36:3 and PG 36:4, *Δcls2* also accumulated L-PG 36:3 and L-PG 36:4: note that none of these four species were increased in the parental OG1RF strain when given linoleic acid (Figure 2.1B, 2.2, 2.3B). Likely these species contained $C_{18:2}$ tails and both strains accumulated $C_{18:2}$ as determined via GC-FAME analysis (Appendix) and our UPLC-HRMS method. While there were some unique alterations in the lipid content upon deletion of *Δcls1* versus *Δcls2,* both strains could clearly produce cardiolipin. Therefore, we generated the double deletion strain, *Δcls1/ Δcls2* to better examine the effects of cardiolipin loss on the lipidome as well as enterococcal physiology.

The resultant strain was unable to produce cardiolipin, as confirmed via UPLC-HRMS (Appendix); thus both genes are bona fide *cl* synthases and contribute to its production. In examining the basal membrane profile, we saw enrichment of most targeted PG and DAG species when compared to the parental strain, and several MGDG species (Supplemental Figure S3). Surprisingly, not only was the strain lacking cardiolipin, we noted significant reduction in most L-PG species as well, suggesting that some of the PG accumulation was in part due to a lack of L-PG synthase activity (Appendix). We note that there were major shifts in the membrane composition of *Δcls1/ Δcls2* compared to the parental wildtype strain, yet CL comprised only a minor portion of the species detected under basal conditions (Fig. 1a).

Supplementation of *Δcls1/ Δcls2* with oleic acid resulted in increased amounts of free fat ($C_{14:0}$, $C_{16:0}$, $C_{18:1}$, $C1_{8:2}$, and $C_{17:0}$), PG species (in particular PG 36:3, PG 36:4), with the higher amounts of $C_{18:1}$ tails corresponding to the

Figure 2.6 OG1RF lacking Δ*cls1* can still produce cardiolipin and alter its lipid composition upon exposure to host fatty acids. (A) Percent totals of lipid species for Δ*cls1* in solvent control: free fatty acids (2.0%), PG (53.5%), L-PG (0.7%), CL (0.7%), DAG (23.8%), and MGDG (19.4%), oleic acid: free fatty acids (9.8%), PG (48.3%), L-PG (0.7%), CL 2.0%), DAG (17.9%), and MGDG (21.3%), linoleic acid: free fatty acids (22.1%), PG (38.9%), L-PG (1.2%), CL (1.8%), DAG (14.7%), and MGDG (21.4%). Species were normalized to $OD_{600\ nm}$. (B) Heat-map of fold changes upon fatty acid supplementation vs. solvent control for Δ*cls1*; OA, oleic acid supplementation; LA, linoleic acid supplementation. Shown are the average fold changes of those detected lipid species above limit of detection for *n* = 5 samples. **P* = 0.1–0.05; ***P* = 0.05–0.01; ****P* < 0.01.

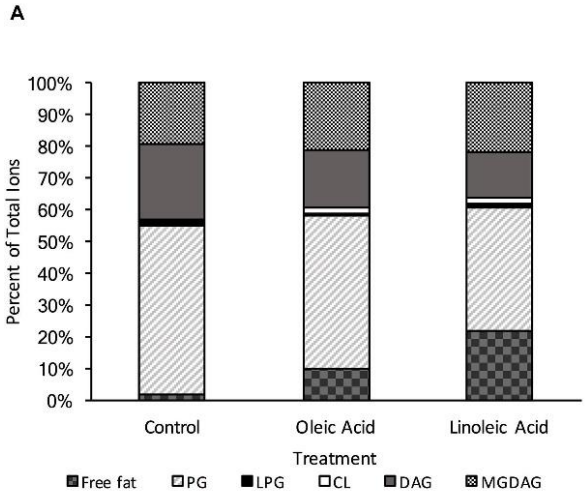
A
100%
90%
80%
70%
60%
50%
40%
30%
20%
10%
0%
Percent of Total Ions
Control
Oleic Acid
Linoleic Acid
Treatment
Free fat
PG
LPG
CL
DAG
MGDAG

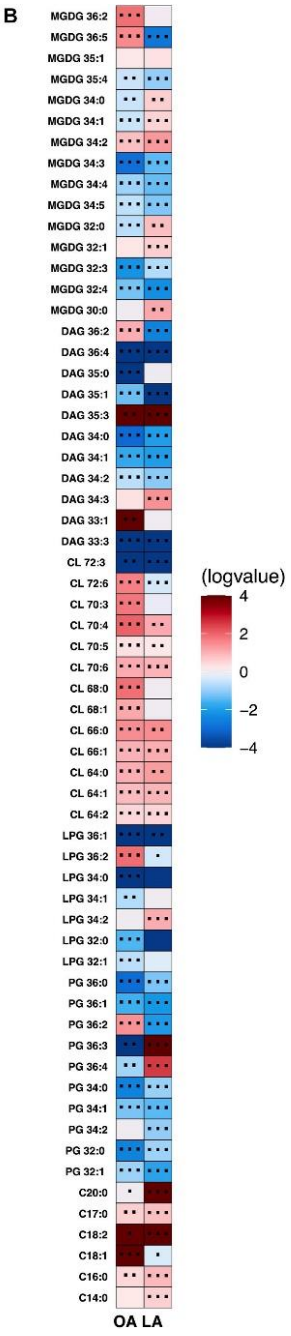
B
MGDG 36:2
MGDG 36:5
MGDG 35:1
MGDG 35:4
MGDG 34:0
MGDG 34:1
MGDG 34:2
MGDG 34:3
MGDG 34:4
MGDG 34:5
MGDG 32:0
MGDG 32:1
MGDG 32:3
MGDG 32:4
MGDG 30:0
DAG 36:2
DAG 36:4
DAG 35:0
DAG 35:1
DAG 35:3
DAG 34:0
DAG 34:1
DAG 34:2
DAG 34:3
DAG 33:1
DAG 33:3
CL 72:3
CL 72:6
CL 70:3
CL 70:4
CL 70:5
CL 70:6
CL 68:0
CL 68:1
CL 66:0
CL 66:1
CL 64:0
CL 64:1
CL 64:2
LPG 36:1
LPG 36:2
LPG 34:0
LPG 34:1
LPG 34:2
LPG 32:0
LPG 32:1
PG 36:0
PG 36:1
PG 36:2
PG 36:3
PG 36:4
PG 34:0
PG 34:1
PG 34:2
PG 32:0
PG 32:1
C20:0
C17:0
C18:2
C18:1
C16:0
C14:0
OA LA
(logvalue)
4
2
0
−2
−4

Figure 2.7 OG1RF lacking Δ*cls2* can still produce cardiolipin and alter its lipid composition upon exposure to host fatty acids. (A) Percent totals of lipid species for Δ*cls2* in solvent control: free fatty acids (1.9%), PG (55.1%), L-PG (1.0%), CL (0.7%), DAG (21.2%), and MGDG (20.1%), oleic acid: free fatty acids (11.1%), PG (51.6%), L-PG (1.2%), CL 2.1%), DAG (9.4%), and MGDG (24.6%), linoleic acid: free fatty acids (35.5%), PG (35.5%), L-PG (1.9%), CL (2.6%), DAG (4.1%), and MGDG (20.4%). Species were normalized to $OD_{600\ nm}$. (B) Heat-map of fold changes Δ*cls2* upon fatty acid supplementation vs. solvent control; OA, oleic acid supplementation; LA, linoleic acid supplementation. Shown are the average fold changes of those detected lipid species above limit of detection for *n* = 5 samples. **P* = 0.1–0.05; ***P* = 0.05–0.01; ****P* < 0.01.

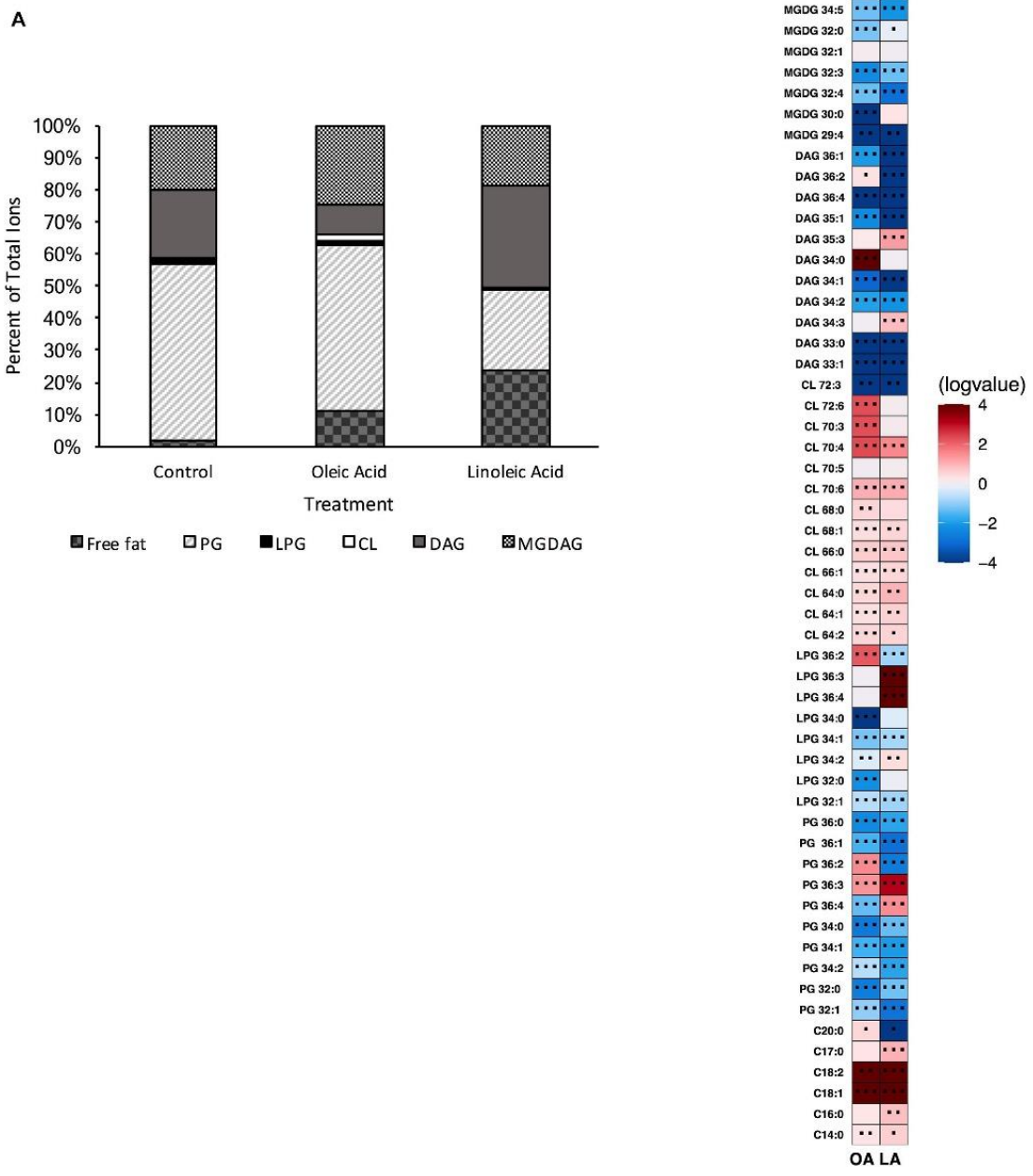
A
100%
90%
80%
70%
60%
50%
40%
30%
20%
10%
0%
Percent of Total Ions
Control
Oleic Acid
Linoleic Acid
Treatment
Free fat
PG
LPG
CL
DAG
MGDAG
B
MGDG 36:2
MGDG 36:5
MGDG 35:1
MGDG 35:4
MGDG 35:6
MGDG 34:0
MGDG 34:1
MGDG 34:2
MGDG 34:3
MGDG 34:4
MGDG 34:5
MGDG 32:0
MGDG 32:1
MGDG 32:3
MGDG 32:4
MGDG 30:0
MGDG 29:4
DAG 36:1
DAG 36:2
DAG 36:4
DAG 35:1
DAG 35:3
DAG 34:0
DAG 34:1
DAG 34:2
DAG 34:3
DAG 33:0
DAG 33:1
CL 72:3
CL 72:6
CL 70:3
CL 70:4
CL 70:5
CL 70:6
CL 68:0
CL 68:1
CL 66:0
CL 66:1
CL 64:0
CL 64:1
CL 64:2
LPG 36:2
LPG 36:3
LPG 36:4
LPG 34:0
LPG 34:1
LPG 34:2
LPG 32:0
LPG 32:1
PG 36:0
PG 36:1
PG 36:2
PG 36:3
PG 36:4
PG 34:0
PG 34:1
PG 34:2
PG 32:0
PG 32:1
C20:0
C17:0
C18:2
C18:1
C16:0
C14:0
OA LA
(logvalue)
4
2
0
−2
−4

abundance of oleic acid and *cis*-vaccenic acid detected via GC-FAME (Appendix). Several MGDG species (MGDG 29:4, MGDG 30:0, MGDG 32:0, MGDG 35:4, MGDG 35:1, and MGDG 36:5) were also elevated when compared to solvent control. For these lipid species, only PG 36:2, MGDG 29:4, MGDG 35:1 and MGDG 36:5 were also induced in a wild type background. A few minor increases in specific DAGs were also increased (Figure 2.4B) with oleic acid supplementation, however the overall percent of DAG in the membrane decreased from 61% to 42% (Figure 2.4A).

The membrane profile of *Δcls1/ Δcls2* when provided linoleic acid was shifted from solvent control: linoleic acid exposed cells had far more free fatty acids and MGDAGs comprising the membrane with a large reduction in DAG species (Figure 2.4A). Linoleic acid supplementation decreased total PG species compared to ethanol, but showed much higher increases in free fat, MGDG, and DAG species compared to both ethanol and oleic acid. When examining individual species, there was a large increase in $C_{18:2}$ within the membrane, in agreement with the GC-FAME analysis (Figure 2.4B, Appendix). Several MGDG species were increased with linoleic acid, as was seen with oleic acid, though not necessarily the same lipids, including, MGDG 30:0, MGDG 32:0, MGDG 32:1, MGDG 35:4 and MGDG 35:1, (Figure 2.4B). While the proportion of the membrane composed of PG species remained relatively constant, there was significant accumulation of both PG 36:3 and PG 36:4 which could include linoleic acid tails.

Given that we were able to alter the membrane composition of *E. faecalis* with both genetic and environmental perturbations, we were interested probing the sensitivity of this altered membrane in response to membrane disrupting agents.

2.4.3 The loss of both cardiolipin synthase 1 and 2 impacts sensitivity to membrane damaging agents

Alterations in cardiolipin synthase activity or in the levels of cardiolipin have been implicated in sensitivity to the antibiotic daptomycin: specifically, increased CL levels potentially reduces the effectiveness of the drug as it does not allow for proper drug interaction with the membrane.[13, 23, 25-27] Given our *Δcls1*/*cls2* strain lacked cardiolipin, we first examined its sensitivity to daptomycin. The *Δcls1/cls2* strain had increased basal sensitivity to daptomycin (P = 0.002) compared to parental OG1RF (Figure 2.5A, 2.5B). This sensitivity was dependent upon deletion of both genes, as single gene deletion strains did not impair survival (Appendix).

We previously demonstrated that the addition of either oleic or linoleic acid could induce a physiological tolerance to daptomycin in OG1RF: cells exposed to either fatty acid survived high concentrations of the drug far better than those without.[10, 11] Given that oleic or linoleic acid also result in increases in cardiolipin in the parental strain, and *Δcls1/ Δcls2* lacks cardiolipin, we hypothesized that oleic or linoleic acid addition would not protect our cardiolipin null strain from the

Figure 2.4 A strain deleted for Δ*cls1/cls2* can alter its lipid composition upon exposure to host fatty acids. (A) Percent totals of lipid species in solvent control: free fatty acids (3.8%), PG (26.3%), L-PG (0.1%), CL (0.0%), DAG (61.3%), and MGDG (8.5%), oleic acid: free fatty acids (11.7%), PG (34.3%), L-PG (0.0%), CL 0.0%), DAG (41.5%), and MGDG (12.5%), linoleic acid: free fatty acids (23.4%), PG (25.7%), L-PG (0.2%), CL (0.0%), DAG (31.9%), and MGDG (19.0%). Species were normalized to $OD_{600\ nm}$. (B) Heat-map of fold changes upon fatty acid supplementation vs. solvent control; OA, oleic acid supplementation; LA, linoleic acid supplementation. Shown are the average fold changes of those detected lipid species above limit of detection for *n* = 5 samples. **P* = 0.1–0.05; ***P* = 0.05–0.01; ****P* < 0.01.

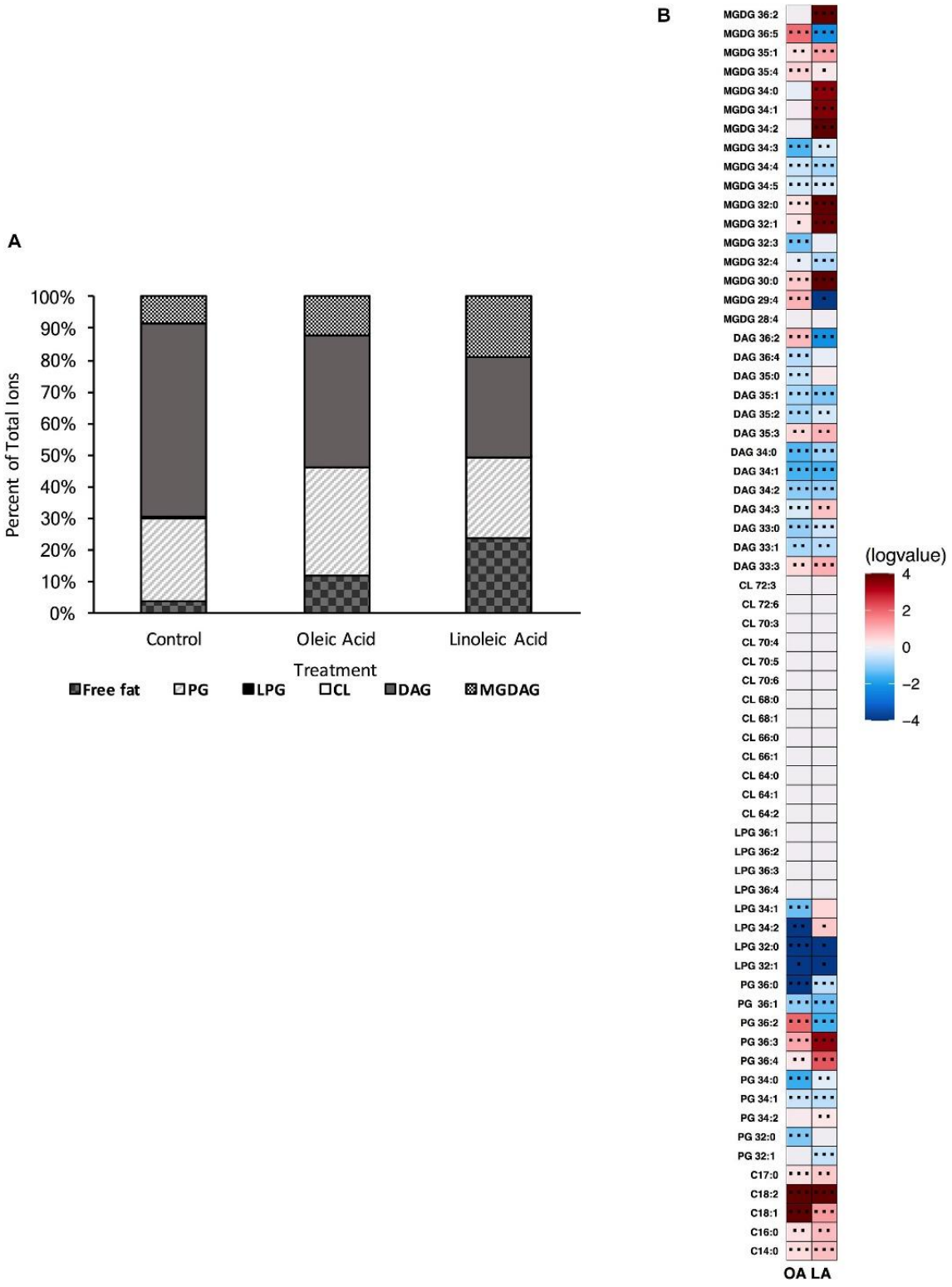
A
100%
90%
80%
70%
60%
50%
40%
30%
20%
10%
0%
Percent of Total Ions
Control
Oleic Acid
Linoleic Acid
Treatment
Free fat
PG
LPG
CL
DAG
MGDAG
B
MGDG 36:2
MGDG 36:5
MGDG 35:1
MGDG 35:4
MGDG 34:0
MGDG 34:1
MGDG 34:2
MGDG 34:3
MGDG 34:4
MGDG 34:5
MGDG 32:0
MGDG 32:1
MGDG 32:3
MGDG 32:4
MGDG 30:0
MGDG 29:4
MGDG 28:4
DAG 36:2
DAG 36:4
DAG 35:0
DAG 35:1
DAG 35:2
DAG 35:3
DAG 34:0
DAG 34:1
DAG 34:2
DAG 34:3
DAG 33:0
DAG 33:1
DAG 33:3
CL 72:3
CL 72:6
CL 70:3
CL 70:4
CL 70:5
CL 70:6
CL 68:0
CL 68:1
CL 66:0
CL 66:1
CL 64:0
CL 64:1
CL 64:2
LPG 36:1
LPG 36:2
LPG 36:3
LPG 36:4
LPG 34:1
LPG 34:2
LPG 32:0
LPG 32:1
PG 36:0
PG 36:1
PG 36:2
PG 36:3
PG 36:4
PG 34:0
PG 34:1
PG 34:2
PG 32:0
PG 32:1
C17:0
C18:2
C18:1
C16:0
C14:0
OA LA
(logvalue)
4
2
0
−2
−4

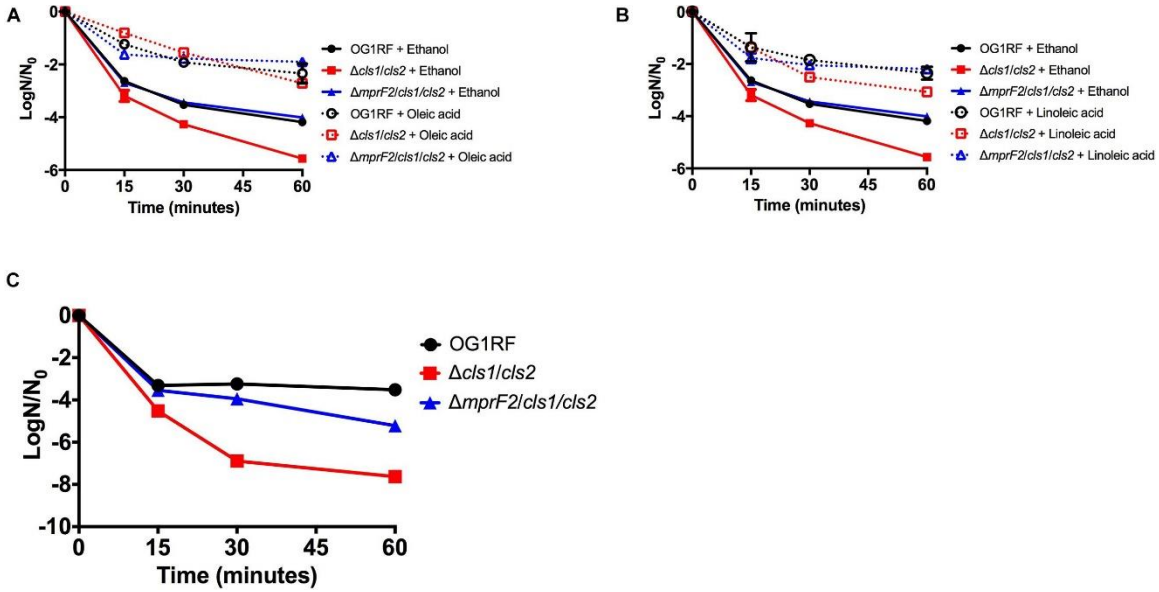

Figure 2.5 Stress sensitivity upon loss of phospholipid synthetic pathways is dependent upon genetic background. (A) Oleic acid supplementation of Δ*cls1/cls2* and Δ*mprF2/cls1/cls2* had statistically increased numbers of survivors vs. the solvent control when treated with daptomycin at all-time points (*P* < 0.0001). (B) Linoleic acid supplementation of Δ*cls1/cls2* and Δ*mprF2/cls1/cls2* had statistically increased numbers of survivors vs. the solvent control when treated with daptomycin at all-time points (*P* = 0.0001). Shown are the averages ± standard deviation for *n* = 3. (C) SDS sensitivity of indicated strains grown in exponential phase. Shown are the averages ± standard deviation for *n* = 3.

daptomycin. However, addition of either oleic or linoleic acid did induce tolerance in *Δcls1/ Δcls2,* yet the protection was not as long lasting as in the parental OG1RF strain (Figure 2.5A, 2.5B, Appendix). To conclude whether *Δcls1*/*cls2* was simply more inherently sensitive to membrane damage, we examined its tolerance to the detergent SDS. The double deletion strain was far more sensitive to SDS than the parental strain (Figure 2.5C). We also noted increased generation time of *Δcls1/ Δcls2* during long-term growth in linoleic acid (see Materials and Methods, Appendix) suggesting additional physiological consequences upon loss of this synthetic pathway.

Upon deletion of a lipid synthetic pathway, cardiolipin, *E. faecalis* was able to adjust its lipid profile and respond to environmental perturbation. To delve further into the plasticity of the lipidome, we deleted the ability OG1RF to produce L-PG as well as L-PG and CL simultaneously.

2.4.4 A strain deleted for mprF2 maintains the ability to alter its lipid composition when supplemented with exogenous fatty acids

To examine how *E. faecalis* would respond to loss of L-PG, we deleted *mprF2* (OG1RF_RS03930), which encodes the enzyme responsible for L-PG synthesis. Although *E. faecalis* contains two separate *mprF* genes, a previous study indicated that *mprF2* encoded the major L-PG synthase.[28] The UHPLC-HRMS analysis confirmed that the *ΔmprF2* strain was unable to produce L-PG, as lipids in this class were below the detection limits under the growth conditions in this study (Supplemental Figure S6, Figure 2.6A, 2.6B; data not shown). With this loss of L-PG, there was a concomitant significant increase in DAG lipid species and a large decrease in total PG species compared to the parental strain (Supplemental Figure S6, Figure 2.6A). There was also a decrease in CL species, similar to how loss of CL resulted in a decrease in L-PG species in *Δcls1/cls2* (compare Supp 3/6). Importantly, there was no impact on generation time when compared to the parental strain (Supplementary Table 5) despite the inability to produce L-PG.

When provided oleic acid, the *ΔmprF2*strain did not accumulate oleic acid to the same extent as other strains examined in this study (Supplemental Table S4). Levels of the native *cis*-vaccenic acid, $C_{18:1}$*cis*$_{11}$, remained far more elevated in this strain compared to the others examined (see Discussion). While *ΔmprF2* had increased levels of free $C_{18:1}$ in the membrane when given oleic acid, we cannot be certain whether this represents an accumulation of native *cis*-vaccenic or oleic acid. Along with these observations, we observed significant increases in PG species (PG 36:4, PG 36:3, and PG 36:2) and MGDG species (MGDG 32:3 and MGDG 36:5). We note that increases in PG 36:2 and PG 36:3 were also induced in *Δcls1/cls2 w*hen provided this fatty acid (Figure 2.4B). Other changes observed in *ΔmprF2* included a decrease of CL and DAG species (Figure 2.6A,B).

Linoleic acid induced some similar membrane changes, including increases in $C_{18:1}$ and $C_{18:2}$, PG 36:4, PG 36:3 (Figure 2.6B). However, the total PG

Figure 2.6 A strain deleted for Δ*mprF2* can alter its lipid composition upon exposure to host fatty acids. (A) Percent totals of lipid species in solvent control: free fatty acids (2.1%), PG (20.9%), L-PG (0.0%), CL (0.5%), DAG (69.8%), and MGDG (6.7%), oleic acid: free fatty acids (19.9%), PG (52.5%), L-PG (0.0%), CL 1.0%), DAG (6.9%), and MGDG (19.7%), linoleic acid: free fatty acids (42.2%), PG (8.6%), L-PG (0.0%), CL (2.1%), DAG (17.6%), and MGDG (29.4%). Species were normalized to $OD_{600\ nm}$. (B) Heat-map of fold changes upon fatty acid supplementation vs. solvent control; OA, oleic acid supplementation; LA, linoleic acid supplementation. Shown are the average fold changes of those detected lipid species above limit of detection for *n* = 5 samples. **P* = 0.1–0.05; ***P* = 0.05–0.01; ****P* < 0.01.

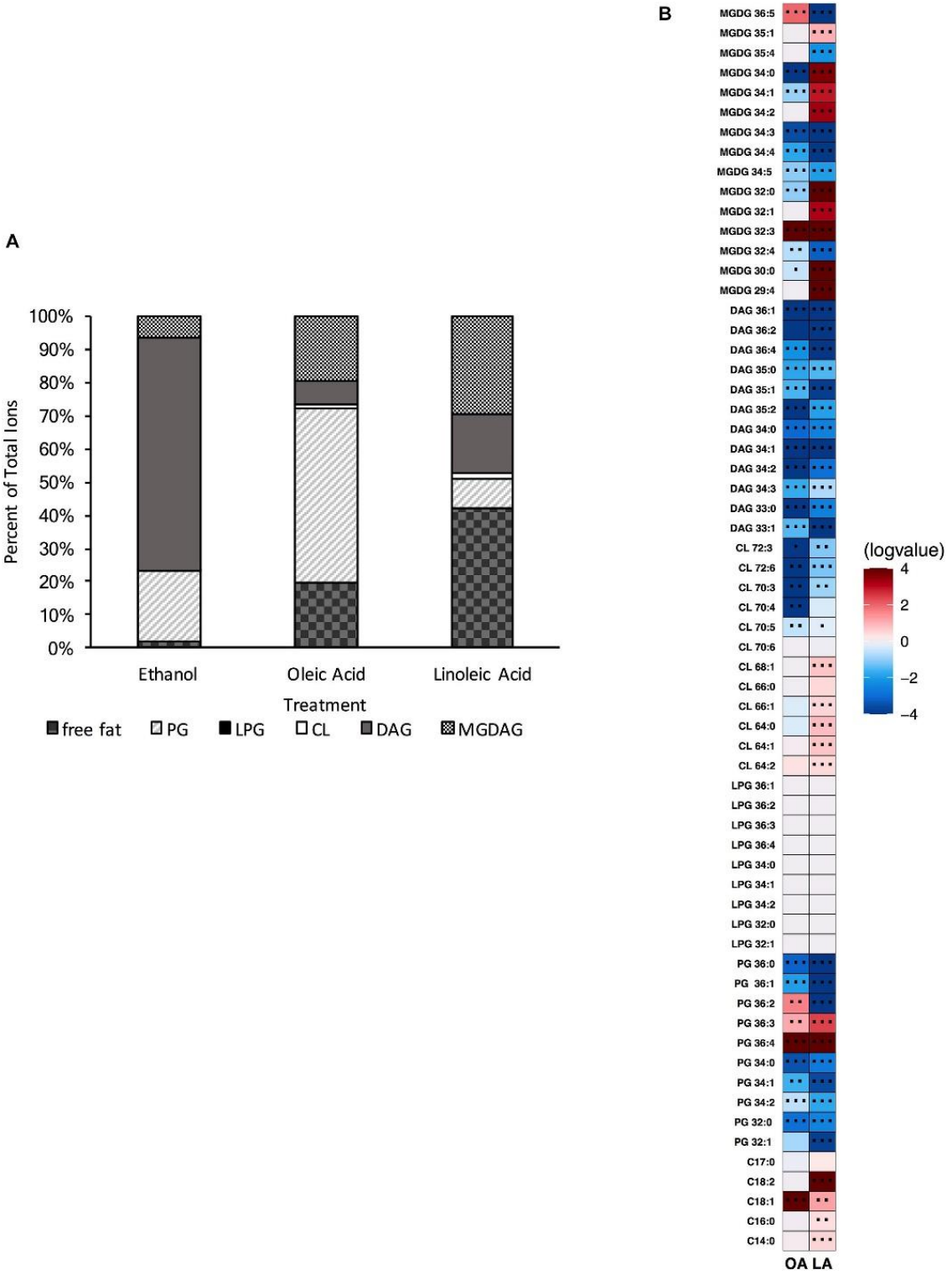
A
100%
90%
80%
70%
60%
50%
40%
30%
20%
10%
0%
Percent of Total Ions
Ethanol
Oleic Acid
Linoleic Acid
Treatment
free fat
PG
LPG
CL
DAG
MGDAG
B
MGDG 36:5
MGDG 35:1
MGDG 35:4
MGDG 34:0
MGDG 34:1
MGDG 34:2
MGDG 34:3
MGDG 34:4
MGDG 34:5
MGDG 32:0
MGDG 32:1
MGDG 32:3
MGDG 32:4
MGDG 30:0
MGDG 29:4
DAG 36:1
DAG 36:2
DAG 36:4
DAG 35:0
DAG 35:1
DAG 35:2
DAG 34:0
DAG 34:1
DAG 34:2
DAG 34:3
DAG 33:0
DAG 33:1
CL 72:3
CL 72:6
CL 70:3
CL 70:4
CL 70:5
CL 70:6
CL 68:1
CL 66:0
CL 66:1
CL 64:0
CL 64:1
CL 64:2
LPG 36:1
LPG 36:2
LPG 36:3
LPG 36:4
LPG 34:0
LPG 34:1
LPG 34:2
LPG 32:0
LPG 32:1
PG 36:0
PG 36:1
PG 36:2
PG 36:3
PG 36:4
PG 34:0
PG 34:1
PG 34:2
PG 32:0
PG 32:1
C17:0
C18:2
C18:1
C16:0
C14:0
OA LA
(logvalue)
4
2
0
−2
−4

composition was greatly reduced upon treatment (Figure 2.6A). There were also notable decreases in DAG production as seen with oleic acid supplementation. Differing from oleic acid, several CL species including CL 64:2, CL 64:1, CL 64:0, CL 66:1, and CL 68:1 were increased. Furthermore, there was a higher percent of MGDG species in the membrane of the *mprF2* mutant when supplementing with linoleic acid (6.7% control vs 30% LA Figure 2.6A), while this trend is not observed in the OG1RF strain.

Considering the altered membrane of this strain, we were interested in the sensitivity of the *mprF2* strain to membrane disrupting agents compared to the previous cardiolipin synthase mutant.

2.4.5 Deletion of mprf2 impacts basal sensitivity to SDS

Given that L-PG has been associated with daptomycin resistance in some bacterial species and that oleic acid has been shown to induce a physiological tolerance to the drug, the relationship between L-PG and daptomycin tolerance upon oleic acid exposure was examined. [8-10, 29, 30] Basal sensitivity to high daptomycin concentrations was equivalent in the parental strain and the Δ*mprF2* strain (Figure 2.7A, B). When Δ*mprF2* was grown in media supplemented with oleic or linoleic acid, there was a similar increased tolerance to the antibiotic as compared to the parental strain. The role of L-PG in membrane stress responses was then examined by evaluating the sensitivity of the Δ*mprF2* strain to SDS. Surprisingly, the deletion strain was less sensitive to SDS compared to the parental strain (Supplementary Figure S7; see Discussion), implying a role of L-PG in detergent sensitivity.

2.4.6 OG1RF lacking mprF2, cls1 and cls2 is viable and can alter its lipid content upon fatty acid supplementation

Thus far, our data has shown that *E. faecalis* can adjust its lipidome in response to genetic disturbances. We wanted to examine further how *E. faecalis* would respond upon loss of two of its three major phospholipid synthetic pathways, L-PG and CL. We therefore generated the triple gene deletion strain Δ*mprF2/cls1/cls2*; this strain grew similar to the original parental strain in laboratory media lacking exogenous fatty acids (Supplemental Table S5). We confirmed the loss of L-PG and CL species via UPLC-HRMS (Supplemental Figure S8; Figure 2.8A, 2.8B). When lipid species were compared to the original parental strain, there were increases in a variety of DAGs, one single MGDG (Supplemental Figure S8). Indeed, DAG species comprised over 64% of the total annotated lipid species examined here, while in the original parental strain, they comprised only 22.4% (Figure 2.1A versus 2.7A). There was a large reduction in total PG species detected however in Δ *mprF2/cls1*/*cls2* versus the original parental strain (23.5% versus 53.7%), supportive of significant remodeling of lipid synthetic pathways, despite both CL and L-PG comprising a minor portion of the total lipid profile of the parental strain under control conditions (Figure 2.1A versus 2.7A).

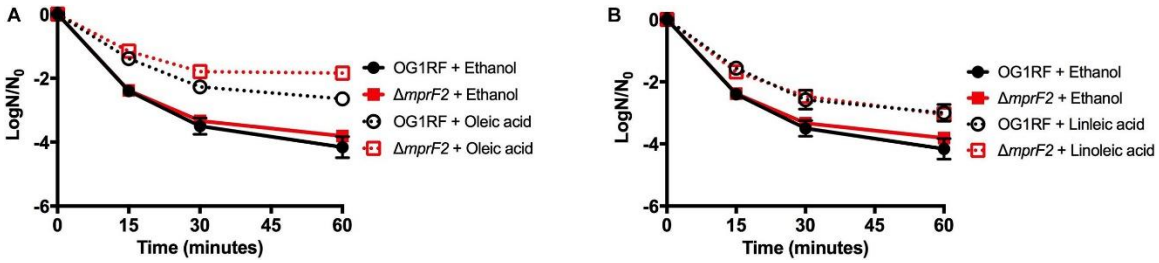

Figure 2.7 Host fatty acid supplementation protects *mprF2* deficient *E. faecalis* OG1RF from daptomycin challenge. (A) All strains supplemented with oleic acid had statistically increased numbers of survivors vs. the solvent control at all-time points analyzed (*P* = 0.002). (B) All strains supplemented with linoleic acid had statistically increased numbers of survivors vs. the solvent control at all-time points analyzed (*P* = 0.005). Shown are the averages ± standard deviation for *n* = 3. OG1RF data is re-plotted from Figures 2.4A,B.

Figure 2.8 A strain deleted for Δ*mprF2/cls1/cls2* can alter its lipid composition upon exposure to host fatty acids. (A) Percent totals of lipid species in solvent control: free fatty acids (2.6%), PG (24.5%), L-PG (0.0%), CL (0.0%), DAG (64.7%), and MGDG (8.3%), oleic acid: free fatty acids (7.0%), PG (35.8%), L-PG (0.0%), CL 0.0%), DAG (64.7%), MGDG (14.8%), linoleic acid: free fatty acids (11.7%), PG (23.0%), L-PG (0.0%), CL (0.0%), DAG (40.8%) MGDG (24.5%). Species were normalized to $OD_{600\ nm}$. (B) Heat-map of fold changes upon fatty acid supplementation vs. solvent control; OA, oleic acid supplementation; LA, linoleic acid supplementation. Shown are the average fold changes of those detected lipid species above limit of detection for *n* = 5 samples. **P* = 0.1–0.05; ***P* = 0.05–0.01; ****P* < 0.01.

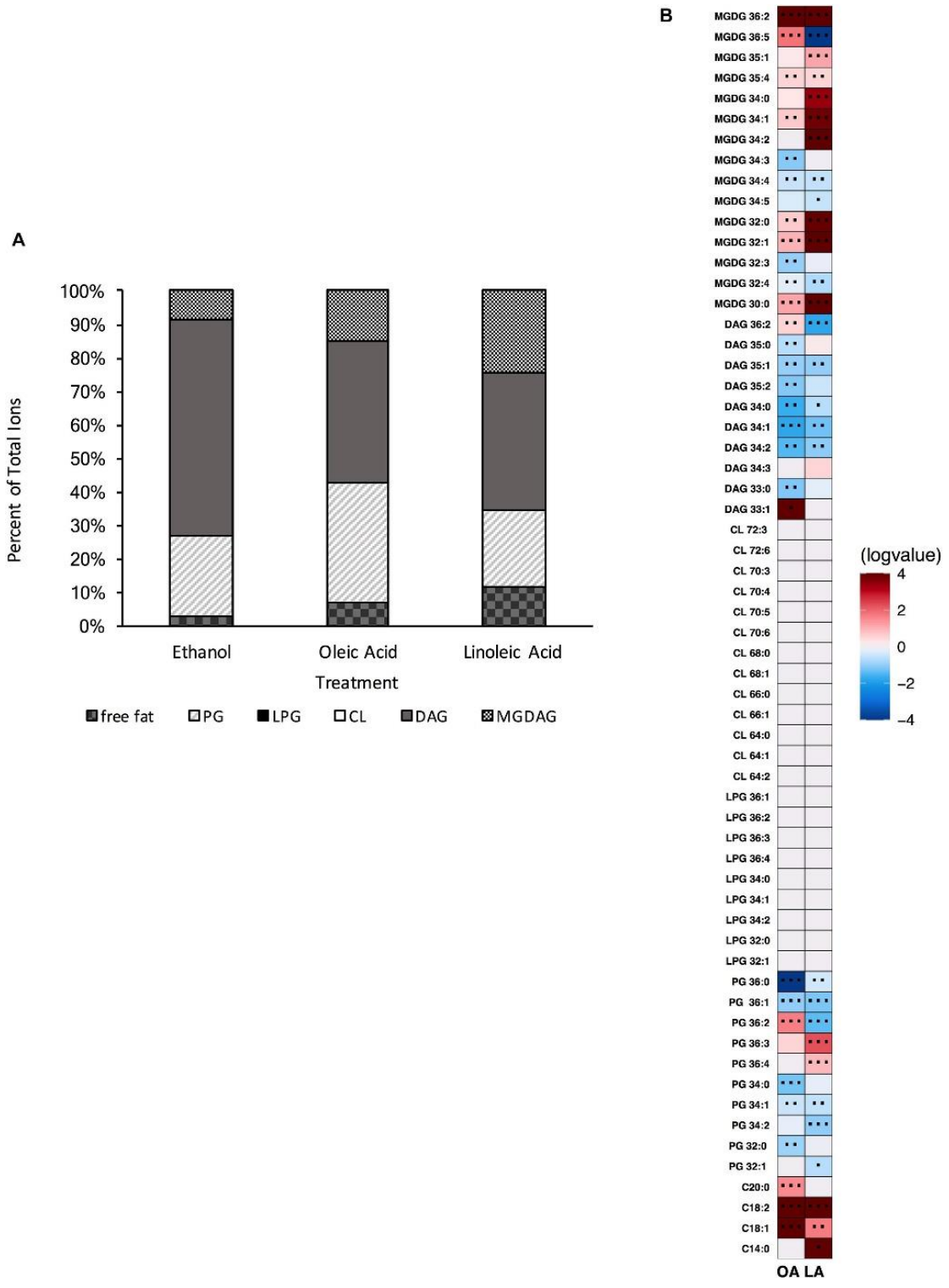
A
Percent of Total Ions
100%
90%
80%
70%
60%
50%
40%
30%
20%
10%
0%
Ethanol
Oleic Acid
Linoleic Acid
Treatment
free fat
PG
LPG
CL
DAG
MGDAG
B
MGDG 36:2
MGDG 36:5
MGDG 35:1
MGDG 35:4
MGDG 34:0
MGDG 34:1
MGDG 34:2
MGDG 34:3
MGDG 34:4
MGDG 34:5
MGDG 32:0
MGDG 32:1
MGDG 32:3
MGDG 32:4
MGDG 30:0
DAG 36:2
DAG 35:0
DAG 35:1
DAG 35:2
DAG 34:0
DAG 34:1
DAG 34:2
DAG 34:3
DAG 33:0
DAG 33:1
CL 72:3
CL 72:6
CL 70:3
CL 70:4
CL 70:5
CL 70:6
CL 68:0
CL 68:1
CL 66:0
CL 66:1
CL 64:0
CL 64:1
CL 64:2
LPG 36:1
LPG 36:2
LPG 36:3
LPG 36:4
LPG 34:0
LPG 34:1
LPG 34:2
LPG 32:0
LPG 32:1
PG 36:0
PG 36:1
PG 36:2
PG 36:3
PG 36:4
PG 34:0
PG 34:1
PG 34:2
PG 32:0
PG 32:1
C20:0
C18:2
C18:1
C14:0
OA LA
(logvalue)
4
2
0
−2
−4

When comparing the basal membrane lipidome to that of cultures supplemented with fatty acids, Δ *mprF2/cls1*/*cls2* was still capable of altering its lipid composition. When pulsed with oleic acid, there was a significant increase in free fatty acids, in particular $C_{18:1}$, $C_{18:2}$ and $C_{20:0}$, though we note that $C_{18:2}$ was not detected via GC-FAME, likely as levels were below detection limits for this analysis (Supplemental Table S4). Similar to Δ *mprF2,* the accumulation of oleic acid, $C_{18:1cis\ 9}$, as determined via GC-FAME, was far less compared to the other strains examined (Supplemental Table S5). Overall, there was a decrease in the total proportion of DAGs and an increase in total proportion of PG species (Figure 2.8A). The increase in PG species was driven primarily through an increase in PG 36:2 (Figure 2.8B). There were increases in MGDG species as well, specifically MGDG 36:2, MGDG 36:5, MGDG 32:1, and MGDG 30:0. Addition of linoleic acid to Δ*mprF2/cls1*/*cls2* also resulted in an altered profile. Similarly we noted increases in free fatty acids, in particular $C_{18:2}$, which corresponds with accumulation of $C_{18:2cis9,12}$ as noted via GC-FAME (Supplemental Table S4). MGDGs, as a group, comprised a larger portion of the examined lipid species (approximately 25% versus control, 8.3% Figure 2.1A vs 2.8A), with specific species like MGDG 34:2, MGDG 36:2, MGDG 32:0, MGDG 34:1 greatly increased (Figure 2.8B). While PG totals were decreased upon supplementation, PG 36:3 and PG 36:4, which likely contain one and two linoleic tails respectively, were enriched.

2.4.7 Loss of both lysyl-phosphatidyl glycerol and cardiolipin synthesis restores basal tolerance to membrane damaging agents

As noted above, loss of cardiolipin synthesis resulted in *E. faecalis* being less tolerant to both daptomycin and the general membrane disruptor SDS. However, loss of lysyl-phosphatidylglycerol *(*Δ*mprF2)* increased tolerance to SDS. Given these observations, we examined how combining these deletions impacted stress sensitivity Δ*mprF2/cls1/cls2.* Basal daptomycin sensitivity of the triple deletion strain was equivalent to the parental strain, unlike Δ*cls1/cls2 (*Figure 2.5A,B*);* addition of oleic or linoleic acid could still induce protection in the triple gene deletion strain. Thus loss of both L-PG and CL has no impact on daptomycin sensitivity or the induction of protection by eukaryotic fatty acids. Basal sensitivity to the SDS was also similar to the parental strain, unlike Δ*cls1/cls2,* although by 60 mins, the survival of Δ*mprF2/cls1/cls2* was reduced (Figure 2.5C).

2.5 Discussion

Within, we examined the plasticity of the enterococcal lipid composition in response to both environmental perturbations and genetic alterations. We refined a lipidomic approach to identify the most common predicted phospholipids based upon known fatty acid tail and head group content (Appendix).[8, 10, 12, 14-16] We also included analyses of previously reported DAG and MGDG species and fatty acids. We observed that the lipid composition responds quickly upon exposure to

the host fatty acids oleic and linoleic acids, resulting in shifts in the proportions of specific PG, CL, L-PG, DAG, and MGDG species. When exposed to exogenous fatty acids, mimicking its environment within humans, OG1RF showed marked increases in lipids containing acyl-chains consisting of the supplemented fatty acid. The parental OG1RF strain appears to respond to exogenous oleic acid by increasing $C_{18:1}$ into the membrane as free fat and as acyl tails onto PG, L-PG, CL, and MGDG. The addition of linoleic acid also increased the amounts of free fat dramatically, as well as increasing specific lipid species containing a $C_{18:2}$ acyl-tail. Further, regardless of the presence or absence of either *mprF2*, *cls1* and/or *cls2*, and the resultant differences in their individual lipid species abundance, the basal membrane fatty acid content was unaltered (Supplementary Table S5). This suggests that *E. faecalis* will re-route its phospholipid synthetic machinery such that there are minimal impacts on fatty acid tail composition. This conservation likely aids in maintaining proper membrane fluidity and membrane protein function. These findings are particularly relevant in that *E. faecalis* does not undergo beta-oxidation, therefore the need to uptake these exogenous lipids into the cell for use as a carbon source is void. Future tracing experiments will better determine the fate of these fatty acids as they enter the lipid biosynthesis pathway of this strain.

We do note that there are major differences in membrane lipid composition upon genetic perturbations of lipid synthetic pathways. While L-PG and CL comprised a minor portion of total lipids detected by our methods (Fig. 1a), loss of either or both resulted in a basal lipid content being dominated by DAG species and not PG species (Figure. 2.4A, 2.6A, 2.8A). Such significant alterations, despite loss of a minor species, demonstrates not only the plasticity of the metabolic capabilities of the organism, but implies the need to maintain proper membrane composition for cellular function. Alterations in membrane composition can have significant impacts on membrane protein function and activity, so this re-wiring of the lipidome likely aids in maintenance of homeostasis.[31-38] We do note that the genetic perturbations performed are deletion strains, thus we are examining the result of acclimation to genetic manipulation; quick changes to genetic disruption will need further investigation. The increase in DAG species in the various deletion strains compared to the parental, as well as increase in specific DAG species upon fatty acid supplementation, may be supportive of active lipid remodeling. Lipid remodeling in yeast refers to the removal of acyl tails from preformed polar head groups and the addition of new tails.[39, 40] In Gram positive bacteria, glycerol phosphate from PG can be transferred to form lipoteichoic acid (in Gram negative bacteria, membrane derived oligosaccharides, MDOs). This generates diacylglycerol, which can be converted to phosphatidic acid and be used to synthesize new lipids.[41, 42] Thus, large accumulations of DAGs may be indicative of cells actively adjusting their membrane profile (note that cells were actively growing for these analyses). Future metabolic flux and isotope tracing experiments are warranted to better examine lipid turnover.

Deletion of cardiolipin synthase 1 or cardiolipin synthase 2 independently resulted in a strain capable of producing detectable levels of CL. Comparing the parental strain to both single deletion strains in ethanol, decreases in CL production for all CL species is shown (Supplemental Figure S1). However, we do note that both Δ*cls1* and Δ*cls2* had a significant increase in CL species when exposed to oleic acid and linoleic acid, similar to the parental strain. This conserved alteration, despite genetic mutation, implied a significant role for CL in acclimating to exogenous host fatty acids in its environment. Further, as increased activity of CL synthase in enterococci and increased levels in liposomes are linked to protection from the antibiotic daptomycin, we noted that both deletion strains maintained a similar tolerance to the drug as the parental.[13, 23, 25-27]

The deletion of both cardiolipin synthase genes resulted in a strain incapable of producing CL (Supplemental Figure S2). The resulting strain produced a membrane vastly different than the parental strain (Fig. 4a versus Fig. 1a; Supplemental Fig S3). The Δ*cls1/cls2* under basal conditions had a membrane dominated by DAG species, while the parental strain was dominated by PG species. Yet, in the parental strain under the control conditions, CL was only about 1% of the total composition examined. Why then would the composition be so dramatically different upon loss of CL? We note that the deletion strain produces high levels of DAGs, precursor of teichoic acid synthesis.[27, 41-45] It could be the loss of CL triggers either wall synthesis or wall recycling, either because its protein machinery activity is altered without the lipid present, or lack of CL results in weakening the organism, and wall synthesis is a compensatory response. Further analysis of wall synthesis is needed to confirm this.

Like Δ*cls1/cls2*, Δ*mprF2* also produced a membrane under control conditions vastly different from the parental strain. It had a membrane dominated by DAG species (69.8%), like Δ*cls1/cls2*, whereas the parental strain was dominated by PG species (53.75%; Figure 2.1A, 2.4A, 2.6A). It is important to note that in the parental strain, L-PG comprised only 1.1% of the total composition, like CL (Figure 2.1A) . When combining these deletions together, generating Δ*mprF2/cls1/cls2*, again DAG species dominate (Figure 2.8A). The conserved increase in DAG species suggest the strains alter wall synthesis or recycling upon loss of phospholipid synthesis.[41] Daptomycin has been shown to disrupt wall synthesis; if wall synthesis levels were similar, then the mutant strains should have equivalent sensitivity to the drug.[46, 47] However, that is not what we observe: Δ*cls1/cls2* was much more sensitive to the antibiotic than the others (Figure 2.5A, B). Further, loss of mprF2 suppressed Δ*cls1/cls2* sensitivity to the drug (Figure 2.5A, B). Clearly, further examination of the consequences on other cellular processes, including wall synthesis, upon such perturbation of the lipidome is needed to explain these observations.

While we note that basal fatty acid tail profiles were consistent across our deletion strains, strains lacking *mprF2* did not accumulate oleic acid to the levels

observed in the other strains (Supplementary Table S4). Enterococci, like *S. aureus* and *S. pneumoniae*, do not have known "active" import systems for exogenous fatty acids. It is thought that environmental fatty acids interact with the membrane, and passively "flip" in. These fatty acids can then be utilized by the Fak system, resulting in their phosphorylation and use in lipid synthesis, or possibly enter the elongation cycle of fatty acid biosynthesis.[47-49] Given this passive mechanism, it is surprising to see such a reduction in oleic acid accumulation specifically: linoleic acid accumulated well in this strain so this is not a generic fatty acid interaction issue (Supplementary Table S4). Even if oleic acid is not used well by the Fak system in a *mprF2* deletion background, we would expect to see it accumulate free in the membrane, and that would be reflected in our GC-FAME analysis. Further analyses examining long-term supplementation, and isotope tracing are warranted to better elucidate this observation.

Regardless, all of our mutant strains were able to alter their lipid profiles if provided oleic or linoleic acids. This in turn resulted in induction of tolerance to daptomycin. Previous findings have noted this protection appears independent of membrane fluidity, growth kinetics, or overall membrane charge.[11] While daptomycin is known to impact wall synthetic machinery, perhaps the addition of oleic or linoleic acid, regardless of genetic background of *E. faecalis*, impacts wall synthesis.[46, 47] We note that all strains examined accumulate free fat within the membrane when given either oleic or linoleic acid: indeed, this seemed to be the only conserved observation across genetic backgrounds(Figure 2.1B, 2.2B, 2.3B, 2.4B, 2.6B). Perhaps the alterations of the lipidome on membrane protein activity is due to free fat accumulation, resulting in stress protection. Ongoing experiments are geared at addressing this.

Loss of L-PG also impacted sensitivity to SDS, however, it rendered Δ*mprF2* more tolerant to the detergent than the parental strain (Supplemental Figure S7). Combining this deletion with Δ*cls1/*Δ*cls2* actually restored basal tolerance to both SDS and daptomycin to that of a wild type strain. This may be due to alterations in membrane protein content and/or activity which in turn could be responsible for the improved survival of Δ*mprF2/*Δ*cls1/*Δ*cls2* compared to Δ*cls1/*Δ*cls2* (Figure 2.5C). Further, differing survival rates upon SDS treatment may be due to altered gene expression in our various deletion strains: a study has shown that SDS can induce a variety of transcriptional changes in enterococci that may aid in acclimation.[50] Combined, alterations in the enterococcal lipid content, directly or indirectly, will impact stress responses.

Taken together, we found that supplementation with host fatty acids, oleic acid and linoleic acid, alter the phospholipid profile of *E. faecalis* regardless of genetic perturbation of phospholipid synthetic pathways, supportive of a plastic lipidome and a flexible metabolism. Supplementation with either host fatty acid could induce protection from daptomycin regardless of the presence of *mprF2, cls1,* and *cls2*. Thus, host fatty acid induced daptomycin tolerance during acute exposure to membrane stressors is through a yet to be determined mechanism.

REFERENCES

1. Silhavy, T. J.; Kahne, D.; Walker, S., The bacterial cell envelope. *Cold Spring Harb Perspect Biol* **2010,** *2* (5), a000414.
2. Strahl, H.; Errington, J., Bacterial Membranes: Structure, Domains, and Function. *Annual Review of Microbiology* **2017,** *71* (1), 519-538.
3. López-Lara, I. M.; Geiger, O., Bacterial lipid diversity. *Biochimica et Biophysica Acta (BBA) - Molecular and Cell Biology of Lipids* **2017,** *1862* (11), 1287-1299.
4. Fozo, E. M.; Rucks, E. A., The making and taking of lipids: The role of bacterial lipid synthesis and the harnessing of host lipids in bacterial pathogenesis. *Advances in microbial physiology* **2016,** *69*, 51-155.
5. de Mendoza, D.; Pilon, M., Control of membrane lipid homeostasis by lipid-bilayer associated sensors: a mechanism conserved from bacteria to humans. *Progress in Lipid Research* **2019,** *76*, 100996.
6. Mendoza, D. d., Temperature sensing by membranes. *Annual review of microbiology* **2014,** *68*, 101-116.
7. Rowlett, V. W.; Mallampalli, V. K.; Karlstaedt, A.; Dowhan, W.; Taegtmeyer, H.; Margolin, W.; Vitrac, H., Impact of membrane phospholipid alterations in Escherichia coli on cellular function and bacterial stress adaptation. *Journal of bacteriology* **2017,** *199* (13), e00849-16.
8. Saito, H. E.; Harp, J. R.; Fozo, E. M., Incorporation of exogenous fatty acids protects Enterococcus faecalis from membrane-damaging agents. *Appl Environ Microbiol* **2014,** *80* (20), 6527-38.
9. Harp, J. R.; Saito, H. E.; Bourdon, A. K.; Reyes, J.; Arias, C. A.; Campagna, S. R.; Fozo, E. M., Exogenous Fatty Acids Protect Enterococcus faecalis from Daptomycin-Induced Membrane Stress Independently of the Response Regulator LiaR. *Applied and Environmental Microbiology* **2016,** *82* (14), 4410-4420.
10. Saito, H. E.; Harp, J. R.; Fozo, E. M., Enterococcus faecalis Responds to Individual Exogenous Fatty Acids Independently of Their Degree of Saturation or Chain Length. *Appl Environ Microbiol* **2018,** *84* (1).
11. Brewer, W.; Harrison, J.; Saito, H. E.; Fozo, E. M., Induction of Daptomycin Tolerance in Enterococcus faecalis by Fatty Acid Combinations. *Applied and Environmental Microbiology* **2020,** *86* (20), e01178-20.
12. Ibbott, F. A.; Abrams, A., The phospholipids in membrane ghosts from Streptococcus faecalis protoplasts. *Biochemistry* **1964,** *3* (12), 2008-2012.
13. Mishra, N. N.; Bayer, A. S.; Tran, T. T.; Shamoo, Y.; Mileykovskaya, E.; Dowhan, W.; Guan, Z.; Arias, C. A., Daptomycin Resistance in Enterococci Is Associated with Distinct Alterations of Cell Membrane Phospholipid Content. *PLOS ONE* **2012,** *7* (8), e43958.
14. Hines, K. M.; Waalkes, A.; Penewit, K.; Holmes, E. A.; Salipante, S. J.; Werth, B. J.; Xu, L., Characterization of the Mechanisms of Daptomycin Resistance among Gram-Positive Bacterial Pathogens by Multidimensional Lipidomics. *mSphere* **2017,** *2* (6), e00492-17.

15. Rashid, R.; Cazenave-Gassiot, A.; Gao, I. H.; Nair, Z. J.; Kumar, J. K.; Gao, L.; Kline, K. A.; Wenk, M. R., Comprehensive analysis of phospholipids and glycolipids in the opportunistic pathogen Enterococcus faecalis. *PLoS One* **2017,** *12* (4), e0175886.
16. Tague, E. D.; Woodall, B. M.; Harp, J. R.; Farmer, A. T.; Fozo, E. M.; Campagna, S. R., Expanding lipidomics coverage: effective ultra performance liquid chromatography-high resolution mass spectrometer methods for detection and quantitation of cardiolipin, phosphatidylglycerol, and lysyl-phosphatidylglycerol. *Metabolomics* **2019,** *15*, 1-10.
17. Schlame, M., Thematic Review Series: Glycerolipids. Cardiolipin synthesis for the assembly of bacterial and mitochondrial membranes. *Journal of lipid research* **2008,** *49* (8), 1607-1620.
18. Peschel, A.; Jack, R. W.; Otto, M.; Collins, L. V.; Staubitz, P.; Nicholson, G.; Kalbacher, H.; Nieuwenhuizen, W. F.; Jung, G.; Tarkowski, A., Staphylococcus aureus resistance to human defensins and evasion of neutrophil killing via the novel virulence factor MprF is based on modification of membrane lipids with l-lysine. *The Journal of experimental medicine* **2001,** *193* (9), 1067-1076.
19. Kristich, C. J.; Chandler, J. R.; Dunny, G. M., Development of a host-genotype-independent counterselectable marker and a high-frequency conjugative delivery system and their use in genetic analysis of Enterococcus faecalis. *Plasmid* **2007,** *57* (2), 131-144.
20. Sasser, M.; Kunitsky, C.; Jackoway, G.; Ezzell, J. W.; Teska, J. D.; Harper, B.; Parker, S.; Barden, D.; Blair, H.; Breezee, J., Identification of Bacillus anthracis from culture using gas chromatographic analysis of fatty acid methyl esters. *Journal of AOAC International* **2005,** *88* (1), 178-181.
21. Guan, X. L.; Riezman, I.; Wenk, M. R.; Riezman, H., Yeast lipid analysis and quantification by mass spectrometry. In *Methods in enzymology*, Elsevier: 2010; Vol. 470, pp 369-391.
22. Bird, S. S.; Marur, V. R.; Sniatynski, M. J.; Greenberg, H. K.; Kristal, B. S., Lipidomics profiling by high-resolution LC− MS and high-energy collisional dissociation fragmentation: Focus on characterization of mitochondrial cardiolipins and monolysocardiolipins. *Analytical chemistry* **2011,** *83* (3), 940-949.
23. Arias, C. A.; Panesso, D.; McGrath, D. M.; Qin, X.; Mojica, M. F.; Miller, C.; Diaz, L.; Tran, T. T.; Rincon, S.; Barbu, E. M.; Reyes, J.; Roh, J. H.; Lobos, E.; Sodergren, E.; Pasqualini, R.; Arap, W.; Quinn, J. P.; Shamoo, Y.; Murray, B. E.; Weinstock, G. M., Genetic basis for in vivo daptomycin resistance in enterococci. *N Engl J Med* **2011,** *365* (10), 892-900.
24. Koprivnjak, T.; Zhang, D.; Ernst, C.; Peschel, A.; Nauseef, W.; Weiss, J., Characterization of Staphylococcus aureus cardiolipin synthases 1 and 2 and their contribution to accumulation of cardiolipin in stationary phase and within phagocytes. *Journal of bacteriology* **2011,** *193* (16), 4134-4142.

25. Palmer, K. L.; Daniel, A.; Hardy, C.; Silverman, J.; Gilmore, M. S., Genetic basis for daptomycin resistance in enterococci. *Antimicrobial agents and chemotherapy* **2011,** *55* (7), 3345-3356.
26. Davlieva, M.; Zhang, W.; Arias, C. A.; Shamoo, Y., Biochemical Characterization of Cardiolipin Synthase Mutations Associated with Daptomycin Resistance in Enterococci. *Antimicrobial Agents and Chemotherapy* **2013,** *57* (1), 289-296.
27. Zhang, T.; Muraih, J. K.; Tishbi, N.; Herskowitz, J.; Victor, R. L.; Silverman, J.; Uwumarenogie, S.; Taylor, S. D.; Palmer, M.; Mintzer, E., Cardiolipin prevents membrane translocation and permeabilization by daptomycin. *J Biol Chem* **2014,** *289* (17), 11584-11591.
28. Bao, Y.; Sakinc, T.; Laverde, D.; Wobser, D.; Benachour, A.; Theilacker, C.; Hartke, A.; Huebner, J., Role of mprF1 and mprF2 in the pathogenicity of Enterococcus faecalis. *PLoS One* **2012,** *7* (6), e38458.
29. Hachmann, A.-B.; Angert, E. R.; Helmann, J. D., Genetic analysis of factors affecting susceptibility of Bacillus subtilis to daptomycin. *Antimicrobial agents and chemotherapy* **2009,** *53* (4), 1598-1609.
30. Bayer, A. S.; Schneider, T.; Sahl, H. G., Mechanisms of daptomycin resistance in Staphylococcus aureus: role of the cell membrane and cell wall. *Annals of the New York Academy of Sciences* **2013,** *1277* (1), 139-158.
31. Carson, D.; Daneo-Moore, L., Effect of cerulenin on Streptococcus faecalis macromolecular synthesis and cell division. *Journal of Bacteriology* **1978,** *133* (2), 472-476.
32. Ma, Y.; Marquis, R., Thermophysiology of Streptococcus mutans and related lactic-acid bacteria. *Antonie Van Leeuwenhoek* **1997,** *72*, 91-100.
33. Fozo, E. M.; Quivey Jr, R. G., The fabM gene product of Streptococcus mutans is responsible for the synthesis of monounsaturated fatty acids and is necessary for survival at low pH. *Journal of bacteriology* **2004,** *186* (13), 4152-4158.
34. Romantsov, T.; Stalker, L.; Culham, D. E.; Wood, J. M., Cardiolipin controls the osmotic stress response and the subcellular location of transporter ProP in Escherichia coli. *Journal of Biological Chemistry* **2008,** *283* (18), 12314-12323.
35. García Montes de Oca, L. Y. J.; Cabellos Avelar, T.; Picón Garrido, G. I.; Chagoya-López, A.; González de la Vara, L.; Delgado Buenrostro, N. L.; Chirino-López, Y. I.; Gómez-Lojero, C.; Gutiérrez-Cirlos, E. B., Cardiolipin deficiency causes a dissociation of the b 6 c: caa 3 megacomplex in B. subtilis membranes. *Journal of bioenergetics and biomembranes* **2016,** *48*, 451-467.
36. Henrich, E.; Ma, Y.; Engels, I.; Münch, D.; Otten, C.; Schneider, T.; Henrichfreise, B.; Sahl, H.-G.; Dötsch, V.; Bernhard, F., Lipid requirements for the enzymatic activity of MraY translocases and in vitro reconstitution of the lipid II synthesis pathway. *Journal of Biological Chemistry* **2016,** *291* (5), 2535-2546.

37. Lin, T.-Y.; Gross, W. S.; Auer, G. K.; Weibel, D. B., Cardiolipin alters Rhodobacter sphaeroides cell shape by affecting peptidoglycan precursor biosynthesis. *Mbio* **2019,** *10* (1), e02401-18.
38. Lin, T.-Y.; Weibel, D. B., Organization and function of anionic phospholipids in bacteria. *Applied microbiology and biotechnology* **2016,** *100*, 4255-4267.
39. Renne, M. F.; Bao, X.; De Smet, C. H.; De Kroon, A. I., Lipid acyl chain remodeling in yeast. *Lipid insights* **2015,** *8*, LPI. S31780.
40. Patton-Vogt, J.; de Kroon, A. I., Phospholipid turnover and acyl chain remodeling in the yeast ER. *Biochimica et Biophysica Acta (BBA)-Molecular and Cell Biology of Lipids* **2020,** *1865* (1), 158462.
41. Neuhaus, F. C.; Baddiley, J., A Continuum of Anionic Charge: Structures and Functions of d-Alanyl-Teichoic Acids in Gram-Positive Bacteria. *Microbiology and Molecular Biology Reviews* **2003,** *67* (4), 686-723.
42. Rock, C. O., CHAPTER 3 - Fatty acid and phospholipid metabolism in prokaryotes. In *Biochemistry of Lipids, Lipoproteins and Membranes (Fifth Edition)*, Vance, D. E.; Vance, J. E., Eds. Elsevier: San Diego, 2008; pp 59-96.
43. Theilacker, C.; Sava, I.; Sanchez-Carballo, P.; Bao, Y.; Kropec, A.; Grohmann, E.; Holst, O.; Huebner, J., Deletion of the glycosyltransferase bgsB of Enterococcus faecalisleads to a complete loss of glycolipids from the cell membrane and to impaired biofilm formation. *BMC Microbiology* **2011,** *11* (1), 67.
44. Theilacker, C.; Sanchez-Carballo, P.; Toma, I.; Fabretti, F.; Sava, I.; Kropec, A.; Holst, O.; Huebner, J., Glycolipids are involved in biofilm accumulation and prolonged bacteraemia in Enterococcus faecalis. *Molecular Microbiology* **2009,** *71* (4), 1055-1069.
45. Horn, W. D. V.; Sanders, C. R., Prokaryotic Diacylglycerol Kinase and Undecaprenol Kinase. *Annual Review of Biophysics* **2012,** *41* (1), 81-101.
46. Müller, A.; Wenzel, M.; Strahl, H.; Grein, F.; Saaki, T. N. V.; Kohl, B.; Siersma, T.; Bandow, J. E.; Sahl, H.-G.; Schneider, T.; Hamoen, L. W., Daptomycin inhibits cell envelope synthesis by interfering with fluid membrane microdomains. *Proceedings of the National Academy of Sciences* **2016,** *113* (45), E7077-E7086.
47. Grein, F.; Müller, A.; Scherer, K. M.; Liu, X.; Ludwig, K. C.; Klöckner, A.; Strach, M.; Sahl, H.-G.; Kubitscheck, U.; Schneider, T., Ca2+-Daptomycin targets cell wall biosynthesis by forming a tripartite complex with undecaprenyl-coupled intermediates and membrane lipids. *Nature Communications* **2020,** *11* (1), 1455.
48. Parsons, J. B.; Rock, C. O., Bacterial lipids: metabolism and membrane homeostasis. *Prog Lipid Res* **2013,** *52* (3), 249-76.
49. Cuypers, M. G.; Subramanian, C.; Gullett, J. M.; Frank, M. W.; White, S. W.; Rock, C. O., Acyl-chain selectivity and physiological roles of Staphylococcus aureus fatty acid-binding proteins. *J Biol Chem* **2019,** *294* (1), 38-49.

50. Solheim, M.; Aakra, Å.; Vebø, H.; Snipen, L.; Nes, I. F., Transcriptional Responses of Enterococcus faecalis V583 to Bovine Bile and Sodium Dodecyl Sulfate. *Applied and Environmental Microbiology* **2007,** *73* (18), 5767-5774.

APPENDIX

Table S2.1 Strains and plasmids used in this study

Strain	**Relevant genotype or description**	**Source**
Enterococcus faecalis OG1RF	Laboratory strain Rif^R, Fus^R	J. Lemos, University of Florida
Escherichia coli EC1000	Cloning strain for *repA*-dependent plasmids;	G. Dunny, University of Minnesota
E. faecalis CK111/pCF10-101	Conjugative donor strain; harbors non-transferrable pCF10 derivative plasmid	G. Dunny, University of Minnesota Kristich *et al.* *(*2007) Plasmid 57(2) 131-144
Plasmid		
pCJK47	Used for markerless exchange	G. Dunny, University of Minnesota Kristich *et al.* *(*2007) Plasmid 57(2) 131-144
pJRH1	pCJK47 derivative containing flanking regions of OG1RF_RS01975 (*cls1)*	This work
pJRH2	pCJK47 derivative containing flanking regions of OG1RF_RS06840 (*cls2)*	This work
pMprF2	pCJK47 derivative containing flanking regions of OG1RF_RS03930 (*mprF2*)	This work

Table S2.2 Oligonucleotides used in this study

Name	Sequence	Use
Oligonucleotides used for splicing by overlap extension (SOE) to generate inserts		
EF1097	GTCCAAGGATTCTCACCATTGATGC AAGGCC	Used to amplify DNA upstream of *cls1*
EF1098	CTGGAGTCATTGTTGTACTATACCAT CAATTACGGATTTGGAATATC	Used to amplify DNA upstream of *cls1*
EF1099	CGTAATTGATGGTATACGTACAACAA TGACTCCAGAAGTTGTTCGTGAC	Used to amplify DNA downstream of *cls1*
EF1105	GACTGTCCATGGTATGTTGCACAGC TTCCATCG	Used to amplify DNA downstream of *cls1*
EF1103	CAAGACTGGTGACCAACGTCATCAT CCATGCTAAAACGCTGG	Used to amplify DNA upstream of *cls2*
EF1108	CCCAAGCCCGGGCGATTGACCAGG ACCACTTAAAACTCC	Used to amplify DNA upstream of *cls2*
EF1113	GGTCACGGATTCTCCAAACAAGGTA ACC	Used to amplify DNA downstream of *cls2*
EF1102	CATGGATGATGACGTTGGTCACCAG TCTTGTAATCAATAAATCAGCAGTG	Used to amplify DNA downstream of *cls2*
Oligonucleotides used for Gibson assembly		
EF1449	CAATCACTAGTGAATTCGCGGCCGC CACGGCGATATCGG	Generate overhangs on pCJK47 for *cls1*
EF1450	CAATCGAATTCCCGCGGCCGCTCTA GAACTAGCGATTCTGAAATCAC	Generate overhangs on pCJK47 for *cls1*
EF1451	CAGAATCGCTAGTTCTAGAGCGGCC GCGGGAATTCGATTGT	Generate overhangs on *cls1* insert
EF1452	CATATGGATCCGATATCGCCGTGGC GGCCGCGAATTCACTAGTGATTGAC TG	Generate overhangs on *cls1* insert
EF1453	GGGAATCACTAGTGAATTCGCGGCC GCACGGCGATATCGGATCC	Generate overhangs on pCJK47 for *cls2*
EF1454	CCGTGACCAATCGAATTCCCGCGGC CGCTCTAGAACTAGCGATTCTGAAA TCAC	Generate overhangs on pCJK47 for *cls2*
EF1455	CAGAATCGCTAGTTCTAGAGCGGCC GCGGGAATTCGATTGG	Generate overhangs on *cls2* insert
EF1456	CATATGGATCCGATATCGCCGTGCG GCCGCGAATTCACTAGTGATTCCCA AG	Generate overhangs on *cls2* insert

Table S2.2 Continued

EF1601	GACAAAACCCCTAATAATTCTTTTGC TTCATCCATGCCCGGGTACCATGGC ATGCTAAGCTTGATTTTCGTTC	Generate overhangs on pCJK47 for *mprF2*
EF1602	CTTTTGATCAAAAACAGGATTTTCTC TAGAACTAGCGATTCTGAAATCACCA TTTAAAAAACTC	Generate overhangs on pCJK47 for *mprF2*
EF1603	GAGTTTTTTAAATGGTGATTTCAGAA TCGCTAGTTCTAGAGAAAATCCTGTT TTTGATCAAAAG	Generate overhangs on DNA upstream of *mprF2*
EF1604	CAATCCAGCTACTTTTAGAATAAAGT GTATAGCAACAACAATAATTGAGACC GCAATAACAAAC	Generate overhangs on DNA upstream of *mprF2*
EF1605	GTTTGTTATTGCGGTCTCAATTATTG TTGTTGCTATACACTTTATTCTAAAA GTAGCTGGATTG	Generate overhangs on DNA downstream of *mprF2*
EF1606	GAACGAAAATCAAGCTTAGCATGCC ATGGTACCCGGGCATGGATGAAGCA AAAGAATTATTAGGGGTTTTGTC	Generate overhangs on DNA downstream of *mprF2*

Table S2.3 Lipid Compound List for UHPLC-HRMS Identification with Tail Composition

Polarity	**Lipid**	**Formula**
-	CL 64:2	C73H138O17P2
-	CL 64:0	C73H142O17P2
-	CL 64:1	C73H140O17P2
-	CL 66:0	C75H146O17P2
-	CL 66:1	C75H144O17P2
-	CL 68:0	C77H150O17P2
-	CL 68:1	C77H148O17P2
-	CL 70:0	C79H154O17P2
-	CL 70:1	C79H152O17P2
-	CL 70:3	C79H148O17P2
-	CL 70:4	C79H146O17P2
-	CL 70:5	C79H144O17P2
-	CL 70:6	C79H142O17P2
-	CL 70:7	C79H140O17P2
-	CL 72:5	C81H148O17P2
-	CL 72:6	C81H146O17P2
-	CL 56:0	C65H126O17P2
-	CL 72:8	C81H142O17P2
-	CL 72:7	C81H144O17P2
-	CL 72:4	C81H150O17P2
-	CL 72:3	C81H152O17P2
-	CL 72:2	C81H154O17P2
-	CL 72:1	C81H156O17P2
-	CL 72:0	C81H158O17P2
-	LPG 32:1	C44H85N2O11P
-	LPG 34:0	C46H91N2O11P
-	LPG 34:1	C46H89N2O11P
-	LPG 34:2	C46H87N2O11P
-	LPG 36:0	C48H95N2O11P
-	LPG 36:1	C48H93N2O11P
-	LPG 36:3	C48H89N2O11P
-	LPG 36:4	C48H87N2O11P
-	LPG 32:0	C44H87N2O11P
-	LPG 36:2	C48H91N2O11P
-	PG 32:0	C38H75O10P
-	PG 32:1	C38H73O10P
-	PG 34:0	C40H79O10P

Table S2.3 Continued

-	PG 34:1	C40H77O10P
-	PG 34:2	C40H75O10P
-	PG 36:3	C42H77O10P
-	PG 36:4	C42H75O10P
-	PG 36:2	C42H79O10P
-	PG 36:1	C42H81O10P
-	PG 36:0	C42H83O10P
-	PG 16:0	C22H43O10P
+	DAG 36:2	C39H75NO5
+	DAG 36:4	C39H71NO5
+	DAG 36:0	C39H79NO5
+	DAG 36:1	C39H77NO5
+	DAG 35:0	C38H77NO5
+	DAG 35:1	C38H75NO5
+	DAG 35:2	C38H73NO5
+	DAG 34:0	C37H75NO5
+	DAG 34:1	C37H73NO5
+	DAG 34:2	C37H71NO5
+	DAG 33:0	C36H73NO5
+	DAG 33:1	C36H71NO5
+	DAG 33:2	C36H69NO5
+	DAG 35:3	C38H71NO5
+	DAG 34:3	C37H69NO5
+	DAG 33:3	C36H67NO5
+	DAG 35:4	C38H69NO5
+	DAG 34:4	C37H67NO5
+	MGDG 28:0	C37H73NO10
+	MGDG 28:1	C37H68O10NH3
+	MGDG 28:2	C37H66O10NH3
+	MGDG 28:3	C37H64O10NH3
+	MGDG 28:4	C37H62O10NH3
+	MGDG 28:5	C37H60O10NH3
+	MGDG 28:6	C37H58O10NH3
+	MGDG 29:0	C38H72O10NH3
+	MGDG 29:1	C38H70O10NH3
+	MGDG 29:2	C38H68O10NH3
+	MGDG 29:3	C38H66O10NH3
+	MGDG 29:4	C38H64O10NH3
+	MGDG 29:5	C38H62O10NH3
+	MGDG 29:6	C38H60O10NH3

Table S2.3 Continued

+	MGDG 30:0	C39H74O10NH3
+	MGDG 30:1	C39H72O10NH3
+	MGDG 30:2	C39H70O10NH3
+	MGDG 30:3	C39H68O10NH3
+	MGDG 30:4	C39H66O10NH3
+	MGDG 30:5	C39H64O10NH3
+	MGDG 30:6	C39H62O10NH3
+	MGDG 31:0	C40H76O10NH3
+	MGDG 31:1	C40H74O10NH3
+	MGDG 31:2	C40H72O10NH3
+	MGDG 31:3	C40H70O10NH3
+	MGDG 31:4	C40H68O10NH3
+	MGDG 31:5	C40H66O10NH3
+	MGDG 31:6	C40H64O10NH3
+	MGDG 32:0	C41H78O10NH3
+	MGDG 32:1	C41H76O10NH3
+	MGDG 32:2	C41H74O10NH3
+	MGDG 32:3	C41H72O10NH3
+	MGDG 32:4	C41H70O10NH3
+	MGDG 32:5	C41H68O10NH3
+	MGDG 32:6	C41H66O10NH3
+	MGDG 33:0	C42H80O10NH3
+	MGDG 33:1	C42H78O10NH3
+	MGDG 33:2	C42H76O10NH3
+	MGDG 33:3	C42H74O10NH3
+	MGDG 33:4	C42H72O10NH3
+	MGDG 33:5	C42H70O10NH3
+	MGDG 33:6	C42H68O10NH3
+	MGDG 34:0	C43H82O10NH3
+	MGDG 34:1	C43H80O10NH3
+	MGDG 34:2	C43H78O10NH3
+	MGDG 34:3	C43H76O10NH3
+	MGDG 34:4	C43H74O10NH3
+	MGDG 34:5	C43H72O10NH3
+	MGDG 34:6	C43H70O10NH3
+	MGDG 35:0	C44H84O10NH3
+	MGDG 35:1	C44H82O10NH3
+	MGDG 35:2	C44H80O10NH3
+	MGDG 35:3	C44H78O10NH3
+	MGDG 35:4	C44H76O10NH3

Table S2.3 Continued

+	MGDG 35:5	C44H74O10NH3
+	MGDG 35:6	C44H72O10NH3
+	MGDG 36:0	C45H86O10NH3
+	MGDG 36:1	C45H84O10NH3
+	MGDG 36:2	C45H82O10NH3
+	MGDG 36:3	C45H80O10NH3
+	MGDG 36:4	C45H78O10NH3
+	MGDG 36:5	C45H76O10NH3
+	MGDG 36:6	C45H74O10NH3
+	MGDG 37:0	C46H88O10NH3
+	MGDG 37:1	C46H86O10NH3
+	MGDG 37:2	C46H84O10NH3
+	MGDG 37:3	C46H82O10NH3
+	MGDG 37:4	C46H80O10NH3
+	MGDG 37:5	C46H78O10NH3
+	MGDG 37:6	C46H76O10NH3
+	MGDG 38:0	C47H88O10NH3
+	MGDG 38:1	C47H86O10NH3
+	MGDG 38:2	C47H84O10NH3
+	MGDG 38:3	C47H82O10NH3
+	MGDG 38:4	C47H80O10NH3
+	MGDG 38:5	C47H78O10NH3
+	MGDG 38:6	C47H76O10NH3
+	MGDG 40:0	C49H92O10NH3
+	MGDG 40:1	C49H90O10NH3
+	MGDG 40:2	C49H88O10NH3
+	MGDG 40:3	C49H86O10NH3
+	MGDG 40:4	C49H84O10NH3
+	MGDG 40:5	C49H82O10NH3
+	MGDG 40:6	C49H80O10NH3
+	MGDG 42:0	C51H96O10NH3
+	MGDG 42:1	C51H94O10NH3
+	MGDG 42:2	C51H92O10NH3
+	MGDG 42:3	C51H90O10NH3
+	MGDG 42:4	C51H88O10NH3
+	MGDG 42:5	C51H86O10NH3
+	MGDG 42:6	C51H84O10NH3
+	MGDG 44:0	C53H100O10NH3
+	MGDG 44:1	C53H98O10NH3
+	MGDG 44:2	C53H96O10NH3

Table S2.3 Continued

+	MGDG 44:3	C53H94O10NH3
+	MGDG 44:4	C53H92O10NH3
+	MGDG 44:5	C53H90O10NH3
+	MGDG 44:6	C53H88O10NH3
-	C14:0	C14H28O2
-	C12:0	C12H24O2
-	C16:0	C16H32O2
-	C16:1	C16H30O2
-	C18:0	C18H36O2
-	C18:1	C18H34O2
-	C18:2	C18H32O2
-	C20:0	C20H40O2
-	C20:4	C20H32O2
-	C20:5	C20H30O2
-	C22:6	C22H32O2
-	C20:1	C20H38O2

Table S2.4 *E. faecalis* OG1RF, Δ*mprF2,* Δ*cls1,* Δ*cls2,* Δ*cls1/cls2*, and Δ*mprF2/cls1/cls2* membrane fatty acid composition during exponential phase growth supplemented with ethanol analyzed via GC-FAME (Microbial ID, Inc.)

% of total membrane content (Avg. ± SD)						
Treatment: Ethanol						
Fatty acid	OG1RF	Δ*mprF2*	Δ*cls1*	Δ*cls2*	Δ*cls1*Δ*cls2*	Δ*mprF2* Δ*cls1* Δ*cls2*
$C_{12:0}$	1.8 ± 0.3	1.2 ± 0.1	1.6 ± 0.1	1.7 ± 0.4	1.7 ± 0.2	1.3 ± 0.3
$C_{14:0}$	4.8 ± 0.1	4.6 ± 0.2	4.6 ± 0.04	4.4 ± 0.4	4.2 ± 0.1	4.4 ± 0.4
$C_{16:1\ cis\ 9}$	7.2 ± 0.1	6.6 ± 0.3	6.7 ± 0.1	7.1 ± 0.4	6.5 ± 0.2	7.0 ± 0.6
$C_{16:0}$	37.8 ± 0.4	38.6 ± 0.4	37.5 ± 0.3	36.0 ± 0.2	37.1 ± 0.3	37.3 ± 0.8
$C_{18:1\ cis\ 9}$	1.7 ± 0.2	ND	1.3 ± 0.1	1.4 ± 0.1	1.3 ± 0.1	0.3 ± 0.5
$C_{18:1\ cis\ 11}$	38.3 ± 0.5	39.6 ± 0.1	39.2 ± 0.4	41.3 ± 0.9	40.2 ± 0.6	41.9 ± 0.9
$C_{18:0}$	5.0 ± 0.1	5.5 ± 0.2	5.5 ± 0.1	4.6 ± 0.1	5.4 ± 0.2	4.9 ± 0.3
$C_{18:2\ cis\ 9,12}$	ND	ND	ND	ND	ND	ND
$C_{17:0\ 2OH}$	2.0 ± 0.2	2.8 ± 0.4	2.1 ± 0.3	1.9 ± 0.3	1.9 ± 0.4	1.6 ± 1.4
$C_{19:0\ cyclo\ 11}$	ND	0.8 ± 0.0	ND	ND	ND	1.0 ± 0.2
$C_{20:0}$	ND	ND	ND	ND	ND	ND
Others[e]	1.3 ± 0.6	0.4 ± 0.7	1.5 ± 0.1	1.5 ± 0.6	1.6 ± 0.3	0.3 ± 0.6
Sat/Unsat	1.1 ± 0.02	1.2 ± 0.04	1.1 ± 0.01	1.0 ± 0.03	1.1 ± 0.01	1.0 ± 0.02
$C_{10} - C_{17}$ / $C_{18} - C_{20}$ [f]	1.2 ± 0.01	1.2 ± 0.01	1.1 ± 0.01	1.1 ± 0.05	1.1 ± 0.02	1.1 ± 0.06

Shown are averages ± standard deviations from three independent cultures
ND=not detected
Ethanol was added at a final concentration of 0.1%
Oleic acid was added at a final concentration of 20 µg ml-1
Linoleic acid was added at a final concentration of 10 µg ml-1
Others indicates fatty acids that comprised <1% of the total membrane content
Fatty acid length ratio includes both saturated and unsaturated fatty acid

Table S2.5 *E. faecalis* OG1RF, Δ*mprF2,* Δ*cls1,* Δ*cls2,* Δ*cls1/cls2*, and Δ*mprF2/cls1/cls2* membrane fatty acid composition during exponential phase growth supplemented with oleic acid analyzed via GC-FAME (Microbial ID, Inc.)

% of total membrane content (Avg. ± SD)						
Treatment: Oleic acid						
Fatty acid	OG1RF	Δ*mprF2*	Δ*cls1*	Δ*cls2*	Δ*cls1*Δ*cls2*	Δ*mprF2* Δ*cls1* Δ*cls2*
$C_{12:0}$	0.7 ± 0.1	1.2 ± 0.1	0.7 ± 0.1	0.8 ± 0.1	0.6 ± 0.1	1.6 ± 0.2
$C_{14:0}$	2.5 ± 0.2	4.2 ± 0.1	2.4 ± 0.1	2.4 ± 0.02	1.6 ± 0.1	4.0 ± 0.2
$C_{16:1\ cis\ 9}$	3.8 ± 0.3	5.7 ± 0.3	3.8 ± 0.1	4.0 ± 0.1	2.7 ± 0.2	5.7 ± 0.4
$C_{16:0}$	19.5 ± 0.6	31.1 ± 0.1	18.6 ± 0.5	18.0 ± 0.3	14.7 ± 0.6	29.5 ± 0.1
$C_{18:1\ cis\ 9}$	46.7 ± 1.7	11.1 ± 1.0	47.1 ± 1.7	42.2 ± 6.0	59.8 ± 2.1	11.5 ± 4.3
$C_{18:1\ cis\ 11}$	19.0 ± 0.6	29.9 ± 0.3	18.3 ± 0.4	19.0 ± 0.7	14.8 ± 0.4	28.0 ± 0.4
$C_{18:0}$	2.9 ± 0.2	3.8 ± 0.2	2.8 ± 0.3	2.6 ± 0.1	2.5 ± 0.1	3.6 ± 0.2
$C_{18:2\ cis\ 9,12}$	ND	ND	ND	ND	ND	ND
$C_{17:0\ 2OH}$	1.1 ± 0.1	1.8 ± 0.3	1.0 ± 0.2	1.1 ± 0.3	0.7 ± 0.1	1.3 ± 0.2
$C_{19:0\ cyclo\ 11}$	ND	0.8 ± 0.1	ND	ND	ND	1.3 ± 0.1
$C_{20:0}$	3.2 ± 0.3	10.0 ± 1.0	4.8 ± 1.2	9.3 ± 5.1	1.8 ± 1.6	13.0 ± 3.3
Others[e]	0.6 ± 0.2	0.5 ± 0.5	0.6 ± 0.1	0.6 ± 0.2	0.8 ± 0.1	0.5 ± 0.4
Sat/Unsat	0.4 ± 0.5	1.1 ± 0.1	0.4 ± 1.0	0.5 ± 0.9	0.3 ± 0.9	1.2 ± 0.2
$C_{10} - C_{17}$ / $C_{18} - C_{20}$ [f]	0.4 ± 0.4	0.8 ± 0.02	0.4 ± 0.3	0.4 ± 0.1	0.3 ± 0.2	0.74 ± 0.03

Shown are averages ± standard deviations from three independent cultures
ND=not detected
Ethanol was added at a final concentration of 0.1%
Oleic acid was added at a final concentration of 20 µg ml-1
Linoleic acid was added at a final concentration of 10 µg ml-1
Others indicates fatty acids that comprised <1% of the total membrane content
Fatty acid length ratio includes both saturated and unsaturated fatty acid

Table S2.6 *E. faecalis* OG1RF, Δ*mprF2,* Δ*cls1,* Δ*cls2,* Δ*cls1/cls2*, and Δ*mprF2/cls1/cls2* membrane fatty acid composition during exponential phase growth supplemented with linoleic acid analyzed via GC-FAME (Microbial ID, Inc.)

% of total membrane content (Avg. ± SD)						
Treatment: Linoleic acid						
Fatty acid	OG1RF	Δ*mprF2*	Δ*cls1*	Δ*cls2*	Δ*cls1*Δ*cls2*	Δ*mprF2* Δ*cls1* Δ*cls2*
$C_{12:0}$	1.2 ± 0.1	1.4 ± 0.2	1.0 ± 0.1	1.1 ± 0.04	1.0 ± 0.1	1.3 ± 0.2
$C_{14:0}$	3.7 ± 0.1	4.3 ± 0.4	3.6 ± 0.1	3.5 ± 0.1	3.0 ± 0.1	3.5 ± 0.3
$C_{16:1\ cis\ 9}$	6.1 ± 0.04	5.9 ± 0.2	5.9 ± 0.2	6.1 ± 0.1	5.4 ± 0.1	5.3 ± 0.3
$C_{16:0}$	29.6 ± 0.5	31.0 ± 2.1	29.2 ± 0.2	29.0 ± 0.6	26.8 ± 0.4	29.0 ± 1.1
$C_{18:1\ cis\ 9}$	ND	ND	ND	ND	ND	ND
$C_{18:1\ cis\ 11}$	28.6 ± 0.5	26.6 ± 1.7	28.4 ± 0.2	30.8 ± 0.9	29.2 ± 0.8	27.0 ± 0.8
$C_{18:0}$	4.3 ± 0.1	4.2 ± 0.5	4.4 ± 0.3	4.0 ± 0.1	4.0 ± 0.2	4.1 ± 0.1
$C_{18:2\ cis\ 9,12}$	24.0 ± 0.9	23.4 ± 3.1	28.4 ± 0.2	22.0 ± 1.4	27.8 ± 0.9	26.1 ± 2.7
$C_{17:0\ 2OH}$	1.6 ± 0.1	1.9 ± 0.2	1.8 ± 0.03	1.7 ± 0.1	1.8 ± 0.1	2.2 ± 0.2
$C_{19:0\ cyclo\ 11}$	ND	0.7 ± 0.1	ND	ND	ND	1.2 ± 0.1
$C_{20:0}$	ND	ND	ND	ND	ND	ND
Others[e]	0.9 ± 0.3	0.7 ± 1.0	0.7 ± 0.2	1.7 ± 0.8	1.1 ± 0.2	0.5 ± 0.4
Sat/Unsat	0.7 ± 0.5	0.8 ± 0.6	0.7 ± 0.7	0.7 ± 0.4	0.6 ± 0.5	0.7 ± 0.5
$C_{10} - C_{17}$ / $C_{18} - C_{20}$ [f]	0.7 ± 0.5	0.8 ± 0.6	0.7 ± 0.5	0.7 ± 0.3	0.6 ± 0.4	0.7 ± 0.6

Shown are averages ± standard deviations from three independent cultures
ND=not detected
Ethanol was added at a final concentration of 0.1%
Oleic acid was added at a final concentration of 20 µg ml-1
Linoleic acid was added at a final concentration of 10 µg ml-1
Others indicates fatty acids that comprised <1% of the total membrane content
Fatty acid length ratio includes both saturated and unsaturated fatty acid

Table S2.7 Exponential phase generation times if given long term

	Generation times in medium constituent (min)		
Strain	Ethanol[a]	Oleic acid[b]	Linoleic acid[c]
OG1RF	37.0 ± 0.3	47.0 ± 1.1	88.2 ± 8.3
Δ*mprF2*	38.3 ± 1.0	36.2 ± 1.5	74.8 ± 6.9
Δ*cls1*	36.7 ± 1.5	47.2 ± 0.2	77.5 ± 1.1
Δ*cls2*	35.9 ± 1.0	50.1 ± 2.3	86.0. ± 6.8
Δ*cls1*/*cls2*	35.0 ± 0.9	52.2 ± 0.4	252.9 ± 98.5
Δ*mprF2*/*cls1*/*cls2*	38.8 ± 5.1	39.7 ± 3.5	195.5 ± 22.2

Shown are averages ± standard deviations from three independent cultures.
Ethanol was added at a final concentration of 0.1%.
Oleic acid was added at a final concentration of 20 µg ml-1
Linoleic acid was added at a final concentration of 10 µg ml-1 .

Figure S2.1 Heat-map of *Δcls1* and *Δcls2* compared to OG1RF in solvent control.Heat-map of fold changes comparing Δcls1 and Δcls2 mutant strains to OG1RF parental strain in solvent control (ethanol). Shown are the average fold changes of those detected lipid species above limit of detection for n = 5 samples. * P = 0.1-0.05; ** P = 0.05-0.01; *** P<0.01.

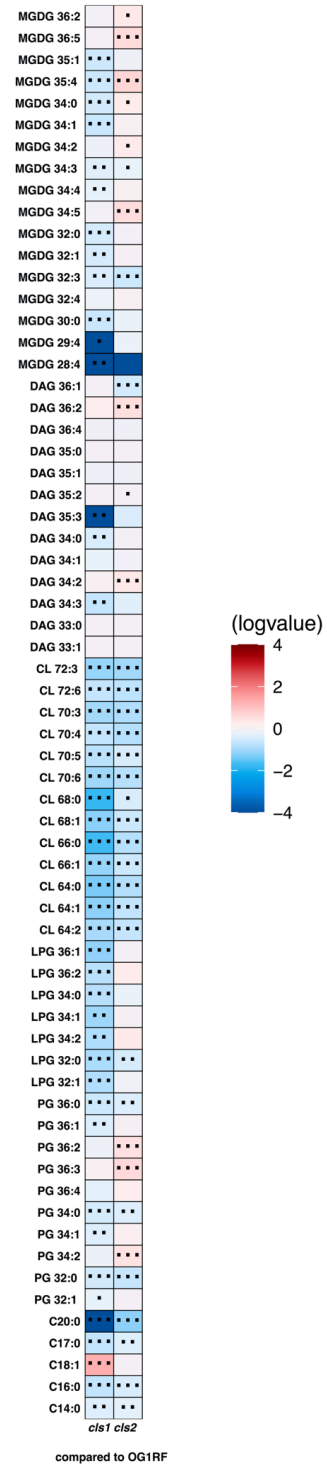
MGDG 36:2
MGDG 36:5
MGDG 35:1
MGDG 35:4
MGDG 34:0
MGDG 34:1
MGDG 34:2
MGDG 34:3
MGDG 34:4
MGDG 34:5
MGDG 32:0
MGDG 32:1
MGDG 32:3
MGDG 32:4
MGDG 30:0
MGDG 29:4
MGDG 28:4
DAG 36:1
DAG 36:2
DAG 36:4
DAG 35:0
DAG 35:1
DAG 35:2
DAG 35:3
DAG 34:0
DAG 34:1
DAG 34:2
DAG 34:3
DAG 33:0
DAG 33:1
CL 72:3
CL 72:6
CL 70:3
CL 70:4
CL 70:5
CL 70:6
CL 68:0
CL 68:1
CL 66:0
CL 66:1
CL 64:0
CL 64:1
CL 64:2
LPG 36:1
LPG 36:2
LPG 34:0
LPG 34:1
LPG 34:2
LPG 32:0
LPG 32:1
PG 36:0
PG 36:1
PG 36:2
PG 36:3
PG 36:4
PG 34:0
PG 34:1
PG 34:2
PG 32:0
PG 32:1
C20:0
C17:0
C18:1
C16:0
C14:0
cls1 cls2
compared to OG1RF
(logvalue)
4
2
0
−2
−4

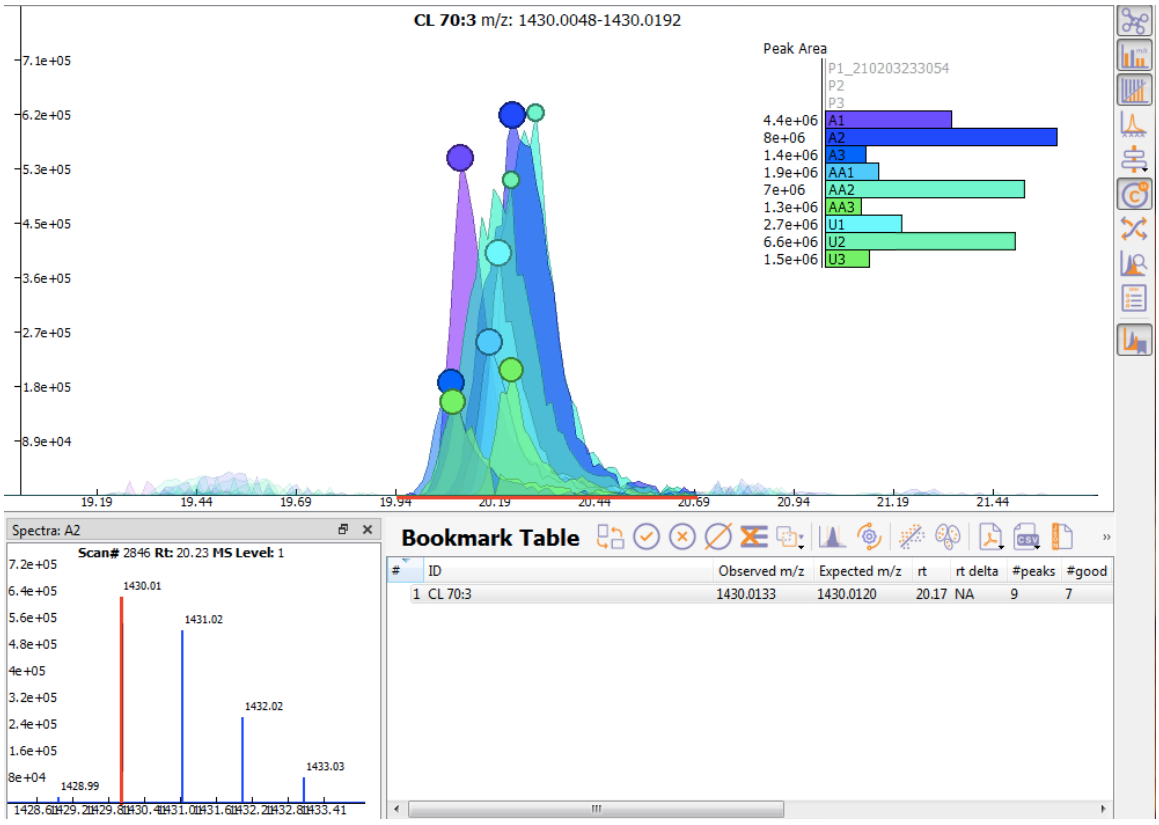

Figure S2.2 Chromatogram of OG1RF, cls1, cls2, and cls1/cls2 displaying cardiolipin 70:3. Sample ID's: A1: OG1RF ETOH, A2: OG1RF OA, A3: OG1RF LA, AA1: cls2 ETOH, AA2: cls2 OA, AA3: cls2 LA, U1: cls1 ETOH, U2: cls1 OA, U3: cls1 LA, P1: cls1/cls2: ETOH, P2: cls1/cls2 OA, P3: cls1/cls2 LA.

Figure S2.3 Heat-map of *Δcls1/Δcls 2* compared to OG1RF in solvent control. Heat-map of fold changes comparing *Δcls1*/ *Δcls2* mutant strain to OG1RF parental strain in solvent control (ethanol). Shown are the average fold changes of those detected lipid species above limit of detection for *n* = 5 samples. * *P* = 0.1-0.05; ** *P* = 0.05-0.01; * *P*<0.01.**

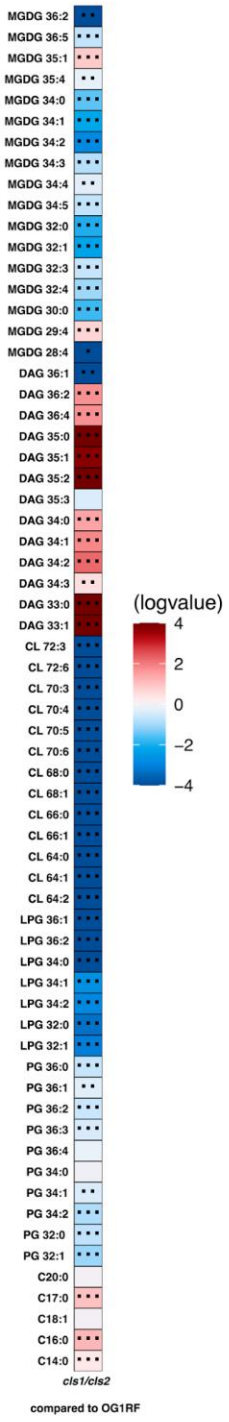
MGDG 36:2
MGDG 36:5
MGDG 35:1
MGDG 35:4
MGDG 34:0
MGDG 34:1
MGDG 34:2
MGDG 34:3
MGDG 34:4
MGDG 34:5
MGDG 32:0
MGDG 32:1
MGDG 32:3
MGDG 32:4
MGDG 30:0
MGDG 29:4
MGDG 28:4
DAG 36:1
DAG 36:2
DAG 36:4
DAG 35:0
DAG 35:1
DAG 35:2
DAG 35:3
DAG 34:0
DAG 34:1
DAG 34:2
DAG 34:3
DAG 33:0
DAG 33:1
CL 72:3
CL 72:6
CL 70:3
CL 70:4
CL 70:5
CL 70:6
CL 68:0
CL 68:1
CL 66:0
CL 66:1
CL 64:0
CL 64:1
CL 64:2
LPG 36:1
LPG 36:2
LPG 34:0
LPG 34:1
LPG 34:2
LPG 32:0
LPG 32:1
PG 36:0
PG 36:1
PG 36:2
PG 36:3
PG 36:4
PG 34:0
PG 34:1
PG 34:2
PG 32:0
PG 32:1
C20:0
C17:0
C18:1
C16:0
C14:0
cls1/cls2
compared to OG1RF
(logvalue)
4
2
0
−2
−4

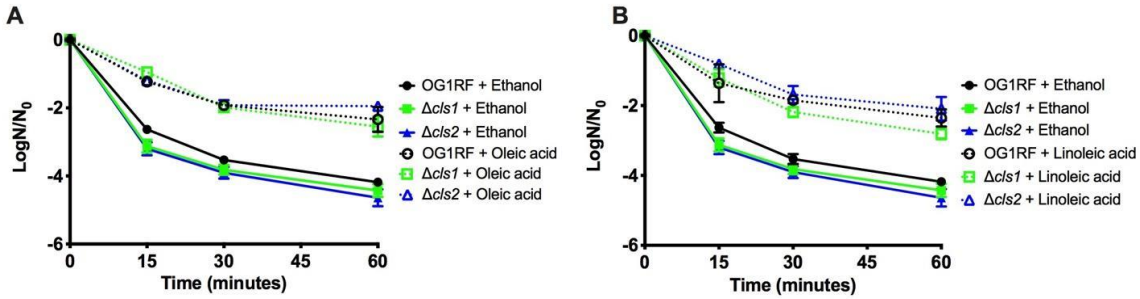

Figure S2.4 Short-term fatty acid supplementation with host fatty acids protects OG1RF *Δcls1* and *Δcls2* from daptomcyin challenge. Supplementation with oleic acid (A) or linoleic acid (B) for either *Δcls1* or *Δcls2* had statistically increased numbers of survivors versus the solvent control at all time points assessed (P = 0.0001). Shown are the average ± standard deviation for n = 3.

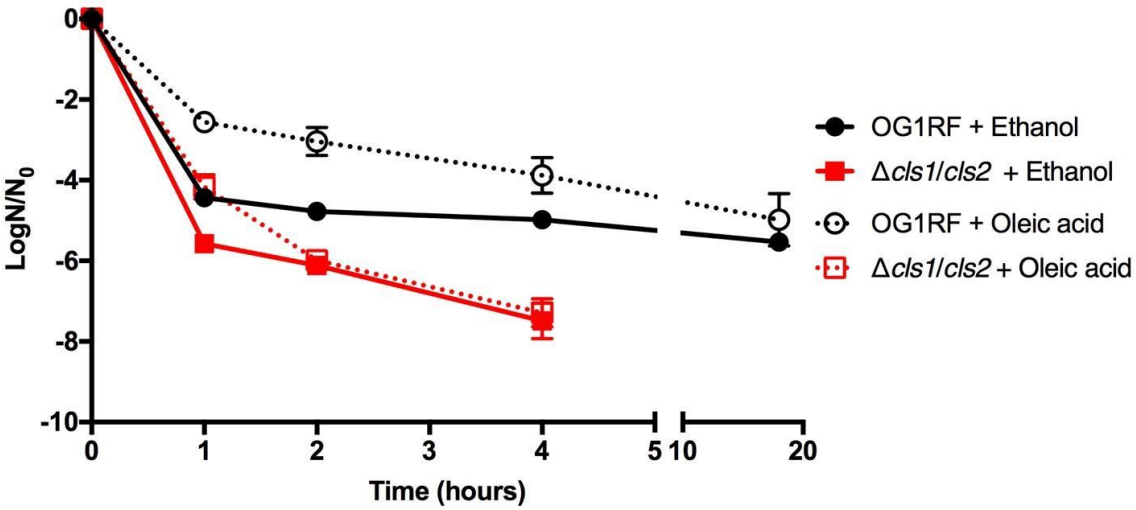

Figure S2.5 Short-term supplementation with oleic acid does not protect *Δcls1/cls2* from extended daptomycin challenge. The *Δcls1/cls2* had no viable colonies after 4 h of exposure. Shown are the averages ± standard deviation for n = 3.

Figure S2.6 Heat-map of *ΔmprF2* compared to OG1RF in solvent control. Heat-map of fold changes comparing *ΔmprF2* mutant strain to OG1RF parental strain in solvent control (ethanol). Shown are the average fold changes of those detected lipid species above limit of detection for *n* = 5 samples. * *P* = 0.1-0.05; ** *P* = 0.05-0.01; * *P*<0.01.**

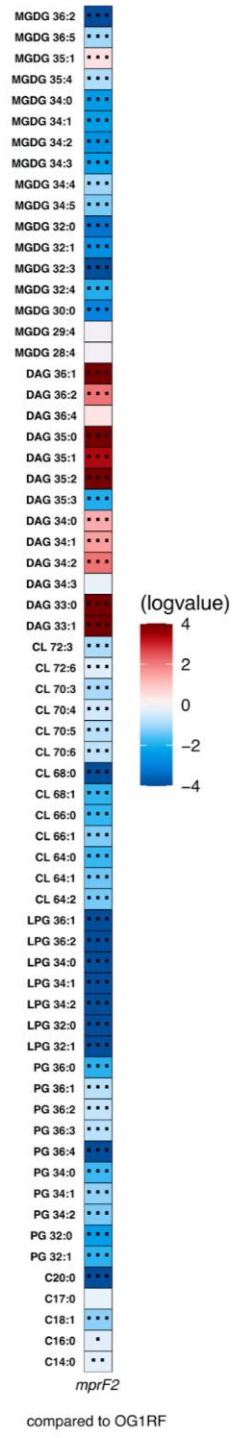
MGDG 36:2
MGDG 36:5
MGDG 35:1
MGDG 35:4
MGDG 34:0
MGDG 34:1
MGDG 34:2
MGDG 34:3
MGDG 34:4
MGDG 34:5
MGDG 32:0
MGDG 32:1
MGDG 32:3
MGDG 32:4
MGDG 30:0
MGDG 29:4
MGDG 28:4
DAG 36:1
DAG 36:2
DAG 36:4
DAG 35:0
DAG 35:1
DAG 35:2
DAG 35:3
DAG 34:0
DAG 34:1
DAG 34:2
DAG 34:3
DAG 33:0
DAG 33:1
CL 72:3
CL 72:6
CL 70:3
CL 70:4
CL 70:5
CL 70:6
CL 68:0
CL 68:1
CL 66:0
CL 66:1
CL 64:0
CL 64:1
CL 64:2
LPG 36:1
LPG 36:2
LPG 34:0
LPG 34:1
LPG 34:2
LPG 32:0
LPG 32:1
PG 36:0
PG 36:1
PG 36:2
PG 36:3
PG 36:4
PG 34:0
PG 34:1
PG 34:2
PG 32:0
PG 32:1
C20:0
C17:0
C18:1
C16:0
C14:0
mprF2
(logvalue)
4
2
0
−2
−4
compared to OG1RF

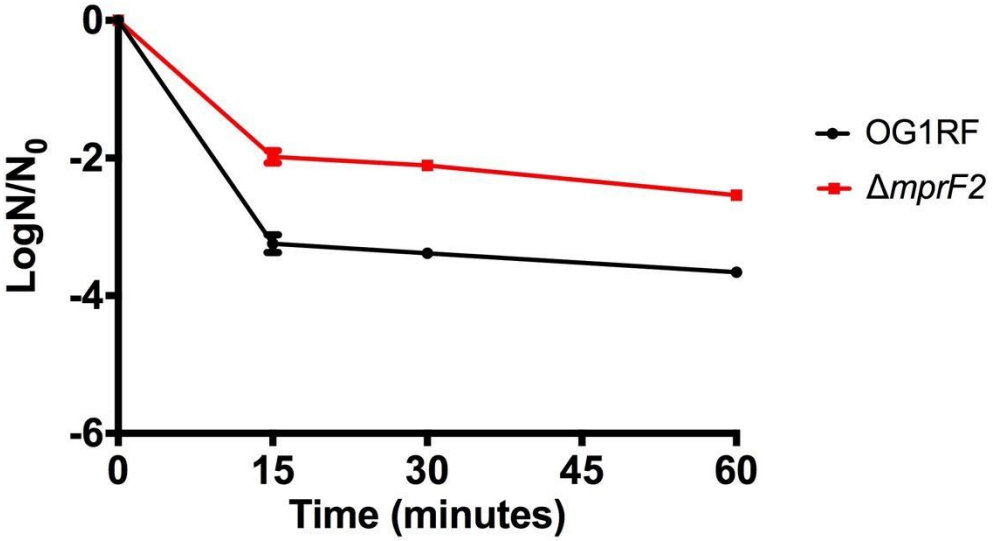

Figure S2.7 *ΔmprF2* survives SDS challenge better than the parental strain. Experimental details are found within the Materials and Methods. *ΔmprF2* had statistically more survivors (P<0.01) than the parental strain at each time point. Shown are the averages ± standard deviation for n=3.

Figure S2.8 Heat-map of *ΔmprF2/cls1/cls2* compared to OG1RF in solvent control. Heat-map of fold changes comparing *ΔmprF2/cls1/cls2* mutant strain to OG1RF parental strain in solvent control (ethanol). Shown are the average fold changes of those detected lipid species above limit of detection for *n* = 5 samples. * *P* = 0.1-0.05; ** *P* = 0.05-0.01; * *P*<0.01**

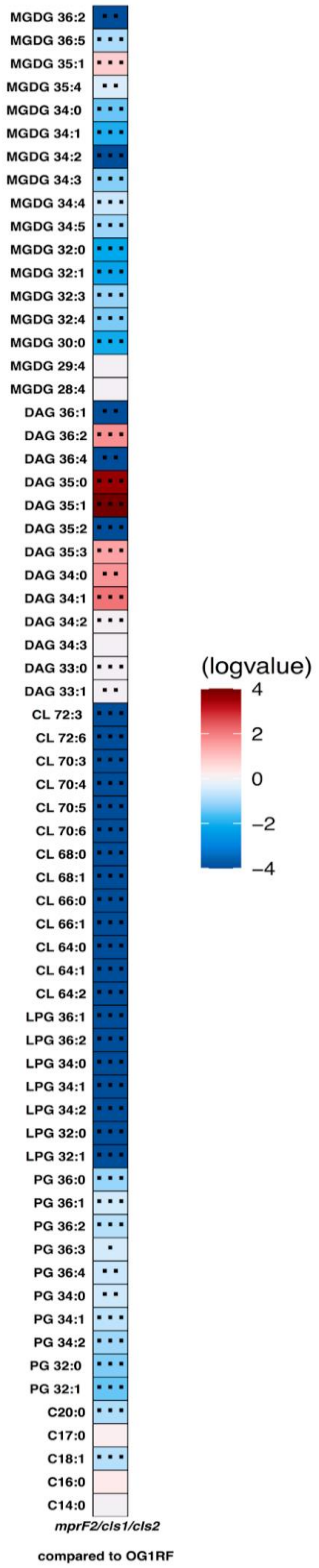
MGDG 36:2
MGDG 36:5
MGDG 35:1
MGDG 35:4
MGDG 34:0
MGDG 34:1
MGDG 34:2
MGDG 34:3
MGDG 34:4
MGDG 34:5
MGDG 32:0
MGDG 32:1
MGDG 32:3
MGDG 32:4
MGDG 30:0
MGDG 29:4
MGDG 28:4
DAG 36:1
DAG 36:2
DAG 36:4
DAG 35:0
DAG 35:1
DAG 35:2
DAG 35:3
DAG 34:0
DAG 34:1
DAG 34:2
DAG 34:3
DAG 33:0
DAG 33:1
CL 72:3
CL 72:6
CL 70:3
CL 70:4
CL 70:5
CL 70:6
CL 68:0
CL 68:1
CL 66:0
CL 66:1
CL 64:0
CL 64:1
CL 64:2
LPG 36:1
LPG 36:2
LPG 34:0
LPG 34:1
LPG 34:2
LPG 32:0
LPG 32:1
PG 36:0
PG 36:1
PG 36:2
PG 36:3
PG 36:4
PG 34:0
PG 34:1
PG 34:2
PG 32:0
PG 32:1
C20:0
C17:0
C18:1
C16:0
C14:0
mprF2/cls1/cls2
compared to OG1RF
(logvalue)
4
2
0
−2
−4

CHAPTER III
Dual stable-isotopes enhance lipidomics studies bacterial model organism *Enterococcus faecalis*

A version of this chapter will be submitted for future publication.

Brittni M. Woodall, Elizabeth M. Fozo, Shawn R. Campagna

BMW performed all experiments and prepared cells for analysis. BMW performed lipid analyses and subsequent data analyses. BMW SRC, and EMF contributed to the writing of the manuscript. SRC and EMF directed the project.

3.1 Abstract

Dual stable isotope probes deuterium oxide and ^{13}C fatty acid were demonstrated to probe the lipid biosynthesis cycle of a Gram-positive bacterium *Enterococcus faecalis*. As external nutrients and carbon sources often interact with metabolic processes, the use of dual labeled isotope pools allowed for the simultaneous investigation of both exogenous nutrient incorporation or modification as well as *de novo* biosynthesis. Deuterium was utilized to trace *de novo* fatty acid biosynthesis through solvent mediated proton transfer during elongation of the carbon chain while ^{13}C-fatty acids were utilized to trace exogenous nutrient metabolism and modification through lipid synthesis. Ultra-high performance liquid chromatography high-resolution mass spectrometry identified 30 lipid species of which incorporated deuterium and/or ^{13}C fatty acid into the membrane. Additionally, MS^2 fragments of isolated lipids identified acyl tail position confirming enzymatic activity of PlsY in the incorporation of the ^{13}C fatty acid into membrane lipids.

3.2 Introduction

Enterococcus faecalis is a Gram-positive bacterium that typically resides as a commensal in the gut of human hosts; however, this organism can cause disease in the immunocompromised if colonization outside of the gut occurs. This microorganism inhabits fatty acid rich environments, and research has demonstrated that the membrane composition of E*. faecalis* is altered when exposed to exogenous fatty acids in a laboratory setting [1-3]. Compared to other gut commensals, such as *Escherichia coli, E. faecalis* has a unique lipid biosynthesis pathway that does not perform β-oxidation and cannot utilize exogenous fatty acids as a primary carbon source [4]. *E. faecalis* synthesizes primarily the following glycerophospholipids: phosphatidylglycerol (PG), lysyl-phosphatidylglycerol (L-PG), cardiolipin (CL), diacylglycerol (DAG) and monoglucosyl-diacylglycerol (MGDG) [5-7]. It has been hypothesized that the Fak system phosphorylates fatty acids, forming acyl phosphates, which are then used in one of two ways: 1.) PlsY can utilize the acyl phosphate to form lyso-phosphatidic acid which can further be used by PlsC or 2.) PlsX can utilize the acyl phosphate mediating the transfer of the acyl phosphate to an acyl carrier protein which can be used by PlsC. Both PlsY and PlsC have unique roles in the lipid biosynthesis cycle in that PlsY adds acyl tails at the sn1 position of the lipid, and PlsC adds acyl tails at the sn2 position. PlsC can also utilize acyl-carrier

protein bound acyl chains synthesized *de novo* by the type II fatty acid biosynthesis cycle (FAS II)[7-9] (Supporting information).

Previously, the membrane of *E. faecalis* has been studied via gas-chromatography—fatty acid methyl ester analysis (GC-FAME), as well as ultra-high performance liquid chromatography—high-resolution mass spectrometry analysis (UHPLC-HRMS) [2, 3, 5, 6, 10-12]. Addition of exogenous fatty acids to the growth environment resulted in alterations of both the fatty acid methyl ester content as well as the global lipidome [3, 10]. Specifically, oleic acid concentrations increased as observed in both the GC-FAME profile, and as a free fatty acid (UHPLC-HRMS) when supplemented into culture during exponential phase growth. Several lipid species (PG 36:2, LPG 36:2, MGDG 36:2 and several CL species) that could contain oleic acid tails also increased in abundance; however, *E. faecalis* can produce *cis*-vaccenic acid (CVA) *de novo*, which is a constitutional isomer of oleic acid with the same exact mass [1, 3, 10]. Without the use of isotopically labeled fatty acids or multiple generation mass spectrometric product spectra, it was not possible to discern which membrane alterations were directly related to exogenous supplementation versus those that could arise via *de novo* synthesis.

Isotope tracing is a technique that allows changes within metabolism and cellular processes to be traced in a wide variety of biological systems. The utilization of isotope tracers supplied as nutrient sources (both organic and inorganic) has been used to study many processes and systems ranging from bacterial pathogenesis, health and human disease, environmental microbiology, and forensic science. Specifically, ^{2}H (D), ^{13}C and ^{15}N containing isotopologues are used routinely to better understand metabolism and nutrient cycling [13, 14]. When considering the lipid membrane specifically, several techniques utilize ^{13}C-labeled carbon sources (e.g., fatty acids, glycerol, or glucose) to trace incorporation or modification of the isotopically labeled substrate [15, 16]. Other studies have utilized D_2O as a stable-isotope tracer to track hydrogen incorporation from the medium into metabolites as biosynthesis or degradation occurs; these efforts have provided a wealth of information on lipid turnover rates in several systems [17-19]. As single isotope probes have progressed the knowledge of lipid metabolism, few studies have investigated the impact of dual isotope probes [20]. Several analytical methodologies utilizing dual isotopes D_2O and ^{13}C have been reported; however, these studies either utilized nuclear magnetic resonance [21], which lacks the ability to measure a breadth of metabolites, or utilized mass spectrometric techniques to measure less than 5 compounds [22, 23]. Further, many of these studies also used the isotopes asynchronously to differentiate metabolites generated at different points in the experiment instead of using them to differentiate simultaneously occurring biological transformations.

As biological systems uptake nutrients from the environment and/or alter *de novo* metabolic processes in response to external stimuli, the need to simultaneously monitor both external inputs into systems and primary

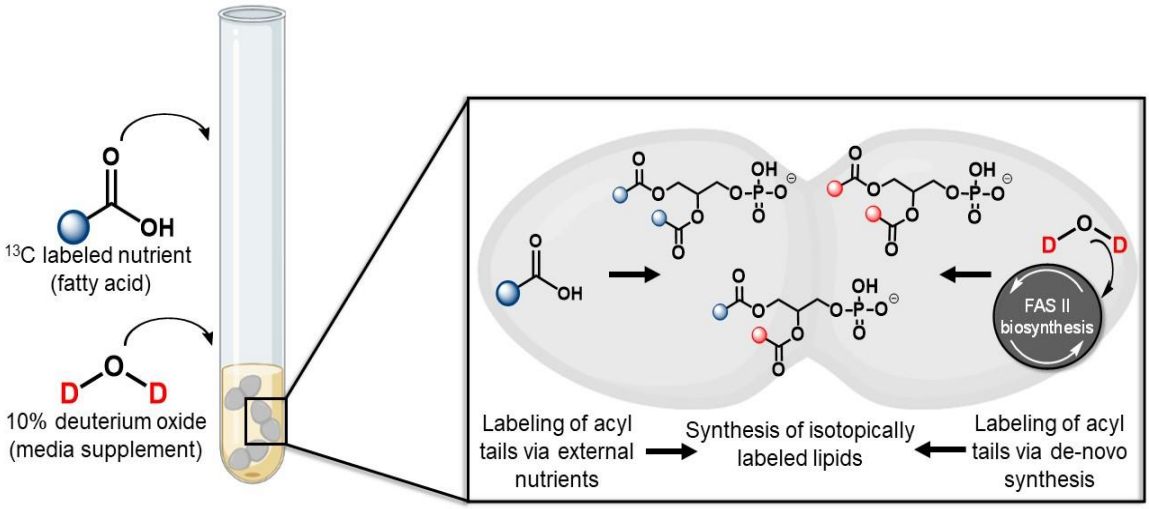

,

Figure 3.0 Graphical abstract of experimental design

metabolism exists. As modern mass spectrometers often have high resolving power and can differentiate almost all isotopologues derived from different elemental isotopes, it is possible to monitor metabolic processes which utilize deuterium or ^{13}C. Although deuterium has been utilized independently to provide lipid synthesis rates in many systems and ^{13}C and ^{15}N have been utilized to probe metabolic fluxes of external nutrients throughout systems, there are no reported studies which combine both methodologies to monitor *de novo* biosynthesis processes as well as exogenous macromolecular input utilization [24, 25]. Given that it is possible to utilize mass spectrometry for differentiation between lipid species that have been altered via incorporation of carbon and/or deuterium isotopes, both of which originate from different biological processes, it was hypothesized that lipids detected with isotope labels could be used to distinguish between lipid biosynthetic processes which utilized an exogenously supplied ^{13}C labeled fatty acid versus those that synthesize fatty acids *de novo*. To further probe lipid biosynthesis and membrane composition of this bacterium, an experiment was designed to trace *de novo* lipid biosynthesis through the incorporation of deuterium from D_2O in the media, as well as the incorporation of exogenous ^{13}C-labelled fatty acid from the addition of ^{13}C-oleic acid. Here in, the benefits of pairing dual stable isotope probes to study lipid metabolism and membrane composition in *E. faecalis* by mass spectrometric identification of lipid moieties and their respective fragments are described.

3.3 Materials and Methods

3.3.1 Lipid standards and materials

Lipid standards were purchased from Avanti Polar Lipids, Alabaster. AL, unless specifically stated otherwise. Oleic acid (U-$^{13}C_{18}$, 98%) and deuterium oxide (99%) were purchased from Cambridge Isotope Laboratories, Tewksbury, MA. Oleic acid and ethanol were purchased from Millipore-Sigma. St. Louis, Missouri. All solvents and buffer components were purchased from Fischer Scientific. Standards included CL 56:0 (internal standard), CL 72:0, CL 72:4 PG 16:0 (internal standard), PG 36:0, LPG 36:0, LPG 36:2, MGDG 34:1, and lipid SPLASH standard mix, commercially available from Avanti Polar Lipids. Internal standards PG 16:0 and CL 56:0 were used to ensure each sample was injected and ionized efficiently, however internal standards for the L-PG, DAG, and MGDG classes were not utilized considering commercially available standards would interfere with lipids found within the bacterial cell. External lipid standards (100uM-5nM) were analyzed to verify retention times of lipids annotated in the previously published liquid chromatography method; further details can be found in supplementary information [10].

3.3.2 Bacterial growth conditions and cell harvest/extraction

Bacterial growth conditions for this experiment were as follows: *E. faecalis* OG1RF was grown statically in brain heart infusion medium (BHI; BD Difco) at 37

°C. Overnight cultures were diluted to a final OD_{600} of 0.01 into fresh BHI media containing 10% D_2O, grown to mid-log phase (OD_{600} ~0.25), then supplemented with one of the following treatments: ^{13}C-oleic acid, oleic acid, or an equal volume of ethanol. Previous reports have observed slowed metabolism due to the kinetic isotope effect, therefore, the concentration of deuterium oxide (10% D_2O) was chosen to avoid kinetic growth effects and metabolic perturbations [18, 26]. An additional control set of samples were inoculated from overnight culture into fresh BHI containing no D_2O and subjected to either equal parts ethanol by volume, ^{13}C-oleic acid, or oleic acid. Oleic acid (labeled and unlabeled) was supplemented at a final concentration of 20 µg/mL. Cells were harvested 30 minutes after supplementation with either ethanol, ^{13}C-oleic acid or oleic acid. Phospholipid extraction was performed in the manner described previously [10, 27]. Full details on extraction protocol can be found in supporting information.

3.3.3 Ultra-high performance liquid chromatography high- resolution mass spectrometry analysis (UHPLC-HRMS)

UHPLC-HRMS analysis was performed on a Vanquish ultra- high performance liquid chromatography system (Dionex, Sunnyvale, CA) coupled to an Exploris 120 (Thermo Scientific) mass spectrometer operated in positive and negative mode adapted from a method previously described [10]. A Thermo C30 column 2.1x150 mm, 2.6 µm pore size, was used to separate 2 µL of sample. Full chromatographic and mass spectrometric parameters can be found in the supporting information. Ions of respective diacylglycerol (DAG) and monoglucosyl-diacylglycerol (MGDG) species were detected in positive mode as ammonium adducts while phosphatidylglycerol (PG), lysyl-phosphatidylglycerol (L-PG), cardiolipin (CL), and free fatty acids (FFA) were detected in negative mode. The mass spectrometer was operated in data dependent acquisition (DDA) mode for which the full scan spectra (100-2,000 *m/z*) were collected at 120,000 resolution (at 200 *m/z)* and the MS^2 spectra were collected at stepped collisional energies of 25, 50, and 75 eV at a resolution of 30,000. The mass spectrometer was calibrated every 24 hours in both modes. Mass calibration was performed utilizing the Pierce™ FlexMix™ calibration solution commercially available from Thermo Scientific to ensure high mass accurary. Both base calibration of the instrument and mass calibration of the instrument were maintained throughout the study.

3.3.4 Data analysis

Raw files acquired from Xcalibur (Thermo Scientific) were converted to .mzML format using MS convert made available by ProteoWizard. El MAVEN was used to integrate the extracted ion chromatogram peaks. Initial data processing utilized a ppm error of 5ppm or less, however; limitations in the El MAVEN software package cause the M+1 isotopologue to be randomly pick as either a D or 13C isotopologue for each compound instead of accurately identifying the M+1 peak as one or the other. Therefore lipid identifications and/or

annotations were made using exact mass (*m/z* error ≤20 ppm) and retention time (deviation from time ≤5 seconds) from a list of potential lipids that was curated to contain lipids expected to be found in *E. faecalis* based on data reported in previously published gas-chromatography fatty acid methyl ester analysis. Single deuterium incorporation versus single ^{13}C incorporation cannot be resolved with 120,000 resolving power (at 200 *m/z)* as described in this method, however; the analysis of non-deuterated cultures allowed for isotope correction to be performed eliminating the need for single isotope resolution. The natural abundance of ^{13}C isotopoglogues present in the bacterial cultures was measured, and these values were subtracted from those for the isomeric peaks measured from the paired deuterated bacterial cultures. This subtraction allowed for any ion detection above that of naturally occurring ^{13}C to be contributed to deuterium incorporation. The equations for these data analyses are described in detail in the supporting information. Any isotopologue above that of the M+1 peak was capable of baseline resolution at 120,000 (200 *m/z*) and was accurately identified as a D or ^{13}C isotopologue by the El MAVEN platform. All deuterium and carbon isotopologues were integrated with parameters identical to those of parent species. The Freestyle Thermo Fischer software package was utilized to filter and export MS^2 data scans for acyl tail identification and position. Fragmentation patterns of lipid species were predicted and identified based on the previously reported work of Murphy and Axelsen [28]. All integrated ion intensities were normalized to OD600 values obtained at time of harvest to account for variation in growth. Biological replicates of n=5 (per group) were analyzed unless stated otherwise.

3.4 Results

3.4.1 UHLPC-HRMS detects stable isotope incorporation into membrane lipids

Global lipidome analysis detected the presence of 30 unique phospholipid species within the membrane of *E. faecalis* along with the associated deuterium and ^{13}C isotopologues. In all experiments utilizing D_2O in the medium, various numbers of deuterium were detected within membrane lipids. Differences in both the number of lipids that incorporated deuterium (% of lipid with deuterium incorporation) and number of deuterium per fatty acyl tail were observed for lipid species in the presence of oleic acid (+) or absence of oleic acid (-) (Table 1, Figure 1 and 2). The addition of unlabeled oleic acid to bacterial cultures grown in the presence of 10% D_2O resulted in decreased deuterium abundance for lipids that could contain a C18:1 acyl tail (CL 70:3, PG 34:1, DAG 34:1, etc); however, lipids that did not contain C18:1 acyl tails incorporated a higher percentage of deuterium (PG 30:0, PG 32:0, PG 34:0);Table 1, Figure 1 and 2). Exposing *E. faecalis* to both ^{13}C-oleic acid and 10% D_2O led to incorporation of intact ^{13}C-oleic acid in 24 of the 30 detected phospholipids (Table 1). Differences in percent incorporation of deuterium and ^{13}C- oleic acid were also detected among lipid species (Table 1). Two tailed lipid species were observed to

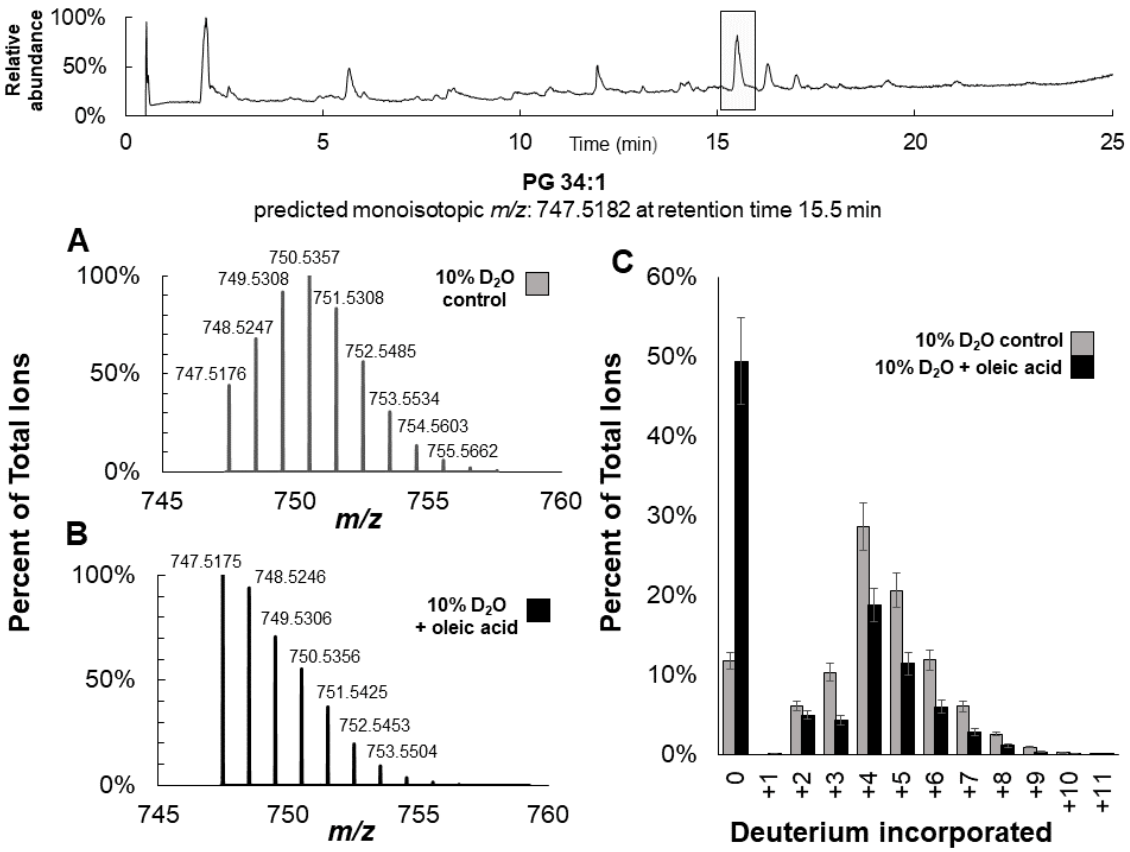

Figure 3.1 Total ion chromatogram highlighting retention time of lipid species. A) Full scan mass spectrum (120,000 resolving power), demonstrating isotopologues for PG 34:1 detected in bacterial culture supplemented with 10% D_2O. B) Full scan mass spectrum (120,000 resolving power), demonstrating isotopologues for PG 34:1 detected in bacterial culture supplemented with 10% D_2O and oleic acid. C) Averaged and corrected deuterium incorporation for bacterial cultures supplemented with ethanol (grey) versus oleic acid (black) grown in the presence of 10% D_2O for PG 34:1.

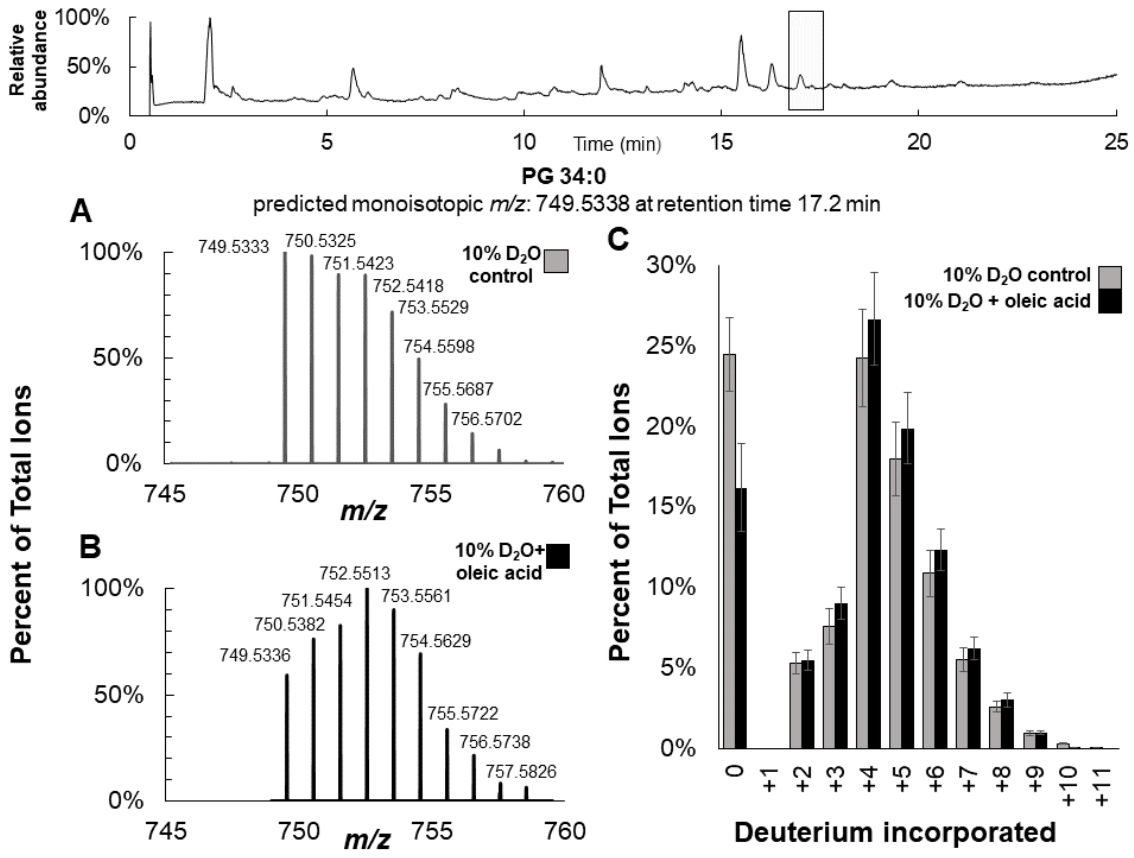

Figure 3.2 Total ion chromatogram highlighting retention time of lipid species. A) Full scan mass spectrum (120,000 resolving power), demonstrating isotopologues for PG 34:0 detected in bacterial culture supplemented with 10% D_2O. B) Full scan mass spectrum (120,000 resolving power), demonstrating isotopologues for PG 34:0 detected in bacterial culture supplemented with 10% D_2O and oleic acid. C) Averaged and corrected deuterium incorporation for bacterial cultures supplemented with ethanol (grey) versus oleic acid (black) grown in the presence of 10% D_2O for PG 34:0.

Table 3.1 . Calculations of isotope incorporation for single and dual labeled experiments

Addition:	10% D_2O	10% D_2O + C18:1		10% D_2O + ^{13}C18:1		
Lipid species	% w/ D incorporation	% w/ D incorporation	% lipid species w/ 0 ^{13}C18:1 (% w/ D incorporation)	% lipid species w/ 1 ^{13}C18:1 (% w/ D incorporation)	% lipid species w/ >1 ^{13}C18:1 (% w/ D incorporation)	max # of D incorporated for all cultures
PG 30:0	57.7±4.6	80.2±5.5	100±12.4 (80.3±5)	-	-	8
PG 30:1	62.3±4.8	61.7±5.0	81.6±10.1 (69.8±5.1)	18.3±1.3 (24.6±4)	-	7
PG 32:0	55.23±4.3	76.1±5.1	100±13 (75.2±5)	-	-	10
PG 32:1	77.1±5.5	56.9±6.1	40.9±4.3 (86.4±5.7)	59±7.7 (36.1±3.8)	-	9
PG 32:2	69.8±4.9	47.1±4.6	42.3±4.4 (75.8±5.4)	57.6±8.3 (34.3±4.2)	-	8
PG 33:1	61.4±4.9	34.2±3.9	100±15.2 (62.2±5.1)	-	-	7
PG 34:0	75.5±4.8	83.8±5.2	100±13 (88±5.5)	-	-	11
PG 34:1	88.1±5.5	50.5±4.1	41.1±4.2 (89.4±5.6)	58.8±8.2 (31.6±3.7)	-	11
PG 35:1	89.9±5.2	72.6±5.0	36.1±3.6 (81.8±5.4)	63.8±7.3 (50.2±4.3)	-	9
PG 36:0	79.5±5.6	41.6±5.1	100±21.6 (52.6±6.4)	-	-	7
PG 36:1	87.6±5.4	66.0±4.8	43.6±4.7 (91.6±5.9)	56.3±5.9 (51.1±4.4)	-	10
PG 36:2	85.1±5.4	31.0±3.1	12.3±1.2 (89.8±5.7)	28.4±2.2 (59.6±4.6)	59.2±2.9 (0±0.0)	10
PG 37:2	84.6±6.1	22.3±2.9	10.8±1.8 (70.2±9.5)	89.1±11.5 (61.9±4.6)	-	7
DAG 34:1	90.9±5.9	60.9±5.7	85.5±22.5 (96.6±12.4)	14.4±0.7 (19.7±3.1)	-	10
DAG 36:1	80.9±5.2	33.4±3.7	57.1±6.5 (62.6±5.3)	42.8±6.3 (13.9±2.3)	-	8
DAG 36:2	95.4±5.9	58.8±5.0	41.2±7.7 (91±10.4)	37±6.3 (100±2.3)	21.8±2.3 (0±0.0)	10
MGDG 34:1	83.6±10.7	50.3±7.0	100±9.6 (96.5±8.6)	47±5.6 (29.8±3.5)	-	5
MGDG 34:0	97±8.9	98.3±11.8	52.9±7.3 (89.4±7.2)	-	-	5
MGDG 36:1	93.7±9.9	68.0±6.7	11.3±2.1 (92.5±11)	88.6±6.3 (16.1±3.2)	-	6
CL 62:1	98.9±4.6	97.3±4.5	83.2±6.5 (99.2±3.8)	16.7±2.2 (91.5±8)	-	10
CL 62:2	99.8±4.8	99.3±4.8	76.8±8.2 (99.4±5.3)	23.1±3.9 (95.5±10.2)	-	8
CL 64:1	96.5±5.6	89.4±5.1	74.2±5.9 (99.3±4)	25.7±1.8 (94.9±4.3)	-	8
CL 64:2	98.8±4.7	95.9±5.0	56.9±4.5 (99.3±4.3)	32±2.9 (98.8±5.5)	11±1.1 (74.4±5.8)	10
CL 66:1	97.2±5.2	91.3±4.5	71.3±5.3 (99.3±3.8)	28.6±2.2 (83.9±4.4)	-	12
CL 66:2	97.8±3.9	91.3±4.8	43.2±3.1 (91.2±3.9)	36.9±3.1 (96.7±4.9)	19.4±1.6 (76.2±4.8)	12
CL 66:3	98.2±5.8	92.7±5.4	41.1±3.1 (98.9±4.4)	38.8±3.7 (94.4±5.4)	20±2 (75.2±5.7)	10
CL 68:2	98.6±3.8	90.3±4.1	43.7±3 (99.6±4)	37±2.9 (96.6±4.6)	19.2±1.5 (75.2±4.7)	14
CL 68:3	97.2±6.5	85.6±6.4	25.7±1.9 (98.4±4.5)	34.9±3 (95.8±4.9)	28.7±2.6 (81.1±5)	11
CL 70:3	98.2±3.6	90.6±4.0	13.4±0.9 (97.7±4.5)	26.4±2.1 (97.0±4.7)	*60.2±3.5 (51.5±4.8)	12
CL 72:4	95.3±6.3	83.8±4.8	2.1±0.3 (76.5±8)	11.5±1.2 (98.1±6.4)	†86.4±5.3 (42.5±6.7)	8

*CL 70:3 incorporated 2 and 3 ^{13}C-18:1 acyl tails, and †CL 72:4 incorporated 2, 3, and 4 ^{13}C-18:1 acyl tails. The reported numbers are derived from the summed abundances of isotopologues containing >1 ^{13}C-18:1 acyl tail for both species

incorporate zero to two ^{13}C-oleic acid tails, and four tailed lipids were observed to incorporate between zero and four ^{13}C-oleic acid tails. Consistent with the data acquired after addition of unlabeled oleic acid, the percentage of lipid species containing deuterium decreased with the addition of ^{13}C-oleic acid.

3.4.2 Data dependent acquisition identifies acyl tail position and provides structural information regarding the number and location of deuterium atoms on lipids

The use of data dependent acquisition (DDA) provided fragmentation data for the top four most abundant ions in each full scan spectra, which allowed for acyl tail identification and confirmed deuterium incorporation on the acyl tails of lipid species (Table 2, Figure 3 and 4). Deprotonated fatty acids (RCO2- ions) were detected to confirm acyl tail structure and position, while glycerol phosphate ions minus the loss of water were detected to confirm head group composition (Figure 3 and 4). The addition of unlabeled oleic acid to bacterial cultures grown in the presence of 10% D_2O did not alter the tail positions of phospholipid species detected (Table 2). However, the addition of oleic acid did result in a shift in both lipid concentrations (as previously reported[11]) and deuterium isotope distribution (Table 1 and 2, Figure 3 and 4, and supporting information). The use of DDA allowed for identification of sn1 and sn2 acyl tails of 29 identified bacterial phospholipids (Table 2).

3.4.3 The use of dual stable isotope tracers elucidates biosynthetic mechanism for exogenous fatty acid incorporation

The addition of ^{13}C-oleic acid to the deuterated bacterial cultures resulted in mass spectrometric detection of species incorporating the intact isotope label. The following lipid species incorporated the ^{13}C isotope based on recorded mass shifts: C18:1 (free fatty acid), CL 62:1, CL 62:2, CL 64:1, CL 64:2, CL 66:1, CL 66:2, CL 66:3, CL 68:2, CL 68:3, CL 70:3, CL 72:4, 30:1, PG 32:1, PG 32:2, PG 34:1, PG 35:1, PG 36:1, PG 36:2, PG 37:2, DAG 34:1, DAG 36:1, MGDG 34:1, MGDG 36:1. Lipids that contained only one ^{13}C oleic acid tail were detected with deuterium isotopologues in full scan mode (Table 1, Figure 5). However, in all cases, none of the exogenously incorporated labeled fatty acid was determined to have been modified by the replacement of an H with a D (Figure 6). Further, there was no evidence of ^{13}C incorporation into other fatty acids. Isolation and fragmentation of lipid species exposed to both stable isotopes such as ^{13}C-PG 34:1 confirmed the presence of ^{13}C oleic acid in the sn1 position on lipid species (Figure 5 and 6). Of the observed bacterial phospholipids, 24 lipid species were observed to incorporate one ^{13}C oleic acid as an acyl tail, 9 lipid species were observed to incorporate two ^{13}C oleic acids as acyl tails, 3 lipid species were observed to incorporate three ^{13}C oleic acids as acyl tails, and one lipid species were observed to incorporate four ^{13}C oleic acids as acyl tails (Table 1).

Table 3.2 Acyl tail position of lipids detected in the absence and presence of oleic acid

Lipid Species	10% D_2O control		10% D_2O + oleic acid	
	sn1	*sn2*	*sn1*	*sn2*
PG 30:0	C16:0	C14:0	C16:0	C14:0
PG 30:1	C16:0	C14:1	C16:0	C14:1
PG 30:2	C16:1	C14:1	N/A	N/A
PG 32:0	C16:0	C16:0	C16:0	C16:0
PG 32:1	C18:1 or C16:0	C14:0 or C16:1	C18:1 or C16:0	C14:0 or C16:1
PG 32:2	C18:1 or 16:1	C14:1 or 16:1	C18:1	C14:1
PG 33:1	C18:1	C15:0	C19:1cyclo	C14:0
PG 34:0	C18:0	C16:0	C18:0	C16:0
PG 34:1	C18:1	C16:0	C18:1	C16:0
PG 35:1	C19:1cyclo	C16:0	C19:1cyclo	C16:0
PG 35:2	C19:1cyclo	C16:1	C19:1cyclo	C16:1
PG 36:0	C18:0	C18:0	N/A	N/A
PG 36:1	C18:0	C18:1	C18:0	C18:1
PG 36:2	C18:1	C18:1	C18:1	C18:1
PG 37:2	C19:1 cyclo	C18:1	C19:1 cyclo	C18:1
CL 62:1	N/A	N/A	C14:0 or 14:0	C18:1 or 16:0
CL 64:1	C14:0 or C18:1	C16:0 or C16:0	C14:0 or C18:1	C16:0 or C16:0
CL 64:2	C14:0 or C16:0	C18:1 or C18:1	C14:0 or C16:0	C18:1 or C18:1
CL 66:1	C18:1 or C16:0	C16:0 or C16:0	C18:1 or C16:0	C16:0 or C16:0
CL 66:2	C16:0 or C16:0	C18:1 or C16:1	C16:0 or C16:0	C18:1 or C16:1
CL 68:2	C16:0 or C16:0	C18:1 or C18:1	C16:0 or C16:0	C18:1 or C18:1
CL 68:3	C18:1 or C16:0	C16:0 or C16:0	C18:1 or C16:0	C16:0 or C16:0
CL 70:3	C16:0 or C18:1	C18:1 or C18:1	C16:0 or C18:1	C18:1 or C18:1
CL 70:4	N/A	N/A	C16:1 or C18:1	C18:1 or C18:1
CL 72:4	C18:1 or C18:1	C18:1 or C18:1	C18:1 or C18:1	C18:1 or C18:1
DAG 34:1	C18:1	C16:0	C18:1	C16:0
DAG 36:2	C18:1	C18:1	C18:1	C18:1
MGDG 34:0	C18:0	C16:0	C18:0	C16:0
MGDG 34:1	C18:1	C16:0	C18:1	C16:0

Acyl tail position assignments for lipid species grown in the presence of 10% D_2O supplemented with solvent control or - oleic acid. Parent ions that were not accompanied by MS^2 data are listed as N/A

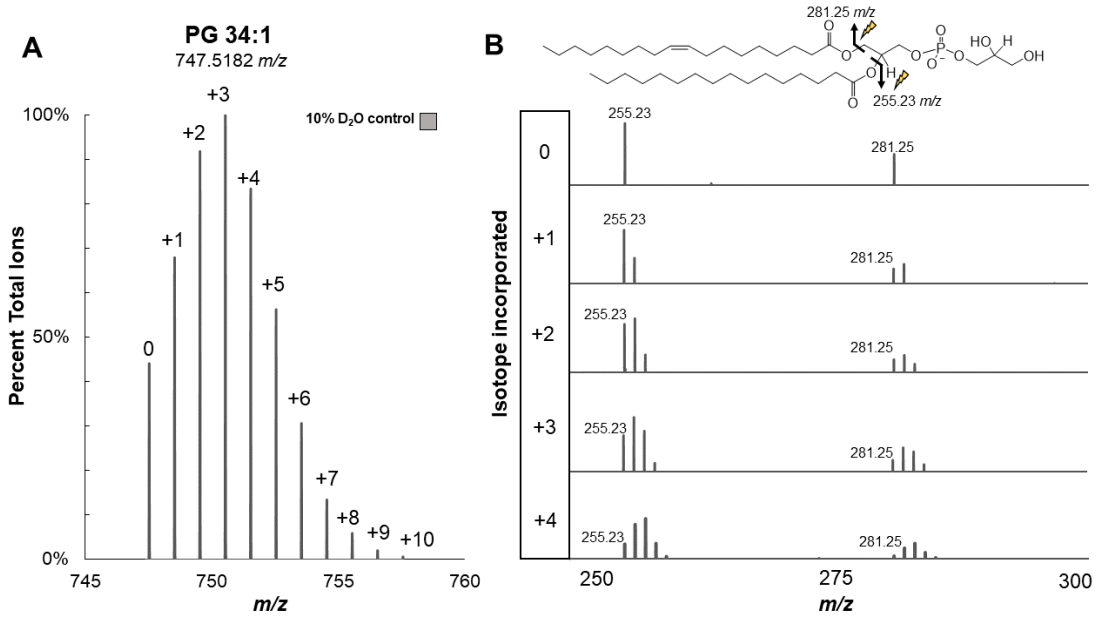

Figure 3.3 A) Full scan mass spectra of lipid species PG 34:1 detected in bacterial culture grown in the presence of 10% D_2O. Mass shifts of isotopologue population denoted as [M+X] species. B) Predicted chemical structure of PG 34:1. Fragmentation events of [M+X] species at 30,000 resolving power shown below.

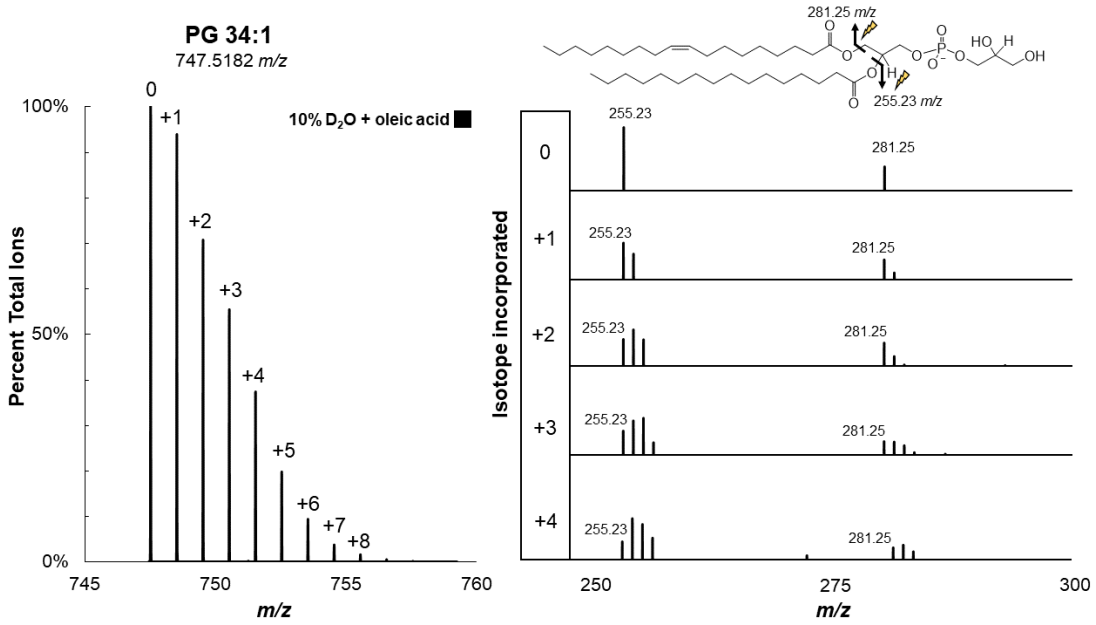

Figure 3.4 A) Full scan mass spectra of lipid species PG 34:1 detected in bacterial culture supplemented with oleic acid and grown in the presence of 10% D_2O. Mass shifts of isotopologue population denoted as [M+X] species. B) Predicted chemical structure of PG 34:1. Fragmentation events of [M+X] species at 30,000 resolving power shown below.

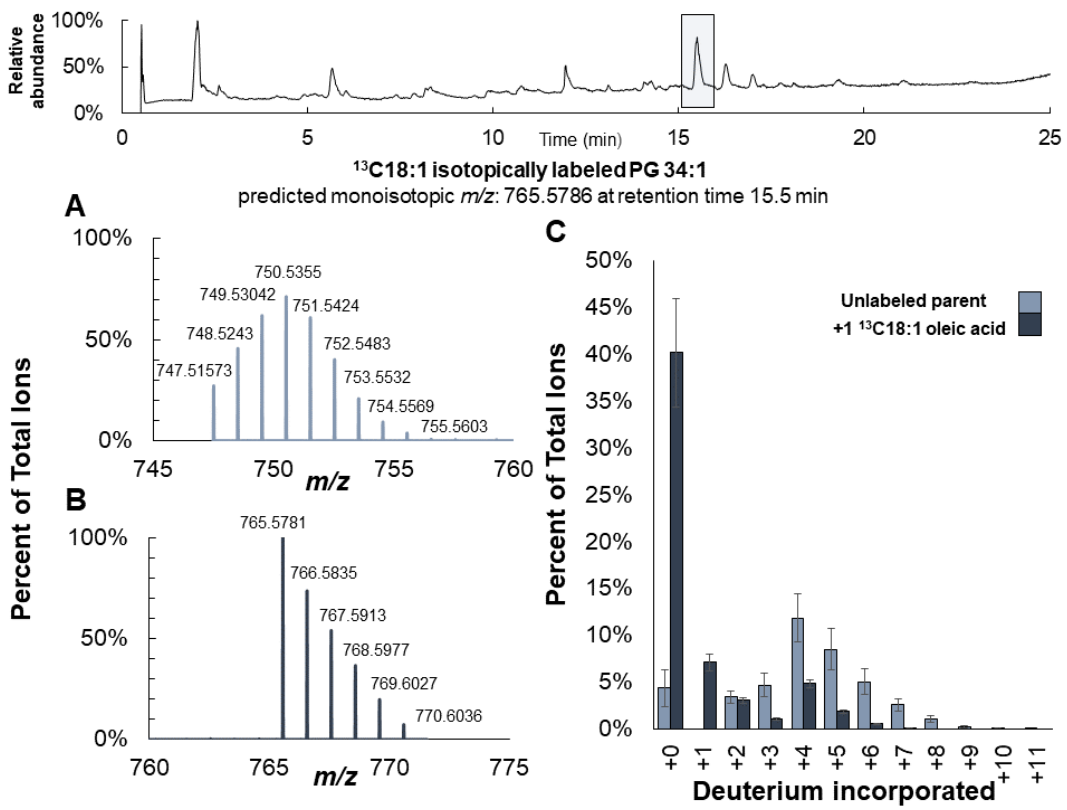

Figure 3.5 Total ion chromatogram highlighting retention time of lipid species. A) Full scan mass spectrum (120,000 resolving power), demonstrating isotopologues for PG 34:1 detected in bacterial culture supplemented with 10% D_2O and ^{13}C oleic acid. B) Full scan mass spectrum (120,000 resolving power), demonstrating isotopologues for $^{13}C18:1$ PG 34:1 detected in bacterial culture supplemented with 10% D_2O and ^{13}C oleic acid. C) Averaged and corrected deuterium incorporation for lipid species containing zero and one $^{13}C18:1$ labeled tail.

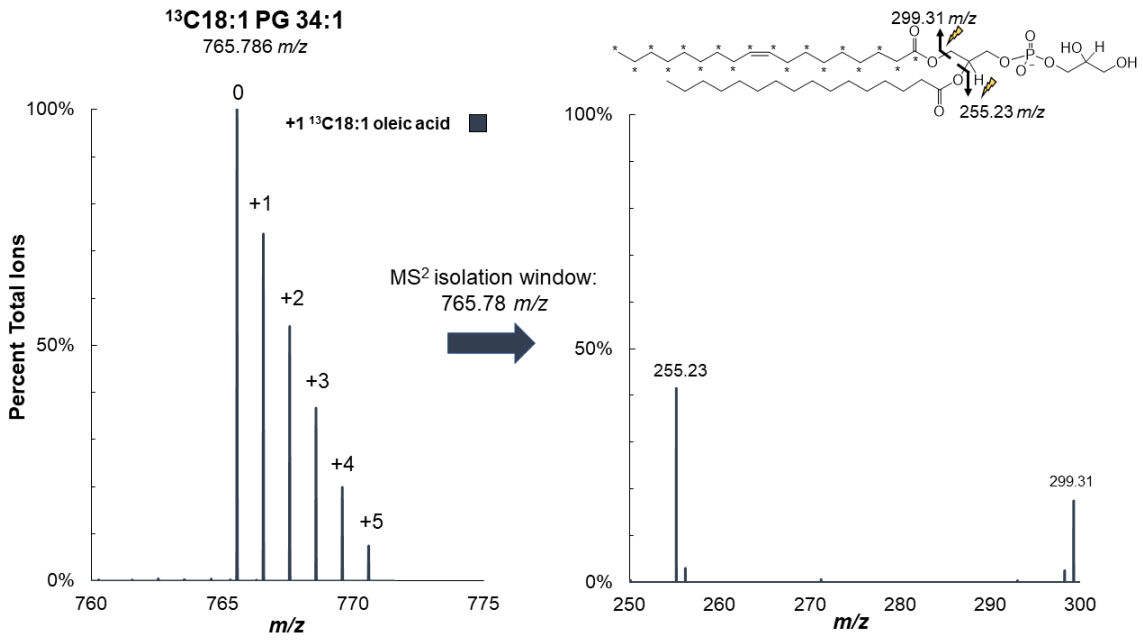

Figure 3.6 A) Full scan mass spectra of lipid species ^{13}C18:1 PG 34:1 detected in bacterial culture grown in the presence 10% D_2O and supplemented with ^{13}C oleic acid. Mass shifts of isotopologue population denoted as [M+X] species. B) Predicted chemical structure of ^{13}C18:1 PG 34:1 with ^{13}carbon isotopes denoted with *. Fragmentation events of [M+X] species at 30,000 resolving power shown below.

3.5 Discussion

Previous research has demonstrated alterations in the lipidome of *E. faecalis* in response to both genetic and environmental perturbation, and a recent publication suggested alterations in lipidome could be due to direct incorporation of oleic acid, a media supplement [10]. However, without the use of stable isotope probes, these hypotheses could not be confirmed due to the organism synthesizing an isomeric *de novo* fatty acid, cis-vaccenic acid. Additionally, oleic acid has been implicated in potential repression of *de novo* biosynthesis of other fatty acids, which could cause membrane alterations [8, 29]. Single stable isotopes experiments utilizing ^{13}C or D could not address these hypotheses independently as neither isotope could monitor *de novo* processes combined with external nutrient incorporation. The aim of this experiment was to design an analytical methodology capable of investigating lipid biosynthesis in a model organism utilizing dual stable isotope tracers that could monitor *de novo* metabolism in addition to competing or exogenous nutrient fluxes in order to differentiate between genetic versus environmental stressors.

If lipid biosynthesis is performed in the presence of deuterium oxide, labeling of fatty acids occurs due to the solvent mediated proton/deuterium transfer from NADPH, which isotopically labels primary fatty acids [18]. This technique can provide measurements of lipid fluxes, and at minimum, can be used to determine whether a fatty acid was synthesized *de novo* or structurally modified via processes such as chain elongation. Deuterium was used in this experiment to isotopically label newly synthesized acyl tails, and the detection of mass additions of 1.0063 *m/z* could be used to determine the number of deuterium added to the fatty acid. Therefore, the % of deuterium labeled lipids gives a direct measure of the fraction of fatty acyl tails that were synthesized *de novo* during the experiment, and the number of deuterium atoms incorporated within the acyl tails is indirectly proportional to the number of acetyl units added during biosynthesis, although this number is likely not an exact measure due to the kinetic isotope effect. For example, examining two lipid species in the presence of 10% D_2O only, PG 34:0 and PG 34:1, demonstrated differences in percent of lipid species that incorporated deuterium: 75.5% PG 34:0 molecules were reported to contain deuterium while 88.1% PG 34:1 molecules were reported to contain deuterium (Table 1). Phospholipids that did not contain deuterium were either present at the initiation of the experiment or were synthesized from intact fatty acids present in the BHI medium, which is known to be rich in C15 and C16 fatty acids [30]. The analyses to determine the percent of phospholipids that contained deuterium did not differentiate those that incorporated deuterium on both fatty acyl tails from those that incorporated deuterium on only one acyl tail. However, the distribution of deuterium containing phospholipid isotopologues provides insight into whether one or both tails are labeled.

The isotopologue distribution for *de novo* synthesized fatty acyl tails could be determined from phospholipids that incorporated either unlabeled or ^{13}C-

labeled oleic acid considering these acyl tails were shown to not incorporate deuterium. Additionally, these data showed that *de novo* synthesized fatty acyl tails had an inverse correlation between the number of deuterium incorporated and the concentration of the isotopologue (Figures 3 and 4). Further inspection of the data showed that PG 30:0, PG 32:0, and PG 34:0 did not display bell shaped distributions of isotopologues (supporting information), and MS^2 data confirmed that each of these species contained C16:0. Fatty acids that are known to be available in high concentrations in BHI, and the incorporation of unlabeled C16:0 can explain the deviation from the expected isotope pattern [30]. The observation that isotopologue distributions of the parent lipid species vary based on the incorporation of deuterium on single versus multiple acyl tails can provide insight into fatty acid origin and allows for further conclusions to be drawn in instances when fragmentation data is difficult to obtain (due to instrumental limitations or low ion abundance) and for compounds of unknown structure.

The addition of oleic acid to the bacterial cultures altered the concentrations of lipid species, the percent of lipids containing deuterium, and the number of deuterium detected within lipids (Table 1, 2 and Figure 4). Previous studies reported decreased abundances of several membrane lipid species after supplementation with oleic acid; however, direct correlations to fatty acid synthesis activity could not be determined. The use of deuterium to trace *de novo* biosynthesis in this experiment made it possible to discern whether lipids were being actively synthesized in the presence of exogenous oleic acid. Examining one case, 88.1% of PG 34:1 molecules were determined to contain deuterium in the absence of exogenous oleic acid (-); however, in the presence of oleic acid (+) only 50.5% of the molecules contained deuterium (Table 1). Considering PG 34:1 could contain a C18:1 acyl tail, the decrease in deuterium incorporation was attributed to direct incorporation of one unlabeled exogenous oleic acyl tail. Additionally, the shift in isotopologue population suggests the incorporation of a non-deuterated acyl tail, as discussed above. It was also noted that several lipids, such as PG 34:0, were determined to contain higher percentages of lipids with deuterium in the presence of oleic acid (75.5% versus 83.8%, respectively; (Table 1)). This suggests that *de novo* biosynthesis was on-going in the presence of exogenous oleic acid for the 30-minute duration of the experiment, although it is possible that this process would be impacted upon longer exposure. If *de novo* biosynthesis were halted by the addition of oleic acid, decreases in the percent of lipid molecules containing deuterium would be also expected for lipids which do not contain C18:1 acyl tails.

Results from the addition of the unlabeled fatty acid suggested incorporation of oleic acid as an acyl tail of actively synthesized lipid moieties; ^{13}C-labeled fatty acids were used to confirm this result. Further, the use of ^{13}C-oleic acid was able to determine whether the exogenous acid was modified before incorporation or catabolized to other metabolites. When considering the possible lipid biosynthesis pathways of *E. faecalis*, exogenous fatty acids could be incorporated into lipid biosynthesis in several ways including: 1.) direct

incorporation (unaltered) into newly synthesized lipid, 2.) replacement of a tail on existing lipid, or 3.) via elongation by FAS II to a longer fatty acid that is later utilized. Catabolism of the ^{13}C-oleic acid was not expected due to the lack of β-oxidation capabilities in this organism; however, the use of ^{13}C-labeled substrates were able to confirm that metabolites derived from oleic acid were not entering the lipidome.

If direct incorporation is the main route of entry for exogenous oleic acid, lipids detected in the dual labeled bacterial culture (10% D_2O and ^{13}C-oleic acid) that incorporate ^{13}C- oleic acid (including but not limited to PG 34:1, PG 36:1, PG 36:2, CL 72:4) would have a mass shifts of 18.0604 *m/z* as well as a fragment *m/z*'s indicative of an unmodified ^{13}C-oleic acid at 299.3089 *m/z* (Figure 5 and 6). Additionally, *de novo* biosynthesized lipids that contained an acyl tail produced via FAS II biosynthesis would also contain a range of 1.0064 *m/z* mass shifts indicative of deuterium labeling on the endogenous lipid tail. If replacement were occurring, masses indicative of non-deuterated lipid incorporating ^{13}C- oleic acid (+18.0604 m/z) would be expected. If elongation of ^{13}C- oleic acid were to occur, lipids containing acyl tails corresponding to C20:1 (or longer) with an isotope label of 18.0604 *m/z*, masses shift of 14.0156 *m/z* for each added methylene (CH_2) unit, as well as range of 1.0064 *m/z* mass shifts would be observed. Modification of the ^{13}C- oleic acid would lead to a lipid with a mass shift of +18.0604 *m/z* from the addition of isotopically labeled carbons, as well as one or more mass shifts arising from addition of CH_2 units and deuterium's.

Several intact phospholipids were detected to contain both the mass shift characteristic of ^{13}C-oleic acid incorporation as well as those for deuterium incorporation. In all cases, the MS^2 spectra confirmed that only 18.0604 *m/z* mass shifts were observed in fragments derived from fatty acyl tails and that this shift was only found in fragments derived from non-deuterated and unmodified ^{13}C-18:1 fatty acids (Figure 6). Together, these data indicate ^{13}C- oleic acid (unaltered) is directly incorporated into an actively synthesized lipid. For example, PG 34:1 was observed to contain unlabeled oleic acid tails 41.1% of the time and to incorporate one ^{13}C-oleic acid tail 58.8% of the time. Deuterium incorporation was detected on both the ^{12}C and ^{13}C isotopologues of this lipid, although the % of lipids containing deuterium was lower for the ^{13}C containing isotopologue (89.4% verses 31.6%) as would be expected given the supplementation with ^{13}C- oleic acid only lasted one generation, 30 minutes (Table 1). Examination PG 36:2, which contains two oleic acid derived tails, indicated that 12.4% of the molecules contained zero ^{13}C-oleic acyl tails, 28.4% contained one ^{13}C-oleic acyl tail, and 59.2% contained two ^{13}C- oleic acid tails yielding a population of lipids in which 85.6% displayed ^{13}C-oleic acid incorporation (Table 1). As 12.4% of PG 36:2 was detected to contain zero ^{13}C-oleic acid labels, 89.8% of the lipid species were detected containing deuterium, indicative of both tails arising from *de novo* biosynthesis. When PG 36:2 was detected containing one ^{13}C- oleic acid label, the percentage of lipids containing deuterium decreased to 59.6%, given one acyl tail was exchanged for a tail

without deuterium. PG 36:2 species detected with two ^{13}C- oleic acid labels were detected without deuterium incorporation as both tails arose from exogenous fatty acid incorporation. There are no known phospholipases annotated within the genome of *E. faecalis*, therefore exchange of oleic acid for a tail on an existing lipid was not expected [31]. However, non-deuterated lipids that incorporated ^{13}C-oleic acid were detected and could have arisen from either exchange of an acyl tail or due to lack of deuterium incorporation during lipid biosynthesis. Further experimentation will be necessary to differentiate the possibilities in this case.

To further investigate this process, acyl tail positions were identified in order to monitor active enzymatic products of lipid biosynthesis in *E. faecalis*. The fatty acid kinase system (FaK) of *E. faecalis* is responsible for binding and phosphorylating exogenous fatty acids for further use by PlsY or PlsX. Both enzymes utilize acyl phosphates produced by the FaK system, however PlsX is responsible for the transfer of the acyl phosphate to an acyl carrier protein (ACP) while PlsY adds the acyl phosphate to a glycerol backbone at the sn1 position forming lyso-phosphatidic acid (lyso-PA). PlsC utilizes acyl-ACP pools generated from PlsX and FAS II biosynthesis to add acyl tails at the sn2 position of lyso-PA (generated by PlsY) [7, 17, 31]. Considering PlsY and PlsC have positional acyl tail specificity, the acyl tails of lipid species were identified to further investigate this process. To our knowledge, acyl tail position of lipids in the *E. faecalis* lipidome have not yet been recorded or investigated. Utilizing data dependent acquisition (DDA) on the Exploris 120 mass spectrometer, allowed for the top 4 most abundant *m/z*, to be independently selected by the quadrupole for fragmentation analysis in the HCD cell.

The ability to isolate and fragment specific *m/z* provided structural information regarding the tail position (sn1 versus sn2) of lipid species, as well as the ability to confirm headgroup composition. Murphy and Axelsen reported characteristic fragmentation patterns of a variety of membrane lipids within the literature and suggested various mechanisms for the observed fragmentation of their lipid standards, including an empirical observation that the sn2 acyl derived fragment was routinely observed in higher abundance than the sn1 acyl derived fragment [28]. These data suggest that the energy required to lose the sn2 fatty acid is lower as well. This can be rationalized based on two structural observations. First, the sn2 acyl tail resides in a more sterically congested position, and repulsions should therefore weaken the C-O bond connecting this moiety to the glycerol backbone in the reactant. Second, the cleavage leading the sn2 fragment forces positive charge onto a 2^{o} carbon during the transition state or produces a 2^{o} carbocation, both of which can be stabilized by interactions with negatively charged phosphate group. Conversely, cleavage leading to the sn1 fragment would lead to a higher energy 1^{o} version of the transition state. Therefore, it is hypothesized that both the weaking of the bond in the reactant and lowering the energy of the transition state and intermediate both work to lower the activation energy required to produce the sn2 $RCOO^-$ ion, and it is therefore observed more often. In both the initial report and in the data

presented here, the relative abundance of the sn2 acyl tails fragments are observed to be ~75% higher than those derived from the sn1 acyl tails (~25% relative abundance). Using these observations, the acyl tail positions could be annotated for 29 lipid species detected in both the presence and absence of oleic acid (Table 2). Examining one such result, lipid species D_3- PG 34:1 isolated from the 10% D_2O (-) oleic acid culture (749.53 *m/z*) was fragmented producing acyl tail fragments of RCO_2^- ions at 255.23 *m/z* and 281.25*m/z* (Figure 3).

These fragments were not detected as single monoisotopic ions but contained isotopologues corresponding to variety of deuterated species. Additionally, the relative abundance of these ions was not equal as the 255.23 *m/z* (or corresponding isotopologues) were detected in higher abundance than those of the 281.25 *m/z* (or corresponding isotopologues), indicating that the C16:0 fatty acyl tail was found preferentially in the sn2 position (Figure 3 and 4). As the PG 34:0 and PG 34:1 species were chromatographically separated (Figure 1 and 2), it was also possible to examine fragmentation data of the PG 34:1 species, independent of the PG 34:0 species. Isolation and fragmentation of D_3-PG 34:1 from the 10% D_2O (+) oleic acid culture produced acyl tail fragments 255.23 *m/z* and 281.25 *m/z*, each with corresponding deuterium isotopologues. Again, the relative abundance of the observed fragments were not equal (Figure 3C and 4C). Further quantitation of the MS^2 data suggested the majority of C16:0 acyl tails (or isotopologues) were in the sn2 position and the C18:1 acyl tails (or isotopologues) were predominantly in the sn1 position. While these results do suggest the dominant acyl tail position of the lipid species are those reported in Table 3, these data do not indicate that only one isomer of each lipid was present. However, they do allow for an assessment of the dominant species for each set of constitutional isomers as a 50/50 ratio for acyl tail fragments would be expected in C16:0 occupied the sn1 and sn2 position equally. Lipid species observed in the 10% D_2O (+) oleic acid culture were observed to have identical structural composition to that of lipids in the 10% D_2O (-) oleic acid culture (Table 2), although ion abundances for some lipid species such as PG 34:0 and PG 34:1 were observed to decrease (Figure 1 and 2). Analysis of the 10% D_2O (+) ^{13}C-oleic acid culture demonstrated the incorporation of one single ^{13}C- oleic acid acyl tail into PG 34:1 (747.5181+ 18.0604= 765.5792 *m/z*). The ^{13}C labeled lipid was detected in the full scan mode with additional deuterium isotopologues (Figure 5). Isolation and fragmentation of the 765.58 *m/z* confirmed the ^{13}C18:1 oleic acid in the sn1 tail position (Figure 6). Further, we note that lipids which could contain acyl tails which have undergone elongation (discussed above), PG 37:2, were not detected to have altered ^{13}C acyl fragments containing deuterium.

This study highlights the benefits of utilizing dual stable isotope probes including the ability to trace multiple nutrient fluxes or metabolic processes simultaneously; however, there are a few pitfalls that exist within this experiment which warrant discussion. As discussed above, the resolving power of the instrument utilized in this study was 120,000 (at 200 *m/z)*, which is a moderate resolving power for a high-resolution instrument, This resolving power cannot

provide baseline resolution between single ^{13}C atom incorporation or single deuterium atom incorporation at the mass to charge range of most lipids (500-2,000 *m/z*). Beyond single atom incorporation (1 D versus 1 ^{13}C), i.e. two, three, four etc. atom incorporation, the high-resolution instrument performs well given the larger mass defect between isotopes. To circumvent this issue, natural abundance correction was performed for this experiment. This mathematical correction highlights the ability of this method to be employed on instruments that are routinely used by many metabolomics and lipidomics facilities. Considering this, quantitative experiments requiring single isotope resolution (1 D versus 1 ^{13}C) would require a higher resolving power, directly increasing the cost of the experiment.

3.6 Conclusions

Given the results from this study, we suggest exogenous fatty acids are incorporated into enterococcal membrane lipids by PlsY in the sn1 position; however, in the case that two or four tailed lipids contain multiple ^{13}C- acyl tails, PlsX transfers the acyl phosphate produced by the FaK system to an acyl-ACP for PlsC sn1 incorporation. Although this analytical method was utilized to investigate the model organism *E. faecalis*, we would like to highlight the versatility of this method for its use in probing lipid biosynthesis by monitoring both exogenous nutrient uptake and/or modification as well as *de novo* biosynthesis. Although phospholipids species specific to the organism were highlighted and discussed, the UHPLC-HRMS described in this work is capable of monitoring lipid species not produced by this organism. As single labeled cultures (10% D_2O (-) oleic acid, 10% D_2O (+) oleic acid,) were analyzed in tandem with dual labeled cultures (10% D_2O ^{13}C-oleic acid), the limitations to single label isotope probes were demonstrated. Dual labeled stable isotope probes can further investigate the relationship between exogenous or environmental supplement influence on the behavior of the membrane itself. As the lipid membrane is a critical structural component of all living cells, methodologies that advance the study of the lipid membrane is warranted and necessary. Understanding and differentiating environmental nutrient fluxes from *de novo* metabolism provides insight on how the organism is surviving or changing in response to perturbation. Although the bacteria utilized in this experiment did not undergo β-oxidation, therefore could not utilize the exogenous nutrient as a carbon source, this method can and should to be applied to other systems in the future.

REFERENCES

1. Brewer, W.; Harrison, J.; Saito, H. E.; Fozo, E. M., Induction of Daptomycin Tolerance in Enterococcus faecalis by Fatty Acid Combinations. *Applied and Environmental Microbiology* **2020,** *86* (20), e01178-20.
2. Harp, J. R.; Saito, H. E.; Bourdon, A. K.; Reyes, J.; Arias, C. A.; Campagna, S. R.; Fozo, E. M., Exogenous Fatty Acids Protect Enterococcus faecalis from Daptomycin-Induced Membrane Stress Independently of the Response Regulator LiaR. *Applied and Environmental Microbiology* **2016,** *82* (14), 4410-4420.
3. Saito, H. E.; Harp, J. R.; Fozo, E. M., Enterococcus faecalis Responds to Individual Exogenous Fatty Acids Independently of Their Degree of Saturation or Chain Length. *Appl Environ Microbiol* **2018,** *84* (1).
4. Iram, S. H.; Cronan, J. E., The β-Oxidation Systems of Escherichia coli and Salmonella enterica Are Not Functionally Equivalent. *Journal of Bacteriology* **2006,** *188* (2), 599-608.
5. Hines, K. M.; Waalkes, A.; Penewit, K.; Holmes, E. A.; Salipante, S. J.; Werth, B. J.; Xu, L., Characterization of the Mechanisms of Daptomycin Resistance among Gram-Positive Bacterial Pathogens by Multidimensional Lipidomics. *mSphere* **2017,** *2* (6), e00492-17.
6. Rashid, R.; Cazenave-Gassiot, A.; Gao, I. H.; Nair, Z. J.; Kumar, J. K.; Gao, L.; Kline, K. A.; Wenk, M. R., Comprehensive analysis of phospholipids and glycolipids in the opportunistic pathogen Enterococcus faecalis. *PLoS One* **2017,** *12* (4), e0175886.
7. Zhang, Y.-M.; Rock, C. O., Membrane lipid homeostasis in bacteria. *Nature Reviews Microbiology* **2008,** *6* (3), 222-233.
8. Zhu, L.; Zou, Q.; Cao, X.; Cronan, J. E., Enterococcus faecalis Encodes an Atypical Auxiliary Acyl Carrier Protein Required for Efficient Regulation of Fatty Acid Synthesis by Exogenous Fatty Acids. *mBio* **2019,** *10* (3), e00577-19.
9. White, S. W.; Zheng, J.; Zhang, Y.-M.; Rock, C. O., THE STRUCTURAL BIOLOGY OF TYPE II FATTY ACID BIOSYNTHESIS. *Annual Review of Biochemistry* **2005,** *74* (1), 791-831.
10. Woodall, B. M.; Harp, J. R.; Brewer, W. T.; Tague, E. D.; Campagna, S. R.; Fozo, E. M., Enterococcus faecalis Readily Adapts Membrane Phospholipid Composition to Environmental and Genetic Perturbation. *Frontiers in Microbiology* **2021,** *12*.
11. Fozo, E. M.; Rucks, E. A., The making and taking of lipids: The role of bacterial lipid synthesis and the harnessing of host lipids in bacterial pathogenesis. *Advances in microbial physiology* **2016,** *69*, 51-155.
12. Mishra, N. N.; Bayer, A. S.; Tran, T. T.; Shamoo, Y.; Mileykovskaya, E.; Dowhan, W.; Guan, Z.; Arias, C. A., Daptomycin Resistance in Enterococci Is Associated with Distinct Alterations of Cell Membrane Phospholipid Content. *PLOS ONE* **2012,** *7* (8), e43958.

13. Jang, C.; Chen, L.; Rabinowitz, J. D., Metabolomics and Isotope Tracing. *Cell* **2018,** *173* (4), 822-837.
14. Dong, W.; Rawat, E. S.; Stephanopoulos, G.; Abu-Remaileh, M., Isotope tracing in health and disease. *Curr Opin Biotechnol* **2022,** *76*, 102739.
15. Triebl, A.; Wenk, M. R., Analytical Considerations of Stable Isotope Labelling in Lipidomics. *Biomolecules* **2018,** *8* (4).
16. Postle, A. D.; Hunt, A. N., Dynamic lipidomics with stable isotope labelling. *Journal of Chromatography B* **2009,** *877* (26), 2716-2721.
17. Zhang, T.; Muraih, J. K.; Tishbi, N.; Herskowitz, J.; Victor, R. L.; Silverman, J.; Uwumarenogie, S.; Taylor, S. D.; Palmer, M.; Mintzer, E., Cardiolipin prevents membrane translocation and permeabilization by daptomycin. *J Biol Chem* **2014,** *289* (17), 11584-11591.
18. Zhang, Z.; Chen, L.; Liu, L.; Su, X.; Rabinowitz, J. D., Chemical Basis for Deuterium Labeling of Fat and NADPH. *Journal of the American Chemical Society* **2017,** *139* (41), 14368-14371.
19. Kim, J.; Kang, D.; Lee, S. K.; Kim, T.-Y., Deuterium Oxide Labeling for Global Omics Relative Quantification: Application to Lipidomics. *Analytical Chemistry* **2019,** *91* (14), 8853-8863.
20. Wegener, G.; Kellermann, M. Y.; Elvert, M., Tracking activity and function of microorganisms by stable isotope probing of membrane lipids. *Current Opinion in Biotechnology* **2016,** *41*, 43-52.
21. Hochuli, M.; Szyperski, T.; Wüthrich, K., Deuterium isotope effects on the central carbon metabolism of Escherichia coli cells grown on a D2O-containing minimal medium. *Journal of Biomolecular NMR* **2000,** *17* (1), 33-42.
22. Wilkinson, D. J.; Cegielski, J.; Phillips, B. E.; Boereboom, C.; Lund, J. N.; Atherton, P. J.; Smith, K., Internal comparison between deuterium oxide (D2O) and L-[ring-13C6] phenylalanine for acute measurement of muscle protein synthesis in humans. *Physiol Rep* **2015,** *3* (7).
23. Malaisse, W. J.; Ladrière, L.; Verbruggen, I.; Willem, R., Metabolism of d-[1-13C]Fructose, d-[2-13C]Fructose, and d-[6-13C]Fructose in Rat Hepatocytes Incubated in the Presence of H2O or D2O. *Molecular Genetics and Metabolism* **2002,** *75* (2), 162-167.
24. Naser, F. J.; Jackstadt, M. M.; Fowle-Grider, R.; Spalding, J. L.; Cho, K.; Stancliffe, E.; Doonan, S. R.; Kramer, E. T.; Yao, L.; Krasnick, B.; Ding, L.; Fields, R. C.; Kaufman, C. K.; Shriver, L. P.; Johnson, S. L.; Patti, G. J., Isotope tracing in adult zebrafish reveals alanine cycling between melanoma and liver. *Cell Metabolism* **2021,** *33* (7), 1493-1504.e5.
25. Fu, X.; Deja, S.; Fletcher, J. A.; Anderson, N. N.; Mizerska, M.; Vale, G.; Browning, J. D.; Horton, J. D.; McDonald, J. G.; Mitsche, M. A.; Burgess, S. C., Measurement of lipogenic flux by deuterium resolved mass spectrometry. *Nature Communications* **2021,** *12* (1), 3756.
26. Gant, T. G., Using Deuterium in Drug Discovery: Leaving the Label in the Drug. *Journal of Medicinal Chemistry* **2014,** *57* (9), 3595-3611.

27. Guan, X. L.; Riezman, I.; Wenk, M. R.; Riezman, H., Yeast lipid analysis and quantification by mass spectrometry. In *Methods in enzymology*, Elsevier: 2010; Vol. 470, pp 369-391.
28. Murphy, R. C.; Axelsen, P. H., Mass spectrometric analysis of long-chain lipids. *Mass Spectrom Rev* **2011,** *30* (4), 579-99.
29. Zou, Q.; Dong, H.; Zhu, L.; Cronan, J. E., The Enterococcus faecalis FabT Transcription Factor Regulates Fatty Acid Biosynthesis in Response to Exogeneous Fatty Acids. *Front Microbiol* **2022,** *13*, 877582.
30. Ehrhardt, C. J.; Chu, V.; Brown, T.; Simmons, T. L.; Swan, B. K.; Bannan, J.; Robertson, J. M., Use of fatty acid methyl ester profiles for discrimination of Bacillus cereus T-strain spores grown on different media. *Appl Environ Microbiol* **2010,** *76* (6), 1902-12.
31. Sohlenkamp, C.; Geiger, O., Bacterial membrane lipids: diversity in structures and pathways. *FEMS Microbiol Rev* **2016,** *40* (1), 133-59.

APPENDIX

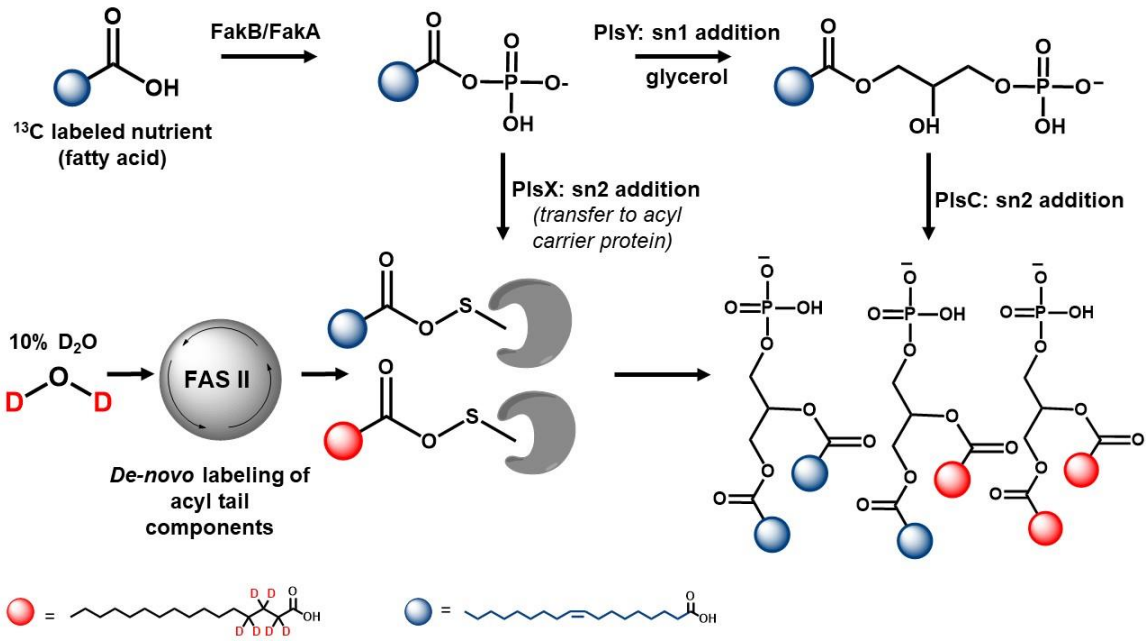

Figure S3.1 Lipid biosynthesis cycle for *Enterococcus faecalis*

Bacterial Extraction Protocol for Lipid Isolation:
Extraction protocol was performed as follows: 5 mL of cell culture were harvested via centrifugation (2739xg, 10 min, 4°C). Supernatant was removed and cell pellets were washed with equal volume phosphate buffered saline (1X PBS) two times. Washed cell pellets were stored at -80°C prior to extraction. Cell pellets were thawed at room temperature and 5 mL of extraction solvent (95% ethanol: water: diethyl ether: pyridine: 4.2N ammonium hydroxide 15:15:5:1:0.18) was added along with glass beads (150-212 µM) and internal standard (10uM PG 16:0/ CL 56:0). Cells, extraction solvent, and glass beads were subject to vortex (10s) and incubated at 60°C for 1 hour. After incubation, pellets were reformed via centrifugation and organic supernatant was harvested by pipetting. An additional 5 mL of extraction solvent was added to the pellet, vortexed and incubated for an additional hour at 60°C, after incubation, pellets were reformed by centrifugation and organic solvent was combined and allowed to dry at room temperature under N_2. Resulting solids were resuspended in 9:1 methanol chloroform and stored at -20°C prior to analysis.

Chromatography Parameters:
2 uL of sample was injected onto the C3) column and separated under the following chromatographic parameters: 0-2 min 30% B, 3 min 40% B, 7 min 50% B, 8 min 60% B, 10 min 65% B, 12 min 68% B, 13 min 70% B, 16 min 75% B, 20 min 80% B, 23-28 min 98% B, 32 min 100% B, 34 min 90% B, 35-40 min 30% B a flow rate of 0.15 µL/min. Solvent A consisted of 60:40 water: acetonitrile with 10 mM ammonium formate and 0.1% formic acid while Solvent B consisted of 90:10 2-propanol: acetonitrile 10 mM ammonium formate and 0.1% formic acid.

Mass Spectrometry Parameters:
Eluent was introduced into the mass spectrometer using a heated- electrospray ionization source with the following parameters: spray voltage (static) 3500 V for positive mode and 2500 V for negative mode, sheath gas 35 (Arb), aux gas 7 (Arb), ion transfer tube 320 °C. Ions of respective diacylglycerol (DAG) and monoglucosyl-diacylglycerol (MGDG) species were detected in positive mode as ammonium adducts while phosphatidylglycerol (PG), lysyl-phosphatidylglycerol (L-PG), cardiolipin (CL), and free fatty acids (FFA) were detected in negative mode. The mass spectrometer was operated in data dependent acquisition (DDA) mode for which the full scan spectra (100-2,000 *m/z*) were collected at 120,000 resolution and the MS^2 spectra were collected at stepped collisional energies of 25, 50, and 75 eV at a resolution of 30,000. The mass spectrometer was calibrated every 24 hours in both modes.

Isotope correction:

Bacterial culture with no deuterium source N_1 -N_5 : natural abundance of ^{13}C only.

Biological replicates N=5 analyzed for natural abundance of ^{13}C (N_1 –N_5)

$\frac{M+1\ total\ ion\ abundance}{\sum \text{M+1,M+2,M+3,ion abundance}}$= N_1 -N_5 percent natural abundance of ^{13}C isotope= [M+1]

$\frac{M+2\ total\ ion\ abundance}{\sum \text{M+1,M+2,M+3,ion abundance}}$ = N_1 -N_5 percent natural abundance of ^{13}C isotope= [M+2]

$\frac{M+2\ total\ ion\ abundance}{\sum \text{M+1,M+2,M+3,ion abundance}}$ = N_1 -N_5 percent natural abundance of ^{13}C isotope= [M+3]

Bacterial culture grown in the presence of 10% deuterium oxide D_1-D_5 : deuterium source for isotope labeling and natural ^{13}C isotope abundance

Biological replicates N=5 analyzed for natural abundance of ^{13}C in the presence of 10% D_2O as a stable isotope source (D_1-D_5)

$\frac{M+1\ total\ ion\ abundance}{\sum \text{M+1,M+2,M+3,ion abundance}}$= D_1-D_5 percent natural abundance of ^{13}C isotope and deuterium isotope [M+1]

$\frac{M+2\ total\ ion\ abundance}{\sum \text{M+1,M+2,M+3,ion abundance}}$ = D_1-D_5 percent natural abundance of ^{13}C isotope and deuterium isotope [M+2]

$\frac{M+2\ total\ ion\ abundance}{\sum \text{M+1,M+2,M+3,ion abundance}}$ =D_1-D_5 percent natural abundance of ^{13}C isotope and deuterium isotope [M+3]

Corrected ion abundance was performed by subtracting the percent of ion abundance for D_1-D_5 [M+X] (containing deuterium and naturally occurring ^{13}C) from the percent of ion abundance N_1 -N_5 [M+X] containing only naturally occurring ^{13}C and scaling the percentage of total to the unlabeled [M] in the deuterated bacterial culture (D_1-D_5). Average ion abundance was calculated by summing all total ions for respective isotopes and dividing by the total number of replicates. For this study N=5. Percent of ion totals were calculated by summing the averaged isotopes and dividing that total by the sum of all ions, including the parent.

Percent of total ion = $\frac{\Sigma \text{ average labeled ion}}{\Sigma \text{ average labeled and unlabeled ion (total ion)}}$

Error of percent of total ion=

$$\sqrt{\left(\frac{standard\ error\ of\ deuterium\ average}{average\ ion\ abundance\ of\ deuterium}\right)^2 + \left(\frac{standard\ error\ of\ total}{average\ ion\ abundance\ of\ total}\right)^2} * percent\ incorporation$$

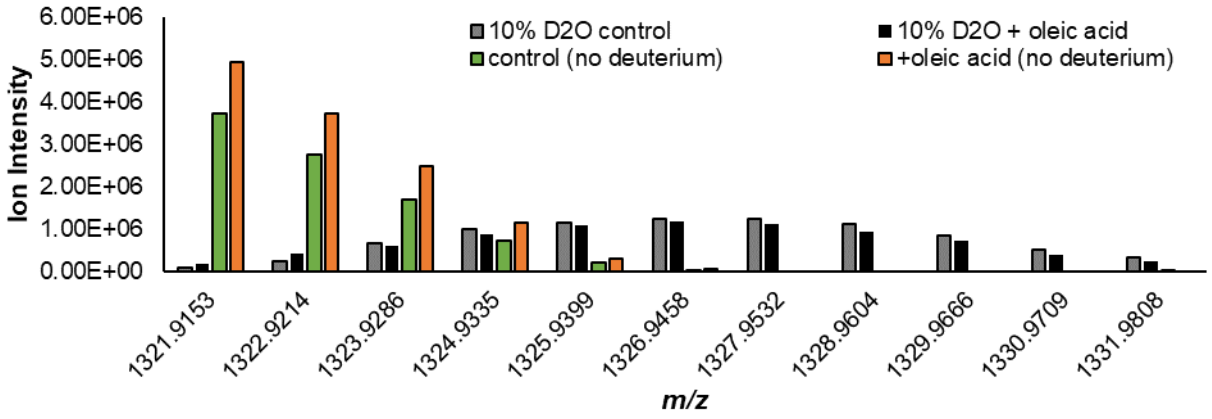

Figure S3.2 Ion intensity for CL 62:1

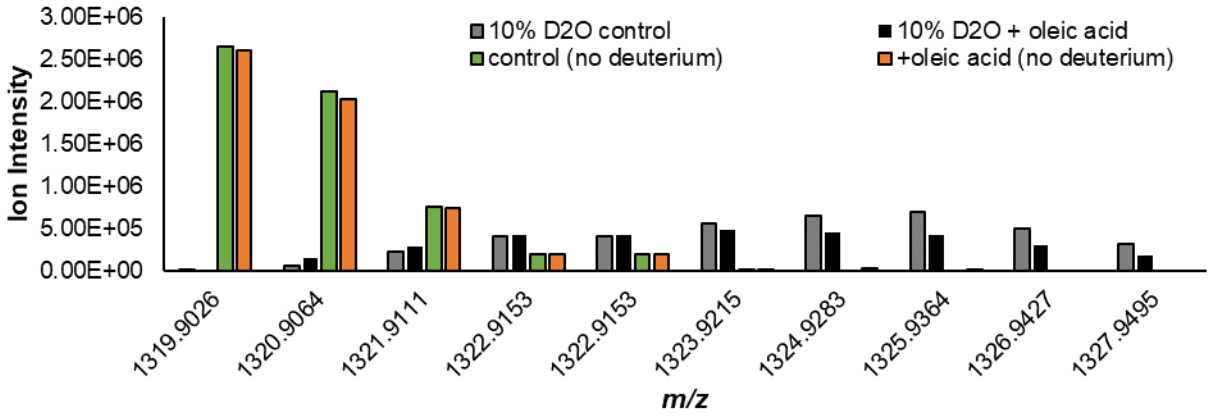

Figure S3.3 Ion intensity for CL 62:2

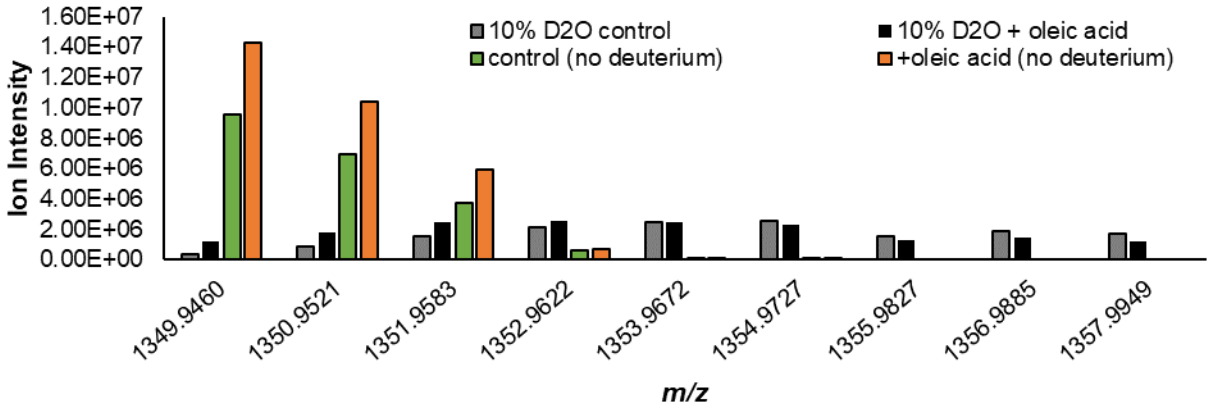

Figure S3.4 Ion intensity for CL 64:1

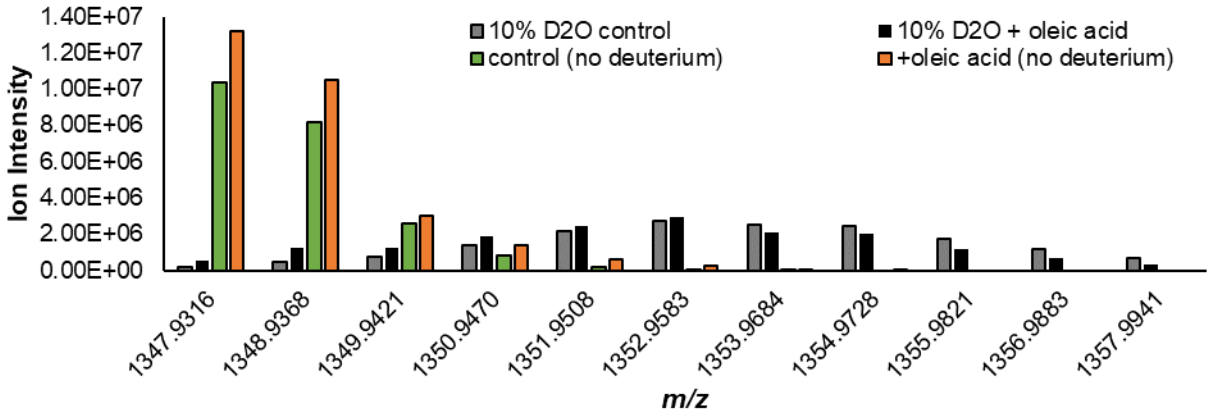

Figure S3.5 Ion intensity for CL 64:2

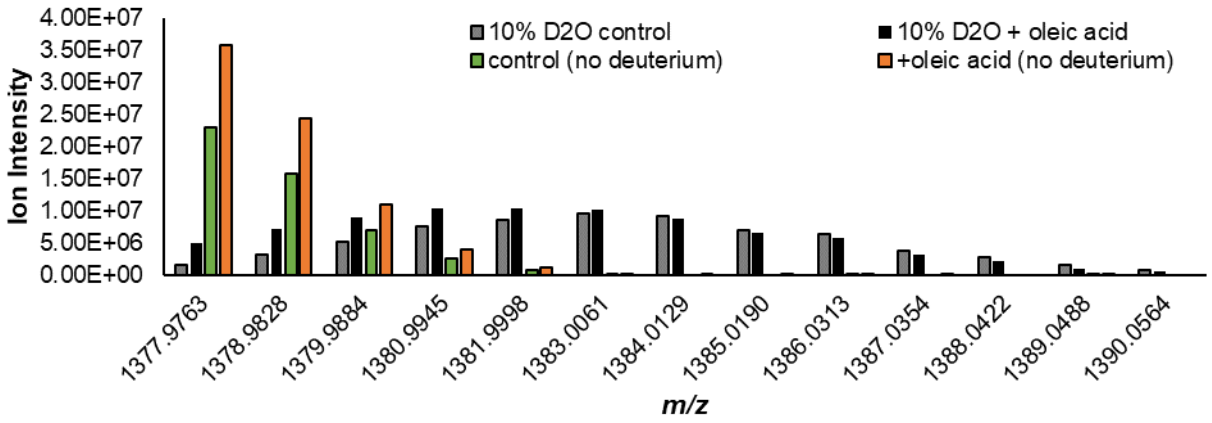

Figure S3.6 Ion intensity for CL 66:1

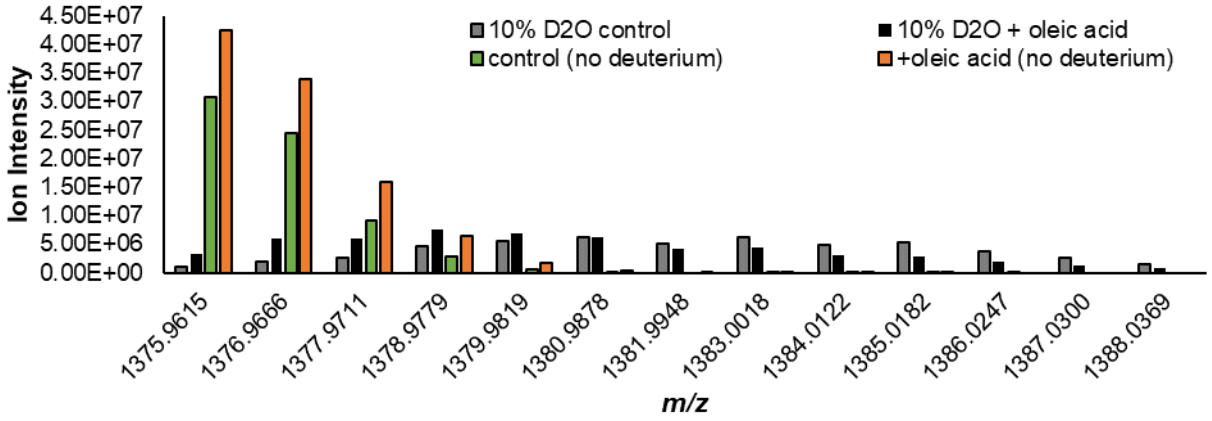

Figure S3.7 Ion intensity for CL 66:2

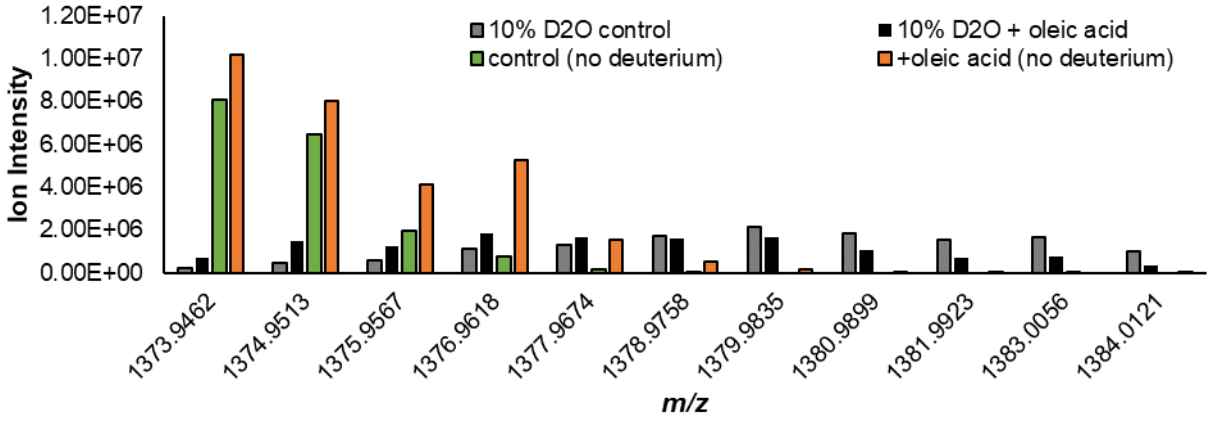

Figure S3.8 Ion intensity for CL 66:3

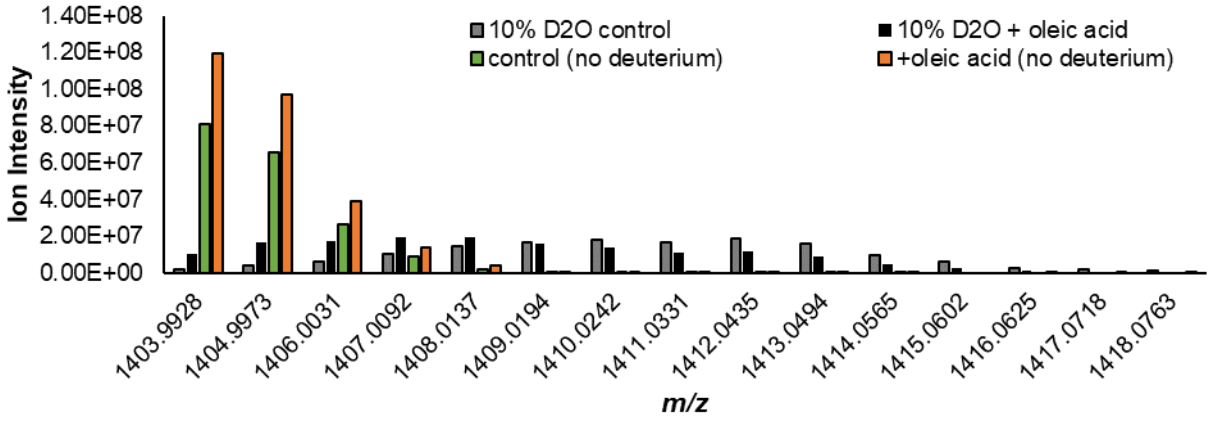

Figure S3.9 Ion intensity for CL 68:2

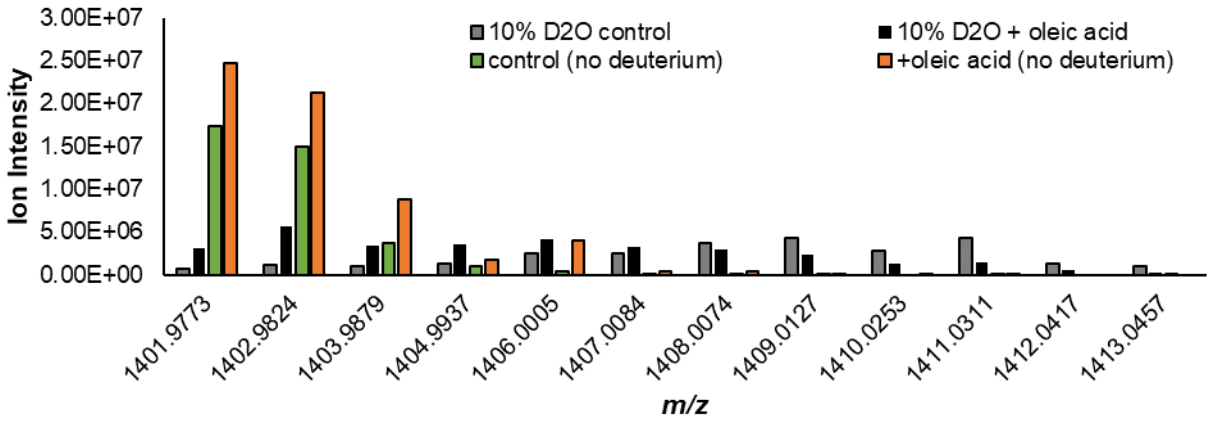

Figure S3.10 Ion intensity for CL 68:3

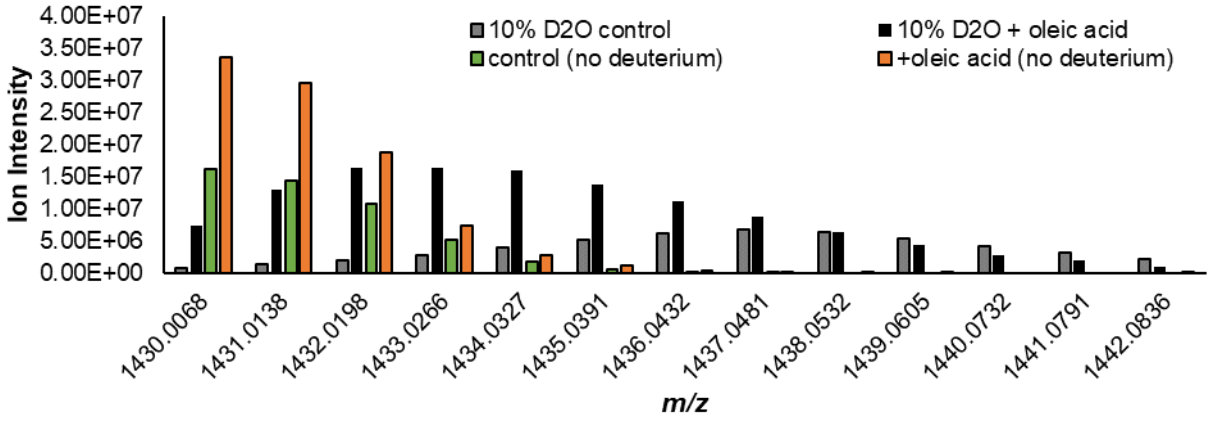

Figure S3.11 Ion intensity for CL 70:3

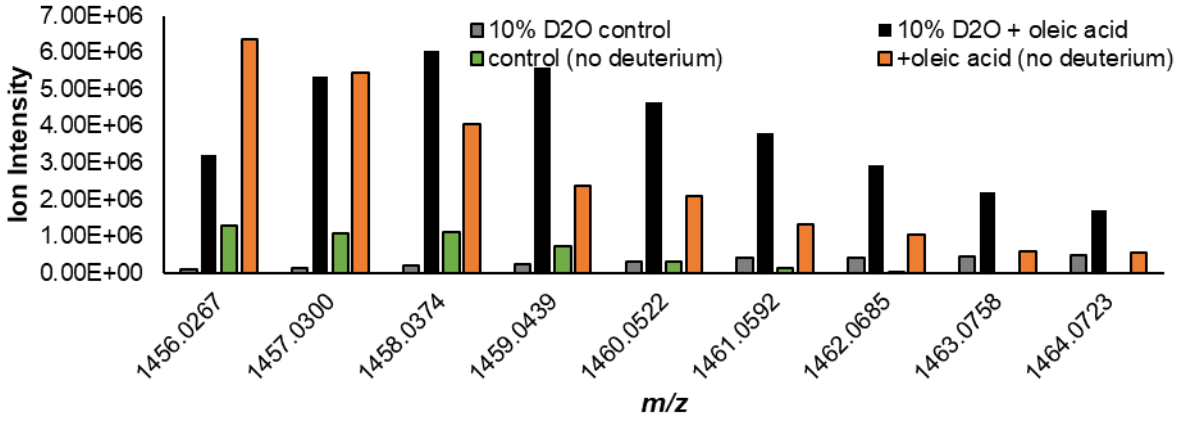

Figure S3.12 Ion intensity for CL 72:4

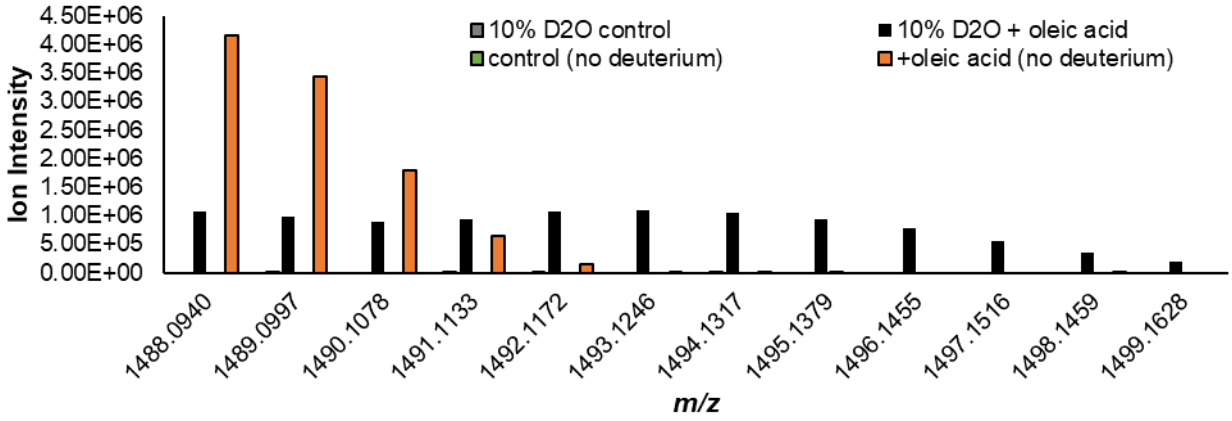

Figure S3.13 Ion intensity for CL 74:2

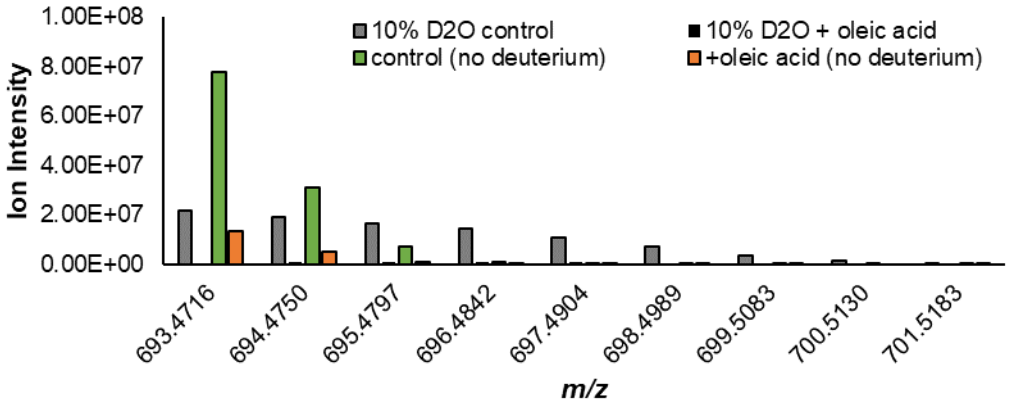

Figure S3.14 Ion intensity for PG 30:0

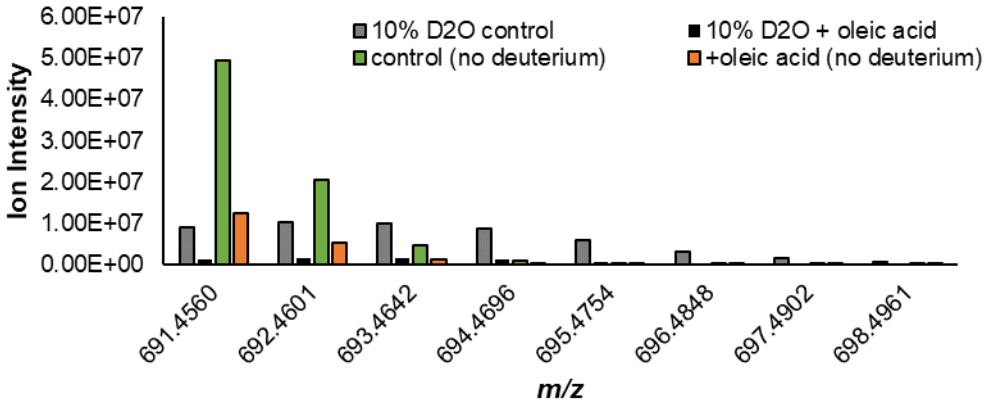

Figure S3.15 Ion intensity for PG 30:1

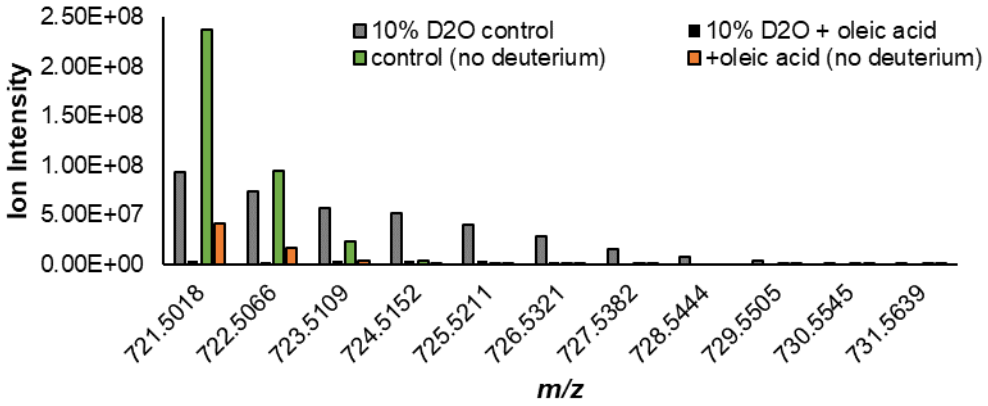

Figure S3.16 Ion intensity for PG 32:0

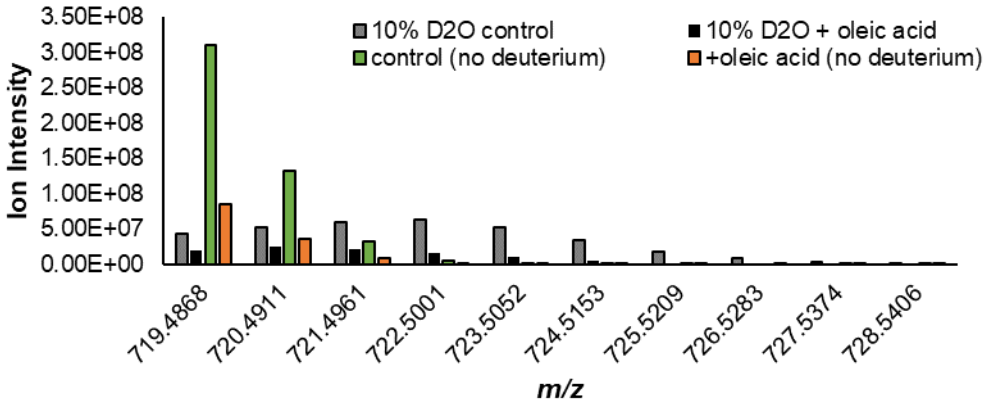

Figure S3.16 Ion intensity for PG 32:1

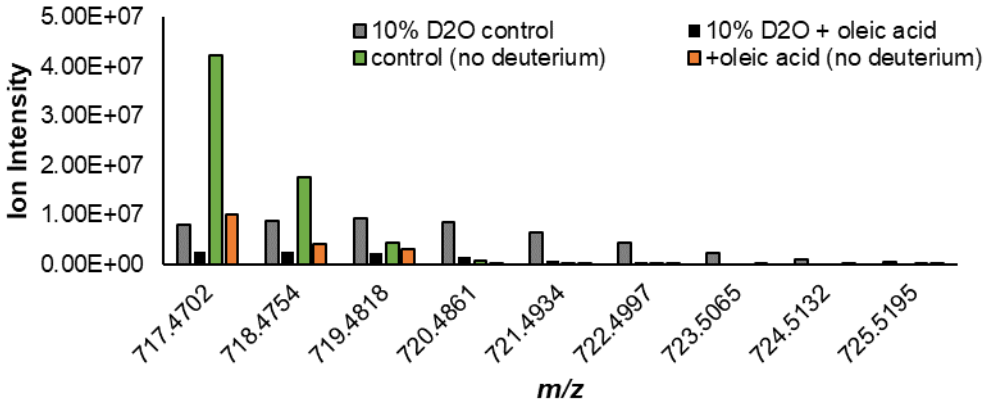

Figure S3.17 Ion intensity for PG 32:2

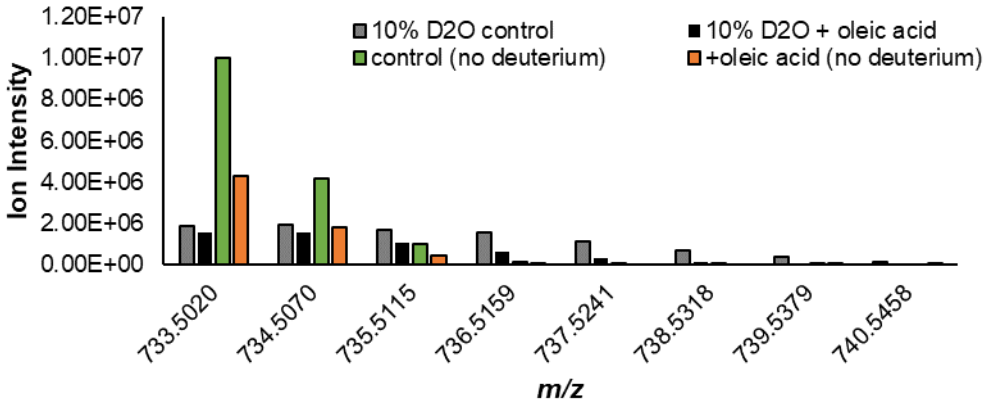

Figure S3.18 Ion intensity for PG 32:2

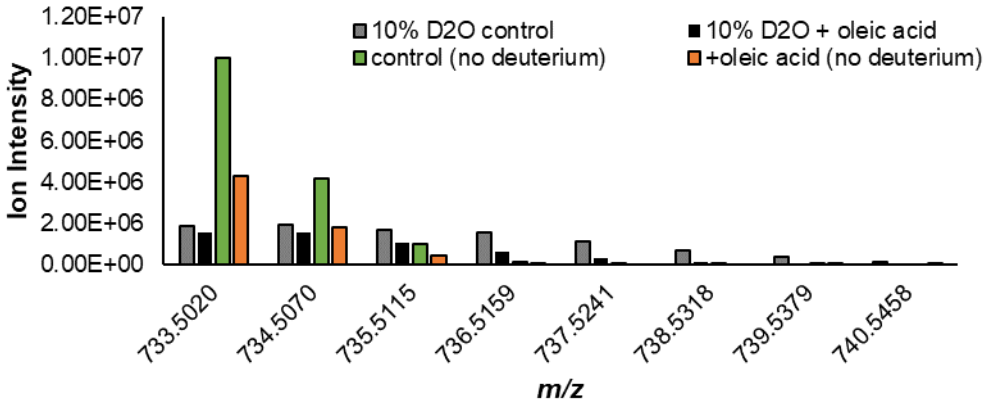

Figure S3.19 Ion intensity for PG 33:1

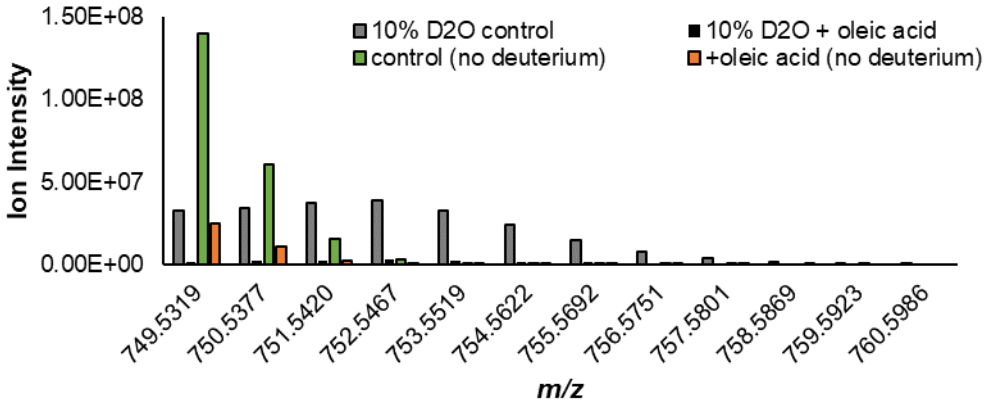

Figure S3.20 Ion intensity for PG 34:0

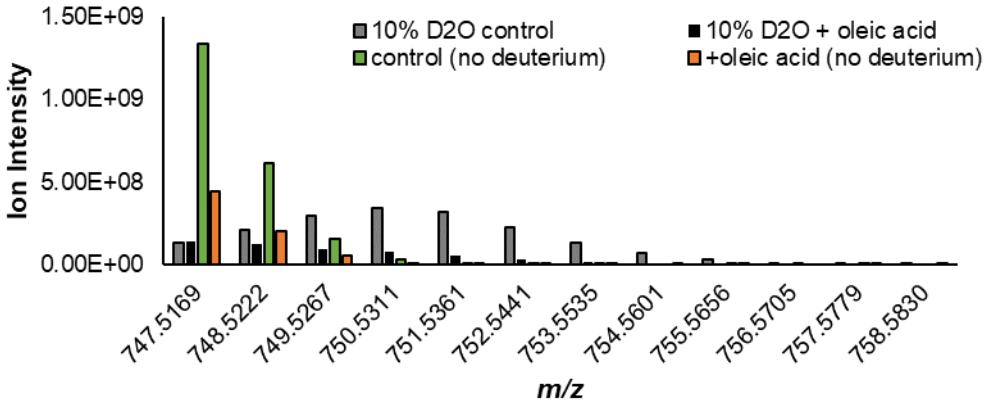

Figure S3.21 Ion intensity for PG 34:1

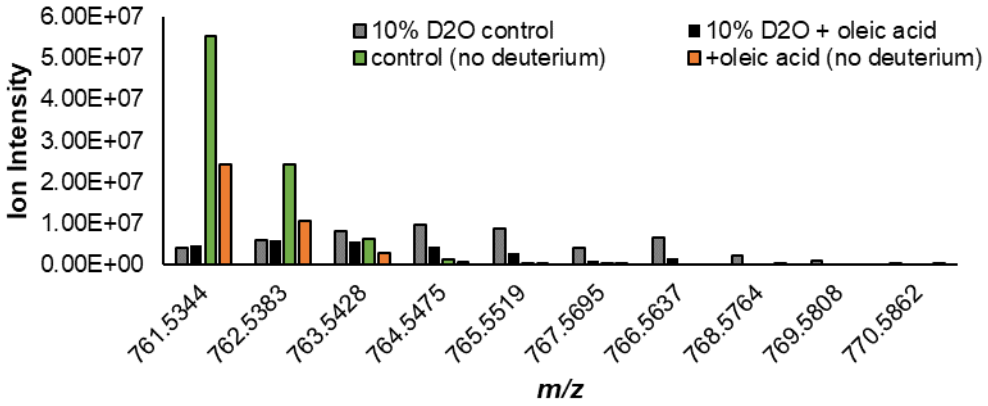

Figure S3.22 Ion intensity for PG 35:1

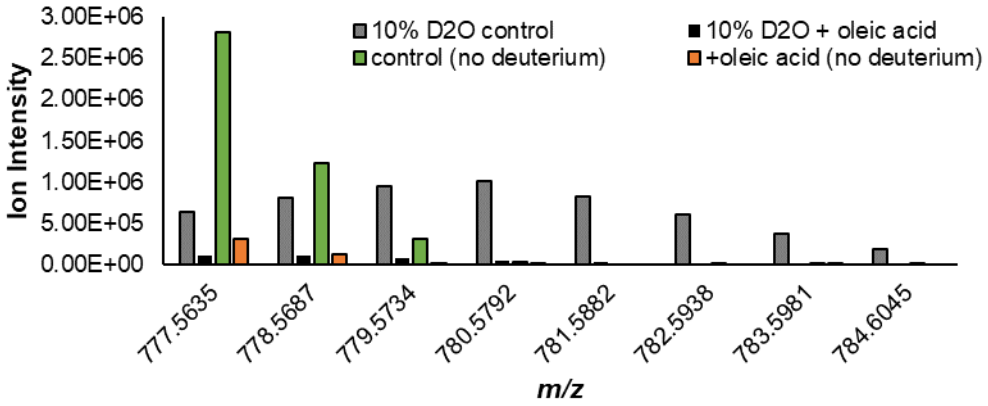

Figure S3.23 Ion intensity for PG 36:0

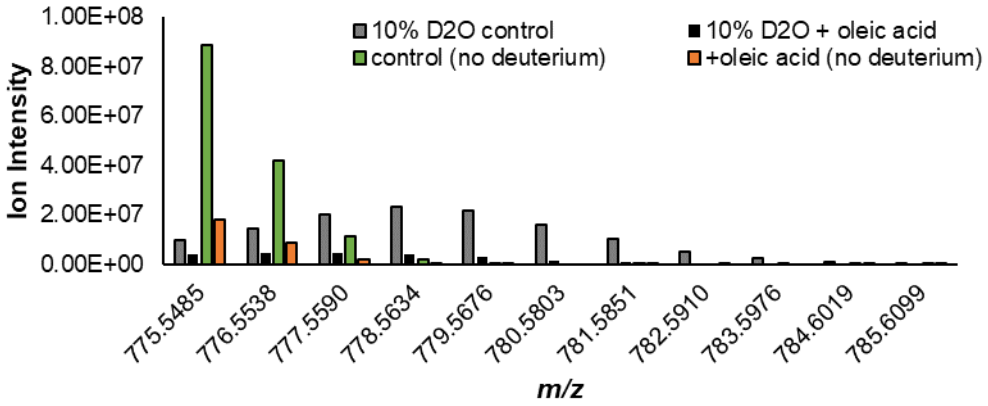

Figure S3.24 Ion intensity for PG 36:1

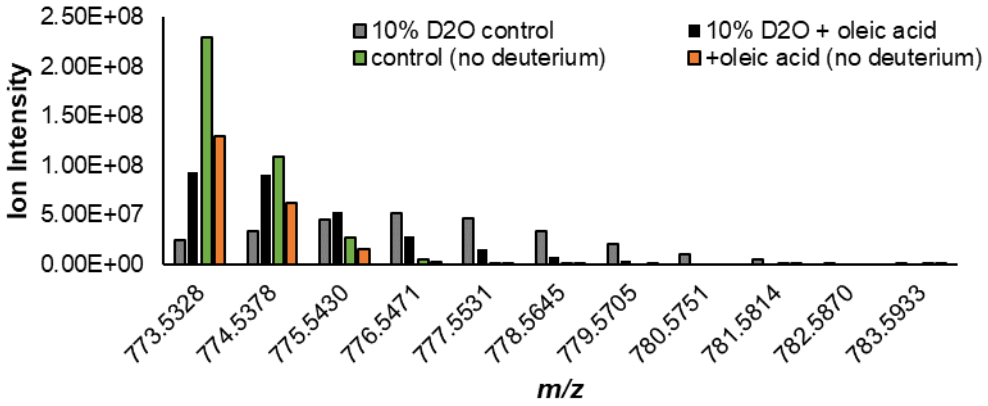

Figure S3.25 Ion intensity for PG 36:2

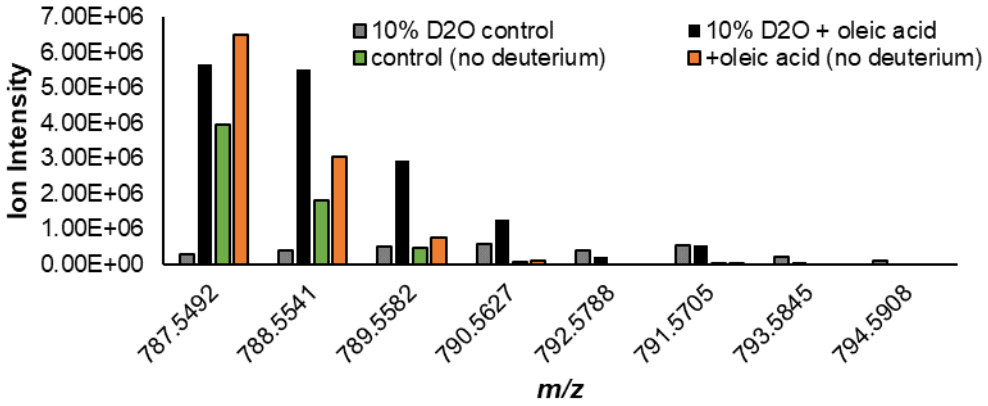

Figure S3.26 Ion intensity for PG 37:1

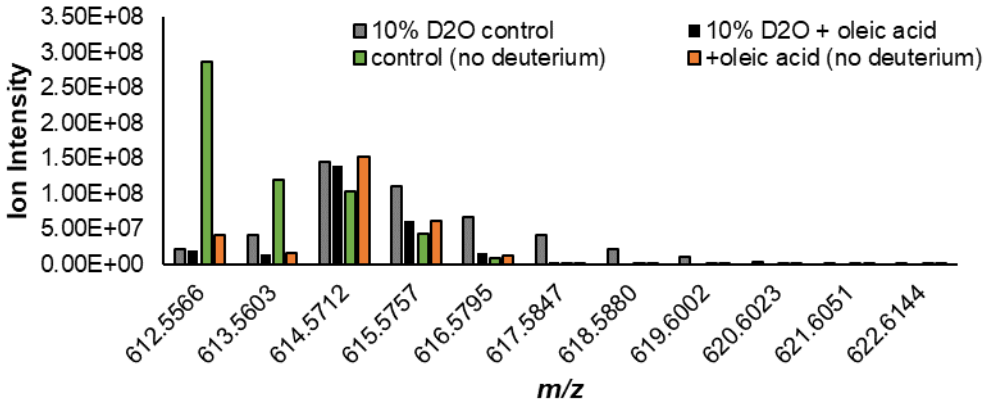

Figure S3.27 Ion intensity for DAG 34:1

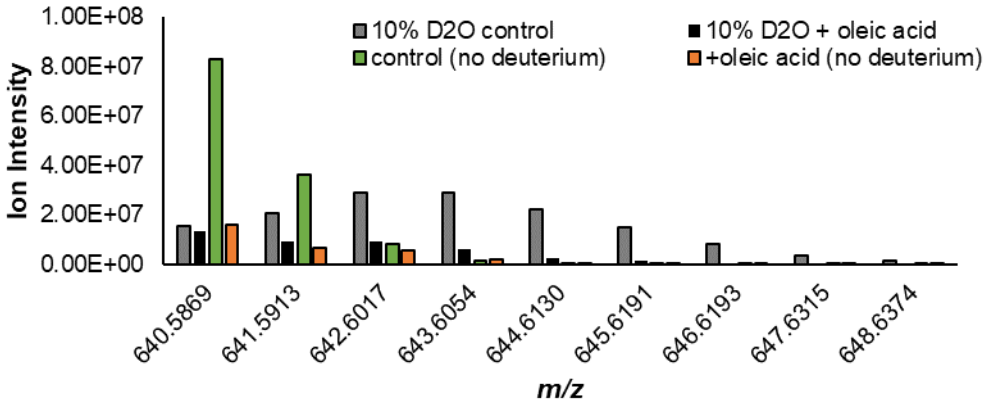

Figure S3.28 Ion intensity for DAG 36:1

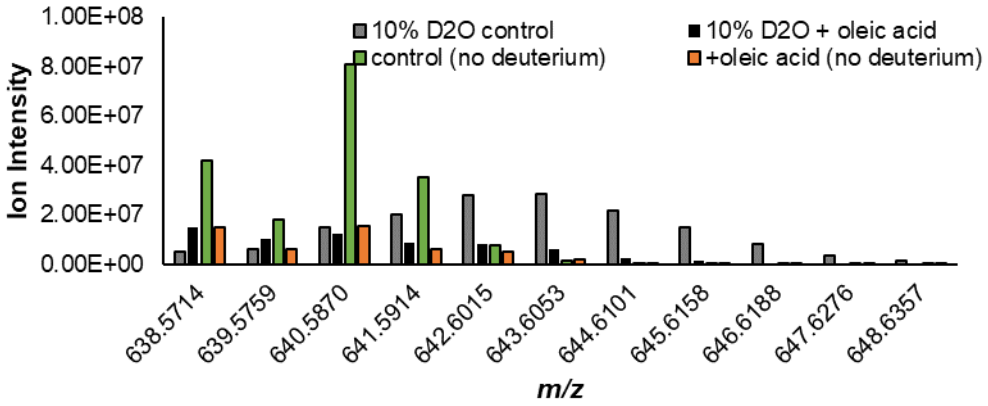

Figure S3.29 Ion intensity for DAG 36:2

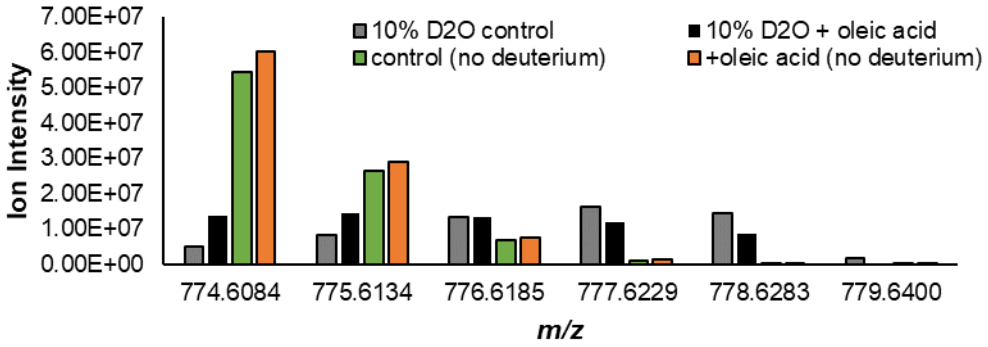

Figure S3.30 Ion intensity for MGDG 34:1

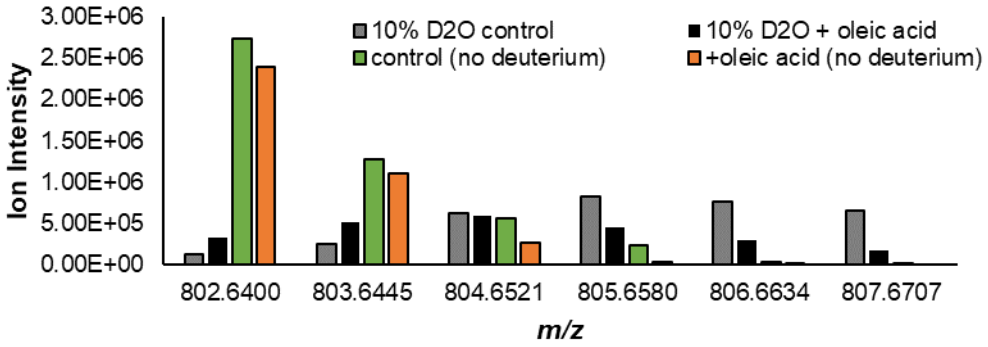

Figure S3.31 Ion intensity for MGDG 36:1

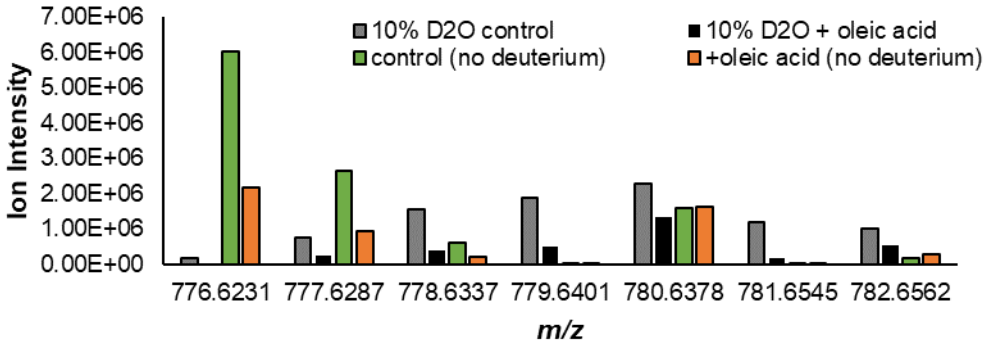

Figure S3.31 Ion intensity for MGDG 36:2

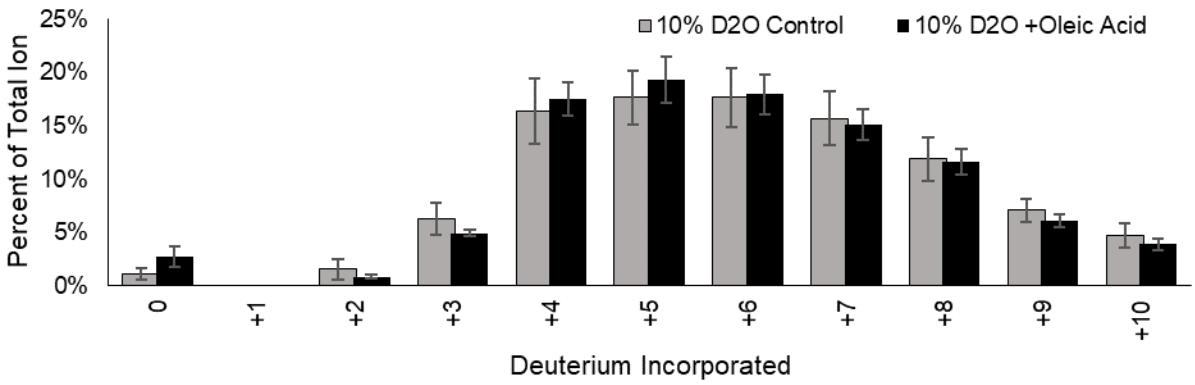

Figure S3.32 Average deuterium incorporation for CL 62:1

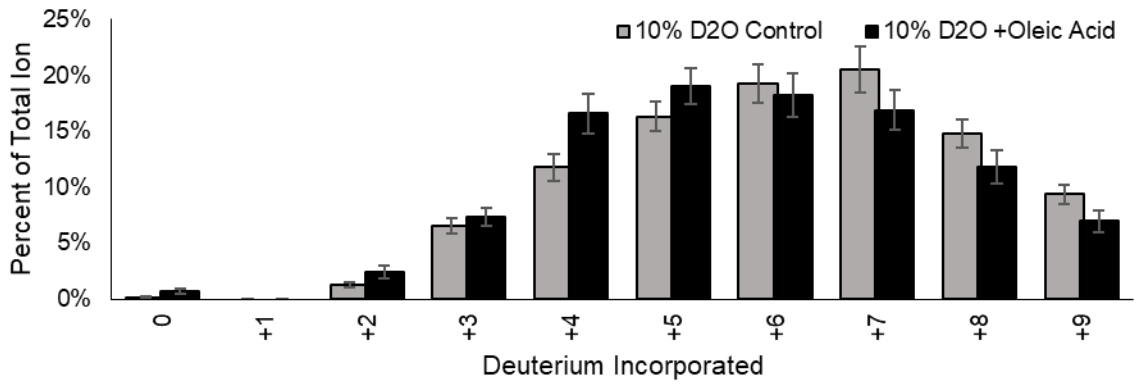

Figure S3.33 Average deuterium incorporation for CL 62:2

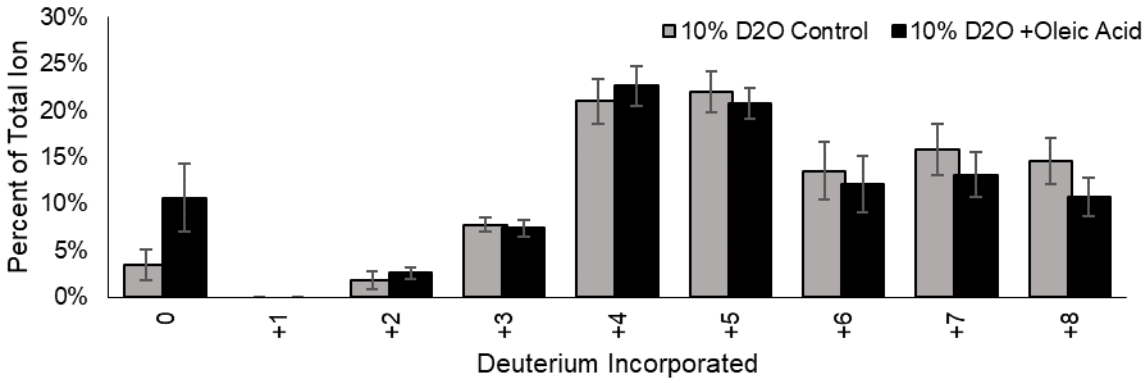

Figure S3.34 Average deuterium incorporation for CL 64:1

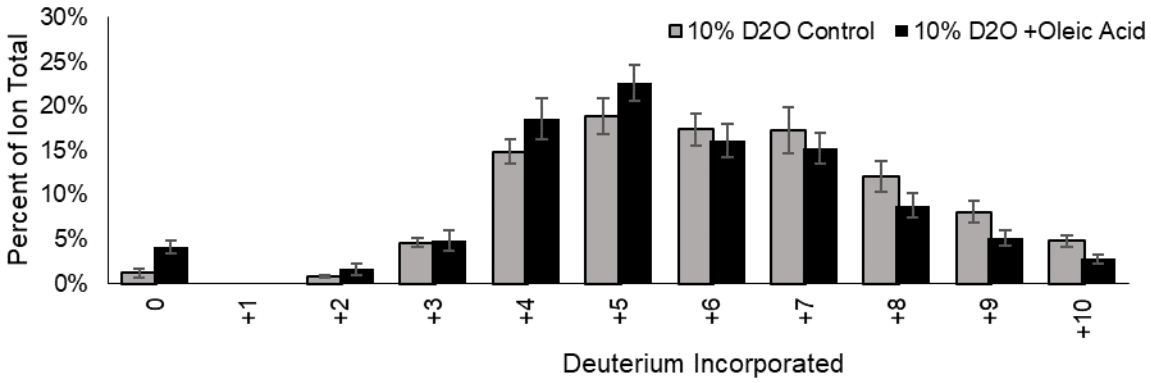

Figure S3.35 Average deuterium incorporation for CL 64:2

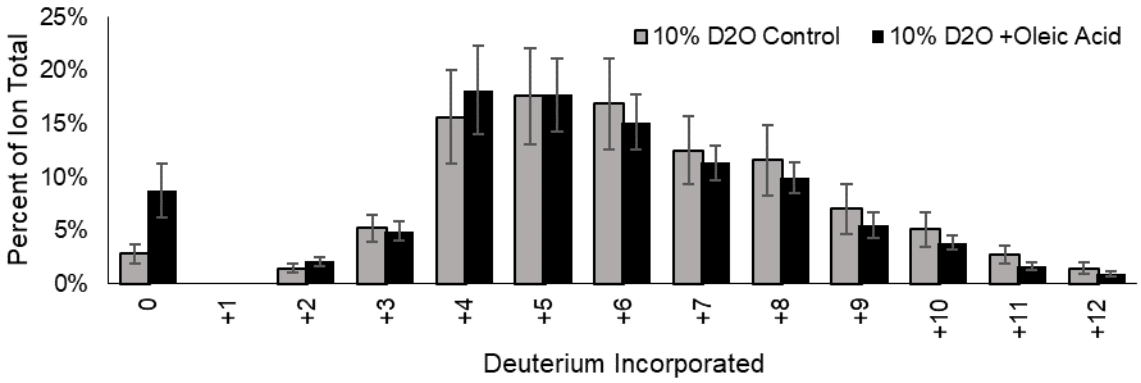

Figure S3.36 Average deuterium incorporation for CL 66:1

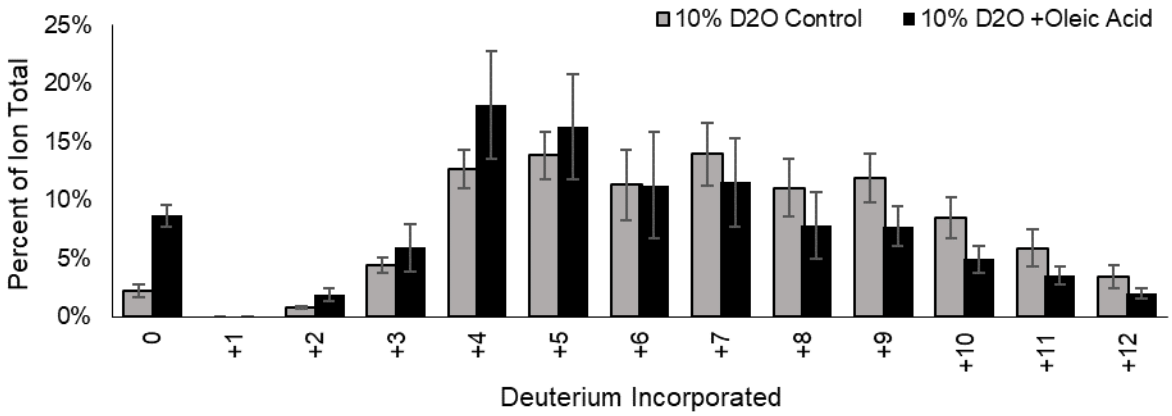

Figure S3.37 Average deuterium incorporation for CL 66:2

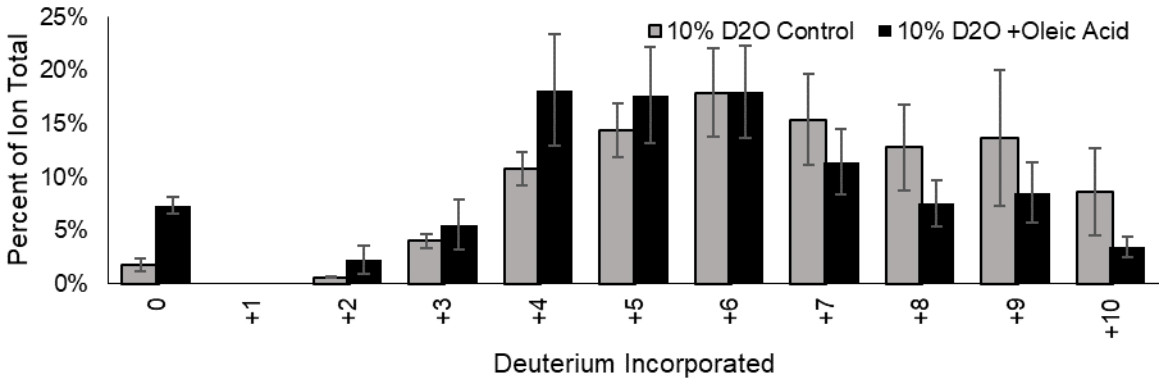

Figure S3.38 Average deuterium incorporation for CL 66:3

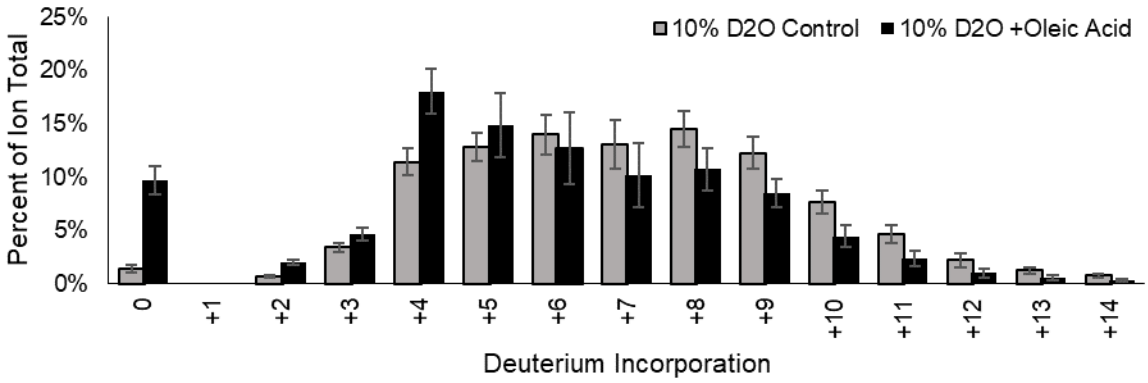

Figure S3.39 Average deuterium incorporation for CL 68:2

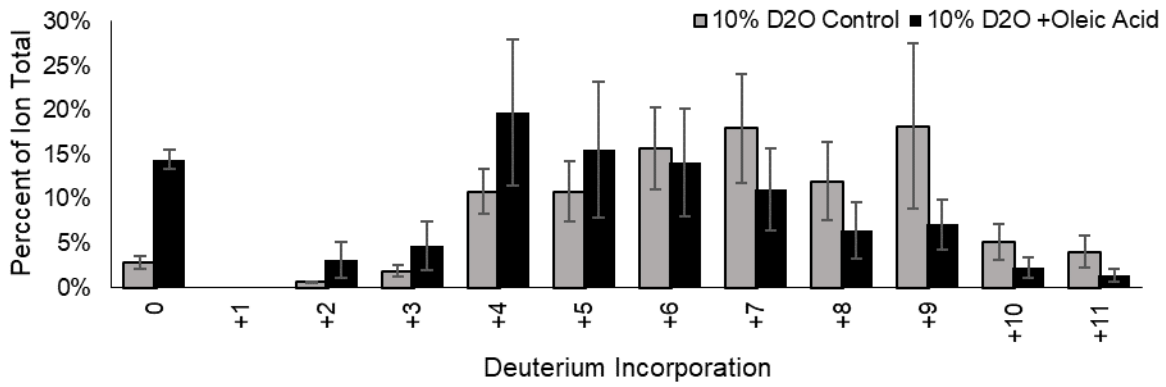

Figure S3.40 Average deuterium incorporation for CL 68:3

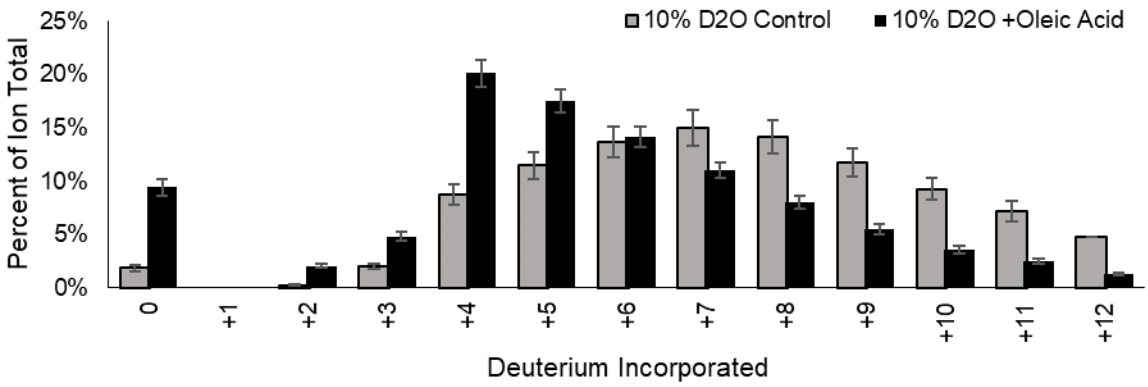

Figure S3.41 Average deuterium incorporation for CL 70:3

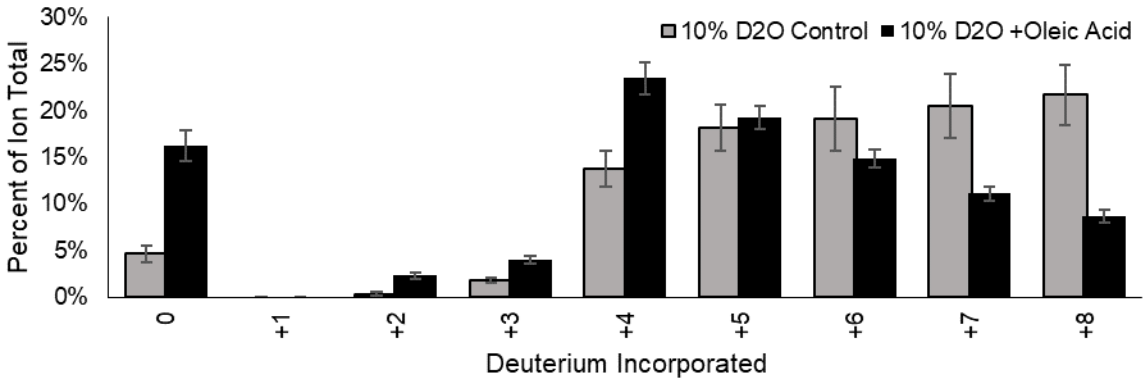

Figure S3.42 Average deuterium incorporation for CL 72:4

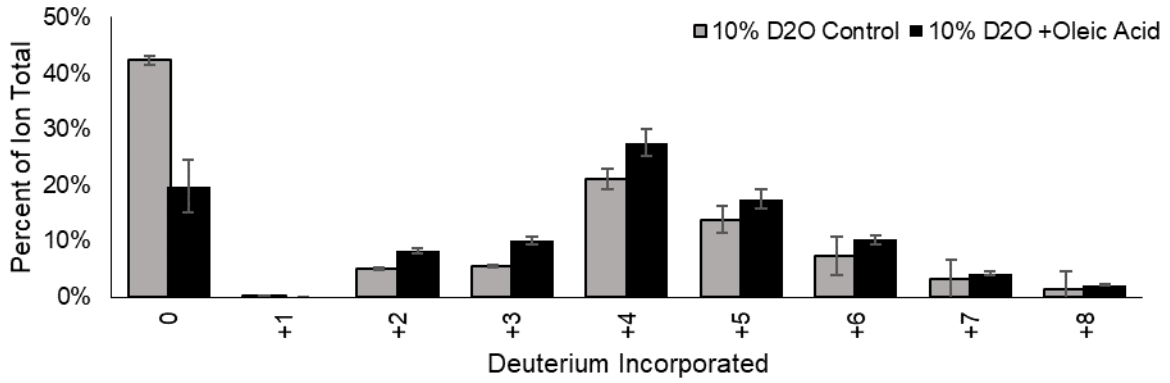

Figure S3.43 Average deuterium incorporation for PG 30:0

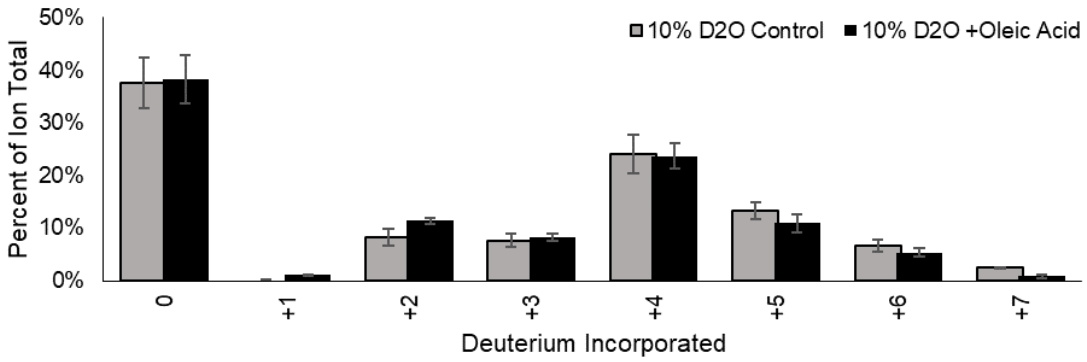

Figure S3.44 Average deuterium incorporation for PG 30:1

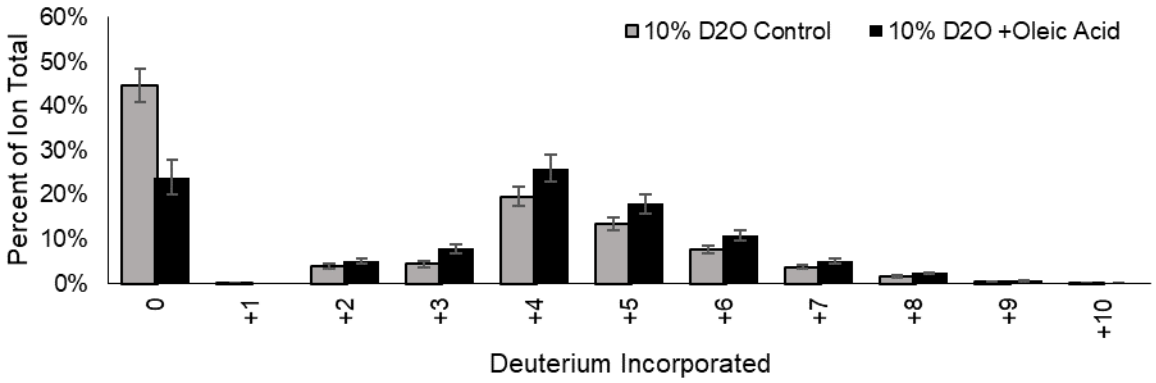

Figure S3.45 Average deuterium incorporation for PG 32:0

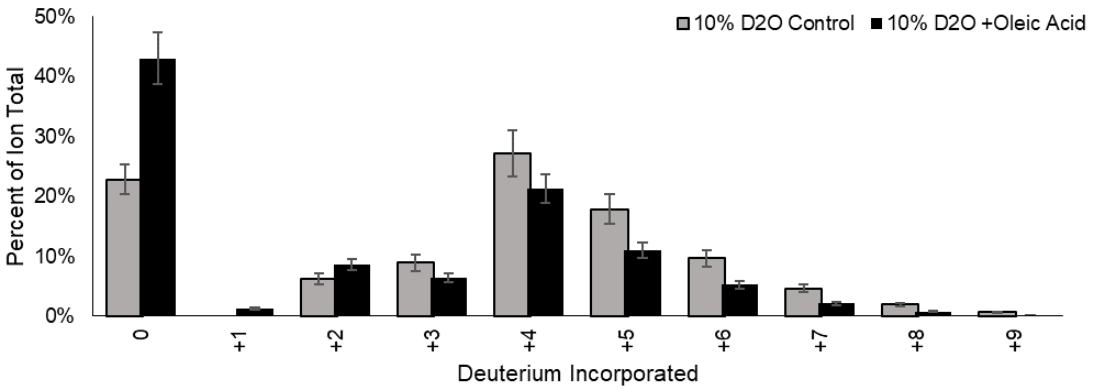

Figure S3.46 Average deuterium incorporation for PG 32:1

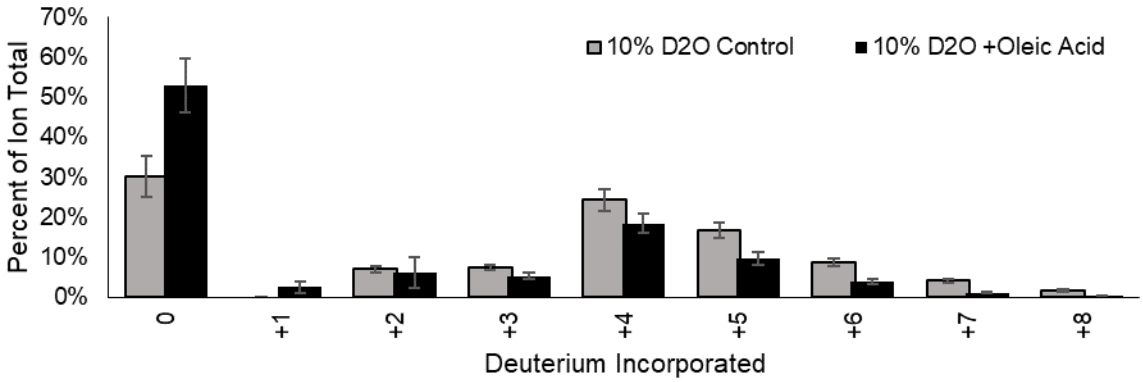

Figure S3.47 Average deuterium incorporation for PG 32:2

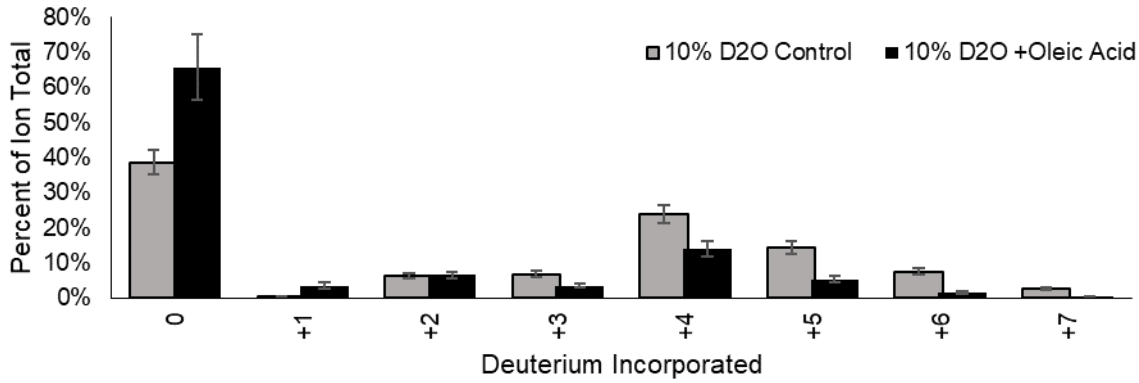

Figure S3.48 Average deuterium incorporation for PG 33:1

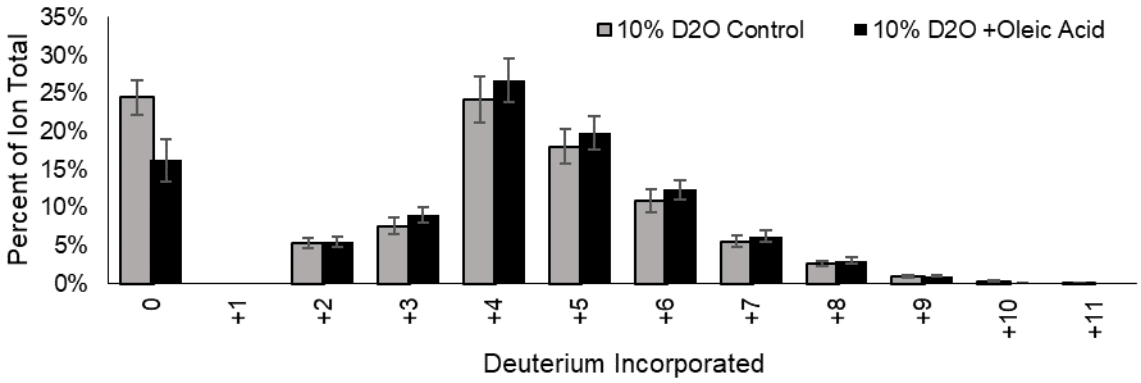

Figure S3.49 Average deuterium incorporation for PG 34:0

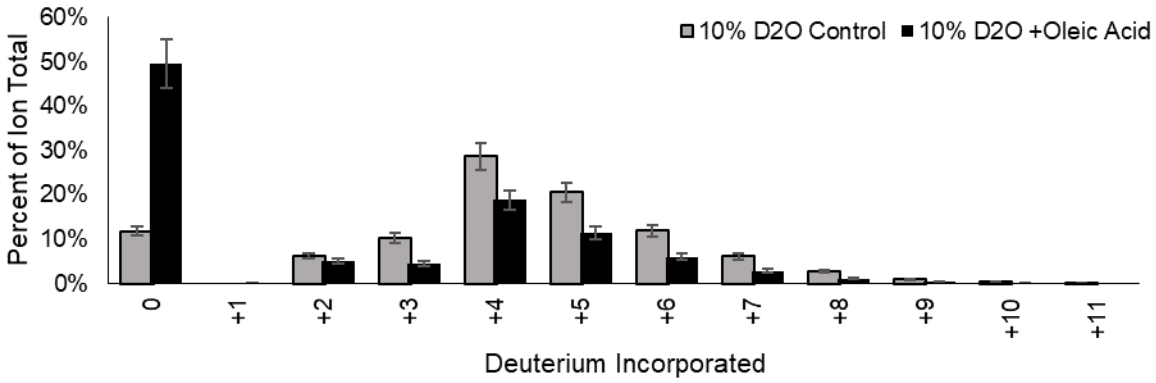

Figure S3.50 Average deuterium incorporation for PG 34:1

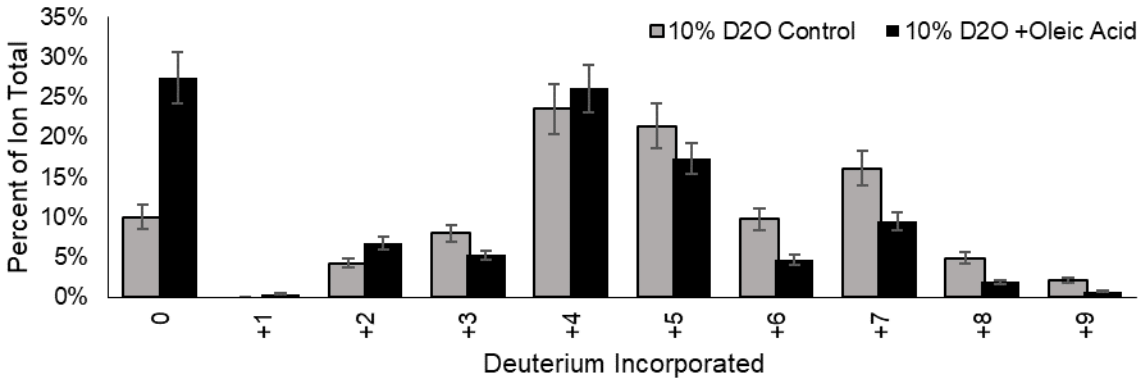

Figure S3.51 Average deuterium incorporation for PG 35:1

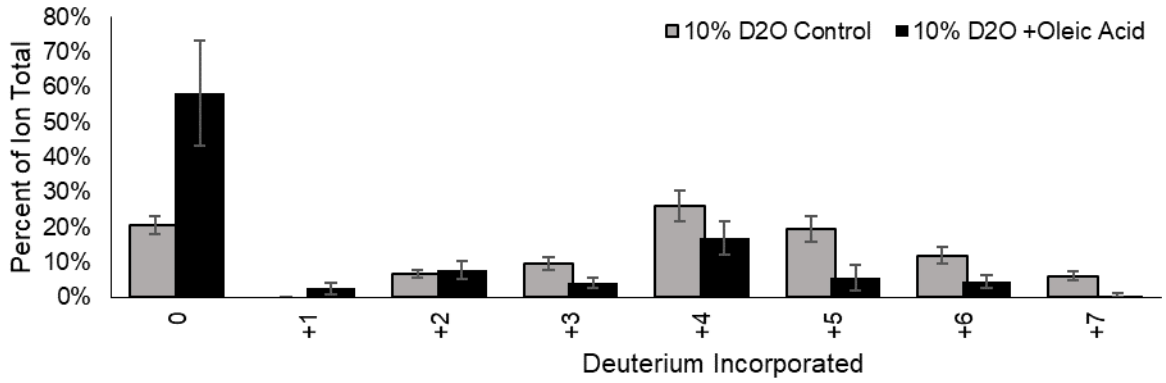

Figure S3.52 Average deuterium incorporation for PG 36:0

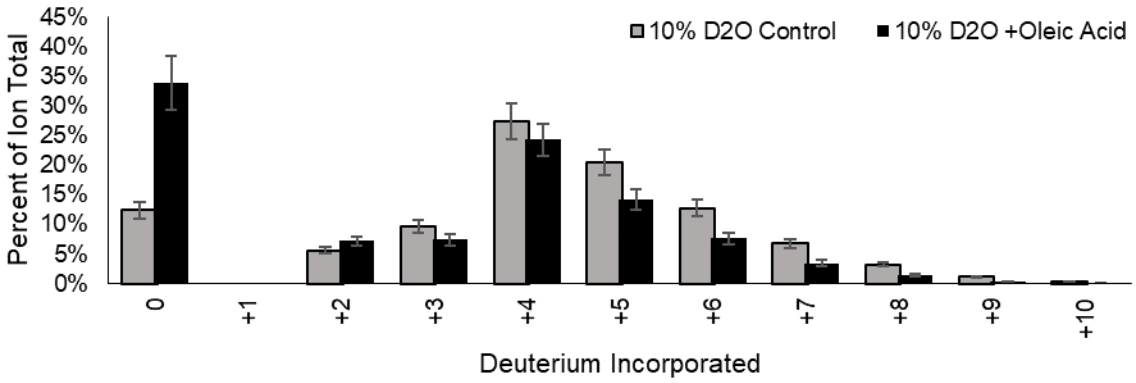

Figure S3.53 Average deuterium incorporation for PG 36:1

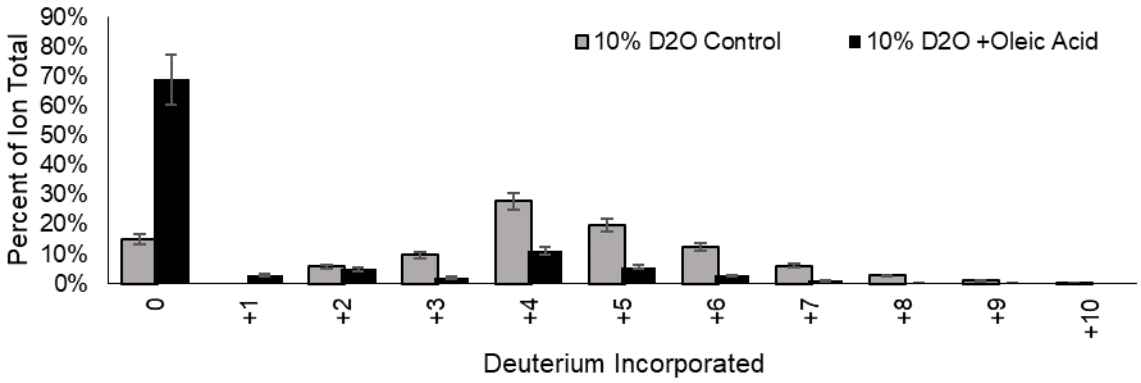

Figure S3.54 Average deuterium incorporation for PG 36:2

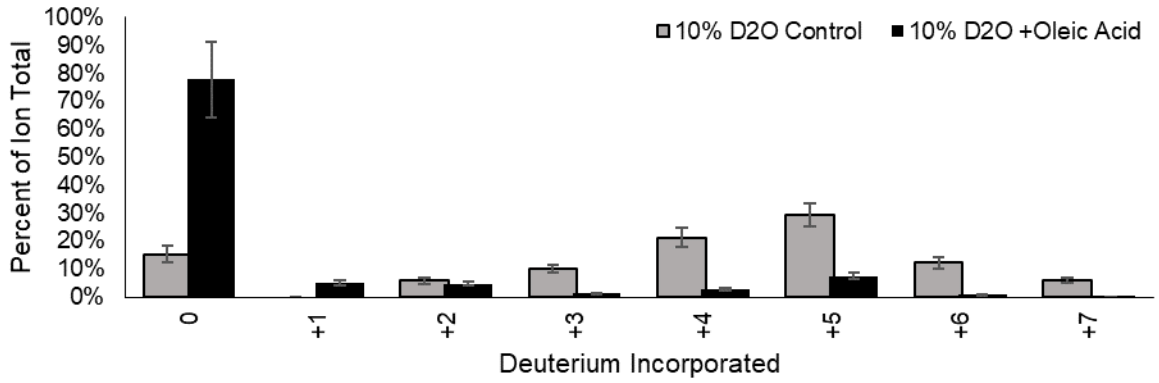

Figure S3.55 Average deuterium incorporation for PG 37:2

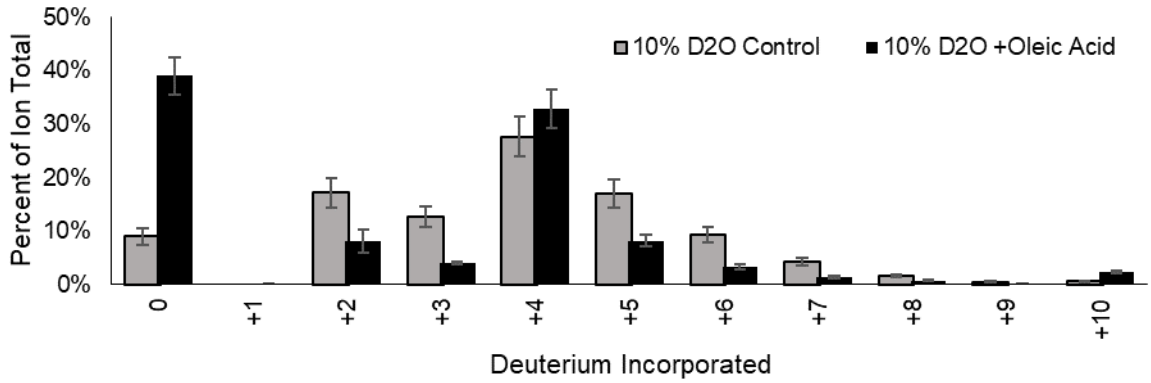

Figure S3.56 Average deuterium incorporation for DAG 34:1

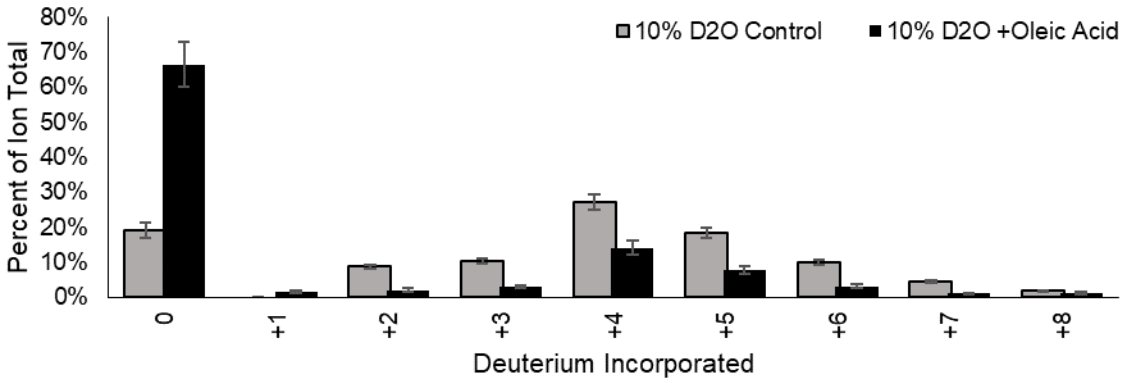

Figure S3.57 Average deuterium incorporation for DAG 36:1

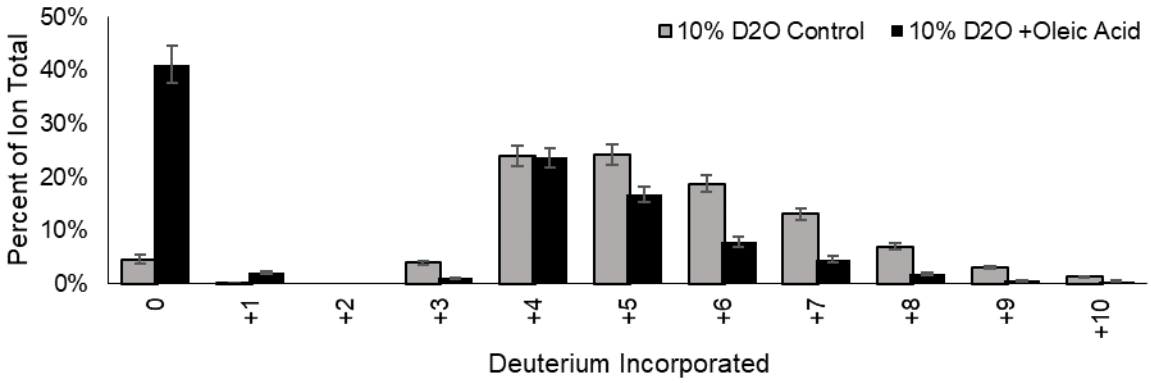

Figure S3.58 Average deuterium incorporation for DAG 36:2

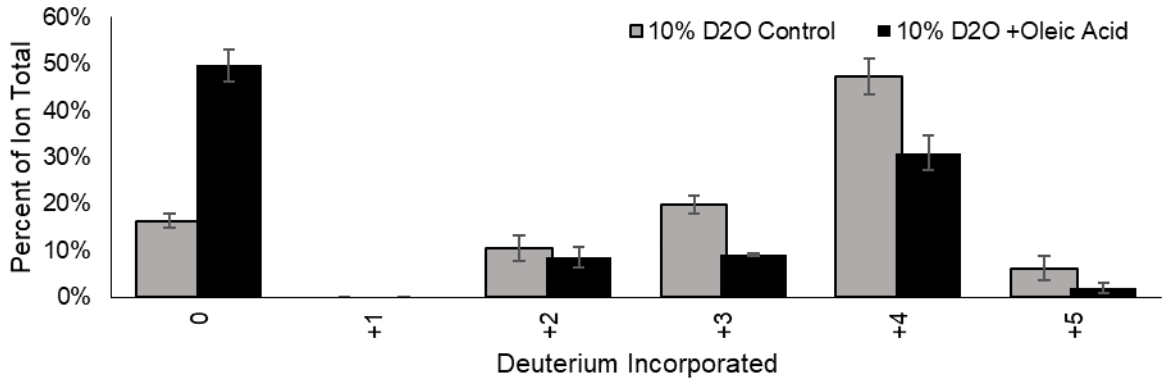

Figure S3.59 Average deuterium incorporation for MGDG 34:1

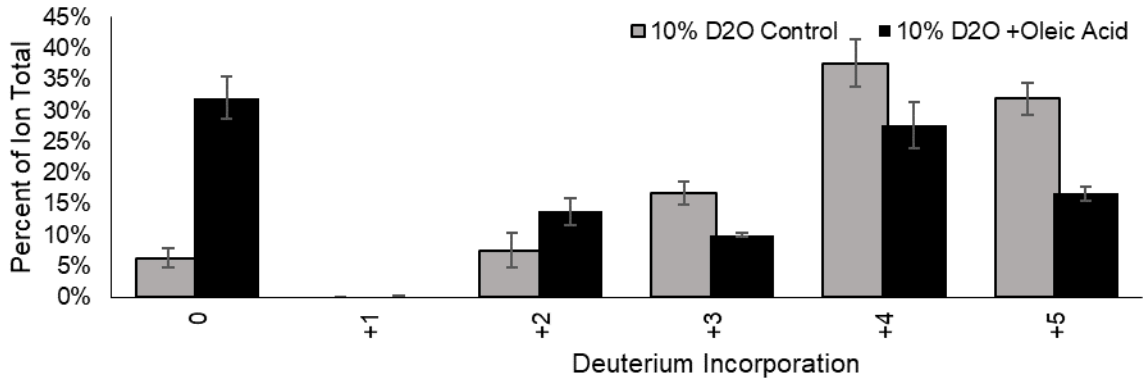

Figure S3.60 Average deuterium incorporation for MGDG 36:1

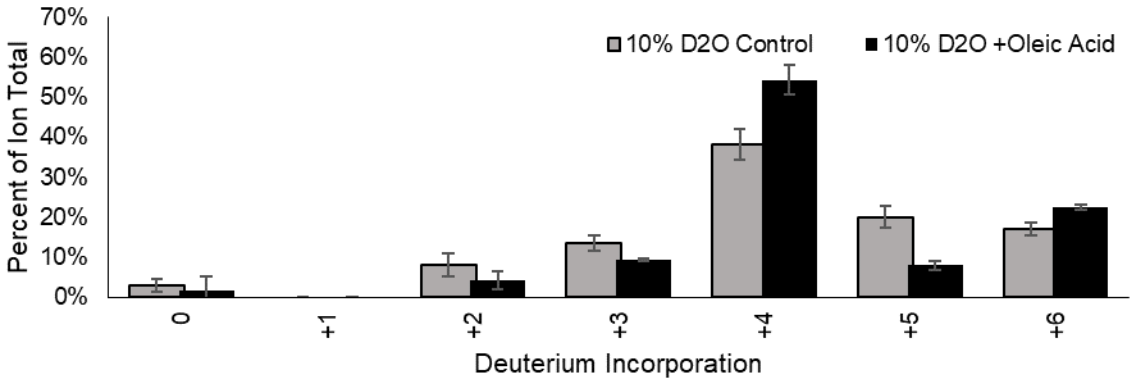

Figure S3.61 Average deuterium incorporation for MGDG 34:0

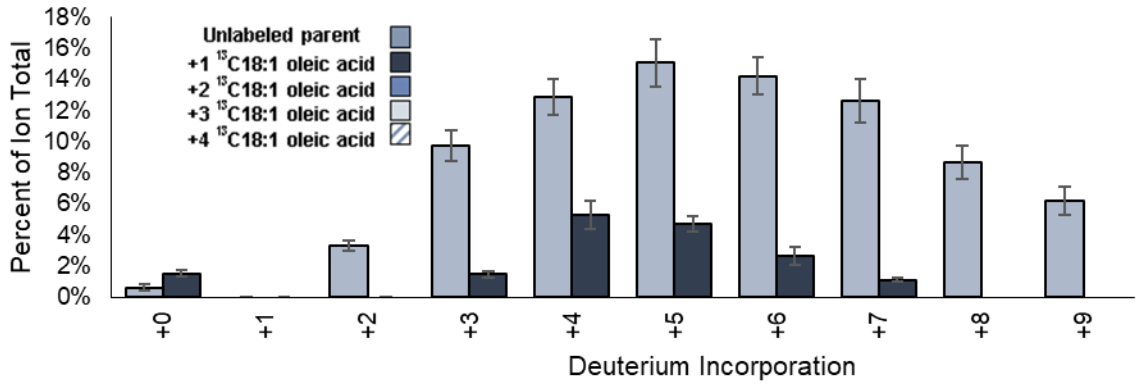

Figure S3.62 Average deuterium incorporation for CL 62:1 in dual labeled culture (10% D_2O + ^{13}C oleic acid)

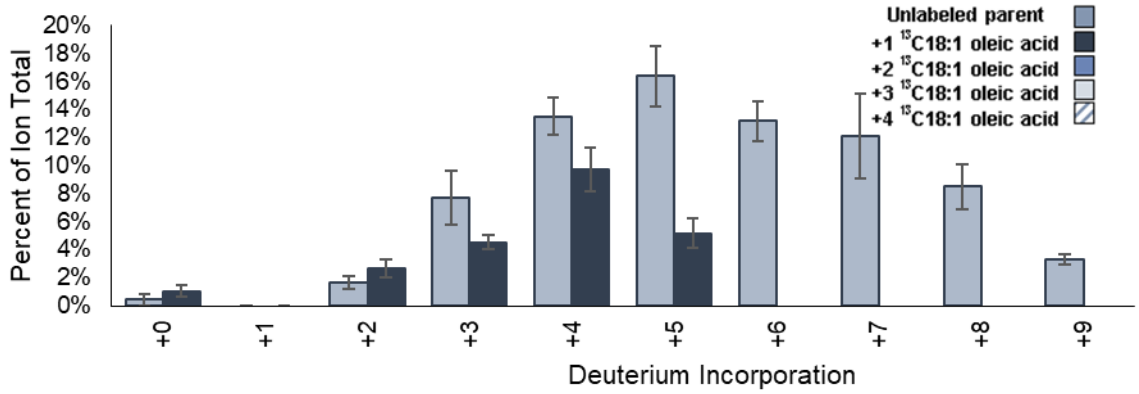

Figure S3.63 Average deuterium incorporation for CL 62:2 in dual labeled culture (10% D_2O + ^{13}C oleic acid)

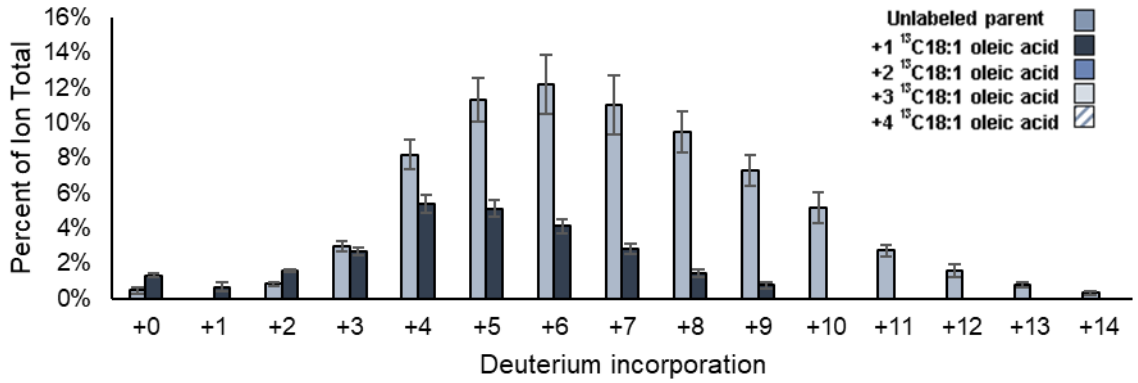

Figure S3.64 Average deuterium incorporation for CL 64:1 in dual labeled culture (10% D_2O + ^{13}C oleic acid)

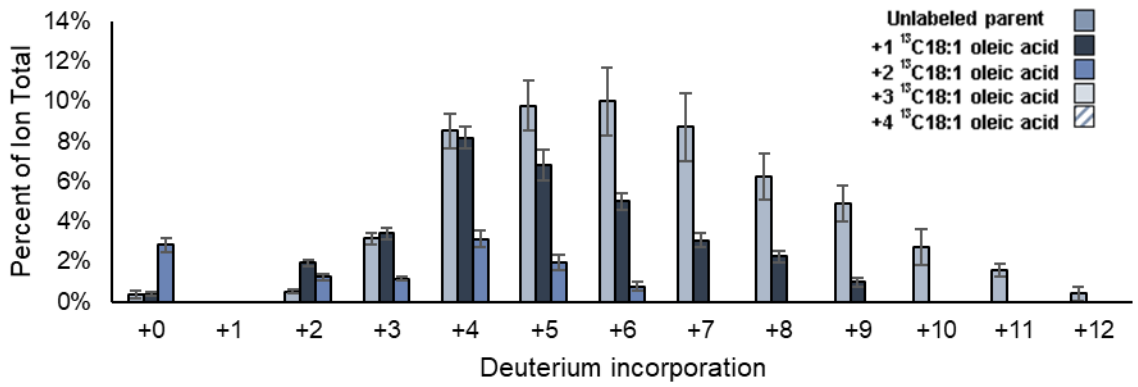

Figure S3.65 Average deuterium incorporation for CL 64:2 in dual labeled culture (10% D_2O + ^{13}C oleic acid)

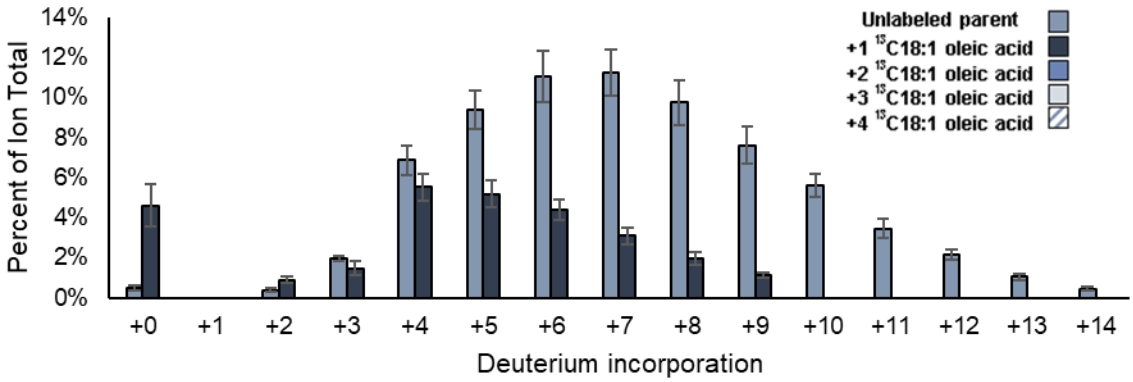

Figure S3.66 Average deuterium incorporation for CL 66:1 in dual labeled culture (10% D_2O + ^{13}C oleic acid)

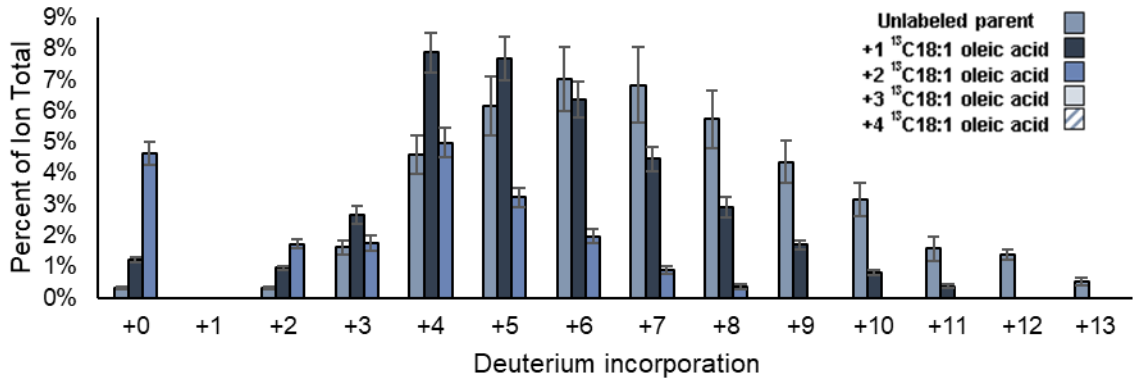

Figure S3.67 Average deuterium incorporation for CL 66:2 in dual labeled culture (10% D_2O + ^{13}C oleic acid)

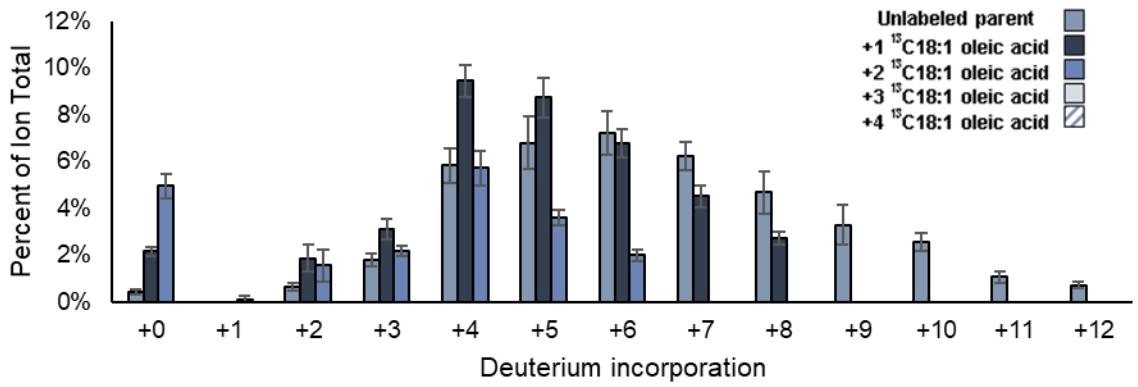

Figure S3.68 Average deuterium incorporation for CL 66:3 in dual labeled culture (10% D_2O + ^{13}C oleic acid)

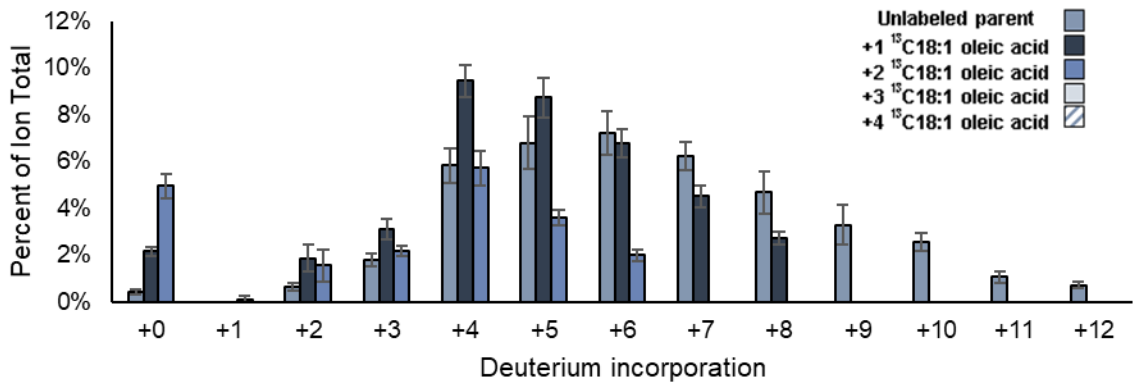

Figure S3.69 Average deuterium incorporation for CL 68:2 in dual labeled culture (10% D_2O + ^{13}C oleic acid)

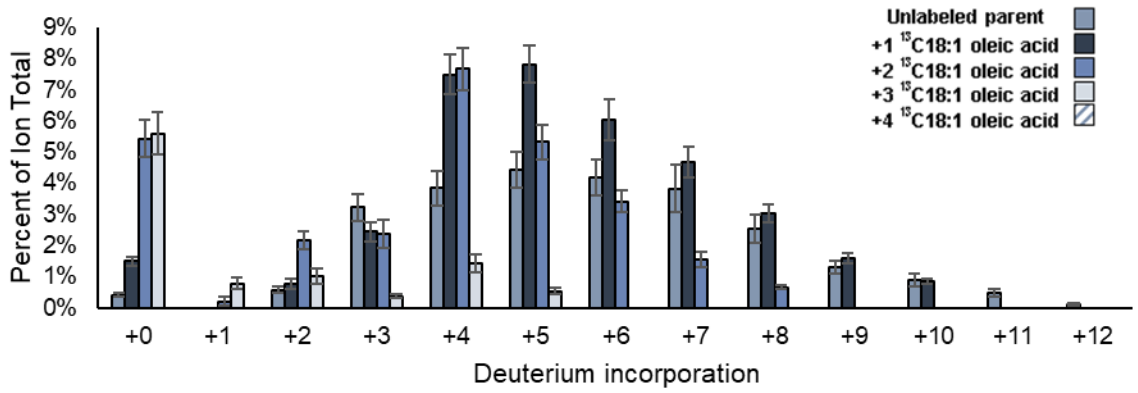

Figure S3.70 Average deuterium incorporation for CL 68:3 in dual labeled culture (10% D2O + 13C oleic acid)

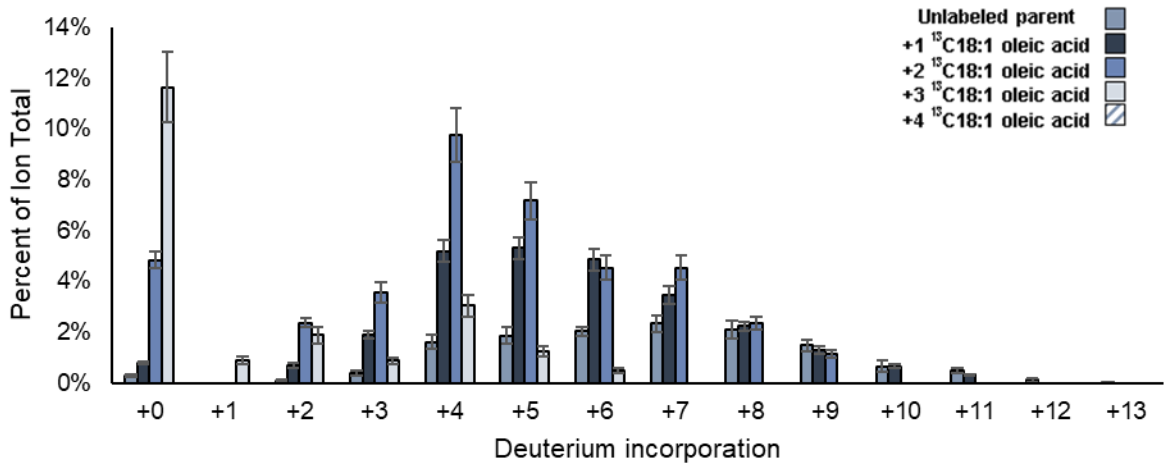

Figure S3.71 Average deuterium incorporation for CL 70:3 in dual labeled culture (10% D_2O + ^{13}C oleic acid)

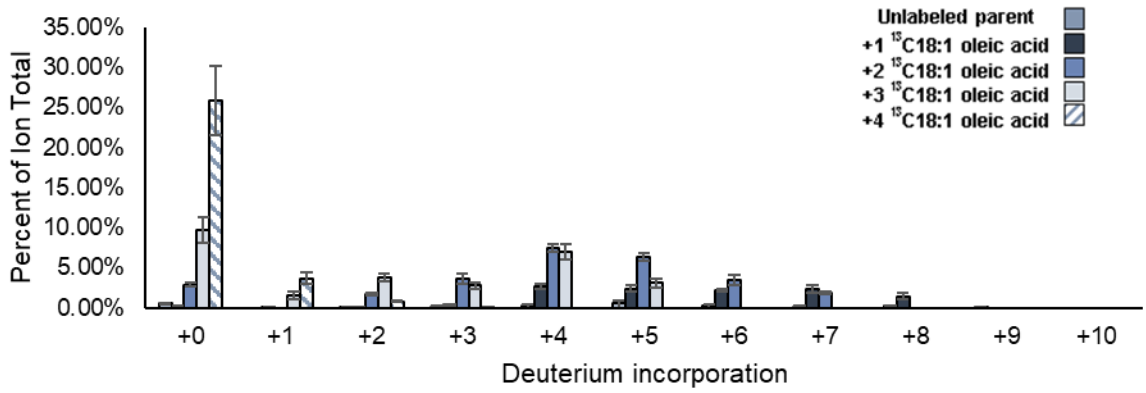

Figure S3.72 Average deuterium incorporation for CL 72:4 in dual labeled culture (10% D_2O + ^{13}C oleic acid)

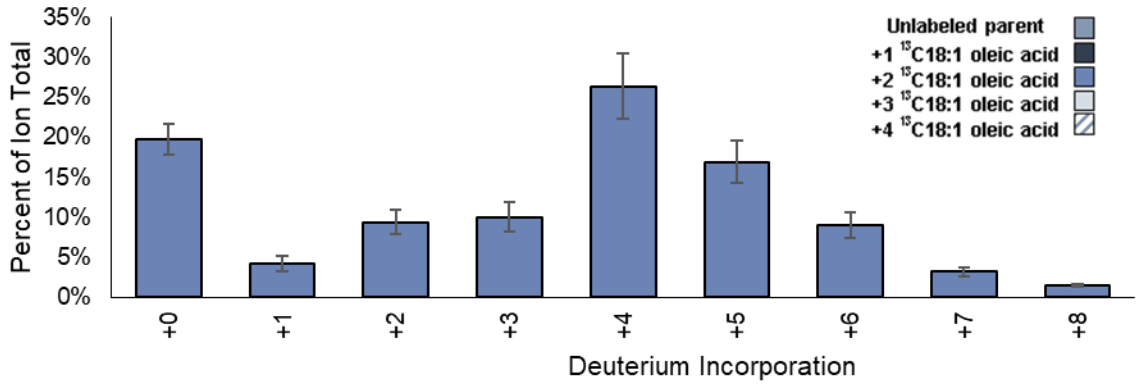

Figure S3.73 Average deuterium incorporation for PG 30:0 in dual labeled culture (10% D_2O + ^{13}C oleic acid)

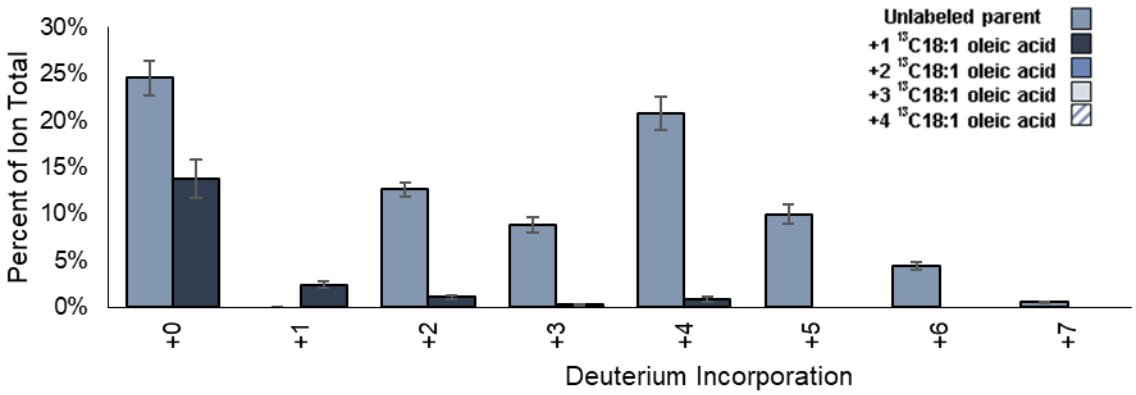

Figure S3.74 Average deuterium incorporation for PG 30:1 in dual labeled culture (10% D_2O + ^{13}C oleic acid)

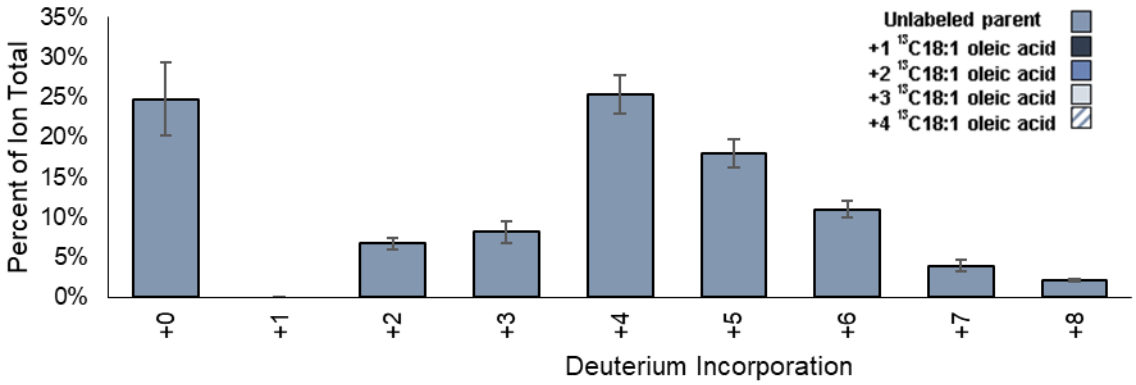

Figure S3.75 Average deuterium incorporation for PG 32:0 in dual labeled culture (10% D_2O + ^{13}C oleic acid)

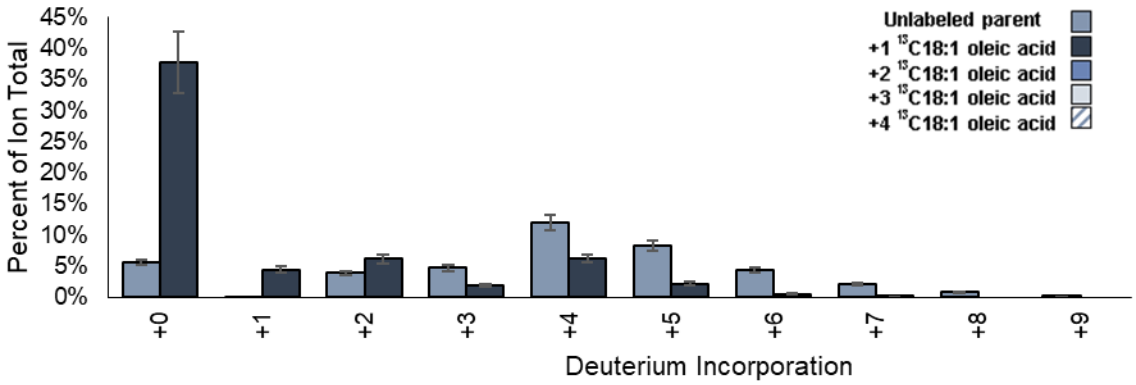

Figure S3.76 Average deuterium incorporation for PG 32:1 in dual labeled culture (10% D_2O + ^{13}C oleic acid)

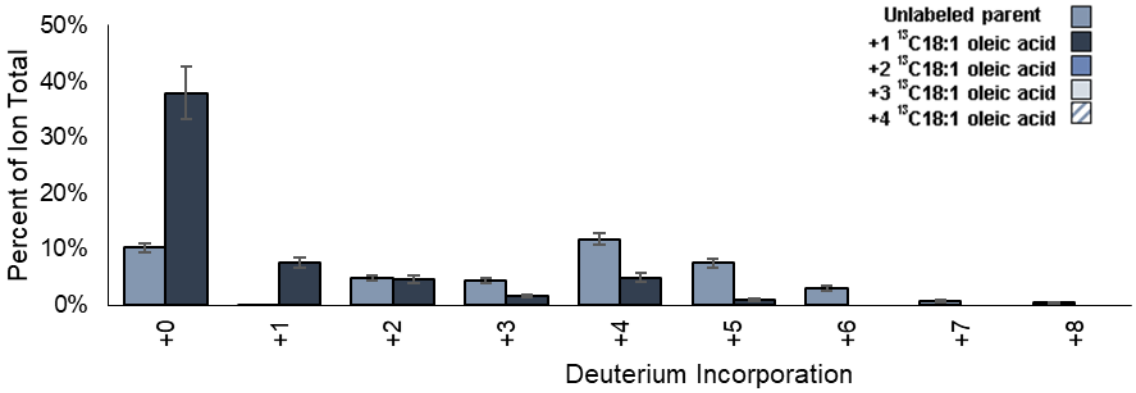

Figure S3.77 Average deuterium incorporation for PG 32:2 in dual labeled culture (10% D_2O + ^{13}C oleic acid)

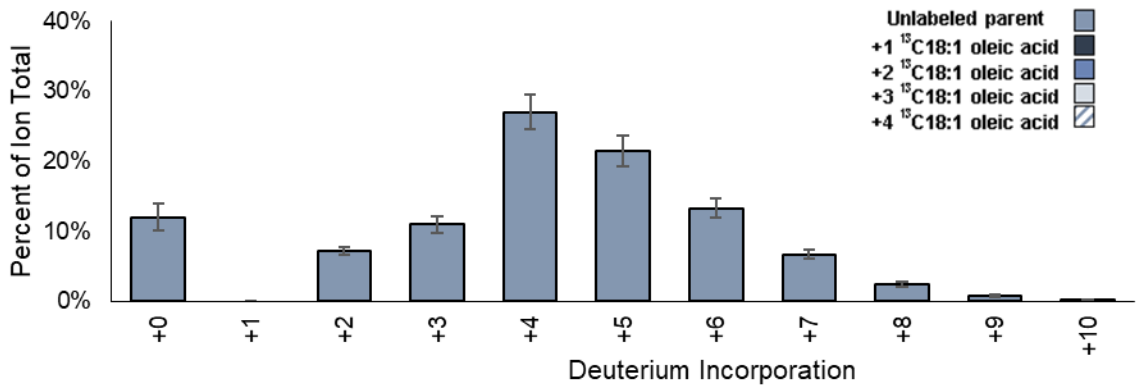

Figure S3.78 Average deuterium incorporation for PG 34:0 in dual labeled culture (10% D_2O + ^{13}C oleic acid)

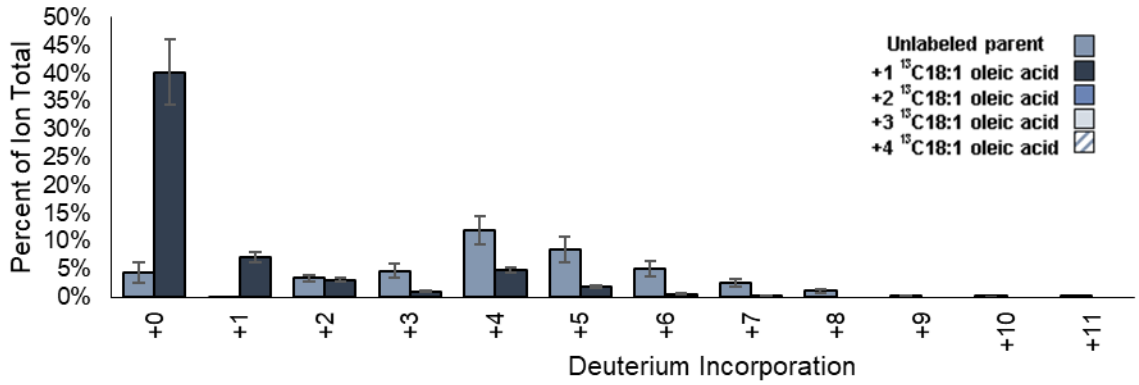

Figure S3.79 Average deuterium incorporation for PG 34:1 in dual labeled culture (10% D_2O + ^{13}C oleic acid)

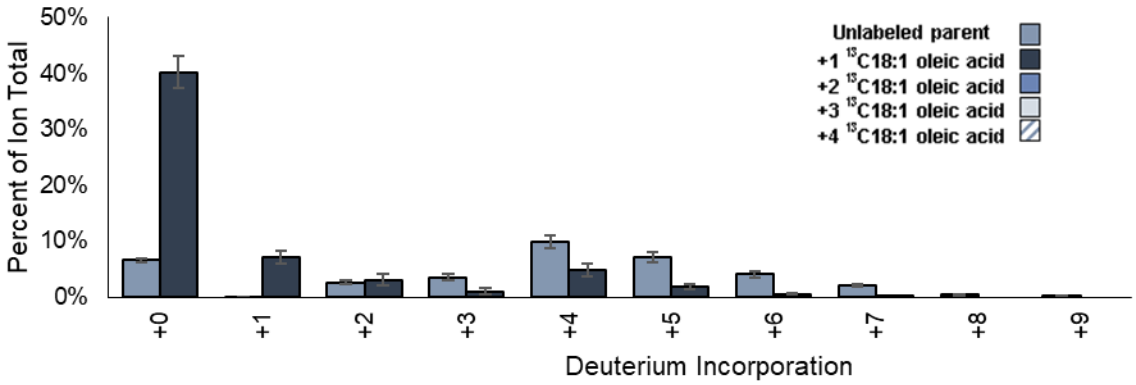

Figure S3.80 Average deuterium incorporation for PG 35:1 in dual labeled culture (10% D_2O + ^{13}C oleic acid)

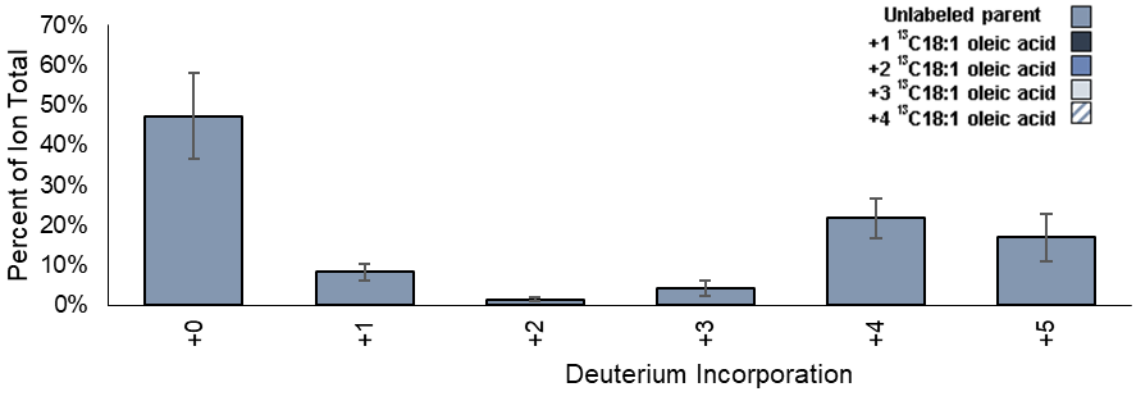

Figure S3.81 Average deuterium incorporation for PG 36:0 in dual labeled culture (10% D_2O + ^{13}C oleic acid)

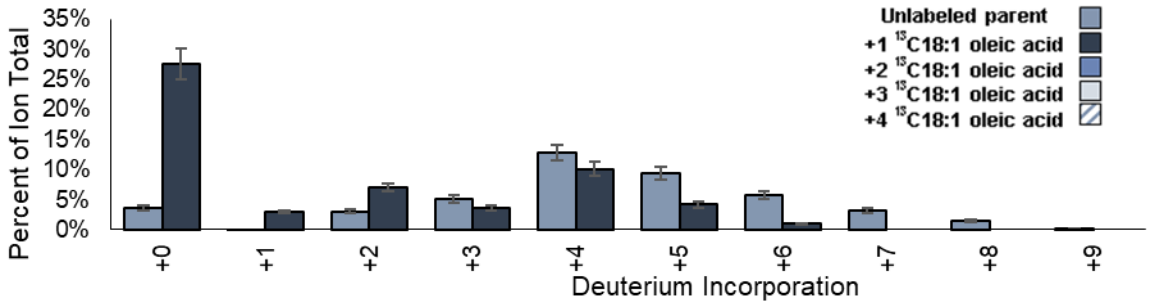

Figure S3.82 Average deuterium incorporation for PG 36:1 in dual labeled culture (10% D_2O + ^{13}C oleic acid)

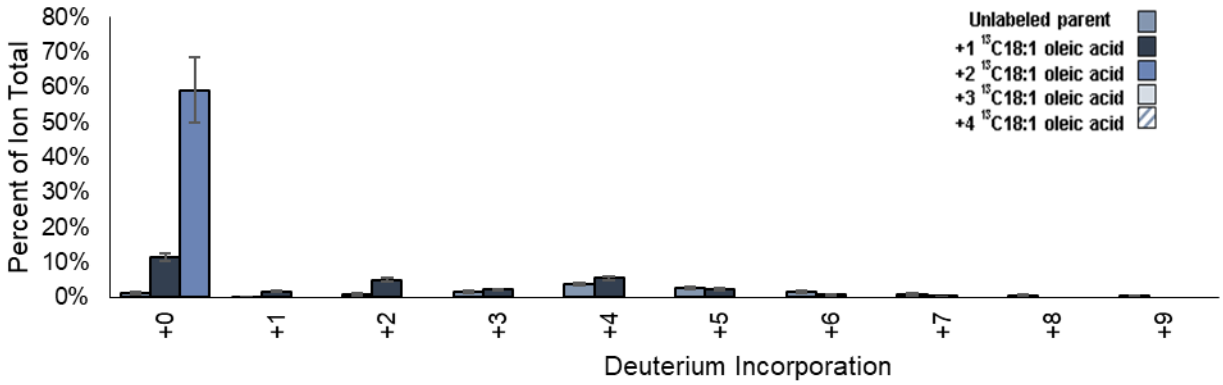

Figure S3.83 Average deuterium incorporation for PG 36:2 in dual labeled culture (10% D_2O + ^{13}C oleic acid)

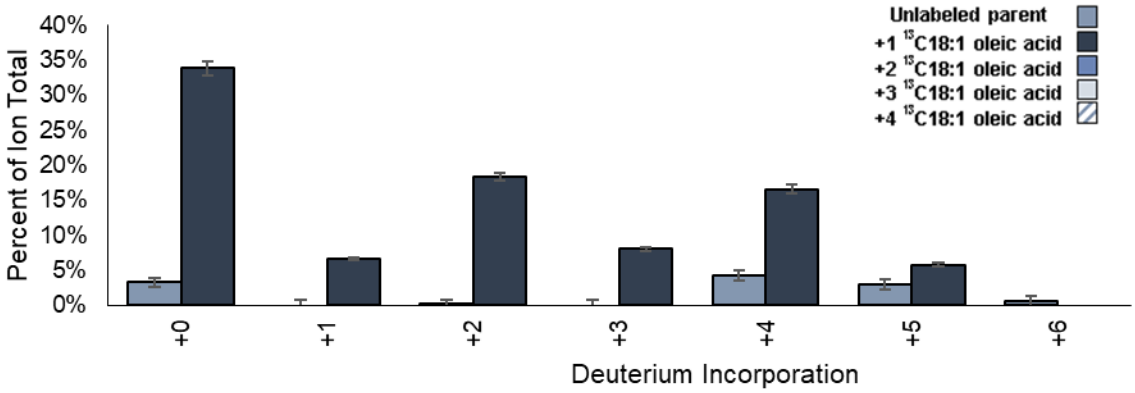

Figure S3.84 Average deuterium incorporation for PG 37:2 in dual labeled culture (10% D_2O + ^{13}C oleic acid)

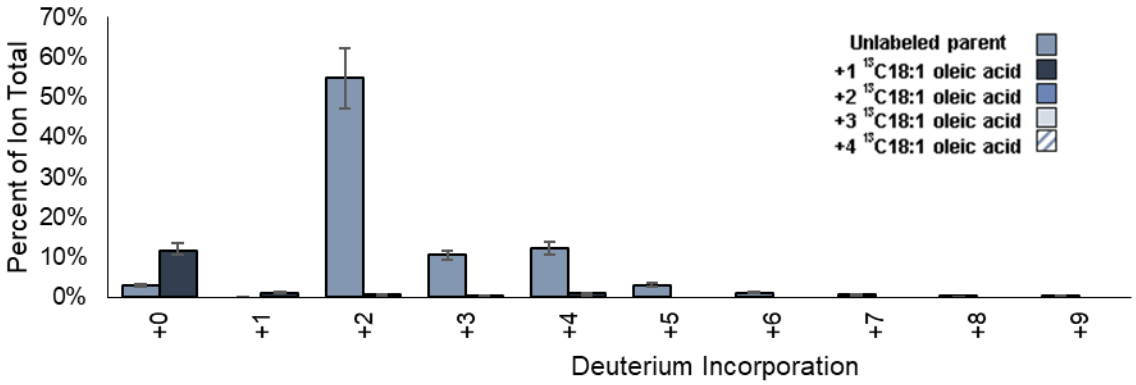

Figure S3.85 Average deuterium incorporation for DAG 34:1 in dual labeled culture (10% D_2O + ^{13}C oleic acid)

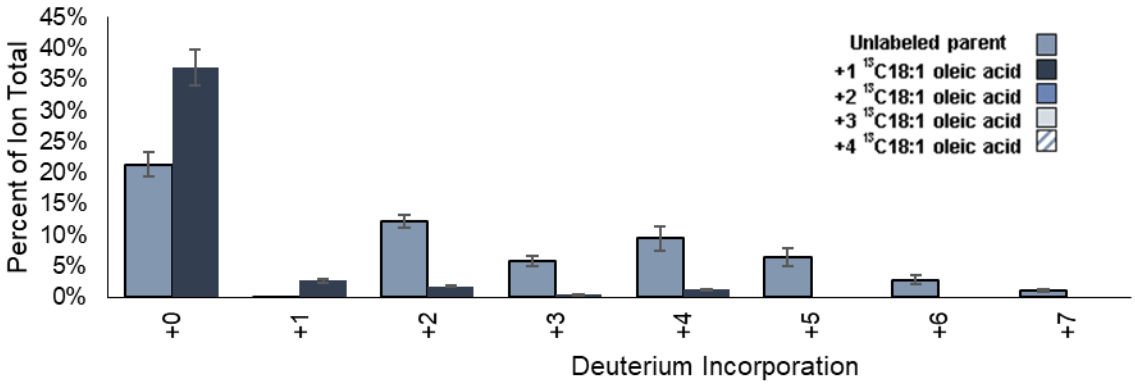

Figure S3.86 Average deuterium incorporation for DAG 36:1 in dual labeled culture (10% D2O + 13C oleic acid)

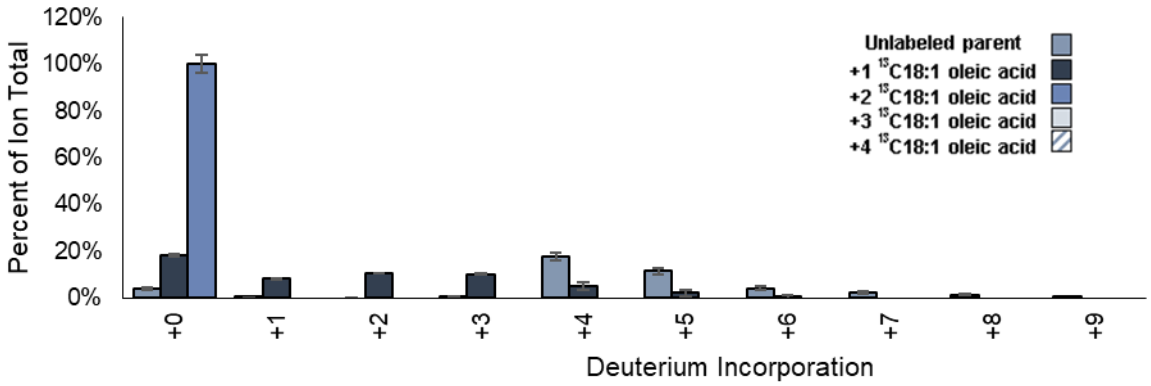

Figure S3.87 Average deuterium incorporation for DAG 36:2 in dual labeled culture (10% D2O + 13C oleic acid)

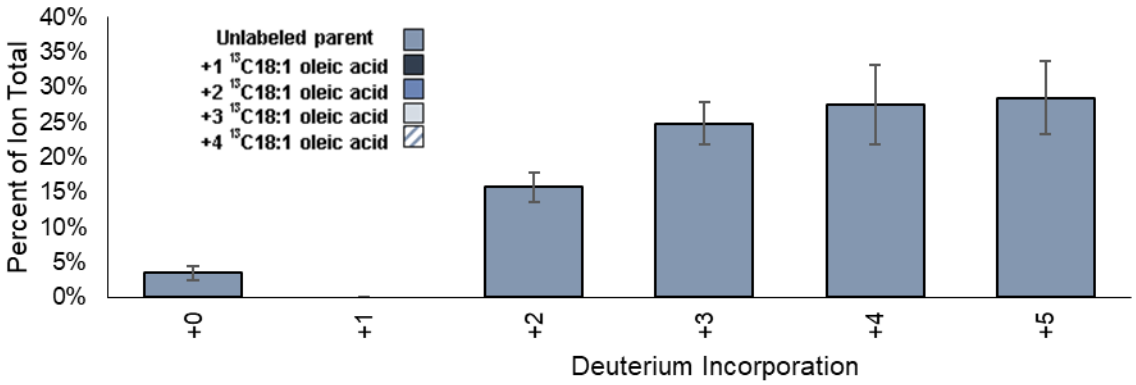

Figure S3.88 Average deuterium incorporation for MGDG 34:0 in dual labeled culture (10% D_2O + ^{13}C oleic acid)

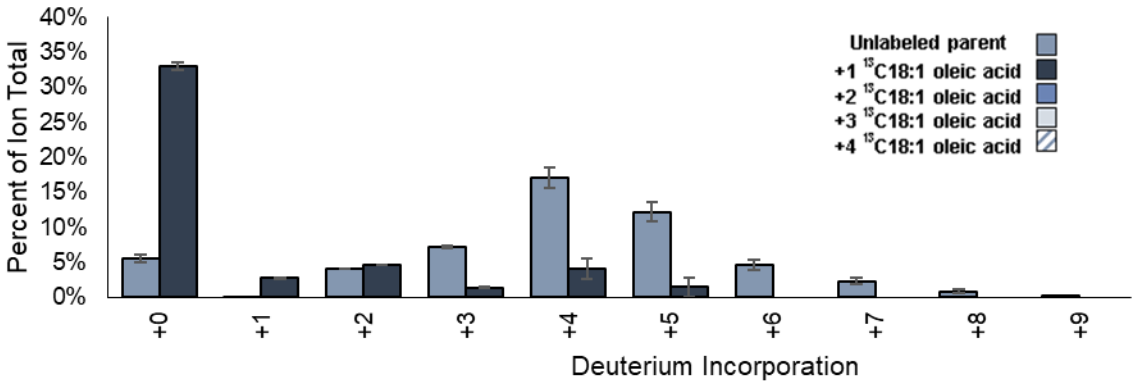

Figure S3.89 Average deuterium incorporation for MGDG 34:1 in dual labeled culture (10% D_2O + ^{13}C oleic acid)

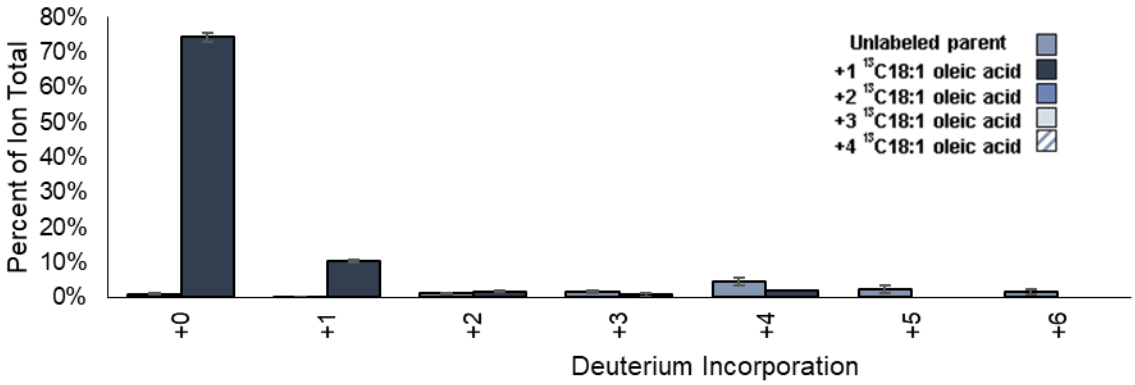

Figure S3.90 Average deuterium incorporation for MGDG 36:1 in dual labeled culture (10% D_2O + ^{13}C oleic acid)

Table S3.1 List of analytical standards utilized to verify retention times

Lipid	Concentration	Internal or External
CL 56:0	10uM	Internal
PG 16:0	10uM	Internal
CL 72:0	100uM-5nM	External
CL 72:4	100uM-5nM	External
PG 36:0	100uM-5nM	External
L-PG 36:0	100uM-5nM	External
L-PG 36:2	100uM-5nM	External
MGDG 34:1	100uM-5nM	External
PC 33:1 (d7)*	150.6ug/mL	External
PE 33:1 (d7)*	5.3ug/mL	External
PS 33:1 (d7)*	3.9ug/mL	External
PG 33:1 (d7)*	26.7ug/mL	External
PI 33:1 (d7)*	8.5ug/mL	External
PA 33:1 (d7)*	6.9ug/mL	External
LPC 18:1 (d7)*	23.8ug/mL	External
LPE 18:1 (d7)*	4.9ug/mL	External
cholesterol 18:1 (d7)*	329.1ug/mL	External
MG 18:1 (d7)*	1.8ug/mL	External
DG 33:1 (d7)*	8.8ug/mL	External
TG 33:1 (d7)*	52.8ug/mL	External
cholesterol (d7)*	98.4ug/mL	External
*Avanti Lipid SLASH Mix		

CONCLUSION

The data presented and discussed in the abovementioned chapters describes the impact of high-resolution mass spectrometry in probing biological systems. Furthermore, the collaborative nature of these studies highlights the importance of combining approaches across disciplines to address hypotheses. Lipidomics and metabolomics workflows provide physical information regarding molecules detected within the system. These techniques aid in understanding how metabolism is altered or influenced in response to external stimuli such as drugs, host nutrients, or genetic alterations. As the lipid membrane is a vital structure required for basic physiological functions and metabolism is the processes by which organisms perform primary chemical reactions required to survive, studying these biological processes can aid in understanding complex behaviors such as antibiotic resistance or tolerance.

The emergence of resistant or tolerant bacterial populations is a growing concern as treatment of these infections at the bedside is cumbersome. Daptomycin, a lipopeptide originally developed to combat vancomycin resistant enterococci, is one such antimicrobial drug becoming less effective at treating enterococcal infections. Although the mechanism by which daptomycin tolerance or resistance occurs is highly debated, lipidomic and metabolic analysis in the presence of the drug has not yet been reported. Chapter 1 aims to fill this void via a dual omics study of *Enterococcus faecalis* in the presence and absence of daptomycin as well as under conditions reported to induce tolerance to the drug. The results from this study suggest that administration of daptomycin influences the lipid membrane of the bacteria by decreasing the prevalence of the primary lipid component, PG, and increasing other membrane components such as PA, FFA, and CL. Administration of daptomycin under conditions reported in this study did not significantly alter the metabolome of the bacteria. As oleic acid has been implicated to induce tolerance to the drug, bacterial populations were exposed to oleic acid for 30 minutes prior to daptomycin administration. These results suggest that daptomycin is capable of altering the lipid membrane in the presence of oleic acid. Exposure to oleic acid did not prevent membrane alterations after treatment with the drug, in fact, similar results were reported in the presence of oleic acid. The primary membrane component, PG, was reported to significantly decrease while PA, FFA, and CL increased after administration of daptomycin in the presence of oleic acid while the metabolome remained unchanged. Additional analysis of tolerant versus susceptible bacterial populations exposed to the drug suggested acyl tail abundance or percentage of oleic acid incorporated into the membrane could be driving tolerance behavior, however; limitations of this study did not allow for further confirmation of these results.

As daptomycin administration altered relative membrane lipid percentages (chapter 1), genetic mutagenesis studies were utilized in chapter 2 to understand if specific lipid classes contributed to antimicrobial tolerance. Knockout strains

resulting in a loss of function were generated for CL, L-PG, and combined CL and L-PG. Loss of function for CL and L-PG mutants were confirmed via UHPLC-HRMS. Deletion of one, two, or three lipid synthesis genes were reported to alter the lipidome both in the percent of lipid species detected as well as relative abundance of specific lipid species compared to the parental strain OG1RF. Bacterial strains (parental and mutant) were exposed to oleic and linoleic acid independently as both fatty acids are reported to induce tolerance to daptomycin. Regardless of mutation, oleic acid or linoleic acid were reported to accumulate in membrane lipids across strains analyzed. Additionally, membrane challenge assays did not identify any mutant strain to have decreased tolerance to membrane damaging agents. Again, incorporation of host fatty acids into membrane lipids is implicated to play a role in antimicrobial tolerance.

Considering results from two independent studies suggested incorporation of exogenous, host fatty acids correlated strongly with antibiotic tolerance, a tracing study was designed to further probe nutrient fluxes compared to *de novo* synthesis. Stable isotope tracing techniques have been paired with mass spectrometry as molecules altered by the incorporation of heavy isotopes reflect altered mass to charge ratios. The study design in chapter 3 was unique in that exogenous nutrient pools needed to be labeled independently of *de novo* synthesis such that exogenous incorporation of fatty acids would have a unique mass to charge ratio compared to lipid synthesized via processes of type II fatty acid biosynthesis. To accomplish this, ^{13}C labeled oleic acid was utilized to trace exogenous incorporation or modification while deuterium was utilized to trace *de novo* lipid biosynthesis. Results from this study suggest oleic acid is incorporated in the sn1 position in 30 phospholipids. Furthermore, there is no evidence of modification of the fatty acid by the organism in the methods utilized. Additional analysis of deuterium fluxes suggests oleic acid does not impact deuterium incorporation, thus *de novo* synthesis does not appear to be significantly impacted by the addition of exogenous fatty acids.

Together, this work highlights significant advancements made within the fields of molecular microbiology and analytical chemistry. While the mechanism of daptomycin tolerance induced by fatty acids is still not completely understood in this organism, this work provides novel data to direct future studies. It is clear the exogenous fatty acids impact the membrane and are related to daptomycin tolerance; however, it is unclear if these alterations are linked to membrane fluidity or rigidity. Future studies should aim to address this correlation in order to better understand how oleic acid influences the membrane from a structural standpoint. Additionally, given decreases in PG were detected upon administration of daptomycin, it would be useful to understand if these alterations are linked to daptomycin tolerance as well. Considering the advancement in isotope tracing techniques highlighted in this work, additional experiments utilizing stable isotopes to better understand membrane structure are warranted. Deuterium has a large collisional cross section making the molecule an ideal target for neutron scattering experiments. As deuterium is reported to be

incorporated in large percentages, neutron scattering experiments could address differences in membrane structure upon the addition of oleic acid. As fatty acids induce tolerance, other studies should address the possibility of a combinatorial therapy aimed at altering the host infection sites, such that a fatty acid profile of the pathogen could be “restored” to a susceptible profile, thus increasing the efficacy of the drug itself.

VITA

Brittni Morgan Woodall was born in Nashville, TN and raised in the small town of Kingston Springs, TN. Upon graduation from Harpeth High School in 2015, she moved to Knoxville, TN to pursue her dream of becoming a doctor. Although the path was a bit different than she imagined, she found her passion for science through working in Dr. Shawn Campagna's laboratory as an undergraduate researcher and ultimately decided to continue her studies as a scientist, receiving her PhD. Brittni graduated from the University of Tennessee in the spring of 2019 with her Bachelor of Science in Biochemistry Cellular and Molecular Biology and a minor in Chemistry, Summa Cum Laude. In the fall of 2019, she returned to the Hill where she began her doctoral degree under the supervision of Dr. Shawn R. Campagna. Brittni has worked with a variety of mass spectrometry instruments and developed new techniques for probing biological systems related to health and human disease. She hopes to make a profound impact on society through her intellectual contributions to the scientific community as well as education and outreach to aid in funding and advancement of scientific ideas.